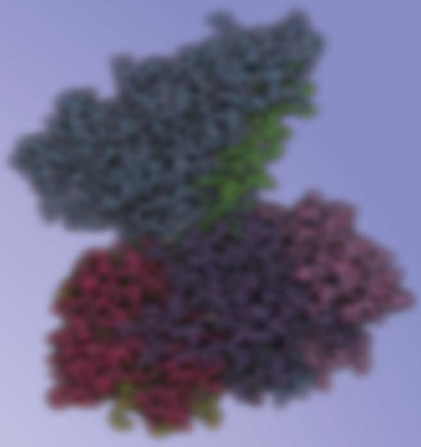

GM1-Derived Carbohydrates for Pathogen and Antibody Detection:

Synthesis and Biological Evaluation

Jaime Garcia Hartjes

GM1-Derived Carbohydrates for Pathogen and Antibody Detection:

Synthesis and Biological Evaluation

Jaime Garcia Hartjes

Thesis Committee

Promotor
Prof. Dr H. Zuilhof
Professor of Organic Chemistry
Wageningen University

Co-promotor
Dr T. Wennekes
Assistant Professor, Laboratory of Organic Chemistry
Wageningen University

Other members
Prof. Dr H.F.J. Savelkoul, Wageningen University
Prof. Dr R.V.A. Orru, VU University Amsterdam
Prof. Dr J.C.M. van Hest, Radboud University Nijmegen
Prof. Dr R.J.Pieters, Utrecht University

This research was conducted under the auspices of the Graduate School VLAG (Advanced studies in Food Technology, Agrobiotechnology, Nutrition and Health Sciences).

GM1-Derived Carbohydrates for Pathogen and Antibody Detection:

Synthesis and Biological Evaluation

Jaime Garcia Hartjes

Thesis

submitted in fulfilment of the requirements for the degree of doctor
at Wageningen University
by the authority of the Rector Magnificus
Prof. Dr M.J. Kropff,
in the presence of the
Thesis Committee appointed by the Academic Board
to be defended in public
on Monday 24 November 2014
at 11 a.m. in the Aula.

Jaime Garcia Hartjes

GM1-Derived Carbohydrates for Pathogen and Antibody Detection:
Synthesis and Biological Evaluation

240 pages.

PhD thesis, Wageningen University, Wageningen, NL (2014)
With summaries in English and Dutch

ISBN 978-94-6257-127-3

Voor mijn ouders

Table of Contents

List of abbreviations

^{13}C-NMR	carbon-13 nuclear magnetic resonance
^{1}H-NMR	proton nuclear magnetic resonance
Abs	antibodies
ACA	anticitrulline antibodies
AIDP	acute inflammatory demyelinating polyneuropathy
ALS	amyotrophic lateral sclerosis
AMAN	acute motor axonal neuropathy
AMSAN	acute motor-sensory axonal neuropathy
APT	attached proton test
BARAC	biarylazacyclooctynone
BCN	9-hydroxymethylbicyclo[6.1.0]nonyne
BSA	bovine serum albumine
C. jejuni	*Campylobacter jejuni*
calcd.	calculated (mass)
chex	cyclohexane
CNS	central nervous system
CTB	cholera toxin B-subunit
CTB-HRP	cholera toxin B-subunit horse raddish peroxidase conjugate
CuAAC	copper-catalyzed azide-alkyne cycloaddition
DCE	1,2-dichloroethane
DCM	dichloromethane
DDQ	2,3-dichloro-5,6-dicyano-1,4-benzoquinone
DFT	density functional theory
DIBAC	aza-dibenzocyclooctyne
DIFBO	difluorobenzocyclooctyne
DIFO	3,3-difluorocyclooctyne
DMF	*N*,*N*-dimethylformamide
DMTST	trifluoromethanesulfonate
DNA	deoxyribonucleic acid
ELISA	enzyme-linked immunosorbent assay
ELLA	enzyme-linked lectin assay
ESI-	electron spray ionization, negative mode
ESI+	electron spray ionization, positive mode
EtOAc	ethyl acetate
EtOH	ethanol
g	gram
Gal	galactose
GalNAc	galactosamine
GBS	Guillain-Barré syndrome
Glc	glucose
GM1os	GM1 oligosaccharide
h	hour(s)
HBTU	*N*,*N*,*N*′,*N*′-Tetramethyl-*O*-(1H-benzotriazol-1-yl)uronium hexafluorophosphate, *O*-(Benzotriazol-1-yl)-*N*,*N*,*N*′,*N*′-tetra-methyluronium hexafluorophosphate
HF	*here*: Hartree-Fock
HMBC	heteronuclear multiple bond correlation
HMDS	here: hexamethyldisilane
HOMO	highest occupied molecular orbital
HR-ESI	high resolution electron spray ionization
HRP	horse radish peroxidase
HSQC	heteronuclear single quantum coherence
IgA	immunoglobine of type A
IgG	immunoglobine of type G
IgM	immunoglobine of type M
ITMS	iodo-trimethylsilane
IVIg	intervenous immunoglobine

List of abbreviations

LUMO	lowest unoccupied molecular orbital
MeCN	acetonitrile
MeOH	methanol
MFS	Miller-Fisher syndrome
mg	milligram
MHz	megahertz
min	minutes
ml	milliliter
mmol	millimole
mol	mole
ms	molecular sieves (depending on context)
ms	multiple sclerosis (depending on context)
MS	mass spectrometry
MW	microwave
NaOMe	sodium methoxide
Neu5Ac	*N*-acetyl neuraminic acid
n-BuLi	*n*-butyllithium
ng	nanogram
nhept	*n*-heptane
nhex	*n*-hexane
NHS	*N*-hydroxy succinimide
nmol	nanomole
NMR	nuclear magnetic resonance
OCT	cyclooctyne
OD	optical density
OPD	*ortho*-phenylenediamine
PBS	phosphate buffered saline
PMB	*para*-methoxy benzyl
PMB-Cl	*para*-methoxy benzyl chloride
pmol	picomole
*p*NP	para-nitrophenylcarbonate
PNS	peripheral nervous system
ppm	parts per million
PTSA	*para*-toluene sulphonic acid
quant.	quantitative yield
Rf	relative retention
RNA	ribonucleic acid
rt	room temperature
sat.	saturated
SCS	spin-component scaling
SET	single electron transfer
S_N1	substitution nucleus type 1
S_N2	substitution nucleus type 2
SPAAC	strain-promoted azide-alkyne cycloaddition
sym	prefix *sym* indicates corannulene 1,3,5,7,9-substitution
TEA	triethylamine
THF	tetrahydrofuran
TMB	3,3′,5,5′-tetramethylbenzidine
TMS	trimethylsilane
TMSOTf	trimethylsilyltriflate
TS	transition state
V. cholerae	*Vibrio cholerae*
W	Watt
µg	microgram
µl	microliter
µmol	micromole

1

General introduction

1.1 Introduction

Carbohydrates, also referred to as sugars, saccharides or glycans, are the most abundant class of organic compounds in nature. They play a key role as food source (*e.g.* sucrose and starch) and are subsequently used in metabolic processes such as energy generation and storage. Carbohydrates are also important for structural purposes. For example, the rigidity of plants is based on the carbohydrate polymer cellulose, and many invertebrates have protective shells made of another carbohydrate polymer called chitin. In addition, the carbohydrate, (deoxy-)ribose is an integral part of the structural framework of DNA and RNA.[1] Essential however for the studies described in this thesis, a dense layer of carbohydrates can also be found on the surface of almost all cells. There they are often linked to proteins and lipids to form so-called glycoconjugates that, among other things,[2] play a vital role in cell-to-cell interactions, communication processes and protein activity regulation. The complex, macromolecular, network of these glycoconjugates and other carbohydrate derivatives on the periphery of cells is called the glycocalyx, and is actually visible on a microscopic level (Figure 1). The collection of all glycan (macro)structures found in an organism is called the glycome and it is thought to be involved in, and lie at the root of, many of such crucial biological events.

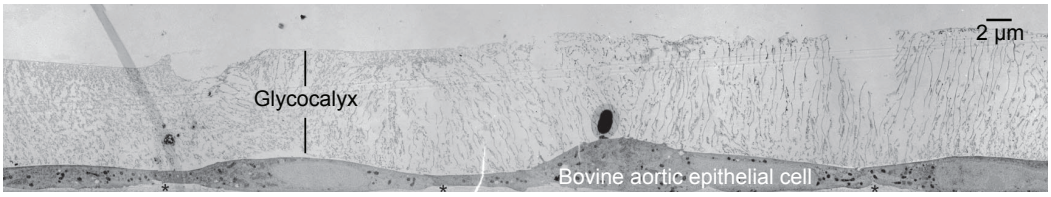

Figure 1. Transmission electron microscopy image of the glycocalyx on a bovine aortic epithelial cell. Figure adapted from reference.[3]

An increasing number of studies focuses on the so-called functional glycomics, *i.e.* mapping the glycome and its functions. The glycocalyx, and the proteins that interact with it, are at the center of interest in functional glycomics.[4] Some concrete examples of such studies are focusing on influenza (the flu) and cholera. At the basis of the pathogeneses of these diseases lie carbohydrates, found in the glycocalyx, that are recognized and targeted by pathogen-produced proteins, which upon binding to the carbohydrates initiate cascades of intracellular processes. Although research activities in the field of functional glycomics are continuously increasing, much still remains unresolved when it comes to

the properties and complexity of the glycocalyx and functions of its individual elements. The structural complexity of carbohydrates, including their chirality, conformation and variable regiochemistry, makes it challenging, however not impossible, to investigate their biological roles.[5] In addition, complex carbohydrate structures and their patterns on cells are very dynamic and, importantly, not encoded in our genome. This makes it difficult to study them *via* a molecular biology approach (*e.g.* gene knock-out techniques[6] or using green fluorescent protein (GFP) fusions[7] for visualization). Hence, this research area is the "turf" of the glycochemist, who is able to design and synthesize tailor-made analogues of natural carbohydrate constructs so that they can be investigated in detail on a smaller scale, while being isolated from interference by other biological processes.

The overall aim of the research described in this thesis is to investigate the interaction of several such tailor-made carbohydrate derivatives with their natural protein binding partners, either both completely solubilized or at an interface. With these functional glycomics studies, we aim for an improved understanding of the nature of these protein-carbohydrate binding events and their relationship with the pathogeneses of the associated ailments. A better understanding can in turn lead to improved/ cheaper/ faster medical treatments, or detection methods in the form of biosensors, based on these same molecules. In line with these

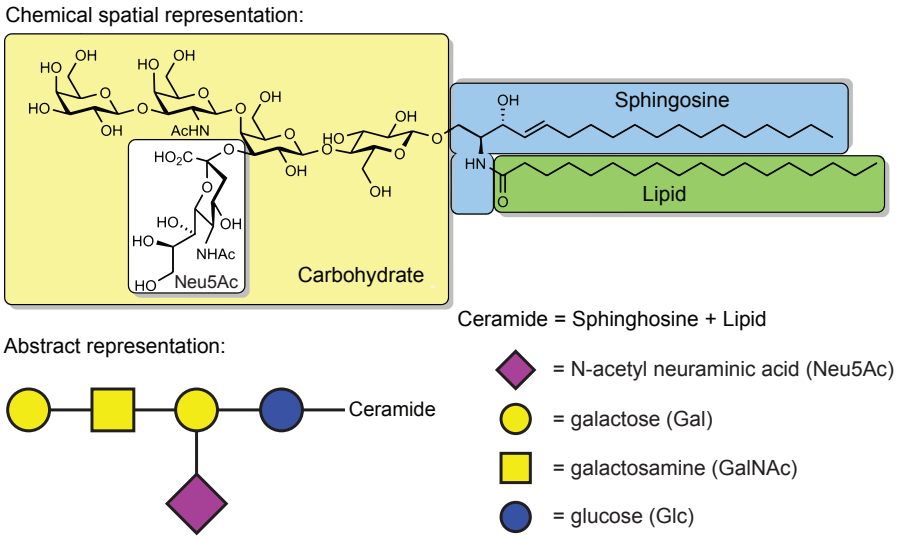

Figure 2. Glycosphingolipid GM1 consists of a carbohydrate part, a sphingosine and lipid part. It belongs to the class of gangliosides, because of the presence of at least one Neu5Ac moiety. Both the chemical spatial and widely accepted abstract representation[9, 10] are depicted here and alternately used throughout this thesis.[9]

envisaged applications, the work described in this thesis formed an integral part of the Interreg "Unihealth" project[8] that focused on the development of a novel type of biosensor for the facile detection of allergens or pathogenic species.

In the following sections, topics will be highlighted that are of particular interest for the studies in this thesis. First, a specific group of carbohydrates, gangliosides, will be discussed in an attempt to create an understanding on their natural purpose and the roles that they play in the pathogenesis of several diseases. The tools that are available for glycochemists to make mimics of these natural carbohydrates are subsequently discussed. This includes general protective group strategies, glycosylations, and chemoenzymatic procedures. To study the biological role of the tailor-made carbohydrates, many techniques exist, some of them will be discussed in more detail later on in this chapter. Finally, an overview is presented of what can be expected in the forthcoming chapters of this thesis.

1.2 Gangliosides

Before introducing the carbohydrate family of the gangliosides it is important to briefly discuss the several ways that the structure of carbohydrates are depicted in the scientific literature and this thesis. The two most commonly used ways, and also in this thesis, are the chemical spatial representation and the more abstract representation with colored icons as shown in Figure 2. The latter, nowadays widely accepted, abstract representation leaves out a lot of chemical and structural information, but does provide a fast overview of the sequence and branching of poly-saccharides and oligo-carbohydrates. Herein, the galactose (Gal) moieties are depicted as yellow circles, galactosamine (GalNAc) as yellow squares, Neu5Ac as purple diamonds and glucose (Glc) as blue circles.[9]

1.2.1 Introduction on gangliosides

In 1942, a specific class of carbohydrate-rich glycosphingolipids was discovered,[11] following the isolation of several of these from mammalian brain tissue.[12] This subclass of glycosphingolipids, termed gangliosides, was found to typically consist of fatty acids, various carbohydrates, and sphingosine (Figure 2). Glycosphingolipids are only characterized as gangliosides if they contain the carbohydrate *N*-acetylneuraminic acid (Neu5Ac). When all types of brain gangliosides are taken into account they together account for ~ 75% of the brain's

sialic acid content and they represent ~ 80% of the total carbohydrate mass.[13] In Figure 2, the ganglioside GM1 is depicted. It contains a pentasaccharide moiety that plays an important role throughout this thesis for reasons that will be clarified later.

Svennerholm[14] was the first to separate individual gangliosides by chromatography and distinguished several compounds that each contained different carbohydrate parts. The gangliosides were separately named according to their chromatographic separation (Figure 3). The chemical composition was identified by a stepwise acid degradation and isolation of the separate ganglioside components.[15] Their nomenclature is now widely accepted to begin with a G for ganglioside, followed by an M, D, T, Q, or P as a designation of the number of Neu5Ac residues present (one, two three, four, or five residues, respectively). In addition, a number was assigned to the gangliosides that were known at that time according to their retention on thin layer chromatography (TLC) plates. For example, the ganglioside that was least retained on the TLC plate was termed GM3, received the "3" for being the highest on the plate.[16] The structurally closely related gangliosides GM1, GD1a, GD1b, and GT1b represent the majority of the gangliosides in the adult human brain, *i.e.,* ~ 97% of all gangliosides (the central four structures in Figure 4).[17]

1.2.2 Natural function of gangliosides

Even though gangliosides have also been isolated from spleen[18] and red

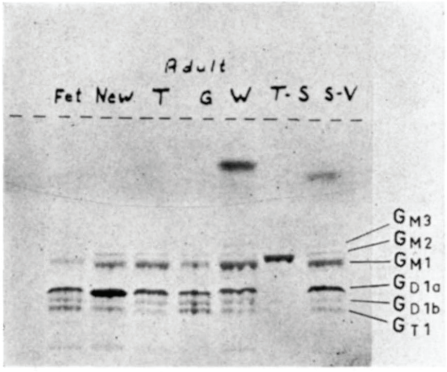

Figure 3. A reproduction of Svennerholm's original TLC plate depicting total ganglioside extracts from various tissues. Fet = fetal brain, New = newborn brain, T = total, adult human brain, G = grey matter of adult human brain, W = white matter of adult human brain, T-S = infantile amaurotic idiocy (=Tay-Sachs disease) brain, and S-V = juvenile amaurotic idiocy brain. Solvent: 1-propanol-water, 7 : 3 (v/v). Figure and adapted caption from reference.[16]

blood cells,[19] they are mainly characteristic components of nerve cells. For most gangliosides, their natural functions have not yet been (fully) determined, but by intense research more and more is being discovered about this class of glycosphingolipids.[13, 20] One way to investigate their natural function is by applying gene knock-out techniques on their biosynthesis machinery. In mouse models, genes can be switched off (knocked out) that are specifically responsible for the expression of, for example, GalNAc transferases.[13] These specific transferases facilitate the enzymatic synthesis of GM2 and GD2, from GM3 and GD3, respectively (Figure 4), by adding a GalNAc moiety to the terminal Gal of the substrates.[21] The absence of such transferases prevents the formation of the more complex, and in adult brains more abundant, four gangliosides GM1, GD1a, GD1b, and GT1b. These knockout mice that lack the GalNAc transferase, display an unusual amount of unmyelinated fibers in the central nervous system (CNS). Myelin serves as a protective sheath on a.o. muscle nerve cells (see Chapter 6 for additional information on this topic). The absence of this protective sheath in the knock-out mice indicates that these gangliosides, GM2 and GD2, are, in part, responsible for the formation of it. On a physiological level, this translated to the observation that these knockout mice displayed loss of function in the lower extremities and loss of coordination. On the contrary, also hyperactivity was noted of which the origin was not established, since this could not be directly related to loss of motor functions or axon conductivity. This indicates possible additional functions of these gangliosides. When additionally also the gene responsible for the biosynthesis of GD3 was knocked out, the mice only displayed GM3. These “GM3-only mice”, additional to earlier mentioned physiological problems, also suffered from seizures and deadly convulsions.[22] Several additional such studies were performed to elucidate the natural function of gangliosides and taken together, these studies imply that complex brain gangliosides like GM1, GD1a, GD1b, and GT1b are required for axon-myelin interactions and long-term axon stability.[13] Other crucial functions of gangliosides include cell signaling for programmed cell death of white blood cells (GD3),[23] whereas specifically GM1 plays a modulatory role in the calcium flux from the cytosol to the plasma through non voltage-gated channels.[24] This is however only the tip of the ice berg as it comes to the natural roles that gangliosides fulfill.[13, 20] Aside from having these roles in healthy cellular functioning, gangliosides are also involved in several diseases and play evident roles in their pathogenesis.

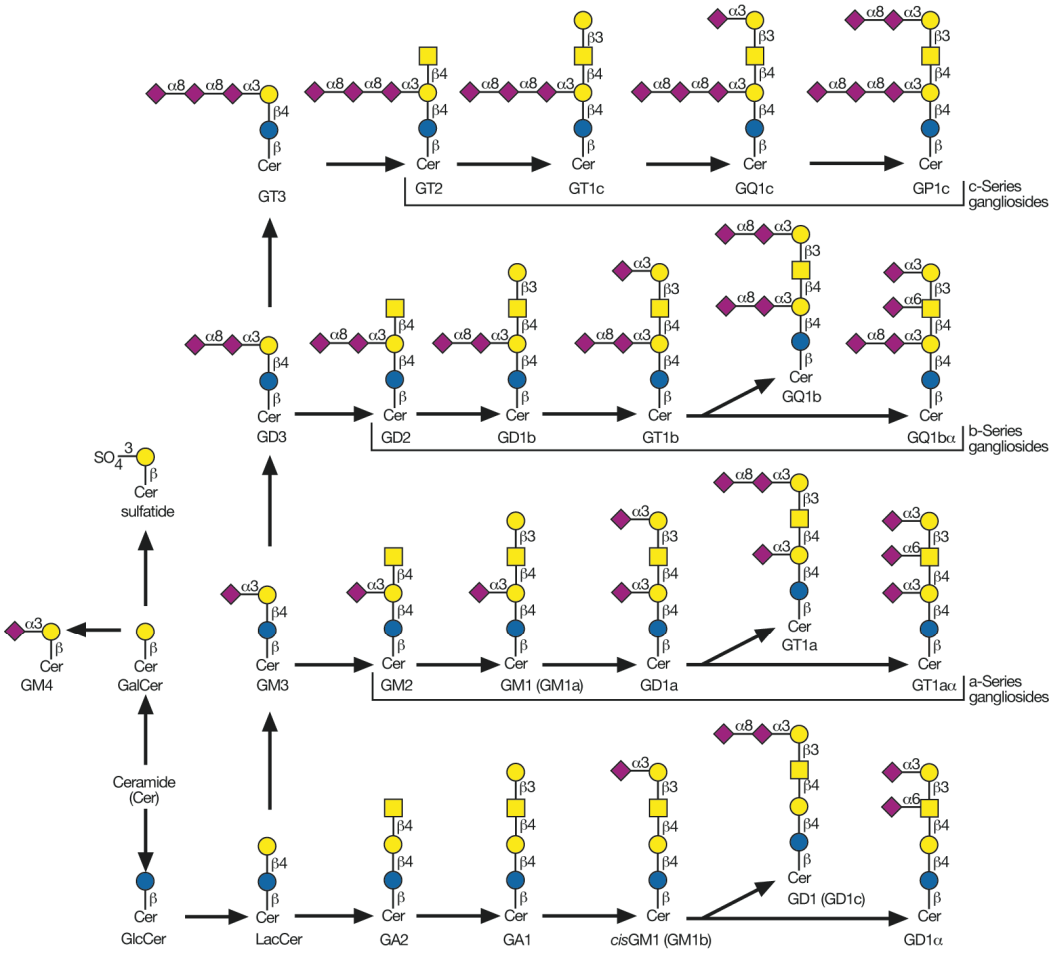

Figure 4. List of gangliosides and other related glycosphingolipids. The biosyntheses of these compounds involve a large array of glycosyltransferases and glycosidases.[25]

1.2.3 Gangliosides and disease

Gangliosides play a role in many disrupted metabolic processes. For example, ganglioside GM2 (Figure 4) accumulates in the brain of patients suffering from Tay-Sachs disease due to a genetic disorder. A mutation in the gene that encodes for the enzymes that break down this ganglioside causes a lowered expression of this enzyme.[15] This results in abnormally high concentrations of the ganglioside in brain nerve cells. Subsequent accumulation in the ganglion lysosomes lead to nerve cell swelling and neuron distubances. The disease GM1 gangliosidosis is quite similar, leading to severe accumulation of GM1 on the

periphery of cells. In many types of cancer, the expression of glycoconjugates, including gangliosides, on the cancer cells have been found to change with respect to their healthy counterparts. In these cases, the exact constitution of these abnormal glycoconjugate levels is often highly specific for each type of cancer.[26] As an example, on carcinoma cells the gangliosides GM1 is above-normally present and therefore more easily recognized by the hemagglutinin of influenza viruses, making the patient more susceptible to infection.[27] Influenza A virus infections are initiated via hemagglutinin (a glycoprotein that can be found on the surface of influenza viruses) that binds to sialylated glycoconjugates exposed on the surface of target cells.[28] In this example, rather than the toxic effects of ganglioside accumulation, the disease is caused by direct gangliosides-targeting by an external pathogen that uses them as recognition and binding points. After successful protein-ganglioside recognition and binding, the pathogen enters the cell *via* endocytosis. This type of involvement of ganlgiosides in the pathogenesis of a disease is also seen in cholera. This disease is initiated by the ingestion of the *Vibrio cholerae* bacterium (*V. cholerae*). Once in the host, this bacterium generates the cholera toxin (CT) that targets intestinal epithelial cells that contain ganglioside GM1 on their periphery. CT plays an important role in the research discussed in Chapters 2, 3 and 5.

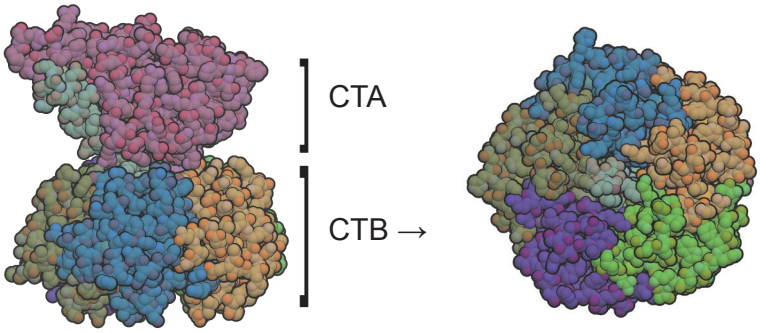

Figure 5. left) CT 3d model; Frontal view; depicting both the toxic CTA and the five CTB units; right) Bottom view of the five identical B_5-subunits. (PDB: 1XTC)[35]

The gastrointestinal life-threatening disease cholera is one of the main causes of death by infectious diseases worldwide. In 2010 alone, almost 320 thousand cases of cholera were reported globally, with a little more than 7500 reported fatalities.[29] The infections and mortality numbers are, however, known to be underreported. Therefore the true total amount of global cases is estimated to be 10-fold higher, with around 3-5 million infections per year and around 150.000

annual mortal cases.[30] Currently, patients affected by cholera are treated *via* oral and intravenous rehydration therapy. Antibiotics are also used in severe cases of cholera infection, but growing antibiotic resistance renders the treatment increasingly less effective. To this date no medical drug has been submitted for clinical trials, making the development of an effective treatment still a highly worthwhile goal.

The CT is a member of the AB_5 toxin family, and contains a pentameric binding domain[31] (Figure 5). These toxins typically have an enzymatically active A subunit (CTA), responsible for inducing toxicity, and a pentavalent toroid-like B_5 subunit (CTB), responsible for binding to cell surfaces. The natural ligand for CT is ganglioside GM1 (Figure 2), which can be found a.o. on the periphery of intestinal cells. Lateral mobility of the gangliosides across cell surfaces ensures an optimal multivalent binding for the toxin, which results in a strong adhesion of the CT molecule to the cell, and subsequent incorporation via endocytosis. This is followed by the release of the toxic A-subunit in the cytosol,[32] which leads to a cascade of biological processes.[33] At the end of the line, this cascade induces the efflux of water from the patients intestinal epithelial cells than in turn causes violent diarrhoea and associated severe dehydration. Preventing these events by capturing the toxin in the intestines would seem to be a logical way of cholera treatment. Natural ganglioside GM1 is however not applicable as such an inhibitory drug for the treatment of toxins like CT, because exogenous gangliosides are readily integrated in cell membranes and thereby become functional components thereof. This occurrence can turn cells that were initially unaffected by CT into more susceptible targets for the toxic agent.[34] To avoid this, the GM1os should be connected to an appropriately designed synthetic scaffold. Some examples on how the GM1os can be presented to toxins when attached to such a scaffold are discussed in §1.3 and in Chapters 2 and 3 of this thesis. Additional research regarding the binding affinity of CTB towards a couple of novel carbohydrate-presenting compounds is discussed in Chapter 5.

Several neurodegenerative diseases also involve gangliosides.[36] Amongst others, these include: amyotrophic lateral sclerosis (ALS), Alzheimer's disease, multiple sclerosis (MS), and Guillain-Barré syndrome (GBS). GBS is also initiated by the ingestion of a pathogen, like in the case of cholera. However, rather than the pathogen itself causing the pathogenesis by targeting cell surface glycans, in GBS, the pathogen displays glycans that resemble carbohydrates that are also displayed on the cell surface of human nerve cells. These glycans, presented on the bacterial cell wall, resemble and mimic gangliosides.[37] This phenomenon is called molecular

mimicry. When the patient's immune system forms antibodies (Abs) that target the carbohydrate moieties that are displayed on the pathogen, these Abs will also target the similar ganglioside epitopes that reside on the patient's nerve cells. As a result, an auto-immune response is imminent. A more extensive discussion on the pathogenesis of GBS will be discussed in Chapter 6. In order to investigate the pathogenesis of abovementioned diseases, and eventually to understand it at a molecular level, carbohydrate structures are needed that resemble the targeted gangliosides. These can be extracted from natural sources. However, natural sources have the disadvantage that the yield is low, purification processes are long and difficult (hence, expensive) and that the obtained products are still potentially (and in practice: regularly) contaminated with other compounds. In contrast, chemically synthesized compounds can be obtained completely pure in higher quantities, and if desired the synthetic route – in this case mainly involving carbohydrate chemistry – can be used to incorporate tailor-made modifications in their structure.

1.3 Carbohydrate chemistry

1.3.1 Glycosylations, glycosyl donors and protective groups

In order to investigate protein-cell or cell-cell interactions, synthetic analogues of the signaling carbohydrates that reside on the cell surface need to be developed. A glycochemist has ample choice of numerous glycosylation reactions. An efficient protective group strategy that is compatible with the glycosylation conditions is essential. In addition, various stereo-electronic effects that are intrinsic for carbohydrates need to be taken into account. An additional challenge in carbohydrate chemistry is that for a standard pyranoside, *e.g.* galactose, five reactive hydroxyl groups are presented with nearly equal reactivity. Only due to small effects – involving charge differences, the anomeric effect, axial or equatorial orientation, or the reactivity difference between primary and secondary hydroxyl functionalities – one can discriminate between these various sites (Figure 6). In order to work with compounds that display so many reactive groups in close proximity of one another, it is imperative to keep in mind the compatibility of the various protective groups and glycosylation conditions.

Over the years, many fine reviews have been published regarding glycosylation reactions.[38] Among the most used glycosyl donors belong the trichloroacetimidates, also called Schmidt imidates (Compound **1**, Scheme 1),[39] which are synthesized by

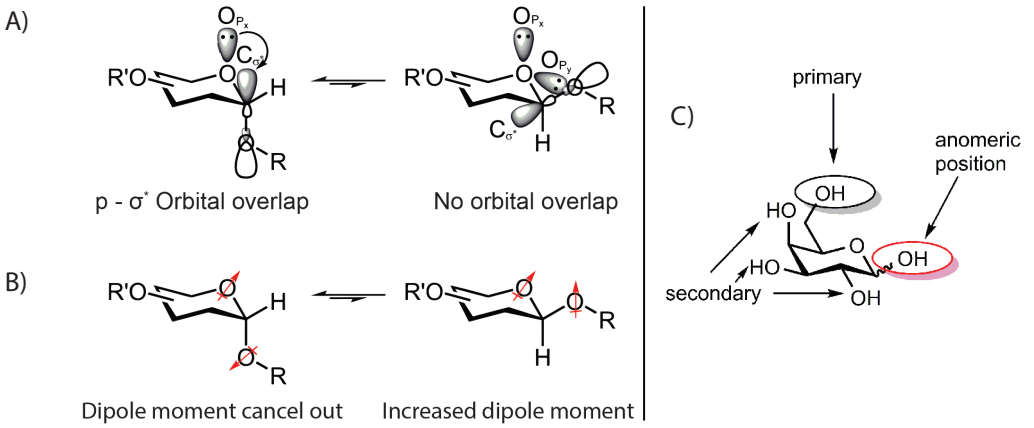

Figure 6. Various stereo-electronic anomeric effects and physical aspects that help to distinguish between the quite similar reactive functionalities on carbohydrates; A) Lone-pair donation to αC-1 σ*; B) Dipole moment; C) carbohydrate pyranosides consist generally of five reactive hydroxyl sites (glycosamines not taken into account) with slightly different reactivities.

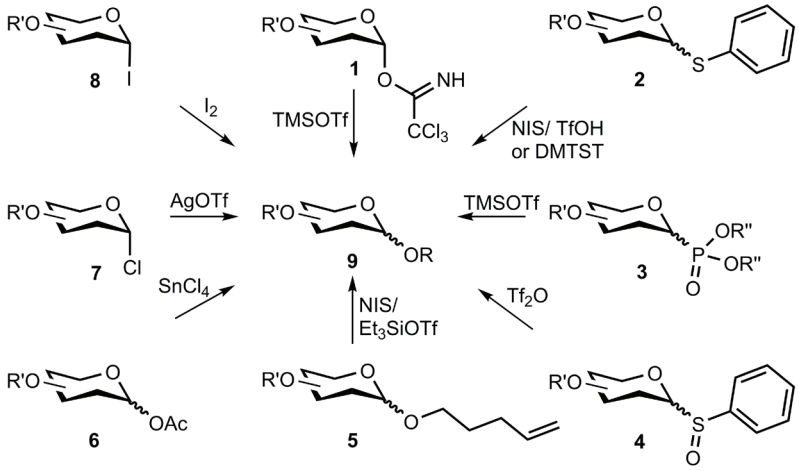

Scheme 1. Common glycosyl donors and typical reactants used in their glycosylation with a nucleophilic alcohol acceptor (R-OH). See text for references.

reacting a pyranosie hemiacetal with tricholoracetonitrile. In general, nucleophiles of various reactivity react with these imidates in the presence of Lewis acids such as equimolar $BF_3 \cdot OEt_2$ or catalytic TMSOTf. Other well-known glycosyl donors include thioglycosides (**2**),[41] phosphates (**3**),[42] sulfoxides (**4**),[43] and pentyl glycosides (**5**).[44] The thioglycosides (**2**) can be conveniently activated in at least two different ways. The first is a "two-step" activation, which involves first forming a glycosyl halide, and then activating this with a halophilic reagent. The second route, which is most

commonly used nowadays, involves a one-step activation with a thiophilic reagent such as methyl trifluoromethanesulfonate (methyl triflate) or dimethyl(methylthio) sulfonium trifluoromethanesulfonate (DMTST).[45] *Per*-acetyl **6** is a substrate for $SnCl_4$-promoted glycosylation.[40] Although the C-1 is equipped with a generally stable acetyl protective group, reactions with relatively low nucleophilic alcohols can still be performed due to the chemical distinction of the anomeric position. This reactivity can be ascribed to the anomeric effect(s) that are depicted in Figure 6. Possibly the oldest type of glycosyl donors are the glycosyl halides. Especially, C-1 chlorides (**7**) and bromides have been extensively used in Koenings-Knorr-type glycosylations.[46] Also glycosyl iodides (**8**) have received a lot of attention in literature and are also used on several occasions in experiments described in this thesis. Scheme 2A shows a proposed mechanism for the formation of iodide donor **13**.[47] The reaction may proceed via oxonium intermediates **11a** - **11d**, in which an iodine anion reacts as a nucleophile on the empty p-orbital on the anomeric position. This leads after equilibration to the desired α-iodo glycoside.

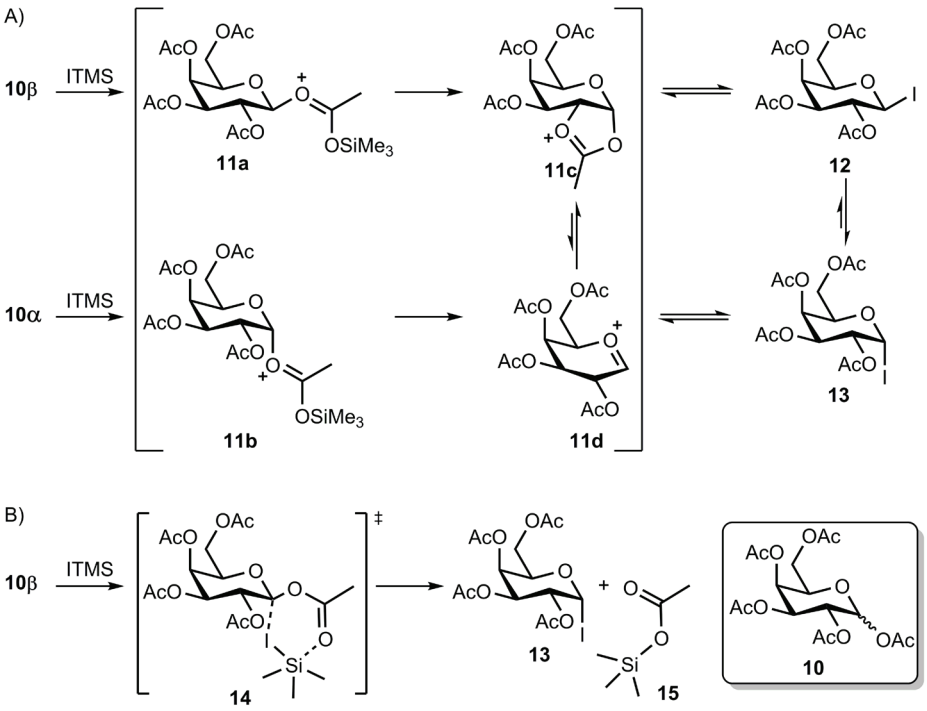

Scheme 2. A) Mechanism for the stereoselective formation of glycosyl iodides by Gervay et al.[47] B) Proposed alternative, concerted mechanism (only shown for the β-acetate).

1.3.2 Protective groups

Successful glycosylation reactions hinge on using the correct protective group strategy. Several good reviews have been published on this topic.[48] In glycosylation reactions with glycosidic halides, several nucleophilic reactions can take place. This may especially require attention when protective groups are used that stimulate anchimeric assistance, a.k.a. neigboring group participation. In the reaction of iodides with alcohols, the β-product is formed by either the S_N2-type mechanism or by the S_N1-type mechanism (Scheme 3A and B, respectively), wheras the α-product is only formed in the S_N1-type reaction. In the case of a S_N2 mechanism, the nucleophilic alcohol displaces the still intact C-I bond resulting in a new β-acetal bond, and iodine acts as the leaving group. Iodine promotes the S_N1 reaction[46b] when it is used as reactant (Lewis acid). It coordinates to the α-iodide and the subsequent dissociation of triiodide (I_3^-) leads to the formation of an oxocarbenium ion (Scheme 3B, **18**). This reaction is feasible because of mesomeric stabilization of the resulting carbocation with one of the oxygen lone-pairs. A nucleophilic reaction of the alcohol at the anomeric centre can now occur from both the axial or equatorial position, leading to α-product **20**, or β-product **16**, respectively.

In this reaction, also the choice of a suitable solvent is of importance to form the desired β-product, since polar protic solvents favor S_N1, and polar aprotic favor S_N2 reactions.[49] In addition, when acetonitrile is used as solvent, another stereo-electronic effect plays an important role, and a stereoselective yield of the β-product is observed (Scheme 3C).[39c, 50] The solvent participation effect that is shown here, involves acetonitrile coordinating to the glycosyl C-1 α-position, effectively blocking that side for nucleophilic reaction in favor of β-product formation. On occasion, also C-2 deprotected glycosides are observed. In that case, the acetyl group on C-2 participates in the glycosylation reaction (Scheme 3D). This C-2 anchimeric assistance works via an additional stabilization of oxocarbenium ion **23**, which is also in equilibrium with its oxonium ion, like galactoside-equivalent oxocarbenium ion **18**. The carbonyl oxygen lone pair of the C-2 acetyl protecting group interacts with the empty p-orbital at C-1, and only the α-position is within reach of the acetyl carbonyl. The resulting dioxolenium ion **24** is then prone to nucleophilic reaction with the alcohol, in two ways. First, direct glycosylation (Scheme 3D, route a) on the activated C-1 leading to the septa-*O*-Ac-protected β-product. Second (route b), the dioxolenium ion reacts with the nucleophile to form an orthoester.[51] Once the unstable orthoester is

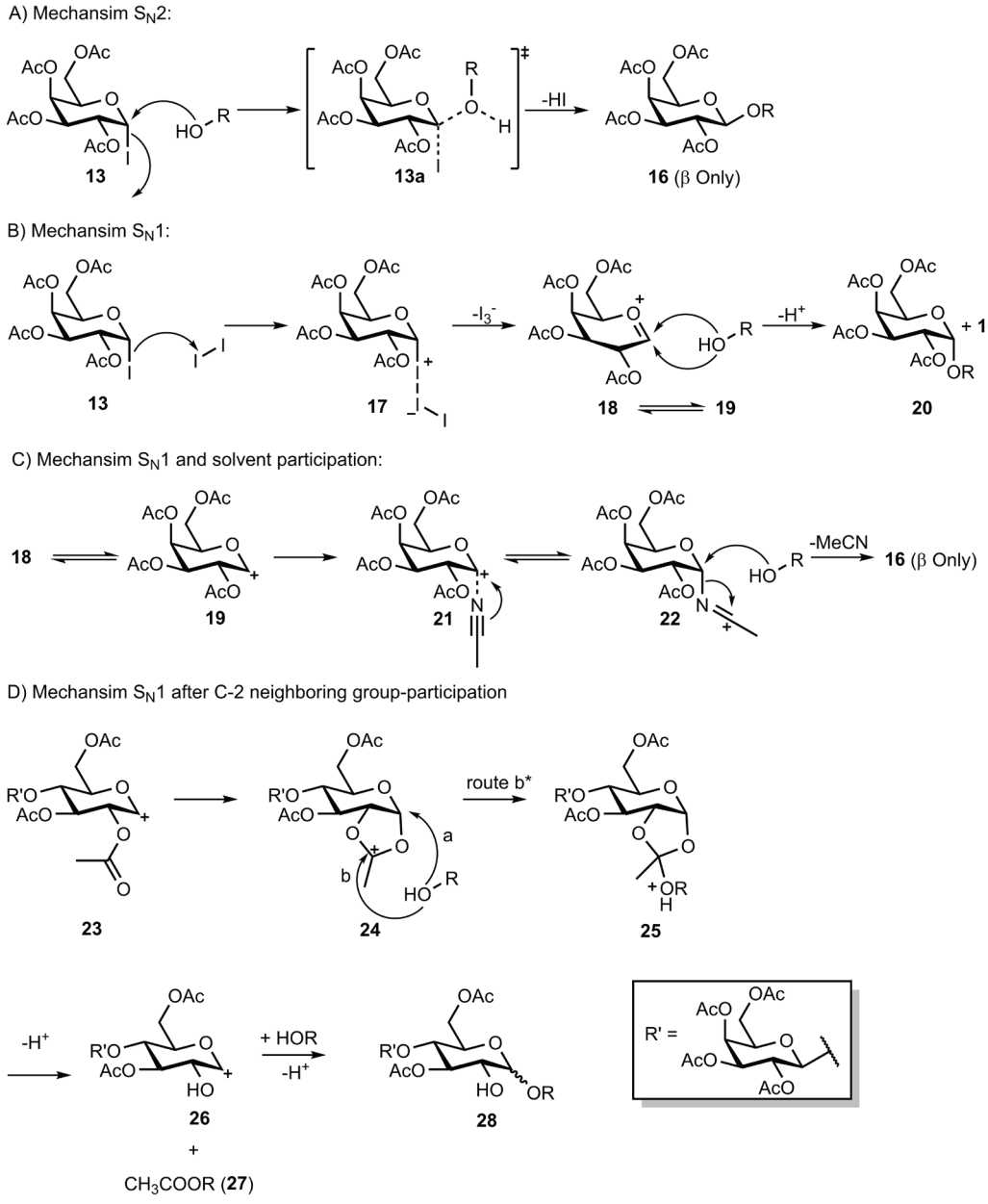

Scheme 3. Glycosylation of α-iodo-glycosides with alcohols *via* A) S_N2-type and B) S_N1-type mechanisms,[46b] C) β-directing acetonitrile solvent participation,[39c, 50] and D) neighboring group-participation;[50] *route a leads to 11-azido undecyl 2,3,4,6-tetra-*O*-acetyl-β-D-galactopyranosyl-(1→4)-2,3,6-tri-*O*-acetyl-β-D-glucopyranoside (not shown) and could be considered an S_N2-type mechanism.

formed, the C-1 oxygen is displaced, deprotecting the C-2 alcohol (compound **26**), while the methyl ester **27** is expelled as byproduct. A second nucleophilic reaction leads to the anomeric mixture of hexa-*O*-acetate compound **28**.

Acetyl (Ac) esters are possibly one of the most used protective groups for hydroxyls in carbohydrate chemistry together with benzyl (Bn) ethers. As shown in the previous example, an advantage of the acetyl group is that in some cases it also facilitates the anchimeric effect that can aid in the stereoselectivity of reactions. The acetyl group is base labile, and can withstand most other reaction conditions, including hydrogenations and mild acids.[52] The more sterically demanding pivaloyl (trimethylacetyl) group is even more stable than the acetyl group and also relatively easy to attach,[53] however, it sometimes suffers from the disadvantage of requiring long or harsh deprotection conditions, which may affect other functionalities in the compound.[54]

In an effort to distinguish between the secondary C-4 hydroxyl and the primary C-6 hydroxyl, acetal groups are often used in carbohydrate chemistry (Scheme 4). Benzylidene acetals can be regioselectively opened depending on the reaction conditions, leading to the 4-OBn, 6-OH (compound **30**)[55] or 4-OH, 6-OBn (compound **31**)[56] glycosides.[57] The benzyl group is able to withstand both basic and acidic conditions and is generally cleaved by hydrogenation with catalytic Pd/C and hydrogen gas. As an alternative for the benzyl groups, *p*-methoxy benzyl is often employed.[58] The electron-deficient DDQ facilitates the mild deprotection of PMB-ethers[59] by a mechanism of multiple single electron transfers (SET) (Scheme 5).[5] In addition, 4,6-PMB acetals can undergo regioselective ring-opening reactions, with $NaCNBH_3$, similar to those described for benzylidene acetals.[56, 58] This is especially useful in strategies wherein hydrogenations are unwanted, for example, when an azide is present in the carbohydrate and it needs to remain intact.

A different approach to carbohydrate synthesis, that also avoids protective

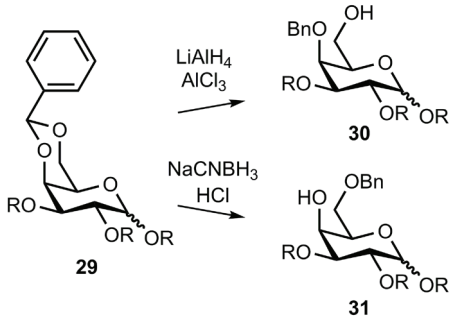

Scheme 4. Reaction conditions for the stereoselective ring opening of glycosylic 4,6-benzylidene acetals.

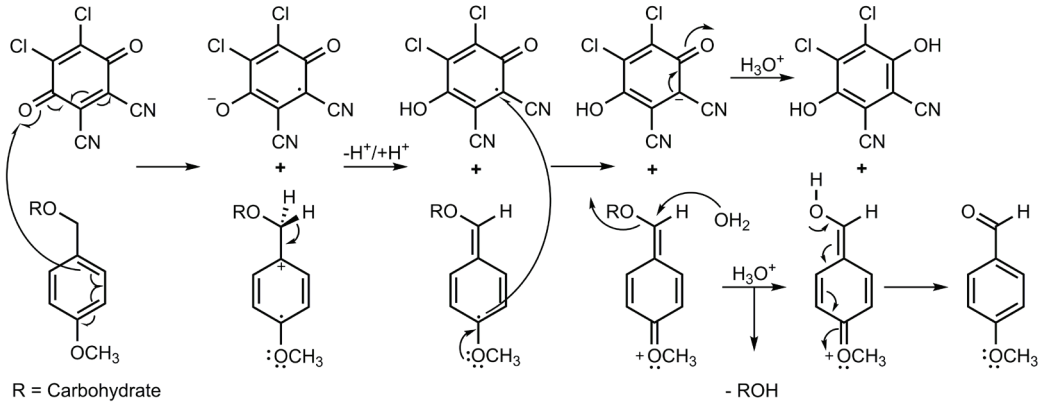

Scheme 5. Single electron transfer mechanism for the deprotection of PMB-ether protected carbohydrates. Scheme reproduced from reference.[5]

groups, is to use enzymatic procedures. A fine example of (chemo)enzymatic synthesis of carbohydrates, or more specifically, ganglioside analogues, is shown in Scheme 6.[60] Ganglioside analogues **34** - **36**. were synthesized by our group starting from acetyl protection of lactose by acetic anhydride in pyridine, followed by selective Lewis acid-mediated glycosylation on the lactoside C-1 with 11-azido-undecan-1-ol. Subsequent deacetylation according to the Zemplén procedure[61] resulted in lactoside **33** (Scheme 6, i - iv). Next, the unprotected lactoside was exposed to a cascade of enzymes in which the corresponding transferases added the Neu5Ac, GalNAc, and terminal Gal-units, respectively. With this procedure, our lab acquired the ganglioside analogues that present the oligosaccharides of gangliosides GM3, GM2, and GM1. The azide functionality was required to allow for subsequent immobilizations on soluble platforms and surfaces. These compounds were then subjected to experiments in which they functioned as substrates for pathogen and antibody (Ab) detection.

1.4 Synthetic carbohydrate derivatives in pathogen detection

The focus of the studies that are described in this thesis was mainly directed to the interaction that proteins display with synthesized carbohydrates that are analogues of naturally occurring structures. One reoccurring topic is the interaction of the complementary set of cholera toxin and its natural substrate ganglioside GM1. The adhesion of CTB to GM1os on cell surfaces is the prerequisite for the endocytosis of CTA, and the subsequent pathogenic biological

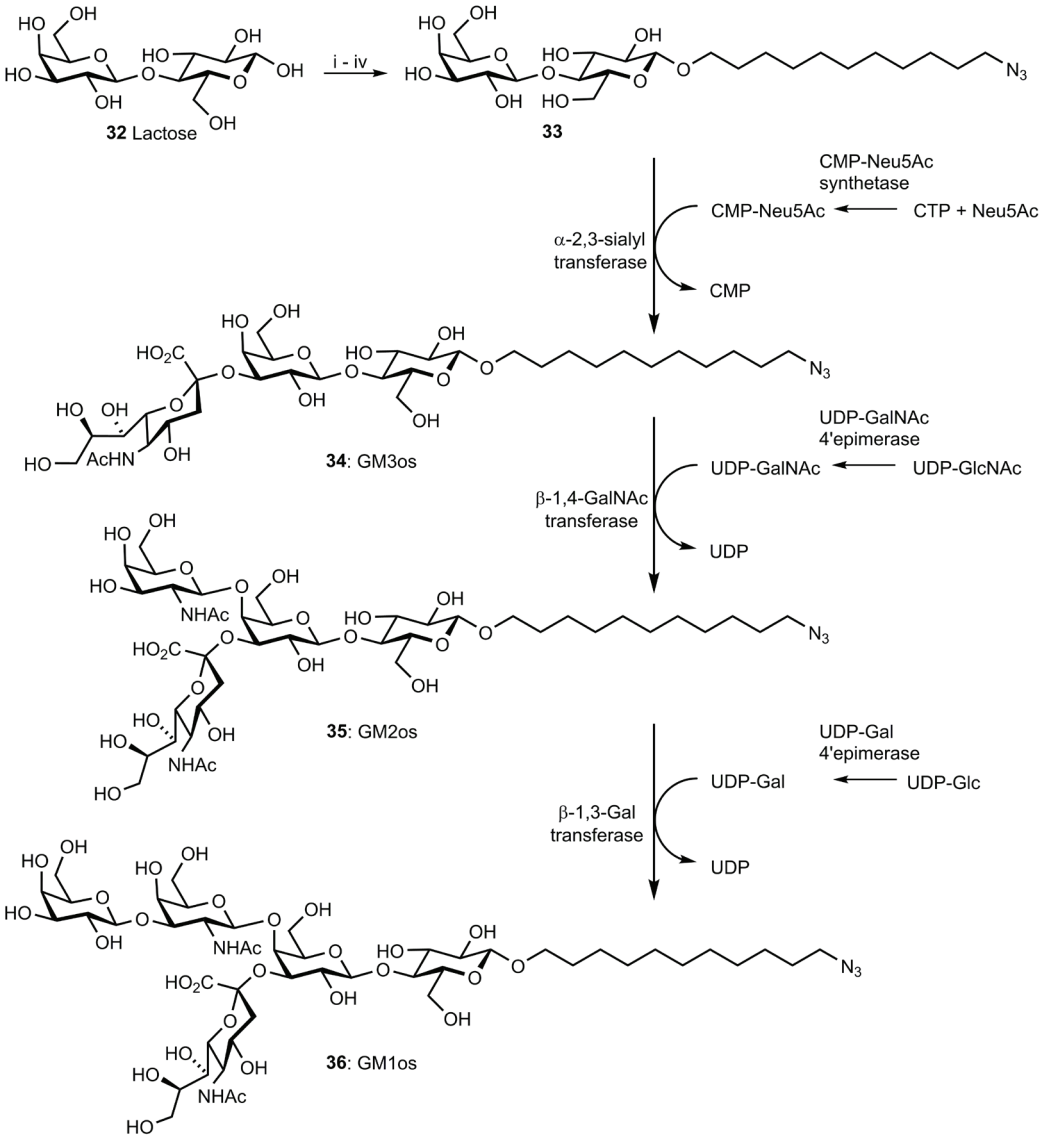

Scheme 6. Chemoenzymatic synthesis procedure for ganglioside oligosaccharides; i) Ac_2O, NaOAc, Δ, 4 h; ii) azido-undecan-1-ol, $SnCl_4$, DCM, rt, overnight; iii) $BF_3{\cdot}Et_2O$ in dry CH_2Cl_2, 0 °C → rt, overnight; iv) NaOMe, MeOH, rt, overnight.[60]

cascade. To stop the pathogenesis in an early stage, several studies have been focused on the synthesis of new multivalent glycosylated ligands,[62] based on the ganglioside GM1 pentasaccharide, which can act as inhibitor by binding to CTB with high affinity. Both natural GM1os-containing derivatives and synthetic

GM1os analogues were used as inhibitor building blocks. In 1997, Thompson and Schengrund described dendritic structures that were functionalized with the GM1os, which lacked the glucose in its pyranose-form (Compound **37**, Figure 7A).[63] With chemiluminiscent enzyme-linked immunosorbent assay (ELISA) experiments (for more information on ELISA see §1.5 of this Chapter), it was shown that IC_{50}-values for the tetra- and octavalent dendrimers are 7 and 3 nM, respectively. The IC_{50} value for the GM1os is reported to be 10 μM.[64]

Two years later, Bernardi *et al*.[65] published a series of GM1-mimics (pseudo-GM1) that present at the same time a good affinity for CTB and a simpler structure compared to the complex natural pentasaccharide of ganglioside GM1. The two-finger appearance of GM1os that in the natural occurring ganglioside is the combination of the terminal Gal and Neu5Ac units – which can be visualized as the index-finger and the thumb, respectively – is maintained in Bernardi's pseudo-GM1 derivatives. The terminal Gal- and the Neu5Ac-units were also identified as the major contributors to the binding of CT.[66] The Neu5Ac-unit, however was substituted by a much simpler structure, which gets around the very labor-intensive synthesis of the GM1 pentasaccharide,[67] or the low-yielding isolation from natural sources, and gives ample possibility for modification. Additionally, it makes these compounds accessible on a multigram scale. These mimics showed good affinity for CT, with dissociation constants (K_d) ranging from 190 to 10 μM, which are noteworthy especially in comparison to simple sugars such as galactose and lactose (K_d = 40 and 81 mM, respectively).[64] Whereas the ganglioside GM1 oligosaccharide is reported to have a K_d of 43 nM.[68] When combining these GM1 mimics with a multivalent presentation, a further enhancement in binding affinity was achieved. This was performed by connecting the pseudo-GM1 to di- or tetra-valent and octavalent dendritic structures,[69] and a calix[4]arene scaffold[70] (Figure 7B). The tetravalent dendrimer showed the best multivalency effect and an 442-fold enhanced binding with respect to a monovalent reference compound. Spectrofluorimetric analyses showed up to 4000-fold enhancement in the complexation efficiency for the multivalent calix[4]arene ligands compared to the monovalent pseudo-GM1.

Together with our group, Pieters reported the synthesis and the biological application of a series of highly effective inhibitors of CTB by using the authentic ganglioside GM1 pentasaccharides linked to a multivalent core (Figure 7C).[71] The potency of these dendritic compounds to be bound by CT was evaluated with ELISA experiments. The combined effect of the high binding efficiency of the single ligand and synergetic the multivalency effect led to inhibitors that showed

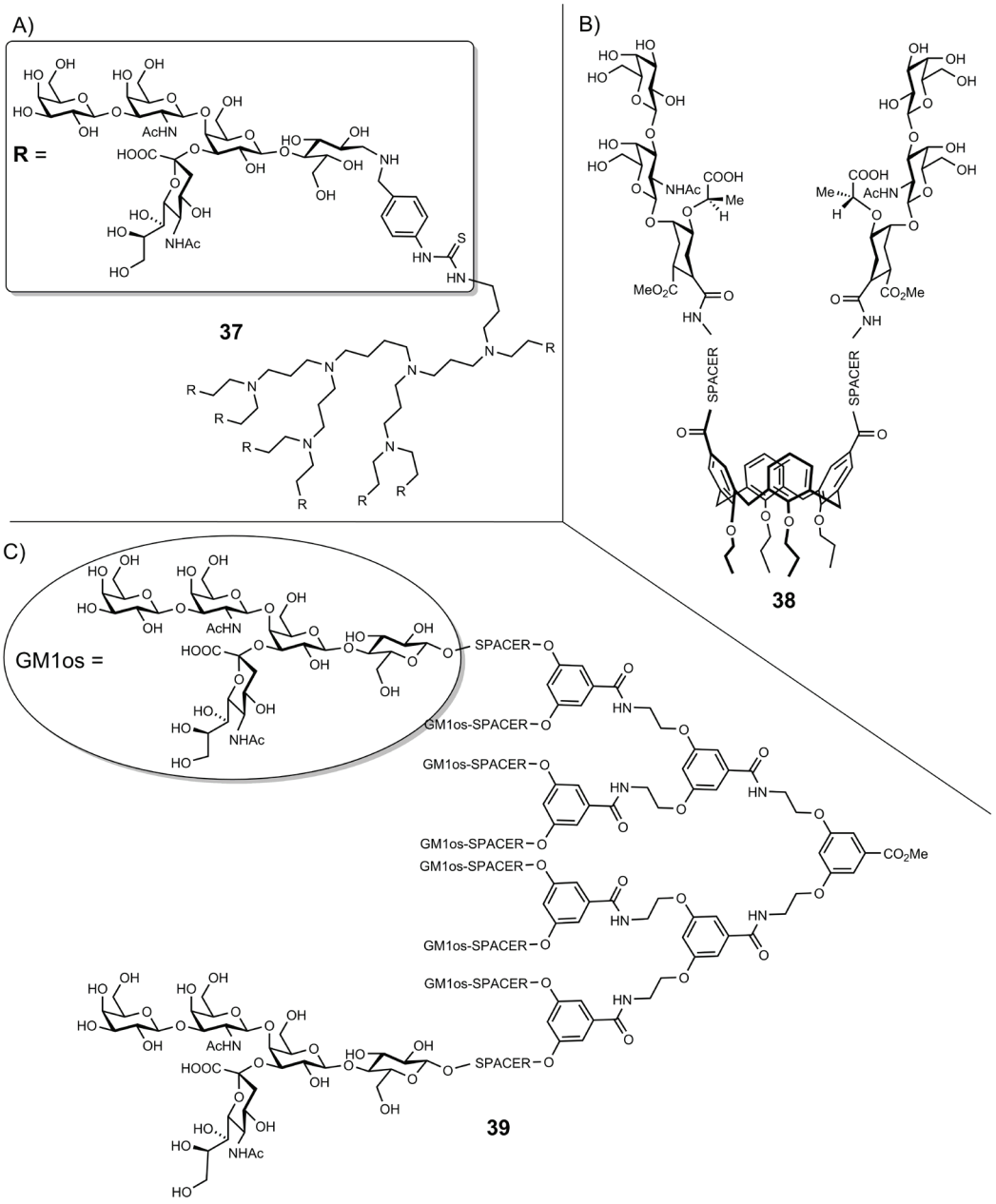

Figure 7. GM1os-based multivalent CTB inhibitors. See text for references.

unprecedented high affinities. While the monovalent derivative, which was used as reference, showed an IC_{50} in the micromolar range (19 μM), the octavalent derivative (**39**) exhibited a record-low IC_{50}-value of only 50 pM. It showed

therefore to be 47,500-fold more potent per GM1os unit, than the monovalent GM1os. The tetravalent variant of compound **39** was later also successfully employed in GBS-related anti-ganglioside antibody binding studies.[72]

1.5 Biological binding assays with synthetic carbohydrates

Biological assays that we performed and discuss in this thesis typically refer to ELISA experiments. This is one way to investigate, on a molecular level, the pathogenesis of a disease by mimicking protein-cell interactions. Other techniques include, surface plasmon resonance (SPR), which is a label-free diagnostic tool based on the variations in the surface resonance of gold-plated chips upon the binding of a protein to antigens on the chip;[73] Western Blot,[74] which is a gel-based electrophoresis technique for the separation of proteins; and isothermal calorimetry (ITC),[75] which measures the enthalpic changes and equilibrium constants relevant for protein-antigen or protein-protein binding. We limit ourselves to ELISA experiments as biological assays, because this is currently still the most widely used technique to measure binding affinity for the specific target proteins that are crucial in our research.

An ELISA is typically performed on a 96 wells microtiter plate.[76] To be measured, compounds can be attached to the plates by hydrophobic interactions, on hydrophobic microtiter plates, or covalently on plates. An adapted version of “indirect ELISA” that was used on several occasions in our research has previously been described (Scheme 7A).[72] The indirect ELISA involves a target substrate (also called an antigen), in our case a carbohydrate, that is coated on the surface of a microtiter plate. For the covalent immobilization of antigens, ester-terminated microtiter plates were coated with propargylamine in the presence of a buffered solution. Azido-terminated carbohydrates could then be attached to the alkyne-terminated microtiter plates via copper-catalyzed azide-alkyne cycloaddtion (CuAAC) reactions. This was followed by a blocking step to prevent aspecific adsorption of biomaterials to unreacted free sites on the surface of the ELISA plates. A typical protein that is used for such purposes is bovine serum albumin (BSA). Blocking allows for a higher signal-to-noise ratio by preventing aspecific adsorption to the surface of solvated elements in the test solution. Then, the protein, for example a toxin or an Ab, is added in solution to the carbohydrate monolayer. A washing step removes all compounds that are not attached and the ganglioside-protein complexes remain on the

surface. The following step requires a secondary antibody that recognizes the first antibody and carries a protein that is able to catalyze coloring reactions. An example of such a protein is horseradish peroxidase (HRP).[77] But, other systems exist that involve fluorescence, chemiluminiscence, and radioactivity. The coloring reaction is started by addition of a substrate that changes color by HRP-mediated oxidation. The optical density (OD) of the coloration is then measured. The OD is a measure for the amount of primary protein present on the plate. By performing binding experiments with various concentrations of the antigen (or the protein) across the plate, it is possible to obtain a binding curve, which is indicative to the protein-ganglioside binding potential.

For a so-called direct ELISA, or "sandwich" ELISA (Scheme 7B), the roles of the antigen (ganglioside) and the protein are inverted. In first instance, the protein is coated on the surface of the microtiter plate via hydrophobic interactions, after which the antigen is added that binds the protein on the surface. A specific primary antibody is then added that "sandwiches" the antigen.

A third type of ELISA experiment is based on competition. As an example, the graphical representation of our competition experiments that are described in Chapter 3 is depicted here (Scheme 7C). It must be noted that technically this type of test is called enzyme-linked lectin assay (ELLA) since it involves interactions between carbohydrates and lectins rather than between carbohydrates and Abs. Nevertheless, the principle is the same. In this case, the native ganglioside GM1 is coated hydrophobically on a microtiter plate. The test antigen (GM1os-calix[5]arene) is allowed to bind with the target protein (CTB) in separate vials. Subsequently, the protein-antigen mixtures are added to the microtiter plate and the natural and synthetic antigens are allowed to compete for inhibition of the protein. After removing the materials that are not bound to the surface, a coloring substrate is added to start the oxidation reaction. Intense coloration indicates the presence of a high amount of CTB on the surface *i.e.* low inhibition of the test antigen, and low coloration less CTB and high inhibition.

1.6 Outline of this thesis

The main focus of this thesis is the rational design and synthesis of carbohydrates that resemble natural gangliosides for the purpose of studying protein-cell interactions *in vitro*. In Chapters 2 and 3, we describe ganglioside analogues that display the GM1os on pentavalent platforms. We test their inhibitory potency

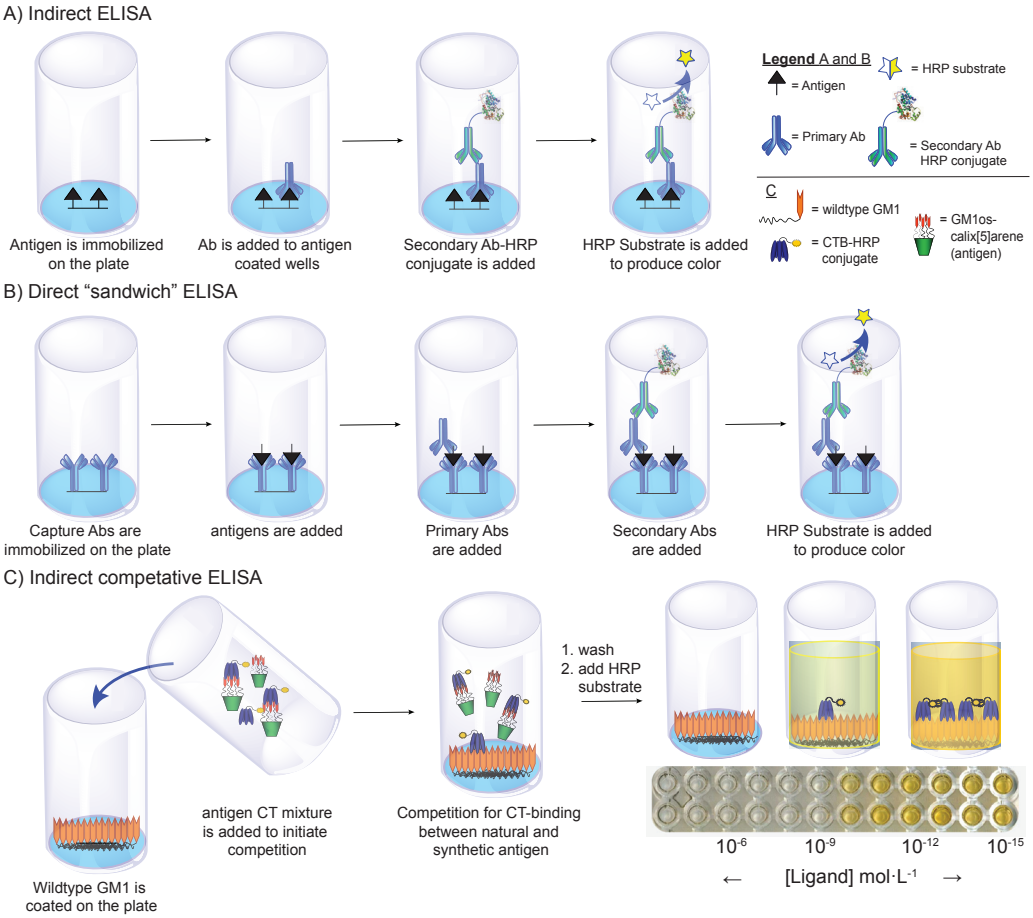

Scheme 7. Graphical representation of A) Indirect ELISA; B) Direct "sandwich" ELISA; C) Competitive ELISA experiment.

towards the "equi-valent" CTB protein. In these studies we employ the highly effective CuAAC reaction. Since copper has, apart from its catalytic function in CuAAC, also detrimental biological effects, copper-free click reactions are of interest. Therefore, Chapter 4 deals with strain-promoted azide-alkyne cycloaddition (SPAAC) reactions. In an investigation on the reactivity of the various SPAAC substrates that are nowadays developed, we employed computational chemistry to find a calculable unit that predicts the reactivity of these compounds. SPAAC continues to be a topic in the study presented in Chapter 5, where it is used in parallel to CuAAC reactions in a direct comparison of their efficiency in immobilizing GM1os on ELISA microtiter plates. In addition, Chapter 5 describes the effect of residual copper from CuAAC on the carbohydrate-CTB binding

affinity. In Chapter 6, we then describe the design and synthesis of a small library of glycan fragments based on the GM1os epitope of GBS-associated antibodies. This library is immobilized on microtiter plates via the CuAAC reaction and then used in subsequent ELISA experiments to detect various GBS-related anti-ganglioside Abs in patient sera. Chapter 7 provides a general discussion and future prospects on the research that is described in this thesis. Chapter 8 concludes with an extensive scientific summary in English and in the Dutch language.

1.7 References

[1] J. Berg, J. Tymoczko, L. Stryer, *Biochemistry 5th Ed.*, W.H. Freeman and Co., New York, **2002**.
[2] S. L. Frey, K. Y. C. Lee, *Biophys. J.* **2013**, *105*, 1421-1431.
[3] E. E. Ebong, F. P. Macaluso, D. C. Spray, J. M. Tarbell, *Arterioscler. Thromb. Vasc. Biol.* **2011**, *31*, 1908-1915.
[4] A. Varki, R. D. Cummings, J. D. Esko, H. H. Freeze, P. Stanley, C. R. Bertozzi, G. W. Hart, M. E. Etzler, *Essentials of Glycobiology 2nd Ed.*, Cold Spring Harbor Laboratory Press, New York, **2009**.
[5] T. K. Lindhorst, in *Essentials of Carbohydrate Chemistry and Biochemistry*, Wiley-VCH Verlag GmbH & Co. KGaA, Weinheim, **2007**, pp. 71-72.
[6] L. A. Galli-Taliadoros, J. D. Sedgwick, S. A. Wood, H. Körner, *J. Immunol. Methods* **1995**, *181*, 1-15.
[7] A. Arnold, I. Sielaff, N. Johnsson, K. Johnsson, S. L. Schreiber, T. M. Kapoor, G. Wess, *Chem. Biol.* **2007**, *1*, 458-479
[8] http://www.unihealth.info/index.php?id=94
[9] RGB colour codes for abstract representation according to the guidelines of the Functional Glycomics Gateway: Neu5Ac (200, 0, 200) Gal and GalNAc (255, 255, 0), Glc (0, 0, 250).
[10] G.-J. Boons, B. A. Cobb, R. D. Cummings, J. A. Hanover, S. Haslam, A. Imberty, J. M. Pierce, R. Raman, C. M. Szymanski, M. Tiemeyer*, Vol. 2014*, May 2012, Functional Glycomics Gateway: http://glycomics.scripps.edu/CFGnomenclature.pdf
[11] E. Klenk, *Z. Physiol. Chem.* **1942**, *273*, 76-86.
[12] a) E. Klenk, K. Lauenstein, *Z. Physiol. Chem.* **1952**, 147-251; b) G. Blix, E. Lindberg, L. Odin, I. Werner, *Nature* **1955**, 340–341.
[13] R. L. Schnaar, R. Gerardy-Schahn, H. Hildebrandt, *Physiol. Rev.* **2014**, *94*, 461–518.
[14] L. Svennerholm, *Nature* **1956**, *177*, 524-525
[15] L. Svennerholm, *Biochem. Biophys. Res. Commun.* **1962**, *9*, 436-.
[16] a) L. Svennerholm, *J. Lipid Res.* **1964**, *5*, 145-155; b) R. Kuhn, H. Wiegandt, *Chem. Ber.* **1963**, *96*, 866-880.
[17] G. Zhang, H. C. Lehmann, S. Manoharan, M. Hashmi, S. Shim, G. L. Ming, R. L. Schnaar, P. H. Lopez, N. Bogdanova, K. A. Sheikh, *J. Neurosci.* **2011**, *31*, 1664–1675.
[18] E. Klenk, F. Rennkamp, *Z. Physiol. Chem.* **1942**, *273*, 253.
[19] E. Klenk, H. Wolter, *Z. Physiol. Chem.* **1952**, *291*, 259.
[20] A. Varki, *Glycobiology* **1993**, *3*, 97-130.
[21] Q. Ma, M. Kobayashi, M. Sugiura, N. Ozaki, K. Nishio, Y. Shiraishi, K. Furukawa, K. Furukawa, Y. Sugiura, *Arch. Histol. Cytol.* **2003**, *66*, 37-44.
[22] K. A. Sheikh, J. Sun, Y. Liu, H. Kawai, T. O. Crawford, R. L. Proia, J. W. Griffin, R. L. Schnaar, *Proc. Natl. Acad. Sci.* **1999**, *96*, 7532-7537.
[23] J. A. Owen, J. Punt, S. A. Stranford, P. P. Jones, *Kuby Immunology 7th Ed.*, W. H. Freeman and Company, New York, **2013**.
[24] R. W. Ledeen, G. Wu, **2006**, *84*, 393-402.

[25] G. Tettamanti, *Glycoconjugate J.* **2004**, *20*, 301-317.
[26] Z. Shriver, S. Raguram, R. Sasisekharan, *Nat. Rev. Drug discov.* **2004**, *3*, 863-873.
[27] L. D. Bergelson, A. G. Bukrinskaya, N. V. Prokazova, G. I. Shaposhnikova, S. L. Kocharov, V. P. Shevchenko, G. V. Kornilaeva, E. V. Fomina-Ageeva, *Eur. J. Biochem.* **1982**, *128*, 467-474.
[28] I. Meisen, T. Dzudzek, C. Ehrhardt, S. Ludwig, M. Mormann, R. Rosenbrück, R. Lümen, B. Kniep, H. Karch, J. Müthing, *Glycobiol.* **2012**, *22*, 1055-1076.
[29] World Health Organisation (WHO), *Weekly epidemiological record* **2011**, *86*, 325-340.
[30] World Health Organisation (WHO), Fact sheet N°107, *Vol. 2012*, **2011**.
[31] E. A. Merritt, S. Sarfaty, F. v. d. Akker, C. l'Hoir, J. A. Martial, W. G. J. Hol, *Protein Sci.* **1994**, *3*, 166-175.
[32] a) N. Sahyoun, P. Cuatrecasas, *Proc. Natl. Acad. Sci. U. S. A.* **1975**, *72*, 3438-3442; b) M. D. Hollenberg, P. H. Fishman, V. Bennett, P. Cuatrecasas, *Proc. Natl. Acad. Sci. U. S. A.* **1974**, *71*, 4224-4228.
[33] J. Moss, M. Vaughan, *Annu. Rev. Biochem.* **1979**, *Vol. 48*, 581-600.
[34] J. Moss, P. H. Fishman, V. C. Manganiello, M. Vaughan, R. O. Brady, *Proc. Natl. Acad. Sci. USA* **1976**, *73*, 1034-1037.
[35] H. M. Berman, J. Westbrook, Z. Feng, G. Gilliland, T. N. Bhat, H. Weissig, I. N. Shindyalov, P. E. Bourne, *Nucl. Acids Res.* **2000**, *28*, 235-242.
[36] T. Ariga, *J. Neurosci. Res.* **2014**, *Early view*, DOI:10.1002/jnr.23411.
[37] a) C. W. Ang, B. C. Jacobs, J. D. Laman, *Trends in Immunology* **2004**, *25*, 61-66; b) N. Yuki, M. Odaka, *Current Opinion in Neurology* **2005**, *18*, 557-561; c) T. Komagamine, N. Yuki, *CNS & Neurological Disorders: Drug Targets* **2006**, *5*, 391-400.
[38] a) G.-J. Boons, A. V. Demchenko, *Chem. Rev.* **2000**, *100*, 4539-4566; b) S. Aubry, A. E. Christina, J. D. C. Codeé, D. Crich, J. C. López, A. V. Demchenko, B. Fraser-Reid, A. M. Gómez, K. S. Kim, G. A. v. d. Marel, H. S. Overkleeft, H. D. Premathilake, R. Roy, K. Sasaki, I. Sharma, T. C. Shiao, D.-H. Suk, M. T. C. Walvoort, C.-H. Wong, C.-Y. Wu, *Reactivity Tuning in Oligosaccharide Assembly*, Springer-Verlag, Berlin, **2011**; c) S. C. Ranade, A. V. Demchenko, *J. Carboh. Chem.* **2013**, *32*, 1-43.
[39] a) G. Grundler, R. R. Schmidt, *Carbohydr. Res.* **1985**, *135*, 203-218; b) R. R. Schmidt, *Angew. Chem., Int. Ed. Engl.* **1986**, *25*, 212–235; c) R. R. Schmidt, M. Behrendt, A. Toepfer, *Synlett* **1990**, 694-696; d) A. T. Carmona, A. J. reno-argas, I. Robina, *Curr. Org. Synth.* **2008**, *5*, 33-60.
[40] a) S. G. Gouin, W. Pilgrim, R. K. Porterb, P. V. Murphy, *Carboh. Res.* **2005**, *340*, 1547–1552; b) M. Polkov, N. Pitt, M. Tosin, P. V. Murphy, *Angew. Chem. Int. Ed.* **2004**, *43*, 2518–2521.
[41] a) S. Hanessian, C. Bacquet, N. Lehong, *Carboh. Res.* **1980**, *80*, C17-C22; b) T. Mukaiyama, T. Nakatsuka, S. Shoda, *Chem. Lett.* **1979**, 487-490.
[42] N. Oka, K. Sato, T. Wada, *Trends in Glycosci. Glyc.* **2012**, *24*, 152-168.
[43] a) D. Kahne, S. Walker, Y. Cheng, D. V. Engen, *J. Am Chem. Soc.* **1989**, *111*, 6881-6882; b) L. Cipolla, L. Lay, F. Nicotra, L. Panza, G. Russo, *Tetrahedron Lett.* **1994**, *35*, 8669-8670.
[44] a) D. R. Mootoo, V. Date, B. Fraser-Reid, *J. Am Chem. Soc.* **1988**, *110*, 2662-2663; b) A. J. Ratcliffe, P. Konradsson, B. Fraser-Reid, *J. Am Chem. Soc.* **1990**, *112*, 5665-5667.
[45] P. Fuegedi, P. J. Garegg, H. Loenn, T. Norberg, *Glycoconjugate J.* **1987**, *4*, 97-108.
[46] a) W. Koenigs, E. Knorr, *Ber. Dtsch. Chem. Ges.* **1901**, *34*, 957–981; b) R. M. v. Well, K. P. R. Kartha, R. A. Field, *J. Carbohydr. Chem.* **2005**, *24*, 463-474.
[47] J. Gervay, T. N. Nguyen, M. J. Hadd, *Carbohydr. Res.* **1997**, *300*, 119-125.
[48] a) J. D. C. Codee, A. Ali, H. S. Overkleeft, G. A. van der Marel, *C. R. Chim.* **2011**, *14*, 178-193; b) J. Guo, X.-S. Ye, *Molecules* **2010**, *15*, 7235-7265.
[49] J. Clayden, N. Greeves, S. Warren, in *Organic Chemistry 2nd Ed.* **2011**, Oxford University Press Inc., New York, **2012**, pp. 344-345.
[50] C.-S. Chao, C.-Y. Lin, S. Mulani, W.-C. Hung, K.-K. T. Mong, *Chem. Eur. J.* **2011**, *17*, 12193-12202.
[51] a) G. Wulff, W. Schmidt, *Carboh. Res.* **1977**, *53*, 33-46; b) V. Magnus, D. Vikić-Topić, S. Iskrić, S. Kveder, *Carboh. Res.* **1983**, *114*, 209-224; c) W. Seebacher, E. Haslinger, R. Weis, *Monatsh. Chem.* **2001**, *132*, 839-847.
[52] H. Weber, H. G. Khorana, *J. Mol. Biol.* **1972**, *72*, 219-249.

[53] A. V. Pukin, H. Zuilhof, *Synlett* **2009**, *20*, 3267-3270.
[54] M. J. Robins, S. D. Hawrelak, T. Kanai, J.-M. Siefert, R. Mengel, *J. Org. Chem.* **1979**, *44*, 1317-1322.
[55] a) B. E. Legetter, R. K. Brown, *Can. J. Chem.* **1964**, *42*, 990–1004; b) A. Lipták, I. Jodál, P. Nánási, *Carbohydr. Res.* **1975**, *44*, 1-11.
[56] P. J. Garegg, H. Hultberg, *Carboh. Res.* **1981**, *93*, C10-C11.
[57] M. Ohlin, R. Johnsson, U. Ellervik, *Carbohydr. Res.* **2011**, *346*, 1358-1370.
[58] R. Johansson, B. Samuelsson, *J. Chem. Soc., Perkin Trans. 1* **1984**, 2371-2374.
[59] a) Y. Oikawa, T. Yoshioka, O. Yonemitsu, *Tetrahedron Lett.* **1982**, *23*, 889-892; b) Z. Zhang, G. Magnusson, *J. Org. Chem.* **1996**, *61*, 2394-2400.
[60] A. V. Pukin, C. A. G. M. Weijers, B. v. Lagen, R. Wechselberger, B. Sun, M. Gilbert, M.-F. Karwaski, D. E. A. Florack, B. C. Jacobs, A. P. Tio-Gillen, A. v. Belkum, H. P. Endtz, G. M. Visser, H. Zuilhof, *Carboh. Res.* **2008**, *343*, 636-650.
[61] G. Zemplén, E. Pascu, *Ber. Dtsch. Chem. Ges.* **1929**, *62*, 1613.
[62] A. Bernardi, J. Jiménez-Barbero, A. Casnati, C. D. Castro, T. Darbre, F. Fieschi, J. Finne, H. Funken, K.-E. Jaeger, M. Lahmann, T. K. Lindhorst, M. Marradi, P. Messner, A. Molinaro, P. Murphy, C. Nativi, S. Oscarson, S. Penadés, F. Peri, R. J. Pieters, O. Renaudet, J.-L. Reymond, B. Richichi, J. Rojo, F. Sansone, C. Schäffer, W. B. Turnbull, T. Velasco-Torrijos, S. Vidal, S. Vincent, T. Wennekes, H. Zuilhof, A. Imberty, *Chem. Soc. Rev.* **2013**, *42*, 4709-4727.
[63] a) J. P. Thompson, C. L. Schengrund, *FASEB J.* **1996**, *10*; b) J. P. Thompson, C. L. Schengrund, *Glycoconjugate J.* **1997**, *14*, 837-845; c) J. P. Thompson, C. L. Schengrund, *Biochem. Pharmacol.* **1998**, *56*, 591-597.
[64] D. Arosio, S. Baretti, S. Cattaldo, D. Potenza, A. Bernardi, *Bioorg. Med. Chem. Lett.* **2003**, *13*, 3831-3834.
[65] a) A. Bernardi, L. Carrettoni, A. Grosso Ciponte, D. Monti, S. Sonnino, *Bioorg. Med. Chem. Lett.* **2000**, *10*, 2197-2200; b) A. Bernardi, A. Checchia, P. Brocca, S. Sonnino, F. Zuccotto, *J. Am. Chem. Soc.* **1999**, *121*, 2032-2036.
[66] W. E. Minke, C. Roach, W. G. J. Hol, C. L. M. J. Verlinde, *Biochemistry* **1999**, *38*, 5684-5692.
[67] H.-Y. Liao, C.-H. Hsu, S.-C. Wang, C.-H. Liang, H.-Y. Yen, C.-Y. Su, C.-H. Chen, J.-T. Jan, C.-T. Ren, C.-H. Chen, T.-J. R. Cheng, C.-Y. Wu, C.-H. Wong, *J. Am. Chem. Soc.* **2010**, *132*, 14849-14856.
[68] W. B. Turnbull, B. L. Precious, S. W. Homans, *J. Am. Chem. Soc.* **2004**, *126*, 1047-1054.
[69] D. Arosio, I. Vrasidas, P. Valentini, R. M. J. Liskamp, R. J. Pieters, A. Bernardi, *Org. Biomol. Chem.* **2004**, *2*, 2113-2124.
[70] D. Arosio, M. Fontanella, L. Baldini, L. Mauri, A. Bernardi, A. Casnati, F. Sansone, R. Ungaro, *J. Am. Chem. Soc.* **2005**, *127*, 3660-3661.
[71] A. V. Pukin, H. M. Branderhorst, C. Sisu, C. A. G. M. Weijers, M. Gilbert, R. M. J. Liskamp, G. M. Visser, H. Zuilhof, R. J. Pieters, *ChemBioChem* **2007**, *8*, 1500-1503.
[72] A. V. Pukin, B. C. Jacobs, A. P. Tio-Gillen, M. Gilbert, H. P. Endtz, A. van Belkum, G. M. Visser, H. Zuilhof, *Glycobiology* **2011**, *21*, 1642-1650.
[73] R. Bakhtiar, *J. Chem. Educ.* **2013**, *90*, 203-209.
[74] T. Mahmood, P.-C. Yang, *N. Am. J. Med. Sci.* **2012**, *4*, 429-434.
[75] M. M. Pierce, C. S. Raman, B. T. Nall, *Methods* **1999**, *19*, 213-221.
[76] S. D. Gan, K. R. Patel, *J. Invest. Dermatol.* **2013**, *133*, e12-e14.
[77] T. M. Hamilton, A. A. Dobie-Galuska, S. M. Wietstock, *J. Chem. Educ.* **1999**, *76*, 642-644.

2

Nanomolar cholera toxin inhibitors based on symmetrical pentavalent ganglioside GM1os-*sym*-corannulenes

This chapter is published as:

Martin Mattarella,‡ Jaime Garcia-Hartjes,‡ Tom Wennekes, Han Zuilhof, Jay S. Siegel, *Org. Biomol. Chem.* **2013**, *11*, 4333-4339, DOI: 10.1039/c3ob40438b

‡Both authors contributed equally to this work.

Abstract:

Eight symmetric and pentavalent corannulene derivatives were functionalized with galactose and the ganglioside GM1-oligosaccharide via copper-catalyzed alkyne-azide cycloaddition reactions. The compounds were evaluated for their ability to inhibit the binding of the pentavalent cholera toxin to its natural ligand, ganglioside GM1. In this assay, all ganglioside GM1os-*sym*-corannulenes proved highly potent nanomolar inhibitors of cholera toxin.

2.1 Introduction

The World Health Organization (WHO) estimates that annually 3-5 million people worldwide are infected with cholera, resulting in over a hundred thousand fatalities.[1] The responsible pathogen, the *Vibrio cholerae* bacterium, produces the cholera toxin (CT) protein that is responsible for the severe clinical symptoms. CT belongs to the protein family of AB_5 bacterial toxins.[2] The structure and activity of CT and other AB_5 toxins have been investigated in detail.[3] These proteins consist of two distinct domains with different roles. The A-subunit is an enzyme that – when delivered inside a host cell – is toxic and responsible for the subsequent disease symptoms. The cholera toxin B-subunit (CTB) is a lectin and plays a crucial role in the recognition and interaction with its natural ligand, ganglioside GM1 (Figure 1a) on the periphery of intestinal cells. The crystal structure of CT[4] shows that the protein complex consists of five identical monomeric CTB subunits, arranged

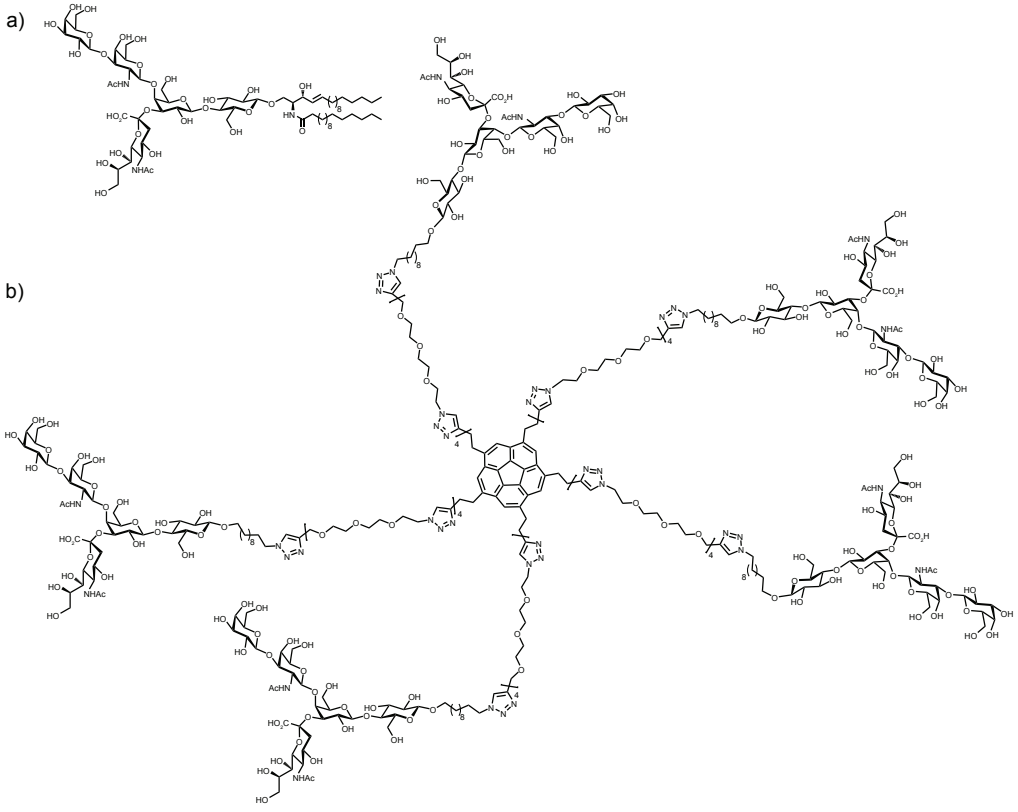

Figure 1. a) Structure of CTB's natural ligand, ganglioside GM1; b) Structure of the pentavalent GM1os-functionalized *sym*-corannulene, a nanomolar inhibitor of cholera toxin.

in a pentagonal symmetry, and each of these subunits can bind the ganglioside GM1 in a one-to-one stoichiometry. Detailed colorimetric studies revealed that CT exhibits allosteric cooperativity,[5] which contributes to increasingly higher binding affinities to CT when more ligands are bound.[6]

One of the possible approaches for the design of CT inhibitors aims to prevent the receptor-recognition process.[7] Two major routes can be discerned in the literature to achieve this goal. The first strategy, monovalent receptor-binding approach, focuses on strong binding interactions, and it is based on the design and synthesis of ligands that closely mimic the natural ligand on the cell surface[8] in order to obtain a strong interaction with the CTB receptor. The second approach, multivalent receptor-binding,[9] exploiting chelate cooperativity, takes advantage of the pentavalent character of the ligand-binding sites of CT. This approach is based on the synthesis of a functionalized branched system, in which each branch carries a single-site inhibitor, like galactose[10,11] or lactose,[12] leading to a compound that has an overall stronger interaction with the toxin than the sum of the independent inhibitors. The synthesis of dendritic multivalent inhibitors, functionalized with the GM1os, has been reported,[13] these displayed unprecedented high inhibitory potencies for CTB, in picomolar range.

An important improvement in the design of multivalent binders was achieved with symmetrical pentameric molecules based on the concept of “finger-linker-core” systems:[12] the pentavalent “core” is connected by flexible “linkers” to “fingers” that include the monovalent receptor-binding ligand. Pentavalent CT inhibitors were synthesized using various “cores”: acylated pentacyclen,[12a] large cyclic peptide[12e] and calix[5]arene.[14]

This Chapter details a study that combines the two strategies to obtain an optimal binding by the design and synthesis of pentavalent GM1os-presenting compounds based on a 5-fold symmetrical *sym*-substituted[15] corannulene scaffold (Figure 1b). Binding assays allowed the determination of the interaction with CTB (the protein complex without the toxic A part) for these and analogous pentavalent galactose corannulenes. This revealed a high inhibitory potency towards CTB by this new class of inhibitors.

2.2 Results and Discussion

Apart from its obvious 5-fold symmetry, the corannulene scaffold is a good candidate to function as the “core” of pentavalent receptor-binding inhibitors for

AB_5 toxins on the basis of the following observations: the recent development of a kilogram-scale synthesis of corannulene (**1**),[16] its further functionalization to *sym*-pentachloro-corannulene (**2**),[17] and the growing number of robust and flexible procedures for the preparation of molecular pentapods displaying functional groups and bioconjugated moieties, by iron-catalyzed[18] cross-coupling and

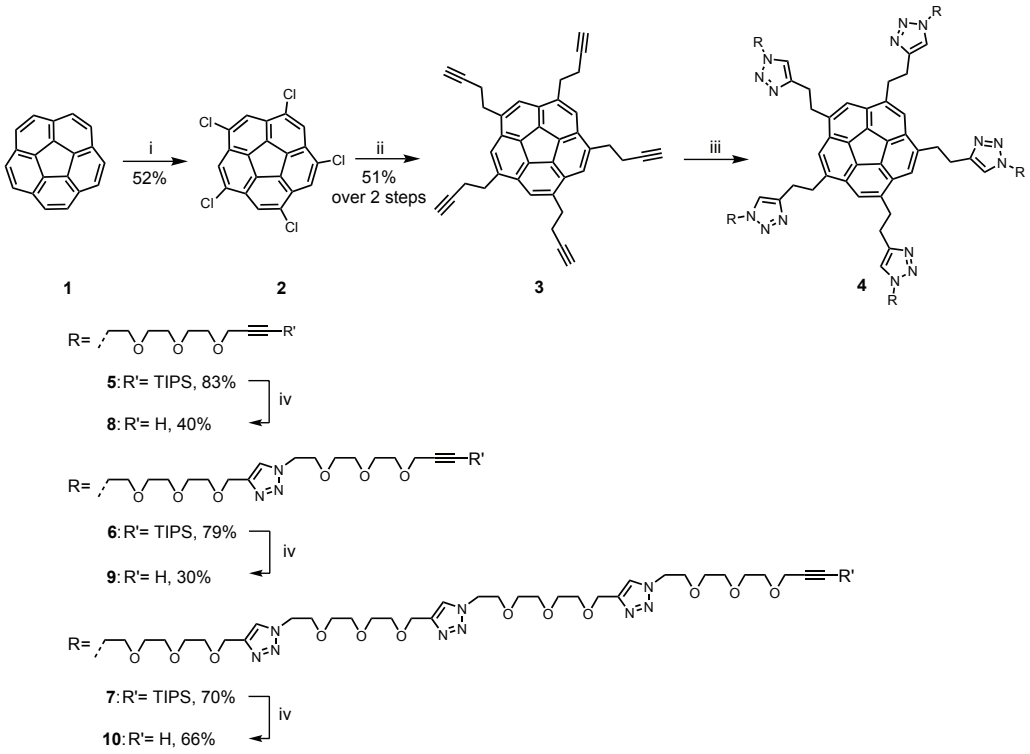

Scheme 1. Synthesis route of the corannulene core and ethylene glycol spacers; i) ICl, DCM, rt, 72 h; ii) (1) $Fe(acac)_3$, 1-bromo-4-trimethylsilyl-3-butyne, THF-NMP, rt, 2.5 h; (2) NaOH, MeOH-H_2O, rt, 24 h; iii) Cu nanoparticles, DMF, microwave, 60 °C, 2 h; iv) TBAF, THF, rt, 2 h.

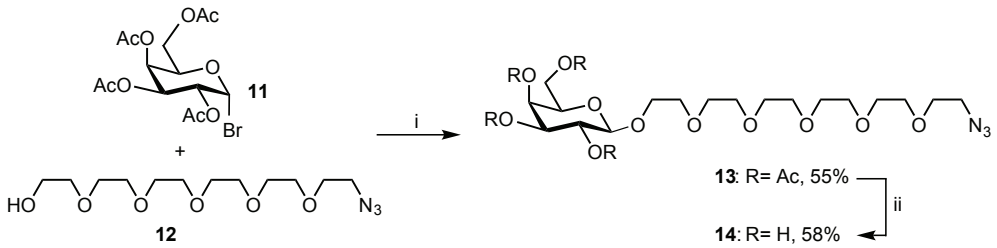

Scheme 2 Synthesis of azido-linked galactoside **14**. i) $HgBr_2$, DCM, rt, 3 d; ii) (1) MeONa, MeOH, rt, 48 h; (2) DOWEX-H^+.

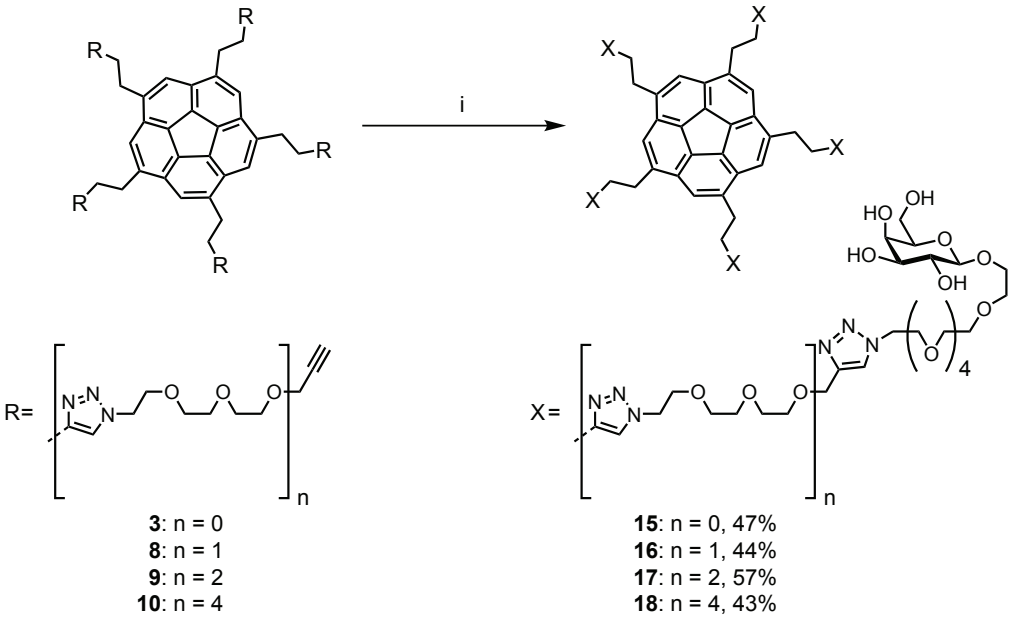

3: n = 0
8: n = 1
9: n = 2
10: n = 4

15: n = 0, 47%
16: n = 1, 44%
17: n = 2, 57%
18: n = 4, 43%

Scheme 3. Microwave-assisted CuAAC-based synthesis of penta-galactose corannulenes; i) **14**, Cu nanoparticles, DMF, microwave, 80 °C, 2 h.

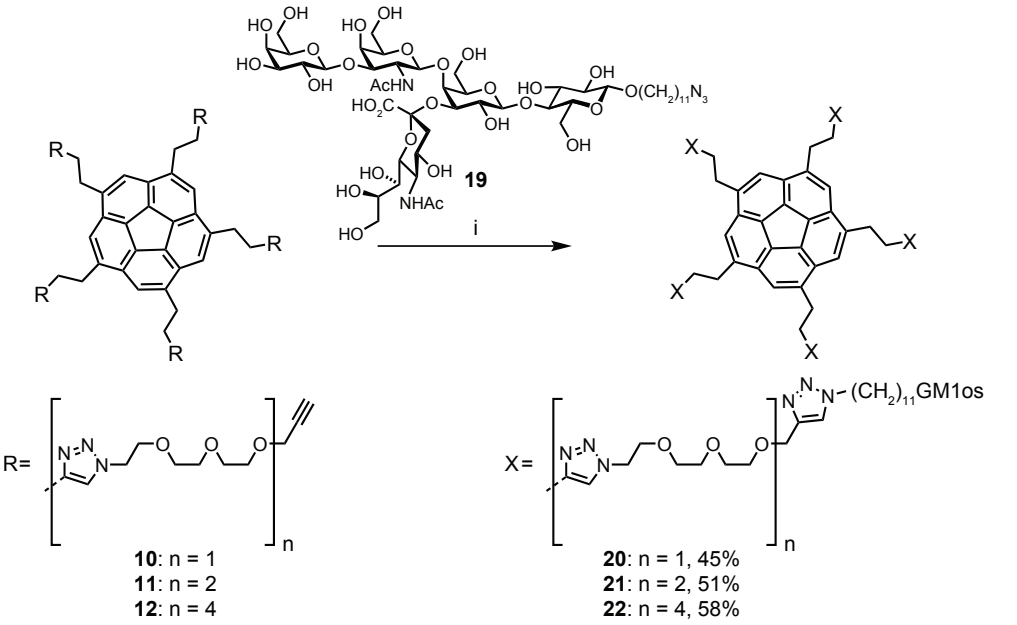

10: n = 1
11: n = 2
12: n = 4

20: n = 1, 45%
21: n = 2, 51%
22: n = 4, 58%

Scheme 4. Synthesis of the GM1os-functionalized PEG-corannulenes; i) Cu nanoparticles, H_2O, microwave, 80 °C, 2 h.

copper-catalyzed azide-alkyne cycloaddition (CuAAC) reaction.

The synthetic pathway towards PEG-corannulene systems starts from the conjugation of the terminal acetylene **3**[18] by an efficient copper nanoparticle-catalyzed CuAAC reaction with *n*-mers of α-azidoethyl-ω-propargyl diglyme (n = 1, 2, 4) (Figure S1 Appendix II).[19] This route gave satisfactory results for the preparation of other *sym*-bioconjugated corannulenes, and was used here to prepare the five-fold symmetric compounds **5**, **6** and **7** in good yield and purity. The PEG arms function as linkers of different lengths and improve water solubility and flexibility of the inhibitor. The terminal TIPS-protected acetylenes were deprotected by reaction with TBAF[19] yielding the alkyne-terminated PEG-corannulenes **8**, **9** and **10** (Scheme 1). After preparing the three PEG-corannulenes the focus shifted to attaching the (oligo)saccharides. In this work, two different CTB binders were used: galactose, an easily obtainable but quite poor binder of CTB, and the oligosaccharide of ganglioside GM1 (GM1os), the natural ligand of CTB. In order to introduce the galactose-based "finger" to the terminal acetylenes **3**, **8**, **9** and **10**, galactoside **11** was functionalized at the anomeric position with a short PEG chain that bears an azido group (compound **12**, Scheme 2). An analogous compound without ethylene oxide moieties belonging to this inhibitor family was previously synthesized[18] by CuAAC reaction on the terminal acetylene **3** and 2-azidoethyl-*β*-D-galactopyranoside.[20,21] The synthetic pathway for the synthesis of azido-PEG-galactoside **14** starts with a Koenigs-Knorr-type glycosylation of azido-PEG hydroxide 12[22,23] with peracetylated galactosyl bromide **11** to afford *β*-galactoside **13**. The deprotected compound **14** was then obtained by treatment of **13** with sodium methoxide. The pentavalent Gal-functionalized *sym*-corannulene inhibitor was prepared in good yield by employing the microwave-assisted CuAAC reaction on the terminal acetylenes **3**, **8**, **9** and **10** with the azido galactose derivative **14** affording the four galactose-based CTB inhibitors **15** - **18** (Scheme 3).

The second family of pentavalent inhibitors displays five GM1os moieties (Scheme 4). The chemo-enzymatic synthesis from lactose of the azide-terminated GM1os oligosaccharide was previously reported.[24] The pentavalent GM1os inhibitors **20**, **21** and **22** were synthesized, in the presence of copper nanoparticles, by microwave-assisted CuAAC reaction of azido-pentasaccharide **19** with the terminal acetylenes **8**, **9** and **10**. Because of the low solubility of the GM1 analog in DMF, the reactions were performed in water, allowing a complete dissolution of **19** in the reaction media. The inhibitory efficiency of the synthesized five-fold symmetric pentavalent CT ligands (**15** - **18** and **20** - **22**) was evaluated

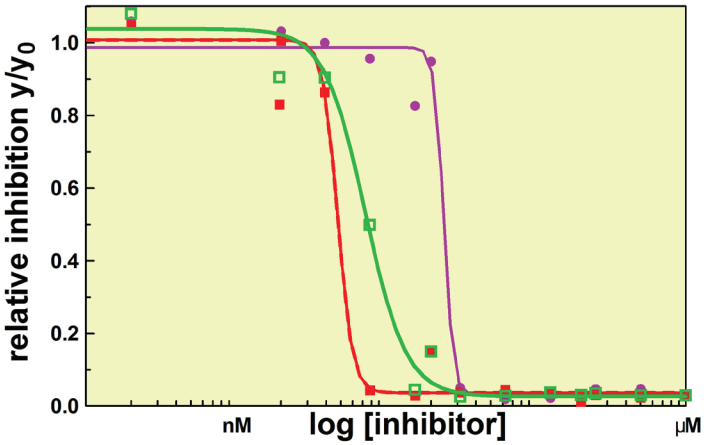

Figure 2. Fitted inhibition curves of compounds ● GM1os-PEG3 corannulene **20**, ■ GM1os-PEG6 corannulene **21**, and ◘ GM1os-PEG12 corannulene **22**.

by an enzyme-linked lectin assay experiment (ELLA) on 96-well plates.[25,26] Solubility issues at concentrations > 1 mM limited the experiments intended to find an IC_{50}-value for galactose-based compounds **15** - **18**. When compared to previously reported IC_{50}-values for multivalent ligands functionalized with galactose,[10,11] these concentrations should not have been limiting. One hypothesis to account for this observation is that the supramolecular aggregation competes against binding to the pentad-complex.

Further investigations by ^{1}H NMR, UV-Vis and fluorescence spectroscopy on the properties of C_5-symmetric galactose conjugated corannulene in aqueous solution suggest the formation of supramolecular aggregates of this amphiphilic molecule in water. If the formation of the supramolecular assemblies is thermodynamically and kinetically favored over the interaction with the CTB, the competition of these two processes might be a plausible explanation for the unexpected results obtained from the ELLA experiment; however, the GM1os-PEG-corannulenes showed high, nanomolar inhibitory potencies (Figure 2; Table 1).

The pentavalent GM1os-functionalized inhibitors, **20**, **21**, and **22**, bind CTB at lower IC_{50} values than monomeric GM1os (cf. Table 1). The lowest IC_{50} value measured is for **21** (Table 1, entry 2) with an inhibition potency that is nearly 4000 times stronger than that of monomeric GM1os.[12f] The lower binding affinity for CTB by compounds **20** and **22** (Table 1, entries 1 and 3) is most probably due to the effects related to the linker length: if the linker is not long enough (compound 20), not all of the five ligands can simultaneously bind the five binding sites of

CTB. In the opposite case (*i.e.* compound **22**), binding would lead to a substantial ordering in the chain, making it entropically less favorable, while enthalpically the necessary folding of the longer linkers to enable binding of CTB by the GM1os fingers might create sufficient steric hindrance to cause an increased IC_{50} value. A further complicating factor is the possibility that galactose and GM1os derivatives undergo supramolecular self-aggregation that competes with binding to CTB and results in apparent higher inhibitory concentrations.

Caveats notwithstanding, compound **21** is as of yet one of the strongest multivalent CT inhibitors,[22,27] and displays the power of combining the natural valency with the natural ganglioside to reach optimal blocking of multivalent lectins. Design efforts to create systems that optimize spacer geometry and avoid self complexation will likely lead to new derivatives with inhibitory concentrations more favorably comparable to other previously reported GM1os-based inhibitors.

Table 1. Inhibitory potency of pentavalent GM1os-functionalized ligands towards CTB

Entry	Compound	IC_{50} (nM)	RIP[a]
1	**20**	25 ± 4	770
2	**21**	5 ± 2	3700
3	**22**	7.3 ± 0.9	2600

[a]RIP = Relative inhibition potency calculated as the ratio between the IC_{50} value of the inhibitor and the IC_{50} value of GM1os.[12f]

2.3 Conclusions

This manuscript reports a powerful method for the synthesis of a new class of cholera toxin inhibitors with a design based on a pentavalent *sym*-substituted corannulene as the core unit and equipped with the galactose and the GM1os as CTB binders. Microwave-assisted CuAAC reactions, catalyzed by copper nanoparticles, were employed for the conjugation of the monovalent CTB ligands (galactose and GM1os) to the corannulene core via azide-presenting PEG-linkers of various lengths. The potent CTB inhibition of 25, 5.0, and 7.3 nM observed for the penta-GM1os corannulenes, **20**, **21**, and **22**, respectively, prove that multivalent systems functionalized with strong CTB binders represents a solid strategic approach for the synthesis CT inhibitors with high potency in comparison with previously reported monovalent inhibitors.

The developed method allows for the use of *sym*-substituted corannulenes

as a possible core unit for the development of new multivalent binders of cholera toxin or other possible biological targets that rely on multivalent binding of their target ligand.

2.4 Representative experimental procedures

Compound 6. A mixture of **3** (9.4 mg, 18 µmol), the proper azide-functionalized PEG (83.0 mg, 0.14 mmol) and copper nanoparticles (11.7 mg, 0.18 mmol) in DMF (1.0 mL) was loaded in a microwave vessel and was heated at 80 °C in a microwave reactor for 2 h. The reaction mixture was filtrated over Celite® and the solvent evaporated. The crude mixture was purified by column chromatography on silica gel (DCM/ MeOH 94 : 6 → 9 : 1) to yield a reddish oil (49 mg, 79%); **^{1}H NMR** (500 MHz, $CDCl_3$): δ = 7.69 (s, 5H), 7.64 (s, 5H), 7.53 (s, 5H), 4.62 (s, 10H), 4.48 (q, 20H, *J* = 5.5 Hz), 4.21 (s, 10H), 3.82 (t, 20H, *J* = 5.0 Hz), 3.69 - 3.47 (m, 90H), 3.26 (t, 10H, *J* = 8.0 Hz), 1.04 (s, 105H); **^{13}C NMR** (125 MHz, $CDCl_3$): δ = 147.1, 144.8, 140.4, 134.9, 129.7, 123.9, 123.1, 122.5, 103.2, 87.8, 70.6, 70.5 70.5, 70.5, 69.7, 69.6, 69.5, 68.7, 64.6, 59.3, 50.3, 50.3, 33.4, 28.5, 18.7, 11.2; **MS** (HR-ESI+) m/z = 1163.6590 $[M+3Na]^{3+}$, calcd. ($C_{175}H_{280}N_{30}Na_3O_{30}Si_5^{3+}$) 1163.6609.

Compound 9. A solution of TBAF in THF (1M, 1.0 mL, 1.0 mmol) was added to a solution of **6** (103 mg, 30.1 µmol) in THF (1.0 mL) and the reaction mixture was stirred at rt for 2 h. The solution was then diluted with a saturated aqueous solution of NH_4Cl and extracted with ethyl acetate. The collected organic phases were dried over Na_sSO_4 and evaporated to yield the crude product. The crude was then heated at 75 °C under high vacuum for 18 h. The product was then purified by column chromatography on silica gel (DCM/ MeOH 9:1) to yield a reddish oil (24 mg, 30%). **^{1}H NMR** (500 MHz, $CDCl_3$): δ = 7.70 (s, 5H), 7.64 (s, 5H), 7.53 (s, 5H), 4.62 (s, 10H), 4.50 - 4.46 (m, 20 H), 4.16 (d, *J* = 2.5 Hz, 10H), 3.82 (t, 20H, *J* = 5.0 Hz), 3.64 - 3.51 (m, 90H), 3.23 (t, 10H, *J* = 8.0 Hz), 2.44 (d, 5H, *J* = 2.5 Hz); **^{13}C NMR** (125 MHz, $CDCl_3$): δ = 147.1, 144.8, 140.5, 134.9, 129.8, 124.0, 123.1, 122.5, 79.7, 74.9, 70.6, 70.6, 70.5, 69.7, 69.5, 69.1, 64.7, 58.5, 50.3, 50.2, 33.4, 28.5; **MS** (HR-ESI+) m/z = 529.2767 $[M+5H]^{5+}$, calcd. ($C_{130}H_{185}N_{30}O_{30}^{5+}$) = 529.2769.

Compound 17. A mixture of **9** (8.5 mg, 3.2 µmol), **14** (11.3 mg, 24.1 µmol) and copper nanoparticles (1.5 mg, 23.6 µmol) in DMF (300 µL) was loaded into a microwave vessel was heated at 80 °C in a microwave reactor for 2 h. The mixture was filtered over Celite® and the solid was washed with water.

The crude was lyophilized and purified by size exclusion chromatography (Sephadex® G-25, water) to yield a reddish solid (9.1 mg, 57%); **^{1}H NMR** (500 MHz, D_2O/ MeOD): δ = 8.01 (s, 5H), 7.88 (s, 5H), 7.68 (s, 5H), 7.60 (s, 5H), 4.58 - 4.39 (m, 50H), 4.08 - 4.06 (m, 5H), 3.98 - 3.12 (m, 255H); **^{13}C NMR** (125 MHz, D_2O/ MeOD): δ = 147.9, 144.8, 141.3, 134.8, 130.4, 126.3, 126.1, 124.8 124.2, 103.9, 76.1, 73.7, 71.7, 70.7, 70.6, 70.5, 70.4, 70.4, 70.4, 70.3, 70.2, 69.9, 69.8, 69.7, 69.7, 69.6, 69.5, 64.0, 61.9, 50.9, 50.8, 49.5, 34.0, 28.1; **MS** (HR-ESI+) m/z = 854.2378 $[M+6Na]^{6+}$, calcd. ($C_{220}H_{355}N_{45}Na_6O_{85}^{6+}$) = 854.2366.

Compound 21. A mixture of **9** (2.88 mg, 1.09 μmol), **19** (11.1 mg, 9.3 μmol) and copper nanoparticles (0.76 mg, 12.0 μmol) in water (300 μL) was loaded into a microwave vessel was heated at 80 °C in a microwave reactor for 2 h. The mixture was filtered over Celite® and the solid was washed with water. The crude was lyophilized and purified by size exclusion chromatography (Sephadex® G-25, water) to yield a colorless solid (4.8 mg, 51%); **^{1}H NMR** (500 MHz, D_2O/ MeOD): δ = 7.96 - 7.75 (m, 20H), 4.57 - 4.54 (m, 70H), 4.18 - 4.05 (m, 45H), 3.94 - 3.34 (m, 286H), 2.70 (d, 5H, *J* = 10.0 Hz), 2.06 (d, 35H, *J* = 15.0 Hz), 1.98 - 1.94 (t, 5H, *J* = 10.0 Hz), 1.62 - 1.45 (m br, 25H), 1.28 - 1.25 (m br, 20H), 1.11 - 0.90 (m br, 75H); **^{13}C NMR** (125 MHz, D_2O/ MeOD): δ = 176.0, 175.1, 105.7, 103.6, 103.5, 103.2, 102.7, 75.8, 75.3, 73.5, 71.7, 70.7, 70.6, 70.6, 70.5, 70.5, 70.5, 70.5, 70.4, 69.6, 69.6, 61,9, 52.6, 52.1, 51.1, 51.1, 29.7, 26.6, 26.2, 23.6, 23.0; **MS** (HR-ESI-) m/z = 1721.1778 $[M-5H]^{5-}$; calc ($C_{370}H_{590}N_{55}O_{175}^{5-}$) = 1720.7797.

ELLA assays. Each well of a 96-well microtiter plate was coated with a 100 μL native GM1 solution (1.3 μM in ethanol) after which the solvent was evaporated. Unattached GM1 was removed by washing with PBS (3 × 450 μL), the remaining free binding sites were blocked by incubation with 100 μL of a 1% (w/v) BSA solution in PBS for 30 min at 37 °C. Subsequently, the wells were washed with PBS (3 × 450 μL). In separate vials, a logarithmic serial dilution, starting from 2.0 mM, of 150 μL saccharide-corannulenes in 0.1% BSA, 0.05% Tween-20 in PBS, mixed with 150 μL of a 50 ng/mL CTB-HRP solution in the same buffer were incubated. This gave an initial inhibitor concentration of 1.0 mM. In the case of potent inhibitors, based on the logarithmic experiments, a more accurate, serial dilution of a factor two was performed around the expected IC_{50} values. The inhibitor-toxin mixtures were incubated at room temperature for 2 h and then transferred to the coated wells. After 30 min of incubation at room temperature, unbound CTB-HRP-corannulene complexes were removed from the wells by

washing with 0.1% BSA, 0.05% Tween-20 in PBS (3 x 500 µL). 100 µL of a freshly prepared OPD solution (25 mg OPD·2HCl, 7.5 mL 0.1M citric acid, 7.5 mL 0.1M sodium citrate and 6 µL of a 30% H_2O_2 solution, pH was adjusted to 6.0 with NaOH) was added to each well and allowed to react with HRP in absence of light, at room temperature, for 15 min. The oxidation reaction was quenched by addition of 50 µL 1M H_2SO_4. Within 5 min, the adsorbance was measured at 490 nm.

2.5 References

[1] World Health Organization, W.H.O. **2011**, Fact sheet Nº107, Vol. 2012.

[2] a) B. D. Spangler, *Microbiol. Rev.,* 1992, **56**, 622. b) E. A. Merritt, W. G. J. Hol, *Struct. Biol.,* **1995**, *5*, 165.

[3] For review, see: E. Fan, C. J. O'Neal, D. D. Mitchell, M. A. Robien, Z. Zhang, J. C. Pickens, X. J. Tan, K. Korotkov, C. Roach, B. Krumm, C. L. M. J. Verlinde, E. A. Merritt, W. G. J. Hol, *Int. J. Med. Microbiol.,* **2004**, *294*, 217.

[4] I. Lonnroth, J. Holmgren, *J. Gen. Microbiol.,* **1973**, *76*, 417.

[5] The following reviews and references therein: a) C. A. Hunter, H. L. Anderson, *Angew. Chem. Int. Ed.,* **2009**, *48*, 7488. b) G. Ercolani, L. Schiaffino, *Angew. Chem. Int. Ed.,* **2011**, *50*, 1762.

[6] D. E. Schafer, A. K. Thakur, *Cell. Biophysics*, **1982**, *4*, 25.

[7] E. Fan, E. A. Merritt, C. L. M. J. Verlinde, W. G. J. Hol, *Curr. Opin. Struc. Biol.,* **2000**, *10*, 680.

[8] A. Bernardi, A. Checchia, P. Brocca, S. Sonnino, F. Zuccotto, *J. Am. Chem. Soc.,* **1999**, *121*, 2032.

[9] A. Bernardi, J. Jiménez-Barbero, A. Casnati, C. D. Castro, T. Darbre, F. Fieschi, J. Finne, H. Funken, K.-E. Jaeger, M. Lahmann, T. K. Lindhorst, M. Marradi, P. Messner, A. Molinaro, P. Murphy, C. Nativi, S. Oscarson, S. Penadés, F. Peri, R. J. Pieters, O. Renaudet, J.-L. Reymond, B. Richichi, J. Rojo, F. Sansone, C. Schäffer, W. B. Turnbull, T. Velasco-Torrijos, S. Vidal, S. Vincent, T. Wennekes, H. Zuilhof, A. Imberty, *Chem. Soc. Rev.,* 2013, **42**, 4709; Y. M. Chambre, R. Roy, *Chem. Soc. Rev.*, **2013**, *42*, 4657; K. T. R. Branson, W. B. Turnbull, Chem. Soc. Rev., **2013**, *42*, 4613.

[10] a) I. Vrasidas, N. J. de Mol, R. M. J. Liskamp, R. J. Pieters, *Eur. J. Org. Chem.,* **2001**, *24*, 4685. b) D. Arosio, I. Vrasidas, P. Valentini, R. M. J. Liskamp, R. J. Pieters, A. Bernardi, *Org. Biomol. Chem.,* **2004**, *2*, 2113. c) Hayama, T. Ph.D. Thesis, University of Zürich, **2008**.

[11] H. M. Branderhorst, R. M. J. Liskamp, G. Visser, R. J. Pieters, *Chem. Comm.*, **2007**, *47*, 5043.

[12] a) E. Fan, Z. S. Zhang, W. E. Minke, Z. Hou, C. L. M. J. Verlinde, W. G. J. Hol, *J. Am. hem. Soc.,* **2000**, *122*, 2663. b) E. A. Merritt, Z. S. Zhang, J. C. Pickens, M. Ahn, W. G. J. Hol, E. Fan, *J. Am. Chem. Soc.,* **2002**, *124*, 8818. c) Z. S. Zhang, E. A. Merritt, M. Ahn, C. Roach, Z. Hou, C. L. M. J. Verlinde, W. G. J. Hol, E. Fan, *J. Am. Chem. Soc.,* **2002**, *124*, 12991. d) J. C. Pickens, D. D. Mitchell, J. Liu, X. Tan, Z. Zhang, C. L. M. J. Verlinde, W. G. J. Hol, E. Fan, *Chem. Biol.,* **2004**, *11*, 1205. e) Z. Zhang, J. Liu, C. L. M. J. Verlinde, W. G. J. Hol, E. Fan, *J. Org. Chem.,* **2004**, *69*, 7737.

[13] A. V. Pukin, H. M. Branderhorst, C. Sisu, C. A. G. M. Weijers, M. Gilbert, R. M. J. Liskamp, G. M. Visser, H. Zuilhof, R. J. Pieters, *ChemBioChem,* **2007**, *8*, 1500.

[14] a) J. Garcia-Hartjes, S. Bernardi, C. A. G. M. Weijers, T. Wennekes, F. Sansone, A. Casnati, H. Zuilhof, *Org. Biomol. Chem.*, **2013**, *11*, 433. b) F. Sansone, L. Baldini, A. Casnati, R. Ungaro, *New J. Chem.,* **2010**, *34*, 2715.

[15] The prefix *sym* is used here to indicate the C_5-symmetric-substituted corannulene corresponding to 1,3,5,7,9-pentasubstitution.

[16] A. M. Butterfield, B. Gilomen, J. S. Siegel, *Org. Process Res. Dev.,* **2012**, *16*, 664.

[17] G. H. Grube, E. J. Elliott, R. J. Steffens, C. S. Jones, K. K. Baldridge, J. S. Siegel, *Org. Lett.,* **2003**, *5*, 713.
[18] M. Mattarella, J. S. Siegel, *Org. Biomol. Chem.,* **2012**, *10*, 5799.
[19] S. Binauld, C. J. Hawker, E. Fleury, E. Drockenmuller, *Angew. Chem. Int. Ed.,* **2009**, *48*, 6654.
[20] M. E. Jung, E. C. Yang, B. T. Vu, M. Kiankarimi, E. Spyrou, J. Kaunitz, J. *J. Med. Chem.*, **1992**, *42*, 3899.
[21] F. Fazio, M. C. Bryan, O. Blixt, J. C. Paulson, C.-H. Wong, *J. Am. Chem. Soc.*, **2002**, *124*, 4397.
[22] A. Bouzide, G. Sauve, *Org. Lett.,* **2002**, *4*, 2329.
[23] M. K. Mueller, L. Brunsveld, *Angew. Chem. Int. Ed.,* **2009**, *48*, 2921.
[24] A. V. Pukin, C. A. G. M. Weijers, B. van Lagen, R. Wechselberger, B. Sun, M. Gilbert, M.-F. Karwaski, D. E. A. Florack, B. C. Jacobs, A. P. Tio-Gillen, A. van Belkum, H. P. Endtz, G. M. Visser, H. Zuilhof, *Carbohydr. Res.*, **2008**, *343*, 636.
[25] R. M. Dawson, *J. Appl. Toxicol.,* **2005**, *25*, 30.
[26] A. M. Svennerholm, J. Holmgren, *Curr. Microbiol.,* **1978**, *1*, 19.
[27] C. Sisu, A. J. Baron, H. M. Branderhorst, S. D. Connell, C. A. G. M. Weijers, R. de Vries, E. D. Hayes, A. V. Pukin, M. Gilbert, R. J. Pieters, H. Zuilhof, G. M. Visser, W. B. Turnbull, *ChemBioChem,* **2009**, *10*, 329.

3

Picomolar inhibition of cholera toxin by a pentavalent ganglioside GM1os-calix[5]arene

This chapter is published as:

Jaime Garcia-Hartjes,‡ Silvia Bernardi,‡ Carel A. G. M. Weijers, Tom Wennekes, Michel Gilbert, Francesco Sansone, Alessandro Casnati and Han Zuilhof *Org. Biomol. Chem.*, **2013**, *11*, 4340-4349, DOI: 10.1039/c3ob40515j

‡Both authors contributed equally to this work.

Abstract:

Cholera toxin (CT), the causative agent of cholera, displays a pentavalent binding domain that targets the oligosaccharide of ganglioside GM1 (GM1os) on the periphery of human abdominal epithelial cells. Here, we report the first GM1os-based CT inhibitor that matches the valency of the CT binding domain (CTB). This pentavalent inhibitor contains five GM1os moieties linked to a calix[5]arene scaffold. When evaluated with an inhibition assay, it achieved a picomolar inhibition potency (IC_{50} = 450 pM) for CTB. This represents a significant multivalency effect, with a relative inhibitory potency of 100.000 compared to a monovalent GM1os derivative, making GM1os-calix[5]arene one of the most potent known CTB inhibitors.

3.1 Introduction

Cholera still represents a serious health problem in areas of the developing world where there is a lack of clean water and proper sanitation. In 2012, the World Health Organization estimated that annually 3 - 5 million cholera cases occur that result in more than 100.000 deaths.[1] Although several treatments exist for cholera,[2] resistance development and mutations in the causative pathogen mean that efforts to better understand the disease pathogenesis and develop new treatments are crucial.[3,4] The symptoms of cholera are caused by cholera toxin (CT), which is produced by the *Vibrio cholerae* bacterium. CT is a member of the AB_5 toxin family that contains a pentameric binding domain, the cholera toxin B-subunit (CTB), for recognition and binding to cell surfaces.[5] The natural target ligand for CTB is the glycosphingolipid ganglioside GM1, on cellular membranes of the infected hosts' intestinal epithelial surface. CTB can bind five GM1 saccharide epitopes simultaneously with the terminal Gal- and the Neu5Ac carbohydrate units of the

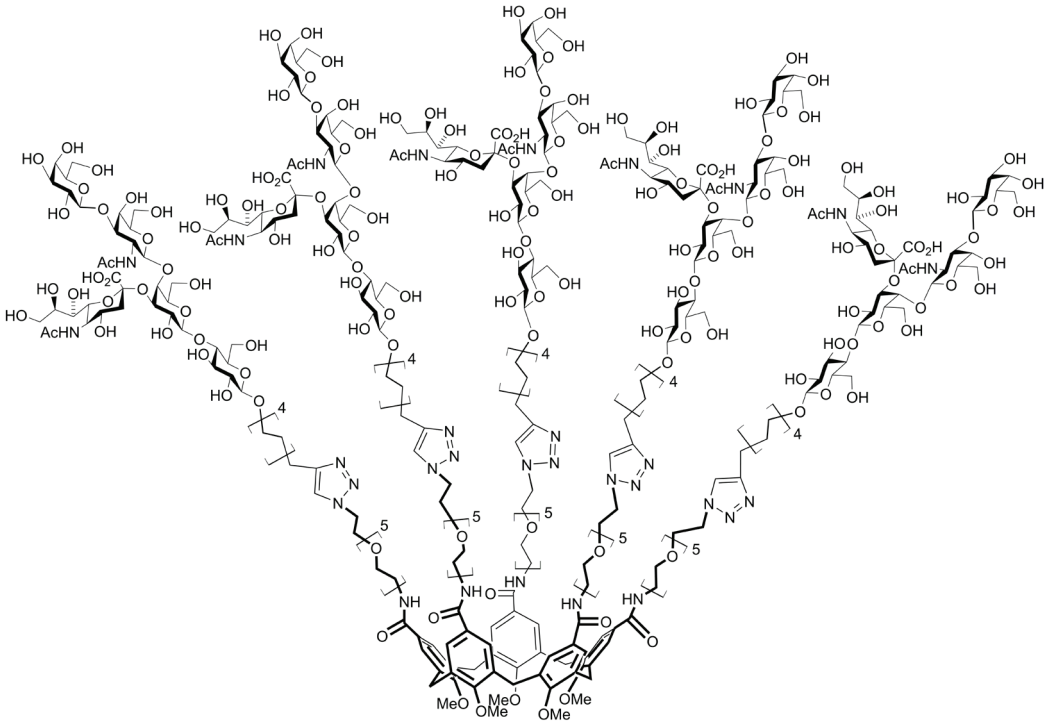

Figure 1. Developed CTB inhibitor: penta-GM1os-calix[5]arene (**1**).

ganglioside as the major contributors to the binding.[6,7] The adhesion of CTB to ganglioside GM1 on cell surfaces is the prerequisite for endocytosis of the toxic enzymatically active A subunit of CT, and the ensuing severe clinical symptoms.[8]

One avenue in cholera research is to study the binding of CTB to GM1 and to develop CTB inhibitors that might prevent CT from binding the hosts' cell surface and thereby also the development of cholera. Here, we present the first example of a pentavalent GM1os-based inhibitor for CTB, GM1os-calix[5]arene (**1**; Figure 1). In Chapter 2, also a pentavalent CTB inhibitors based on a GM1os-presenting corannulene scaffold was described. In the past, several studies have focused on the development of multivalent glycosylated inhibitors for CTB based on ganglioside GM1.[9] It is noteworthy that in none of these studies, inhibitors were investigated with a pentavalent structure that matches the pentavalent structure of CTB. On the other hand, pentavalent cyclens[10,11] and cyclic peptides[12] have been described as CTB inhibitors, but those contained only the much simpler galactose epitope, likely to get around the difficulty to obtain sufficient tailor-made GM1os.

Therefore, also GM1 mimics have been used, e.g. Thompson and Schengrund described poly(propylene) imine dendrimers that present the Galβ1-3GalNAcβ1-4(Neu5Acα2-3)Galβ-epitope of GM1 (see Chapter 1 for structure),[13] with IC_{50} values for the tetravalent and octavalent dendrimer of 7 and 3 nM, respectively. Bernardi *et al*. published a series of GM1-mimics (pseudo-GM1), in which the residues in the GM1os that are not essential for binding were replaced by a conformationally restricted cyclohexane-diol and the Neu5Ac-unit was substituted by various α-hydroxy acids.[14,15] When attached to multivalent dendritic structures,[16] the relative inhibitory potency (RIP) per mimic unit of the tetravalent and octavalent inhibitors were 111 and 55, respectively. Interestingly, when the same mimic was linked to a divalent calix[4]arene scaffold,[17] a 4000-fold enhancement in binding efficiency was achieved compared to the monovalent pseudo-GM1. These data suggested to us that the calixarene macrocycle, from which the binding inhibitors are projected, could be a promising multivalent scaffold[18-20] to design CTB inhibitors with improved efficiency. In collaboration with the group of Pieters, our lab previously published divalent, tetravalent, and octavalent dendritic structures decorated with GM1os (see for structure §1.4 on p.39).[21,22] For the octavalent compound the unprecedentedly low IC_{50} value of 50 pM was observed with a relative inibititory potency (RIP) of 17500 per each arm compared to its monovalent counterpart. However, its mismatched valency compared to CTB, prompted us to investigate

a pentavalent scaffold as core structure that when decorated with GM1os has the potential to form 1 : 1 inhibitor-CTB complexes. The current paper presents the convergent synthesis of the first, water-soluble, pentavalent CTB inhibitor (**1**), which was made by coupling five GM1os units to a calix[5]arene scaffold.

3.2 Results and Discussion

We designed a 5-fold symmetric calix[5]arene as a pentavalent scaffold structure. This calix[5]arene (Figure 1) presents small methoxy groups at the lower rim, which confer a high conformational flexibility to the macrocyclic structure.[23] The upper rim of the calixarene inhibitor is decorated with the GM1 pentasaccharide separated from the macrocyclic core by appropriate linkers. Fan and coworkers[12] have demonstrated that an optimal linker length is vital for the potency of a synthetic multivalent inhibitor. For the calix[5]arene, described here, a 31 atom-containing linker was chosen. This should allow the simultaneous interaction of the five GM1os units with the five B-subunits of a single toxin.[5]

The route towards our target (**1**) started with the synthesis of the pentavalent scaffold that began with the preparation of the known *p-tert*-butyl-calix[5]arene.[24] This product was converted into *p*-H-calix[5]arene **2**[25] by following literature procedures. Next, penta-aldehyde **3** was obtained in 57% yield from **2** by exploiting the Duff formylation reaction.[26,27] Compound **3** was subsequently methylated at the

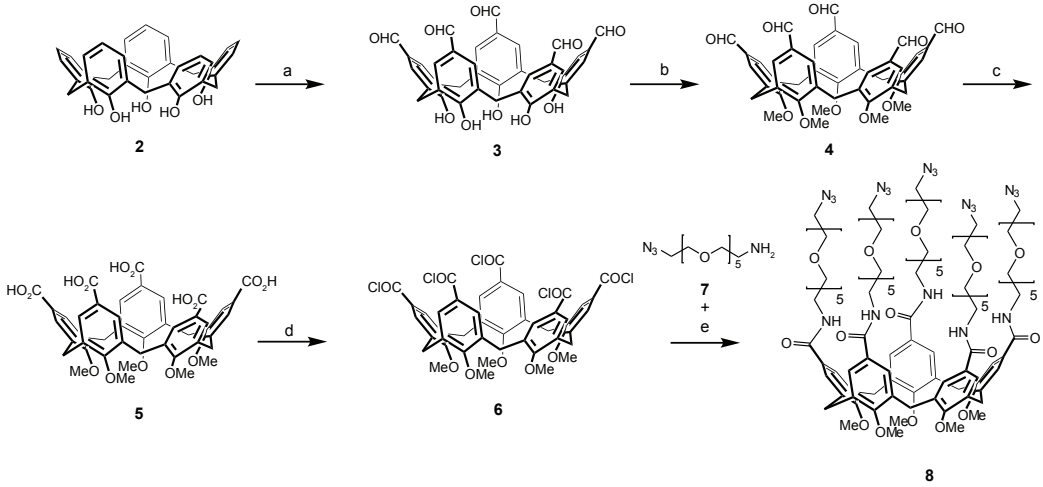

Scheme 1. Synthesis of the azido-calix[5]arene (**8**) scaffold. Reagents and conditions: a) HMTA, CF_3COOH, Δ, N_2, 5 days, 57%; b) CH_3I, K_2CO_3 CH_3CN, reflux, N_2, 20 h, 68%; c) $NaClO_2$, NH_2SO_3H, $(CH_3)_2CO$, $CHCl_3$, H_2O, rt, 24 h, 79%; d) $(COCl)_2$, CH_2Cl_2, N_2, rt, 18h, quant.; e) Et_3N, dry CH_2Cl_2, N_2, rt, 20 h, 44%.

lower rim by using CH_3I and K_2CO_3 in acetonitrile affording the penta-methoxy-calix[5]arene **4** in 68% yield (Scheme 1). Oxidation of compound **4** with $NaClO_2$ and NH_2SO_3H produced the penta-carboxylic acid **5**. The unsymmetrically substituted by ditosylation, substitution to the diazide, and finally selective Staudinger reduction of one azide.[28,29] Initial attempts to condense amine **7** with the carboxylic azido-penta-(ethyleneglycol)-amine **7** was synthesized from hexa-ethylene glycol

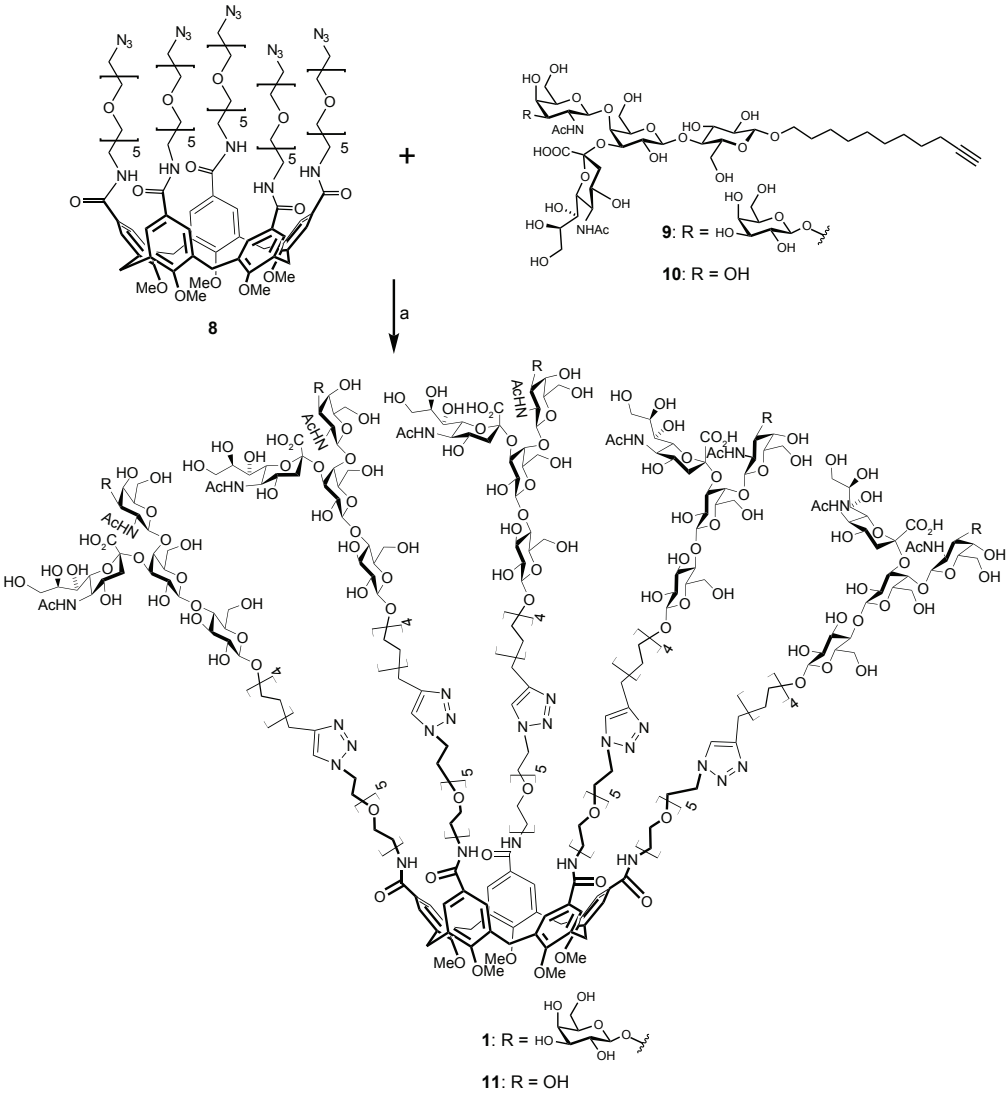

Scheme 2. Synthesis of GM1os-calix[5]arene (**1**) and GM2os-calix[5]arene (**11**); a) $CuSO_4 \cdot 5H_2O$, sodium ascorbate, Triton X-100, CH_3OH, H_2O, MW (150W), 80 °C, 1 h; 51% **1**, 59% **11**

acids in **5** using HBTU resulted in difficult purification and low yields (~ 20%) of **8**. However, when this spacer (**7**) was attached to calix[5]arene **5** *via* penta-acyl chloride intermediate **6** it provided penta-azido-calix[5]arene **8** in a 44% yield.

With the calix[5]arene (**8**) scaffold in hand we proceeded to the next stage, attaching five GM1 oligosaccharides. We chose the copper-catalyzed azide-alkyne cycloaddition (CuAAC) reaction to achieve this, which meant a GM1os derivative with a terminal alkyne was required. This C_{11}-alkyne-terminated GM1os **9** (Scheme 2) was made via a chemo-enzymatic procedure previously reported by us,[30] which allowed the production of **9** on gram scale. Compound **9** was subsequently "clicked" to scaffold **8** under standard CuAAC conditions in H_2O while exposed to microwave irradiation to successfully provide our crude target inhibitor **1**. With our target pentavalent GM1os-calix[5]arene **1** in hand, in order to properly assess the role of the GM1os in inhibitor **1**, we also set out to synthesize derivatives of **1** containing fragments of the GM1os to use for comparison in the biological assays. The first of these was penta-GM2os-calix[5] arene (**11**) that lacks the terminal galactose epitope compared to the GM1os. We synthesized **11** using the same CuAAC reaction conditions from scaffold **8** and a chemo-enzymatically produced alkyne-terminated C_{11}-linked GM2os sugar (**10**).

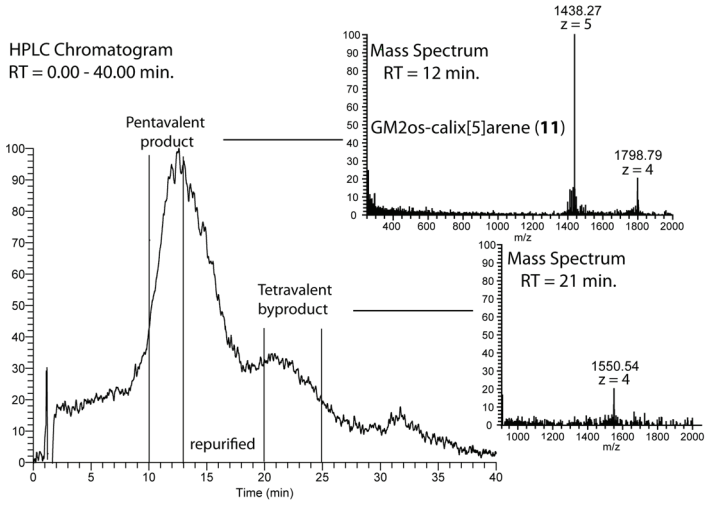

Figure 2. LCMS trace of the purification of GM2-calix[5]arene **11**. (left) Chromatogram of the purification on a reversed phase column (see Sup. Info. for details). (right) Mass spectra for two fractions, the pentavalent product **11** at RT = 12 min, and the tetravalent at 21 min.

With both our target **1** and its derivative **11** in hand as crude products, we investigated what purification method would be suitable for these large complex

molecules. An initial purification by size exclusion chromatography (SEC) efficiently removed excess of alkyne-terminated GM1os **9** and GM2os **10**, respectively. However, the crude products both also contained a minor amount of tetravalent byproducts as could be clearly seen with mass spectrometry and their separation proved quite challenging. Initial attempts to separate these by aqueous GPC on HPLC failed, but after extensive optimization, reversed phase HPLC purification proved the most successful for this final purification step. Figure 2 shows a typical HPLC chromatogram for the separation for both the GM1os- and GM2os-calix[5] arenes. Despite attempts to improve the moderate resolution, the purification remained quite complicated because of long elution times (up to 40 minutes per run) and high affinity of the products with the column material. Collecting of small fractions in a specific retention time window over multiple HPLC injections and subsequent lyophilization resulted indeed in pure pentavalent GM1os- and GM2os-calix[5]arenes (**1** and **11)** as shown by HR-MS and NMR analyses. The other impure fractions that also contained **1** or **11** were collected, pooled, lyophilized and

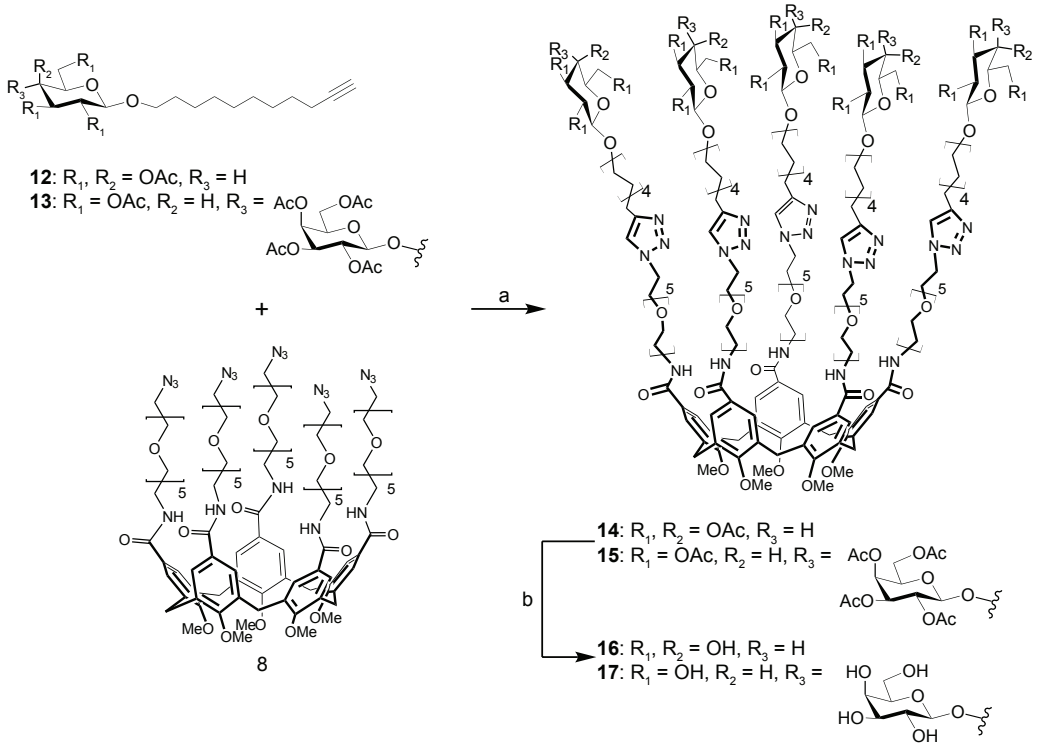

Scheme 3. Synthesis of galactoside-calix[5]arene (**16**), and lactoside-calix[5]arene (**17**); a) $CuSO_4 \cdot 5H_2O$, sodium ascorbate, DMF, H_2O, MW (150 W), 80 °C, 1 h; 67% **14**, 57% **15**; b) NaOMe/MeOH, 4 h - 18 h, H^+-resin; 90% **16**, 72% **17**.

re-injected to achieve optimal yields. Attempts were made to isolate the tetravalent byproducts, but insufficient amounts could be obtained for further analysis. Besides the GM2os containing calixarene (**11**), we also prepared two further derivatives of **1** that contained fragments of GM1os, a pentavalent *β*-galactoside- (**16**) and *β*-lactoside-calix[5]arene (**17**) (Scheme 3). These more simple carbohydrates enabled a modified synthesis procedure that circumvented the potentially challenging HPLC purification, as encountered for compounds **1** and **11**. The coupling was also performed by employing the microwave-assisted CuAAC reaction on penta-azido-calixarene scaffold **8**, but instead of using the deprotected carbohydrates, acetyl-protected galactoside **12**, and lactoside **13** were reacted. The resulting products could now be purified by normal phase silica gel chromatograpy. The acetyl-protected **14** and **15** were deprotected by employing standard Zemplén[31] conditions to obtain galactoside-calix[5]arene **16**, and lactoside-calix[5]arene **17**, respectively, which did not require further purification after work up.

Finally, in order to properly determine the multivalency effect of the interaction of **1** with CTB in our biological assays, we also synthesized the monovalent GM1os derivative **20** (Scheme 4). This was achieved by first *in situ* generation of the acyl chloride of commercially available 4-methoxybenzoic acid with oxalyl chloride and, subsequently, reacting this with amino-azide **7**, yielding azide **19** in 20% over two steps. Again, by employing the microwave-assisted CuAAC reaction on alkyne-terminated **9** and azide **19**, GM1os-monomer **20** was obtained in reasonable yield (49%).

The inhibitory potency of the four pentavalent compounds (**1**, **11**, **16**, and **17**), was determined by enzyme-linked lectin assay (ELLA) experiments. In the assays, the ability of **1**, **11**, **16** and **17** to compete with the natural antigen GM1 for binding HRP-labeled CTB was measured, which was adsorbed to the well surface of the microtiter plate. GM1os-calix[5]arene **1** showed a high inhibition potency, *i.e.*, a very low IC_{50} value of 450 pM (Figure 3, Table 1). Comparing the IC_{50} value

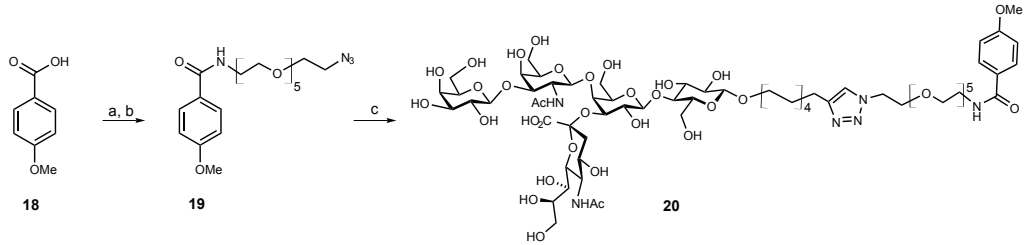

Scheme 4. Synthesis of GM1-monomer **20**; a) $(COCl)_2$, dry CH_2Cl_2, N_2, rt, 18 h; b) **7**, Et_3N, dry CH_2Cl_2, N_2, rt, 20 h; 20% in two steps; c) **9**, $CuSO_4 \cdot 5H_2O$, sodium ascorbate, Triton X-100, CH_3OH, H_2O, MW (150 W), 80 °C, 1 h; 49%.

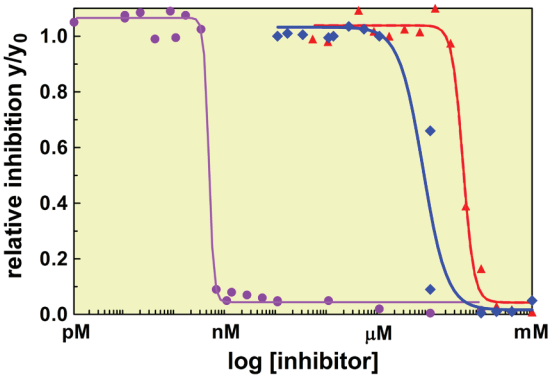

Figure 3. ● GM1os-calix[5]arene ♦ GM2os-calix[5]arene ▲ GM1os-monomer; Fitted curves of the experimental ELLA inhibition data. For details of the inhibition assays see §3.4.

Table 1. CTB inhibition potency for reported compounds.

Entry	Saccharide	Valency	#	IC_{50}
1	GM1os	5	**1**	450 pM
2	GM1os	1	**20**	44 μM
3	GM2os	5	**11**	9 μM
4	Galactose	5	**16**	>1 mM
5	Lactose	5	**17**	>1 mM

(44 μM) of the monovalent control compound (**20**) to that of **1**, revealed a 100-thousand fold increase in inhibitory potency, and a RIP of 20-thousand per arm. Pentavalent inhibitors based on a more rigid corannulene scaffold, which we also report in this issue, inhibited CTB in the nanomolar range.[32] Assay results for the GM2os-calix[5]arene **11** confirmed the importance of using GM1os. Lacking only the terminal galactose compared to **1**, it produced an IC50 of 9 μM, which is 20-thousand fold worse compared to **1**. The galactose-terminated (**16**) and lactose-terminated (**17**) calix[5]arenes displayed a higher inhibition concentration than their solubility in the assay medium, and their IC_{50} could therefore only be determined as being >1 mM (Table 1).

3.3 Conclusions

In summary, the study described in this chapter dealt with the synthesis and initial biological evaluation of the first known example of a pentavalent GM1os-based

inhibitor of cholera toxin that matches the valency of the cholera toxin B-subunit. With an IC_{50} of 450 pM, the pentavalent GM1os-calix[5]arene (**1**) also displays the highest relative inhibitory potency, 20-thousand per arm (compared to **20**), documented thus far for CT inhibitors. We are currently using the here reported convergent synthetic route to further explore the structure-activity-relationship of **1** and improve its potency. Among other issues we are interested in investigating the effect of the length, rigidity and hydrophobicity of the used spacer and restricting the flexibility of the calix[5]arene scaffold to a fixed cone structure.

3.4 Experimental section

General experimental information

All moisture sensitive reactions were carried out under nitrogen atmosphere, using previously oven-dried glassware. All dry solvents were prepared according to standard procedures, distilled before use and stored over 3 Å or 4 Å molecular sieves. Reagents were obtained from commercial sources and used without further purification unless stated otherwise. Analytical TLC was performed using prepared plates of silica gel (Merck 60 F-254 on aluminium) and then, according to the functional groups present on the molecules, revealed with UV light or using staining reagents: $FeCl_3$ (1% in H_2O/ CH_3OH 1 : 1), H_2SO_4 (5% in EtOH), ninhydrin (5% in EtOH), basic solution of $KMnO_4$ (0.75% in H_2O). Merck silica gel 60 (70 - 230 mesh) was used for flash chromatography and for preparative TLC plates. ^1H NMR and ^{13}C NMR spectra were recorded on Bruker AV300, Bruker AV400, Bruker DPX400, and Bruker AV600 equipped with cryoprobe spectrometers (observation of ^1H nucleus at 300 MHz, 400 MHz, 600 MHz, respectively, and of ^{13}C nucleus at 75 MHz, 100 MHz, and 151 MHz, respectively). Chemical shifts are reported in part per million (ppm), calibrated on the residual peak of the solvent, whose values are referred to tetramethylsilane (TMS, δ_{TMS} = 0 ppm), as internal standard. ^{13}C NMR spectra were performed with proton decoupling. Electrospray ionization (ESI) mass analyses were performed with a Waters spectrometer, while high resolution ESI mass analyses were recorded on a Thermo Scientific Q Exactive spectrometer. Melting points were determined on an Electrothermal apparatus in closed capillaries. Microwave reactions were performed on a CEM Discovery System reactor running on Discover Application Chemdriver Software v3.6.0. HPLC was performed on a HP 1100 series with a DAP 190-600 nM detector, equipped with a Waters Xterra 100 × 4.6 mm C18 column eluted with isocratic

iPrOH/ H_2O 35 :65, and a flow of 0.4 mL/min, unless stated otherwise. Materials for the ELLA experiments i.e. bovine serum albumin (BSA), bovine brain GM1, ortho-phenylenediamine (dihydrochloride salt) (OPD), cholera toxin horseradish peroxide (CTB-HRP) conjugate, tween-20, 30% H_2O_2 solution, sodium citrate, and citric acid were purchased at Sigma Aldrich and used without further modification, phosphate-buffered saline (PBS) 10 × concentrate was diluted ten times with demineralized water prior to use. Nunc F96 MaxisorpTM 96-wells microtiter plates were used as purchased at Thermo Scientific. The microtiter plates were washed using an automated Denville® 2 Microplate Washer. Optical density (OD) was measured between 1.5 and 0.5 units on a Thermo Labsystems Multiskan Spectrum Reader running on Skanit software version 2.4.2. Data analysis and curve fitting of inhibition experiments were performed on Prism Graphpad software v5.04. Simplified nomenclature proposed by Gutsche[33] is used to name the calix[5]arene compounds. Compounds 31,32,33,34,35-pentahydroxycalix[5]arene **2**,[25] 17-azide-3,6,9,12,15-pentaoxaheptadecane-1-amine **7**,[29] Undec-10-ynyl-2,3,4,6-tetra-*O*-acetyl-*β*-D-galactopyranoside **12**,[30] undec-10-ynyl-2,3,4,6-tetra-*O*-acetyl-*β*-D-galactopyranosyl-(1→4)-2,3,6-tri-*O*-acetyl-*β*-D-glucopyranoside **13**[30] were prepared according to literature procedures.

GM1-calix[5]arene (**1**)

Calix[5]arene **8** (15.7 mg, 6.93 µmol) was dissolved in 0.5 mL of CH_3OH in a microwave tube. Then the GM1os derivative **9** (59.8 mg, 52.1 µmol), previously synthesized by chemo-enzymatic procedures,[30,34] was combined with $CuSO_4 \cdot 5H_2O$ (0.52 mg, 2.1 µmol), sodium ascorbate (0.82 mg, 4.2 µmol), 4 mL of H_2O and a drop of Triton X-100. The mixture was heated at 80 °C by microwave irradiation (150 W) for 60 min. The reaction progression was monitored via TLC (eluent: AcOEt/ CH_3OH/ H_2O/ AcOH 4 : 2 : 1 : 0.1) and ESI-MS analyses. The crude mixture was purified via size exclusion column chromatography (Sephadex G-15, eluent: H_2O 100%) and HPLC purification (see General Information) giving product **1** as a white solid. Yield: 51%; **^{1}H NMR** (D_2O, 600 MHz): δ = 7.61 (s, 5H, H5 triazole), 7.50 (s, 10H, Ar), 4.69 (bs, 5H, H1-GalNAc), 4.43 (d, 5H, *J* = 8.0 Hz, H1-Gal'), 4.44 - 4.41 (m, 5H, H1-Gal), 4.38 - 4.37 (m, 5H), 4.32 - 4.31 (5H, d, *J* = 7.9 Hz, H1-Glc), 4.05 - 4.02 (m, 15H), 3.94 - 3.92 (m, 5H, H2-GalNAc), 3.86 - 3.60 (m, 105H), 3.60 - 3.45 (m, 80H), 3.46 - 3.33 (m, 75H), 3.26 - 3.24 (m, 5H, H2-Gal); 3.18 - 3.15 (m, 5H, H2-Glc), 3.10 (bs, 10H), 2.56 - 2.54 (m, 5H, H3a-Neu5Ac), 2.45 - 2.42 (m, 10H, triazole-C$\underline{H}_2CH_2CH_2$), 1.92 (s, 15H, NC(O)CH_3-Neu5Ac), 1.89 (s,

15H, NC(O)CH_3-GalNAc), 1.85 - 1.80 (m, 5H, H3b-Neu5Ac), 1.44 - 1.35 (m, 20H, CH_2 aliphatic chain), 1.14 - 1.08 (m, 10H, C$\underline{H}_2$CH_2OC1-Glc), 1.03 (m, 40H, CH_2 aliphatic chain); **^{13}C NMR** (D_2O, 151 MHz): δ = 175.4, 175.1, 174.5 (C(O)),169.1 (Ar$\underline{C}$(O)NH); 159.7 (Ar-ipso); 134.8 (Ar-ortho); 129.2 (Ar-para); 128.9 (Ar-meta); 123.7 (C5 triazole), 105.1 (C1-Gal'), 103.0 (C1-Gal), 102.8 (C1-GalNAc), 102.5 (C1-Glc), 102.0 (C2-Neu5Ac), 80.7 (C3-GalNAc), 79.0 (C4-Glc), 77.6 (C4-Gal), 75.2 (C5-Gal'), 75.1 (C5-Glc), 74.9 (C3-Gal), 74.7, 74.4 (C5-Gal), 73.4 (C6-Neu5Ac), 73.1 (C2-Glc), 72.8 (C3-Gal'), 72.6 (C7-Neu5Ac), 71.0 (C2-Gal'), 70.9 (β-CO$\underline{C}H_2$), 70.4 (C2-Gal), 70.1 - 69.8, 69.4, 69.2, 69.0, 68.9, 68.4, 68.3 (C4-GalNAc), 63.1, 61.4, 61.3, 60.9, 60.5, 52.0, 51.5 (C2-GalNAc), 50.3, 40.0, 37.2, 31.1 (Ar$\underline{C}H_2$Ar), 29.3, 29.1, 29.0, 28.9, 28.8 (CH_2 aliphatic chain), 25.6 ($\underline{C}H_2CH_2$OC1-Glc), 25.0 (triazole-$\underline{C}H_2CH_2CH_2$), 23.0 (NHC(O)$\underline{C}H_3$-GalNAc), 22.4 (NHC(O)$\underline{C}H_3$-Neu5Ac); **MS** (HR-ESI-): m/z = 1600.5013 [100% $(M-5H)^{5-}$], calcd: 1600.7112.

5,11,17,23,29-Pentaformyl-31,32,33,34,35-pentahydroxycalix[5]arene (**3**)
Calix[5]arene **2**[25] (0.41 g, 0.78 mmol) was added to a solution of HMTA (2.5 g, 17.8 mmol) in 50 mL TFA and the mixture was refluxed for 5 days under N_2. The solvent was then removed under reduced pressure and the residue dissolved in 12 mL of a 1 : 1 CH_2Cl_2/ HCl 1 M solution. The mixture was stirred at room temperature for 24 h. The aqueous phase was extracted with CH_2Cl_2 (5 × 5mL). The combined organic phases were washed with water (2 × 10mL), dried over anhydrous Na_2SO_4, filtered and the solvent removed under reduced pressure. The residue was purified by trituration in $CHCl_3$/ hexane 1 : 1 to give the product **3** as a brownish solid. Yield: 57%; **^{1}H NMR** (300 MHz, $CDCl_3$/ CD_3OD 9 : 1): δ = 9.75 (s, 5H, CHO), 7.70 (s, 5H, ArOH), 7.22 (s, 10H, ArH), 3.45 (s, 10H, Ar$\underline{H}_2$Ar); **^{13}C NMR** (75 MHz, $CDCl_3$/ CD_3OD 9 : 1): δ = 192.1 (CHO), 150.6 (Ar-ipso), 131.9 (Ar-para), 128.1 (Ar-meta), 127.2 (Ar-ortho), 31.4 (Ar$\underline{C}H_2$Ar); **MS**(HR-ESI+): m/z = 671.1921 [100% $(M+H)^+$], calcd: 671.1917; **m.p.** > 300 °C.

5,11,17,23,29-Pentaformyl-31,32,33,34,35-pentamethoxy- calix[5]arene (**4**)
In a two-neck round-bottomed flask, pentaformylcalix[5]arene **3** (0.7 g, 1.1 mmol) was dissolved in 150 mL of dry CH_3CN, then K_2CO_3 (4.5 g, 32 mmol) and CH_3I (2 mL, 32 mmol) were added and the mixture was refluxed for 20 h under nitrogen atmosphere. The solvent was removed under reduced pressure and the residue dissolved in 150 mL of a 1:1 solution CH_2Cl_2/ HCl 1 M. The mixture was stirred for 2 h at room temperature. The organic layer was separated, and

the aqueous phase extracted with CH_2Cl_2 (2 x 50 mL). The combined organic phases were washed with water (2 x 100 mL), dried over anhydrous Na_2SO_4, filtered and the solvent removed under reduced pressure. The product **4** was obtained as a brown solid. Yield: 68%; **^{1}H NMR** (300 MHz, $CDCl_3$): δ = 9.72 (s, 5H, CHO), 7.50 (s, 10H, ArH), 3.92 (s, 10H, Ar$\underline{C}H_2$Ar), 3.25 (s, 15H, OCH_3); **^{13}C NMR** (75 MHz, $CDCl_3$/ CD_3OD 9 : 1): δ = 191.4 (CHO), 161.8 (Ar-ipso), 134.8 (Ar-para), 132.0 (Ar-ortho), 130.8 (Ar-meta), 60.6 (OCH_3), 30.7 (Ar$\underline{C}H_2$Ar); **MS** (HR-ESI +): m/z = 741.2700 [100% $(M+H)^+$], calcd: 741.2700; **m.p.** = 217 - 219 °C.

5,11,17,23,29-Pentacarboxy-31,32,33,34,35-pentamethoxycalix[5]arene (**5**)
Pentaformyl-pentamethoxycalix[5]arene **4** (0.25 g, 0.34 mmol) was dissolved in a two-neck round-bottomed flask in 100 mL of a mixture acetone/ $CHCl_3$ 1 : 1, and cooled to 0 °C with an ice-water bath. In another flask, a solution of $NaClO_2$ 80% pure (0.47 g, 4.20 mmol) was dissolved in the minimum amount of water. Subsequently, sulfamic acid (0.49 mg, 5.04 mmol) was added. This solution was slowly poured into the reaction flask. The mixture was stirred at 0 °C for 15 min and gradually warmed to room temperature while it remained being stirred for 24 h. The solvent was then removed under reduced pressure and the residue triturated with 1 M HCl. After filtration on a Büchner funnel, product **5** was obtained as a solid. Yield: 79%; **^{1}H NMR** (300 MHz, CD_3OD): δ = 7.75 (s, 10H, ArH), 3.93 (s, 10H, Ar$\underline{C}H_2$Ar), 3.30 (s, 15H, OCH_3); **^{13}C NMR** (75 MHz, CD_3OD): δ (ppm) 169.6 (CO), 162.1 (Ar-ipso), 135.8 (Ar-ortho), 132.0 (Ar-meta), 126.8 (Ar-para), 61.3 (-OCH_3), 31.9 (Ar$\underline{C}H_2$Ar); **MS**(HR-ESI+): m/z = 843.2269 [100% $(M+Na)^+$], calcd: 843.2265.

5,11,17,23,29–Pentakis[(17-azide-3,6,9,12,15-pentaoxahepta-decane-1-amino)carbonyl]–31,32,33,34,35–pentamethoxy-calix[5]arene (**8**)
In a round-bottomed flask, 0.12 g of calix[5]arene **5** (0.14 mmol) and 0.51 mL of oxalyl chloride (5.82 mmol) were solubilized in 15 mL of dry CH_2Cl_2 under nitrogen atmosphere. The solution was stirred for 18 h at room temperature and then the solvent evaporated to dryness. The residual compound **6** was dissolved again in 5 mL of dry CH_2Cl_2 and then added dropwise to a solution of amine compound **7** (0.29 g, 0.87 mmol) and NEt_3 (0.12 mL, 0.87 mmol) in 5 mL of dry CH_2Cl_2. The mixture was stirred for 20 h at room temperature under nitrogen atmosphere. The mixture was then washed with 1 M HCl, an aqueous solution of Na_2CO_3 and water till neutral pH was reached. The solvent was removed under reduced pressure and the crude purified by flash chromatography (eluent: $CHCl_3$/CH_3OH 95:5) to give the product **8**

as a yellow oil. Yield: 44%; **^{1}H NMR** (400 MHz, $CDCl_3$): δ = 7.50 (s, 10H, ArH), 7.07 (bs, 5H, CONH), 3.89 (s, 10H, ArC$\underline{H}_2$Ar), 3.65 - 3.50 (m, 110H, OCH_2, C$\underline{H}_2$NHCO), 3.34 (t, 10H, *J* = 4.8 Hz, CH_2N_3), 3.28 (s, 15H, OCH_3); **^{13}C NMR** (100 MHz, $CDCl_3$): δ = 167.3 (CO), 159.2 (Ar-ipso), 134.2 (Ar-para), 129.8 (Ar-ortho), 128.2 (Ar-meta), 70.6, 70.5, 70.2, 70.0, (OCH_2), 60.8 (OCH_3), 50.6 (CH_2N_3), 39.7 ($\underline{C}H_2$NHCO), 30.9 (Ar$\underline{C}H_2$Ar); **MS** (HR-ESI+): m/z = 1131.5698 [100% $(M+2H)^{2+}$], calcd: 1131.5756.

GM2-calix[5]arene (**11**)

Calix[5]arene **8** (15.7 mg, 6.93 μmol) was dissolved in 0.5 mL of CH_3OH in a microwave tube. Then the GM2os derivative **10** (50.5 mg, 52.1 μmol), previously synthesized by chemo-enzymatic procedures,[30,34] was added together with samples of $CuSO_4 \cdot 5H_2O$ (0.52 mg, 2.1 μmol), sodium ascorbate (0.82 mg, 4.2 μmol), 4 mL of H_2O and a drop of Triton X-100. The mixture was heated at 80 °C by microwave irradiation (150 W) for 60 min. The reaction progress was monitored via TLC (eluent: AcOEt/ CH_3OH/ H_2O/ AcOH 4 : 2 : 1 : 0.1) and ESI-MS analyses. The crude material was purified via size exclusion column chromatography (Sephadex G-15, eluent: H_2O 100%), followed by HPLC purification (see General Information) giving pure product **11** as a white solid. Yield: 59%; **^{1}H NMR** (D_2O/ CD_3OD, 400 MHz): δ = 7.65 (s, 5H, H5 triazole), 7.54 (s, 10H, ArH), 4.70 (m, 5H, H1-Gal), 4.47 - 4.42 (m, 15H, H1-GalNAc), 4.36 - 4.35 (d, 5H, H1-Glc, *J* = 7.6 Hz), 4.08 - 4.06 (m, 10H), 3.89 - 3.66 (m, 95H, ArC$\underline{H}_2$Ar), 3.58 - 3.43 (m, 150H); 3.32 - 3.30 (m, 5H, H2-Gal), 3.23 - 3.19 (m, 5H, H2-Glc), 3.14 (bs, 10H), 2.61 - 2.58 (m, 5H, H3a-Neu5Ac), 2.48 (bs, 10H), 1.97 (s, 15H, NHC(O)C$\underline{H}_3$-Neu5Ac), 1.95 (s, 15H, NHC(O)C$\underline{H}_3$-GalNAc), 1.89 - 1.84 (m, 5H, H3b-Neu5Ac), 1.51-1.36 (bs, 20H, CH_2 aliphatic chain), 1.23 - 0.95 (50H, m, CH_2 aliphatic chain); **MS** (HR-ESI-): m/z 1440.4670 [100% $(M-5H)^{5-}$], calcd: 1438.6588.

Peracetylated-galactosylcalix[5]arene (**14**)

Calix[5]arene **8** (32.0 mg, 14.1 μmol) and the β-galactoside derivative **12** (52.9 mg, 106 μmol) were dissolved in 2.5 mL of DMF in a microwave tube. $CuSO_4 \cdot 5H_2O$ (2.0 mg, 8.5 μmol), sodium ascorbate (3.3 mg, 16.9 μmol) and 0.5 mL H_2O were then added. The mixture was heated at 80 °C by microwave irradiation (150 W) for 60 min. When the reaction was completed (checked via TLC, eluent: CH_2Cl_2/ CH_3OH 20 : 1), it was quenched by addition of water (15 mL) and extracted with AcOEt (5 × 15 mL). The combined organic layers were dried over anhydrous Na_2SO_4, filtered and the solvent removed under reduced pressure. The crude

material was purified on preparative TLC plates (eluent: CH_2Cl_2/ CH_3OH 9 : 1) giving product **14** as a yellow oil. Yield: 67%; **^{1}H NMR** (300 MHz, CD_3OD): δ = 8.21 (bs, 5H, C(O)NH), 7.77 (s, 5H, H5 triazole), 7.61 (bs, 10H, ArH), 5.38 (d, 5H, *J* = 2.7 Hz, H-4), 5.16 - 5.02 (m, 10H, H3, H2), 4.61 (d, 5H, *J* = 7.3 Hz, H1), 4.51 (t, 10H, *J* = 5.0 Hz, $OCH_2C\underline{H}_2$-triazole), 4.20 - 4.05 (m, 15H, H5, H6a, H6b), 3.94 (bs, 10H, $ArC\underline{H}_2Ar$), 3.88 - 3.77 (m, 15H, $OC\underline{H}_2CH_2$-triazole, β-COCHa), 3.70 - 3.44 (m, 105H, OCH2, β-COCHb, $C(O)NHC\underline{H}_2$), 3.29 (s, 15H, $ArOC\underline{H}_3$), 2.67 (t, 10H, *J* = 7.6 Hz, triazole-$C\underline{H}_2CH_2CH_2$), 2.13 (s, 15H, Ac), 2.02 (s, 15H, Ac), 2.01 (s, 15H, Ac), 1.94 (s, 15H, Ac), 1.71 - 1.59 (m, 10H, triazole-$CH_2C\underline{H}_2CH_2$), 1.59 - 1.47 (m, 10H, β-$COCH_2C\underline{H}_2$), 1.40 - 1.23 (m, 50H, CH_2 aliphatic chain); **^{13}C NMR** (75 MHz, CD_3OD): δ = 172.0, 171.5, 171.2 (Ac), 169.6 (C(O)NH), 160.9 (Ar-ipso), 149.0 (C4 triazole), 135.8 (Ar-ortho), 130.7 (Ar-para), 129.7 (Ar-meta), 123.9 (C5 triazole), 102.2 (C1), 72.4 (C3), 71.7 (C5), 71.5, 71.4, 71.3, 70.9 (OCH_2), 70.6 ($O\underline{C}H_2CH_2$-triazole), 70.5 (C2), 68.8 (C4), 62.6 (C6), 61.5 ($ArO\underline{C}H_3$), 51.3 ($OCH_2\underline{C}H_2$-triazole), 41.0 ($C(O)NH\underline{C}H_2$), 32.0 ($Ar\underline{C}H_2Ar$), 30.6, 30.4, 30.2 (CH_2 aliphatic chain), 27.0 (triazole-$\underline{C}H_2CH_2CH_2$), 26.3 (CH_2 aliphatic chain), 20.8, 20.6, 20.5 ($\underline{C}H_3C(O)$); **MS**(HR-ESI+): m/z = 1607.7872 [100% $(M+3Na)^{3+}$], calcd: 1607.7813.

Peracetylated-lactosylcalix[5]arene (**15**)

Calix[5]arene **8** (27.5 mg, 12.0 μmol) and the *β*-lactoside compound **13** (70.0 mg, 89.0 μmol) were dissolved in 2.5 mL DMF in a microwave tube. $CuSO_4 \cdot 5H_2O$ (2.6 mg, 10.4 μmol), sodium ascorbate (4.4 mg, 22.2 μmol) and 0.5 mL H_2O were then added. The mixture was heated at 80 °C by microwave irradiation (150 W) for 60 min. When the reaction was completed (checked via TLC, eluent: CH_2Cl_2/ CH_3OH 94 : 6), it was quenched by addition of water (15 mL) and extracted with AcOEt (5 × 15 mL). The combined organic layers were dried over anhydrous Na_2SO_4, filtered and the solvent removed *in vacuo*. The crude was purified by flash chromatography (elution in gradient: CH_2Cl_2/ CH_3OH 96 : 4 → 95 : 5) giving product **15** as a yellow oil. Yield: 57%; **^{1}H NMR** (300 MHz, $CDCl_3$): δ = 7.46 (bs, 10H, ArH), 7.40 (s, 5H, H5 triazole), 6.83 (bs, 5H, C(O)N$\underline{H}$), 5.33 (d, 5H, *J* = 3.3 Hz, H4'), 5.17 (t, 5H, *J* = 9.3 Hz, H3), 5.09 (dd, 5H, $J_{1'\text{-}2}$' = 7.9 Hz, $J_{2'\text{-}3'}$ = 10.4 Hz, H2'), 4.93 (dd, 5H, $J_{2'\text{-}3'}$ = 10.4 Hz , $J_{3'\text{-}4'}$ = 3.3 Hz, H3'), 4.86 (dd, 5H, $J_{2\text{-}3}$ = 9.3 Hz, $J_{1\text{-}2}$ = 8.1 Hz, H2), 4.50 - 4.38 (m, 25H, H1', H1, H6a, $OCH_2C\underline{H}_2$-triazole), 4.15 - 4.00 (m, 15H, H6b, H6a', H6b'), 3.90 - 3.71 (m, 35H, H5', H4, *β*-COCHa, $ArC\underline{H}_2Ar$, $OC\underline{H}_2CH_2$-triazole), 3.65 - 3.47 (m, 105H, OCH_2, H5, $C(O)NHC\underline{H}_2$), 3.42 (m, 5H, *β*-COCHb), 3.21 (s, 15H, $ArOCH_3$), 2.65 (t, 10H, *J* = 7.7 Hz, triazole-$C\underline{H}_2CH_2CH_2$), 2.12 (s, 15H, Ac),

2.09 (s, 15H, Ac), 2.04 - 1.98 (m, 60H, Ac), 1.94 (s, 15H, Ac), 1.65 -,1.55 (m, 10H, triazole-$CH_2C\underline{H}_2CH_2$), 1.55 - 1.44 (m, 10H, β-$COCH_2C\underline{H}_2$), 1.39 - 1.15 (m, 50H, CH_2 aliphatic chain); **^{13}C NMR** (100 MHz, $CDCl_3$): δ = 170.4, 170.3, 170.2, 170.1, 169.8, 169.6, 169.1 (Ac); 167.3 ($\underline{C}$(O)NH), 159.2 (Ar-ipso), 148.2 (C4 triazole), 134.2 (Ar-ortho), 129.9 (Ar-para), 128.2 (Ar-meta), 121.7 (C5 triazole), 101.1 (C1'), 100.6 (C1), 76.3 (C4), 72.8 (C3), 72.5 (C5), 71.7 (C2), 71.0 (C3'), 70.6 (C5'), 70.5 (OCH_2), 70.2 (β-$CO\underline{C}$H2), 69.8 (OCH_2), 69.6 ($O\underline{C}H_2CH_2$-triazole), 69.1 (C2'), 66.6 (C4'), 62.1 (C6), 60.8 (C6'), 60.7 ($ArO\underline{C}H_3$), 50.0 ($OCH_2\underline{C}H_2$-triazole), 39.7 (C(O)$NH\underline{C}H_2$), 31.0 ($Ar\underline{C}H_2Ar$), 29.5, 29.3, 25.8, 25.7 (CH_2 aliphatic chain), 20.9, 20.8, 20.6, 20.5 ($\underline{C}H_3C(O)$); **MS** (HR-ESI+): m/z = 1571.9445 [100% $(M+4Na)^{4+}$], calcd: 1571.940.

Galactosylcalix[5]arene (**16**)

The peracetylated-galactosylcalix[5]arene **14** (45.0 mg, 9.46 μmol) was dissolved in 5 mL of CH_3OH, dropwise a freshly prepared MeONa in methanol solution was added till pH 8 - 9. The mixture was stirred at room temperature for 4 h. The progress of the reaction was monitored via ESI-MS analysis. Amberlite resin IR 120/H^+ was subsequently added to quench the reaction, and the mixture was gently stirred for 30 min. until neutral pH was reached. The resin was then filtered off and the solvent removed under reduced pressure to give pure product **16** as a yellow oil. Yield. 90%; **^{1}H NMR** (300 MHz, CD_3OD): δ = 8.23 (bs, 5H, C(O)NH), 7.77 (s, 5H, H5 triazole), 7.61 (s, 10H, ArH), 4.51 (t, 10H, *J* = 5.0 Hz , $OCH_2C\underline{H}_2$-triazole), 4.20 (d, 5H, *J* = 7.1 Hz, H1), 3.94 (bs, 10H, $ArC\underline{H}_2Ar$), 3.92-3.80 (m, 20H, H4, *β*-COCHa, $OC\underline{H}_2CH_2$-triazole), 7.77 - 7.69 (m, 10H, H6a, H6b), 3.66 - 3.40 (m, 120H, β-COCHb, H2, H3, H5, OCH_2, C(O)$NHC\underline{H}_2$), 3.29 (s, 15H, OCH_3), 2.67 (t, 10H, *J* = 7.6 Hz, triazole-$C\underline{H}_2CH_2CH_2$), 1.72 - 1.53 (m, 20H, triazole-$CH_2C\underline{H}_2CH_2$, *β*-$COCH_2C\underline{H}_2$), 1.44 - 1.24 (m, 50H, CH_2 aliphatic chain); **^{13}C NMR** (75 MHz, CD_3OD): δ = 169.6 (C(O)NH), 160.9 (Ar-ipso), 149.0 (C4triazole), 135.8 (Ar-ortho), 130.7 (Ar-para), 129.7 (Ar-meta), 124.0 (C5 triazole), 105.0 (C1), 76.6, 75.1, 72.6 (C2, C3, C5), 71.5, 71.4, 71.3, 70.8, 70.6, 70.4, 70.3 (OCH_2, β-$CO\underline{C}H_2$, C4), 62.5 (C6), 61.5 ($ArO\underline{C}H_3$), 51.3 ($OCH_2\underline{C}H_2$-triazole), 41.0 (C(O)$NH\underline{C}H_2$), 32.0 ($Ar\underline{C}H_2Ar$), 30.8, 30.6, 30.5, 30.4, 30.3, 27.1 (CH_2 aliphatic chain), 26.3 (triazole-$\underline{C}H_2CH_2CH_2$); **MS** (HR-ESI+): m/z = 1305.0569 [100% $(M+3H)^{3+}$], calcd: 1305.0601.

Lactosylcalix[5]arene (**17**)

The peracetylated-lactosylcalix[5]arene **15** (42.0 mg, 6.8 μmol) was dissolved in 5 mL of CH_3OH, and drops of a freshly prepared methanol solution of MeONa

were added till pH 8-9. The mixture was stirred at room temperature for 18 h. The progress of the reaction was monitored via ESI-MS analysis. Amberlite resin IR 120/H^+ was subsequently added for quenching, and the mixture was gently stirred for 30 min. till neutral pH. The resin was then filtered off and the solvent removed under reduced pressure to give pure product **17** as a yellow oil. Yield: 72%; **^{1}H NMR** (300 MHz, CD_3OD): δ = 7.79 (s, 5H, H5 triazole); 7.60 (s, 10H, ArH), 4.51 (t, 10H, *J* = 5.0 Hz, $OCH_2C\underline{H}_2$-triazole), 4.35 (d, 5H, *J* = 7.3 Hz, H1'), 4.26 (d, 5H, *J* = 7.8 Hz, H1), 3.93 (bs, 10H, $ArC\underline{H}_2Ar$), 3.90 - 3.65 (m, 40H, H4', H6ab', H6ab, Glc β-COC<u>Ha</u>, $OC\underline{H}_2CH_2$-triazole), 3.65 - 3.35 (m, 135H, H3, H4, H5, H2', H3', H5', Glc β-COC<u>Hb</u>, OCH_2, $C(O)NHCH_2$), 3.28 (s, 15H, OCH_3), 3.23 (t, 5H, *J* = 8.4 Hz , H2), 2.66 (t, 10H, *J* = 7.6 Hz, triazole-$C\underline{H}_2CH_2CH_2$), 1.69 - 1.53 (m, 20H, CH_2 aliphatic chain), 1.42 - 1.23 (m, 50H, CH_2 aliphatic chain); **^{13}C NMR** (75 MHz, CD_3OD): δ ppm = 169.6 (C(O)NH), 160.9 (Ar-ipso), 148.8 (C4 triazole), 135.7 (Ar-ortho), 130.7 (Ar-para), 129.7 (Ar-meta), 124.2 (C5 triazole), 105.1 (C1'), 104.2 (C1), 80.7 (C4), 77.0, 76.5, 76.4, 74.8, 74.7, 72.5 (C2, C3, C5, C2', C3', C5'), 71.5, 71.4, 71.3, 70.9, 70.6, 70.4 (OCH_2, β-$CO\underline{C}H_2$,), 70.3 (C4'), 62.5, 61.9 (C6, C6'), 61.5 ($ArO\underline{C}H_3$), 51.4 ($OCH_2\underline{C}H_2$-triazole), 41.0 ($C(O)NH\underline{C}H_2$), 32.0 ($Ar\underline{C}H_2Ar$), 30.8, 30.6, 30.5, 30.4, 30.2, 27.1 (CH_2 aliphatic chain), 26.2 (triazole-$\underline{C}H_2CH_2CH_2$); **MS** (HR-ESI+) m/z = 1575.1475 [100% $(M+3H)^{3+}$], calcd = 1575.1481.

17-Azide-3,6,9,12,15-pentaoxaheptadecane-1-aminocarbonyl-p-methoxybenzene (**19**) Oxalyl chloride (1.5 mL, 16.0 mmol) was added to a solution of 4-methoxybenzoic acid (0.30 g, 2.0 mmol) in 15 mL of dry CH_2Cl_2 and the mixture was stirred at room temperature under N_2 for 18 h. The solvent was then removed under reduced pressure and the residue dissolved again in 5 mL of dry CH_2Cl_2. This solution was added dropwise to a round bottomed flask containing the azidoamine compound **7** (0.91 g, 3.0 mmol) and NEt_3 (0.5 mL, 3.0 mmol) in 10 mL of dry CH_2Cl_2. The mixture was let react for 20 h at room temperature under N_2 atmosphere. The reaction was monitored via TLC (eluent: AcOEt). A 1 M HCl solution (20 mL) was then added to quench the reaction, and the product extracted with CH_2Cl_2 (2 × 20 mL). The combined organic phases were washed with $NaHCO_3$ saturated aqueous solution (15 mL), brine (15 mL), water (15 mL), dried over anhydrous Na_2SO_4, filtered and the solvent evaporated under reduced pressure. The crude was purified by flash chromatography (eluent: AcOEt/acetone 9 : 1). Product **19** was obtained pure as a yellow oil. Yield: 20%; **^{1}H NMR** (300 MHz, $CDCl_3$): δ (ppm) 7.74 (d, 2H, *J* = 8.9 Hz, Ar-meta); 6.87 (d, 2H, *J* = 8.9 Hz, Ar-ortho); 6.78 (bs, 1H, C(O)NH); 3.80 (s, 3H, OCH_3);

3.65 - 3.54 (m, 22H, OCH_2, C(O)NHC$\underline{H}_2$); 3.32 (t, 2H, *J* = 5.0 Hz, C$\underline{H}_2N_3$); **^{13}C NMR** (75 MHz, $CDCl_3$): δ ppm 167.0 (Ac); 162.0 (Ar-ipso); 128.8 (Ar-meta); 126.9 (Ar-para); 113.6 (Ar-ortho); 70.6, 70.5, 70.2, 70.0, 69.9 (OCH_2); 55.4 (OCH_3); 50.6 (CH_2N_3); 39.7 (C(O)NH$\underline{C}H_2$); **MS** (ESI+) m/z = 463.0 [100% $(M+Na)^+$]; 435.0 [60% $(M-N_2+Na)^+$].

GM1os-monomer (**20**)

Starting from compounds **19** and **9**, following the same procedure as for compound **1**, and using reversed phase column chromatography for the purification (gradient MeOH/ H_2O/ AcOH), monomer **20** was obtained as a white solid in 49% yield. **^{1}H NMR** (D_2O, 400 MHz): δ = 7.81 (3H, m, triazole, Ar), 6.98 (2H, d, *J* = 8.4 Hz, Ar), 4.71 (1H, s, H1-GalNAc), 4.39 (1H, d, *J* = 8.4 Hz, H1-Gal'), 4.42 (1H, m, H1-Gal), 4.38 (1H, m), 4.31, (1H, d, *J* = 8.2 Hz, H1-Glc), 4.05-4.01 (3H, m), 3.93 (1H, m, H2-GalNAc), 3.75 - 3.40 (21H, m) , 3.60-3.47 (16H, m), 3.36-3.28 (14H, m), 3.25 (1H, m, H2-Gal), 3.18 (1H, m, H2-Glc), 3.10 (2H, s), 2.54 (1H, m, H3a-Neu5Ac), 2.35 (2H, m, C$\underline{H}_2$-triazole), 1.92 (3H, s, NHC(O)C$\underline{H}_3$-Neu5Ac), 1.85 (3H, s, NHC(O)C$\underline{H}_3$-GalNAc), 1.75 (1H, m, H3b-Neu5Ac), 1.40 (4H, m), 1.11 (2H, m, Glc β-$COCH_2C\underline{H}_2$), 1.03 (8H, m, -$CH_2C\underline{H}_2CH_2$-); **^{13}C NMR** (D_2O, 75 MHz): δ (ppm) 174.8, 174.5, 173.9, 168.5, 159.2, 128.4 (2 x CH Ar), 123.1 (C4 triazole), 113.2 (2 × CH Ar) 104.6 (C1-Gal'), 102.7 (C1-Gal), 102.4 (C1-GalNAc), 102.0 (C1-Glc), 101.5 (C2-Neu5Ac), 80.2 (C3-GalNAc), 78.5 (C4-Glc), 77.0 (C4-Gal), 74.7, 74.6, 74.4, 74.2, 74.1, 74.0, 73.9 (C2 Glc), 72.6 (C3 Gal'), 72.3, 72.1 (C2-Gal'), 70.6 (Glc β-$CO\underline{C}H_2$), 70.4 (C2-Gal), 70.4 - 68.5 (-OCH_2-, PEG, Glc β-$CO\underline{C}H_2$), 68.4 (C4-GalNAc), 67.8, 62.7, 60.9, 60.8, 60.4, 60.0, 51.4, 51.0 (C2 GalNAc), 49.8, 39.5, 36.7, 28.8 - 28.3 ($CH_2\underline{C}H_2CH_2$), 25.0 (Glc β-$COCH_2C\underline{H}_2$), 24.5 ($\underline{C}H_2$-triazole), 22.5 (NHC(O)$\underline{C}H_3$-GalNAc), 21.9 (NH(O)$\underline{C}H_3$-Neu5Ac); **MS** (HR-ESI-) m/z: 1587.7009 [100% $(M-H)^-$], calcd = 1587.7034.

CTB5 inhibition assays

Each well of a 96-well microtiter plate was coated with a 100 µL native GM1 solution (1.3 µM in ethanol) after which the solvent was evaporated. Unattached GM1 was removed by washing with PBS (3 × 450 µL), the remaining free binding sites were blocked by incubation with 100 µL of a 1% (w/v) BSA solution in PBS for 30 min. at 37 °C. Detection limits were determined by placing CT-horseradish peroxidase conjugate (CT-HRP), without inhibitor, on the plate, which gives the highest response, and the lowest response was determined by the optical density of the blank, *i.e.* the native GM1-coated well with all components except the inhibitor and toxin. These two values represent the minimum and the maximum

values of optical density, 0% and 100% of binding of the CT to the GM1-coating of the wells. Subsequently, the wells were washed with PBS (3 × 450 µL). In separate vials, a logarithmic serial dilution, starting from 2.0 mM, of 150 µL saccharide-calixarenes in 0.1% BSA, 0.05% Tween-20 in PBS, mixed with 150 µL of a 50 ng/mL CTB-HRP solution in the same buffer were incubated. This gave an initial inhibitor concentration of 1.0 mM. In the case of potent inhibitors, based on the logarithmic experiments, a more accurate, serial dilution of a factor two was performed around the expected IC_{50} values. The inhibitor-toxin mixtures were incubated at room temperature for 2 h and then transferred to the coated wells. After 30 min. of incubation at room temperature, unbound CTB-HRP-calixarene complexes were removed from the wells by washing with 0.1% BSA, 0.05% Tween-20 in PBS (3 × 500 µL). 100 µL of a freshly prepared OPD solution (25 mg OPD·2HCl, 7.5 mL 0.1 M citric acid, 7.5 mL 0.1M sodium citrate and 6 µL of a 30% H_2O_2 solution, pH was adjusted to 6.0 with NaOH) was added to each well and allowed to react with HRP in absence of light, at room temperature, for 15 minutes. The oxidation reaction was quenched by addition of 50 µL 1 M H_2SO_4. Within 5 min., the absorbance was measured at 490 nm.

3.5 References

[1] World Health Organisation, W.H.O. **2011**, *Fact sheet N°107*, 2012.
[2] World Health Organisation *Weekly epidemiological record* **2011**, *86*, 325.
[3] N. Lycke, *Nat. Immunol.*, **2012**, *12*, 592.
[4] J. Holmgren and A.-M. Svennerholm, *Curr. Opin. Immunol.*, **2012**, *24*, 343.
[5] E.A. Merritt, S. Sarfaty, F. v.d. Akker, C. l'Hoir, J.A. Martial and W.G.J. Hol, *Protein Sci.*, **1994**, *3*, 166.
[6] W.E. Minke, C. Roach, W.G.J. Hol and C.L.M.J. Verlinde, *Biochemistry*, 1999, **38**, 5684.
[7] W.B. Turnbull, B.L. Precious and S.W. Homans, *J. Am. Chem. Soc.*, 2004, **126**, 1047.
[8] N. Sahyoun and P. Cuatrecasas, *Proc. Natl. Acad. Sci. U. S. A.*, 1975, **72**, 3438; M.D. Hollenberg, P.H. Fishman, V. Bennett and P. Cuatrecasas, *Proc. Natl. Acad. Sci. USA* Bernardi, J. Jiménez-Barbero, A. Casnati, C.D. Castro, T. Darbre, F. Fieschi, J. Finne, H. Funken, K.-E. Jaeger, M. Lahmann, T.K. Lindhorst, M. Marradi, P. Messner, A. Molinaro, P. Murphy, C. Nativi, S. Oscarson, S. Penadés, F. Peri, R.J. Pieters, O. Renaudet, J.-L. Reymond, B. Richichi, J. Rojo, F. Sansone, C. Schäffer, W.B. Turnbull, T. Velasco-Torrijos, S. Vidal, S. Vincent, T. Wennekes, H. Zuilhof and A. Imberty, *Chem. Soc. Rev.*, 2013, **42**, 4709; T.R. Branson and W.B. Turnbull, *Chem. Soc. Rev.*, **2013**, *42*, 4613.
[10] E. Fan, Z. Zhang, W.E. Minke, Z. Hou, C.L.M.J. Verlinde and W.G.J. Hol, *J. Am. Chem. Soc.*, **2000**, *122*, 2663.
[11] Z. Zhang, J.C. Pickens, W.G.J. Hol, E. Fan, *Org. Lett.*, **2004**, *6*, 1377.
[12] Z. Zhang, J. Liu, C.L.M.J. Verlinde, W.G.J. Hol and E. Fan, *J. Org. Chem.*, **2004**, *69*, 7737.
[13] J.P. Thompson and C.L. Schengrund, *Glycoconjugate J.*, **1997**, *14*, 837.
[14] A. Bernardi, L. Carrettoni, A. Grosso Ciponte, D. Monti and S. Sonnino, *Bioorg. Med. Chem. Lett.*, **2000**, *10*, 2197.
[15] A. Bernardi, D. Arosio, D. Potenza, I. Sànchez-Medina, S. Mari, F.J. Cañada and J.

Jiménez-Barbero, *Chem. Eur. J.*, **2004**, *10*, 4395.
[16] D. Arosio, I. Vrasidas, P. Valentini, R.M.J. Liskamp, R.J. Pieters and A. Bernardi, *Org. Biomol. Chem.*, **2004**, *2*, 2113.
[17] D. Arosio, M. Fontanella, L. Baldini, L. Mauri, A. Bernardi, A. Casnati, F. Sansone and R. Ungaro, *J. Am. Chem. Soc.*, **2005**, *127*, 3660.
[18] F. Sansone and A. Casnati, *Chem. Soc. Rev.*, **2013**, *42*, 4623-4639
[19] F. Sansone, L. Baldini, A. Casnati and R. Ungaro, *New J. Chem.*, **2010**, *34*, 2715.
[20] A. Dondoni and A. Marra, *Chem. Rev.*, **2010**, *110*, 4949.
[21] A.V. Pukin, H.M. Branderhorst, C. Sisu, C.A.G.M. Weijers, M. Gilbert, R.M.J. Liskamp, G.M. Visser, H. Zuilhof and R.J. Pieters, *ChemBioChem*, **2007**, *8*, 1500.
[22] C. Sisu, A.J. Baron, H.M. Branderhorst, S.D. Connell, C.A.G.M. Weijers, R. de Vries, E.D. Hayes, A.V. Pukin, M. Gilbert, R.J. Pieters, H. Zuilhof, G.M. Visser and W.B. Turnbull, *ChemBioChem*, **2009**, *10*, 329.
[23] D.R. Stewart, M. Krawiec, R.P. Kashyap, W.H. Watson and C.D. Gutsche, *J. Am Chem. Soc.*, **1995**, *117*, 586.
[24] D.R. Stewart and C.D. Gutsche, *Org. Prep. Proced. Int.*, **1993**, *25*, 137.
[25] S.E.J. Bell, J.K. Browne, V. McKee, M.A. McKervey, J.F. Malone, M. O'Leary and A. Walker, *J. Org. Chem.*, **1998**, *63*, 489.
[26] J.C. Duff, *J . Chem. Soc.*, **1941**, 547.
[27] W.E. Smith, *J. Org. Chem.*, **1972**, *37*, 3972.
[28] A.W. Schwabacher, J.W. Lane, M.W. Scheisher, K.M. Leigh and C.W. Johnson, *J. Org. Chem.*, **1998**, *63*, 1727.
[29] S.S. Iyer, A.S. Anderson, S. Reed, B. Swanson and J.G. Schmidt, *Tetrahedron Lett.*, **2004**, *45*, 4285.
[30] A.V. Pukin, C.A.G.M. Weijers, B. van Lagen, R. Wechselberger, B. Sun, M. Gilbert, M.-F. Karwaski, D.E.A. Florack, B.C. Jacobs, A.P. Tio-Gillen, A van Belkum, H.P. Endtz, G.M. Visser and H. Zuilhof, *Carboh. Res.*, **2008**, *343*, 636.
[31] G. Zemplén and E. Pascu, *Ber. Dtsch. Chem. Ges.*, **1929**, *62*, 1613.
[32] M. Matarella, J. Garcia-Hartjes, T. Wennekes, H. Zuilhof and J.S. Siegel, *Org. Biomol. Chem.*, **2013**, *11*, 4333.
[33] C.D. Gutsche, *Calixarenes Revisited*; Cambridge: Royal Society of Chemistry, **1998**.
[34] C.A.G.M. Weijers, M.C.R. Franssen and G.M. Visser, *Biotech. Adv.*, **2008**, *26*, 436.

4

Electronic effects versus distortion energies during strain-promoted alkyne-azide cycloadditions:

A theoretical tool to predict reaction kinetics

This chapter is published as:

Jaime Garcia-Hartjes, Jan Dommerholt, Tom Wennekes, Floris L. Van Delft, Han Zuilhof, *Eur. J. Org. Chem.* **2013**, *18*, 3712-3720, DOI: 10.1002/ejoc.201201627

Abstract:

Second-order reaction kinetics of known strain-promoted azide-alkyne cycloadditions (SPAAC) were compared with theoretical data from various ab initio methods. This produced both detailed insight into determining the reaction rates and two straightforward theoretical tools to predict a priori the reaction kinetics of novel cyclooctynes for strain-promoted cycloadditions. Multiple structural and electronic effects contribute to the reactivity of cyclooctynes with azides in cycloaddition reactions. It is therefore hard to relate a physical or electronic property directly and independently to the reactivity of the cyclooctyne. However, we show that Hartree-Fock LUMO energies, which were acquired while calculating activation energies on MP2 level of theory, correlate with second-order kinetic rate data and are therefore usable for reactivity predictions of cyclooctynes towards azides. Using this correlation we developed a simple theoretical tool to predict reaction kinetics of (novel) cyclooctynes for SPAAC reactions.

4.1 Introduction

The strain-promoted azide-alkyne cycloaddition (SPAAC) reaction is increasingly investigated for bio-orthogonal purposes. Cyclooctynes have proven valuable because of their relative biological inertness, their strain-induced high efficiency, and selectivity towards azides in cycloaddition reactions.[1] Unlike the copper-catalyzed variant of Huisgen's 1,3-dipolar cycloaddition,[2] – *i.e.* the Copper-catalyzed azide-alkyne cycloaddition reaction, which emerged over the years as the prototypical "click-reaction"[3] – there is no need for toxic additives like Cu(I). This is advantageous, since copper ions can induce undesirable side-reactions such as non-specific binding to thiol groups and oxidative damage that both Cu(I) and Cu(II) ions are able to inflict on biomolecules.[4] Also, since cyclooctynes are generally not reactive towards other cellular components in aqueous media, they can be used in studies on cellular level.[5]

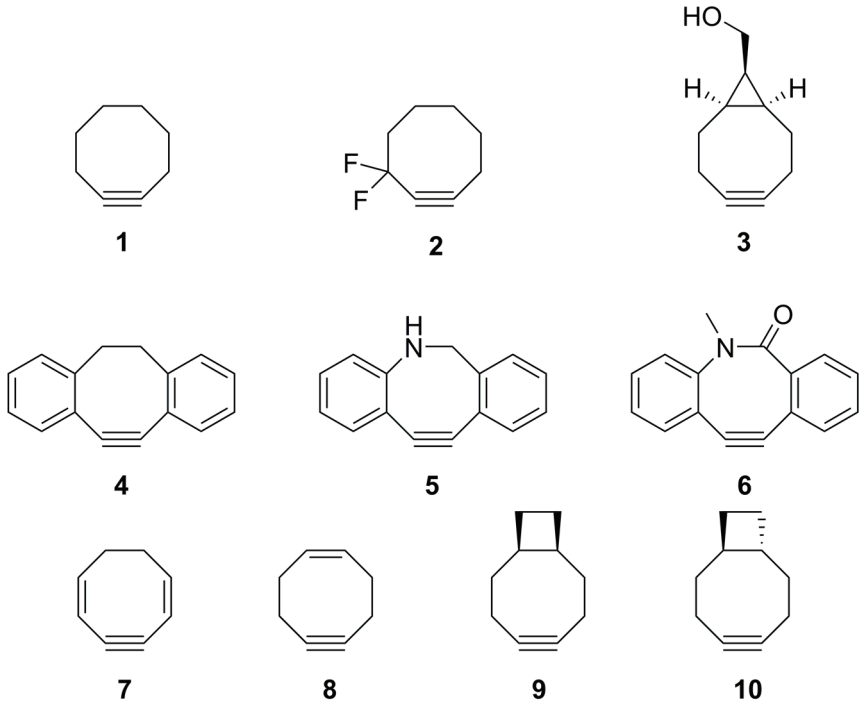

Figure 1. Cyclooctynes under study. See text for details.

In 1953, Blomquist,[6] and later, Wittig and Krebs[7] described the reaction of cyclooctyne (OCT, **1**, Figure 1) with phenyl azide as an "explosive reaction". Based

on work by Turner *et al.*[8] on ΔH of hydrogenation of unsaturated aliphatic compounds (including cyclooctyne), Bertozzi later assigned significant rate enhancements to the ring strain of 18 kcal/mol[9] for **1** compared to unstrained alkynes. Subsequently, the use of electron-poor cyclooctynes was shown to speed up the reaction significantly, specifically in 3,3-difluorocyclooct-1-yne (DIFO, **2**).[5d, 10] Dommerholt *et al.* developed bicyclo[6.1.0]non-4-yne (BCN, **3**)[11] with the additional advantage over earlier cyclooctynes that it is readily prepared and symmetrical, thus avoiding the formation of regioisomeric adducts upon cycloaddition with an organic azide (Figure 2). Apart from electron-withdrawing groups, like the fluorine groups in compound **2**, the addition of extra ring strain was also shown to be advantageous, as for example implied from the observed high rates for 3,7-dibenzocyclooctyne (DIBO) **4**.[13]

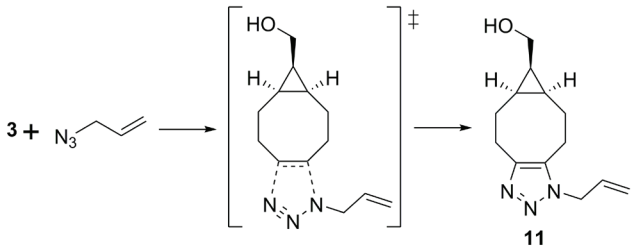

Figure 2. SPAAC of strained cyclooctyne BCN (**3**) and allyl azide, yielding triazole **11**.

In 2010, difluorobenzocylooctyne (DIFBO) was described[14] that combines the electron-withdrawing effect of the fluorine atoms of **2** with the ring strain of **4**. This compound was shown to be the most rapidly reacting cyclooctyne towards azides reported to date, but was not taken up in the current study because of its lack of stability outside a protective cyclodextrin shell. Based on the framework of **4**, two endocyclic nitrogen-containing dibenzocyclooctyne derivatives have been published. These contain either a CH_2 group and a nitrogen atom in the ring (DIBAC, compound **5**),[15, 16] or an endocyclic amide (lactam) functionality and no saturated carbon atoms in the cyclooctyne ring (BARAC, compound **6**).[17] Kinetic data are available for **2** - **6** as summarized in Table 1, while the kintetic data of **1** is only available for an analogue that contains an alkoxy moiety at the 3-position.[9] Therefore, we performed our own kinetic study on compound **1** (*vide infra*). Compound **7** was described in literature,[12] but not in reaction with azides. Compounds **8** - **10** are strained models that have not been described in literature at the time of writing.

Relatively little theoretical work has been published up to now that correlates experimental and calculated data of these strain-promoted cycloadditions. Various

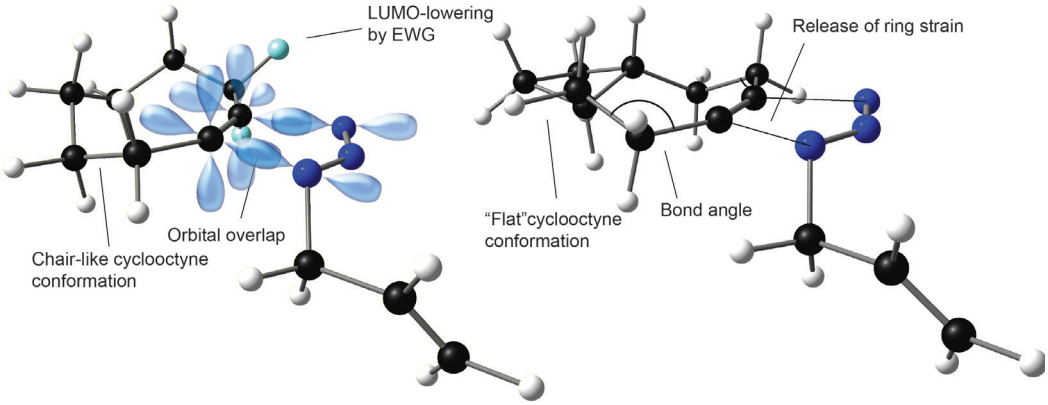

Figure 3. Various properties of the cycloocytnes that influence their SPAAC reaction kinetics; left) Transition state conformation of DIFO (**2**); right) *trans*-cyclobutyl-substituted **10** with allyl azide.

properties are known to influence the reaction kinetics of these cyclooctynes in SPAAC reactions (Figure 3). For example, Houk and co-workers performed B3LYP/6-31G(d) optimizations to compare the reactivity of **1** and **2**,[19] which were more recently complimented with a more extensive series of SCS-MP2/6-311G(d) single-point computations on B3LYP-optimized geometries.[20] These studies concluded that the difference in the reactivity of various cyclooctynes is based on the difference in distortion energies of the alkynes, which is required to deform it from the reactant geometry to the geometry it has in the transition state (TS). In addition, the ring strain in cyclooctynes has been investigated systematically by Bach with B3LYP/6-311+G(3df,2p) calculations.[21] He calculated that the barrier for cycloaddition of benzyl azide and DIFO (**2**) is 2.3 kcal/mol lower than addition to OCT (**1**). This method was also used to investigate the trends in activation barriers for the 1,3-dipolar cycloadditions of azides with various cyclooctynes, dibenzocyclooctynes

Table 1. Experimental data of SPAAC second-order reaction kinetics of cyclooctynes with benzyl azide.

Compound	k [$\cdot 10^{-3}$ $M^{-1} \cdot s^{-1}$]	Solvent	Reference
1	5.8	CD_3CN/D_2O	a
2	76	CH_3CN	[5d]
3	140	CD_3CN/D_2O	[11]
4	170	CD_3OD	[13]
	120	CD_3CN	[18]
5	310	CD_3OD	[15]
6	960	CH_3CN	[17]

[a] Current work; see Appendix II for details.

and azacyclooctynes. Subsequently, Goddard and co-workers concluded that proper placement (*e.g.* on the position next to the *sp*-hybridized alkyne carbons) of electron-withdrawing substituents leads to LUMO-lowering effects on the alkyne, and that this is accompanied by higher reactivity of cyclooctynes towards cycloaddition with azides.[22]

Houk *et al.* showed an approximately 2 kcal/mol increase in reactivity of DIFO (**2**) with respect to the parent compound OCT (**1**). Gold *et al.* confirmed this finding and elaborated with Natural Bond Order (NBO) analyses that showed that hyper-conjugative donation of the alkyne π-system to the σ*C−F orbital directly leads to the TS stabilization via assistance in alkyne bending,[23] which is the apparent drive for the 50-fold increase of reactivity of DIFO (**2**), together with the LUMO-lowering effect, described by Goddard earlier. Both Gold and Goddard pleaded for the strategy of lowering the energy of the TS to increase reactivity towards azides rather than reactant destabilization. In case of DIFO, increased reactivity is a direct result of E_a lowering. Gold and co-workers hinted at a theoretical tool to predict reactivity in the form of a combination of the above described calculable molecule properties.

Recently, the reaction kinetics of BARAC (**6**) derivatives were shown to vary depending on the addition of several substituents.[24] The reaction kinetics of the derivatives were subsequently compared with B3LYP/6-31G(d) calculations. It was found that addition of fluorine groups on the aryl-groups of BARAC (**6**), resulted in an increase in reactivity of ~ 75% compared to its parent compound (**6**). By using B3LYP calculations, this was attributed to increased stabilizing interaction energy in the TS. In the same study, a decrease in the alkyne bond angle was correlated to an increase in reactivity. The authors suggested that the calculated TS distortion and interaction energies could be used in the design of novel cyclooctynes.

To date, however, a generally applicable computational tool to correlate the structures of these cyclooctynes to their reaction kinetics, has not yet been described. In the current paper, we will focus in more detail on the transition states of SPAAC reactions, and describe tools that predict *a priori* the reaction kinetics of novel cyclooctynes for application in these cycloaddition reactions. Given the still growing interest in SPAAC reactions, it is highly desirable to have a simple theoretical tool that can predict the reactivity of novel, hypothetical cyclooctynes. Up till now, scientists have mainly focused on the development of faster reacting cyclooctynes. However, the cost of increased reactivity is often paid by decreased stability. This is for example seen in DIBO (**4**)[13] that needs to be stored while deprived of light and oxygen. The decreased

stability of highly reactive cyclooctynes hampers the further development of SPAAC reactions in material sciences like, in our own experience, in the development of biosensors.[26] Additionally, these compounds with a high intrinsic energy are prone to lose their selective reactivity, by also being able to undergo – apart from SPAAC reactions – *e.g.* a thiol-yne reaction with cysteines, which would complicate the application of these cyclooctynes in biosciences. The ability to tune the reactivity of cyclooctynes by combining an increase in reactant stability with a high efficiency during SPAAC, is therefore of paramount importance in both biological and material sciences.[25] Hence, it would be advantageous if the design of novel cyclooctynes with, for example, additional groups that increase the water solubility, could be guided by predicting their reactivity before going through the effort of synthesizing them.

We here present precisely this: a theoretical tool that can accurately predict SPAAC reaction kinetics. Furthermore, we describe an even simpler, though less accurate, tool to be used by non-theoreticians that only requires a ChemDraw-like chemical structure as input to quickly give an indication of the reactivity of new cyclooctynes before they are actually developed. In the here presented study, we further elucidate the relationship between SPAAC kinetics and cyclooctyne electronic properties, by investigating the SPAAC transition state structures and energies for a structurally diverse set of ten cyclooctynes (**1** - **10**; Figure 1). This was performed with a combination of DFT (B3LYP[27], M06-2X[28]) and SCS-MP2[29] calculations. Among the ten selected cyclooctynes, six (**1** - **6**) have been previously used in SPAAC reactions and four (**7** - **10**) have not been used yet. Finally, to improve the benchmarking of our calculations additional competition experiments and kinetic constant determinations were performed on cyclooctynes **1 - 3**.

4.2 Computational and experimental methods

Calculations were performed using the Gaussian 09 set of programs.[30] Structures (reactants and transition states) were optimized, and the resulting geometries were shown to be real minima or transition states on the potential energy surface via vibrational frequency computations. The standard IEFPCM dielectric continuum solvent model for MeOH with UA0 radii was used. Optimization was consistently performed using the 6-311G(d,p) basis set, at the B3LYP, M06-2X, and MP2 levels of theory. Following the optimization, single-point energies were obtained using the 6-311+G(2d,2p) basis set for all these three methods,

while for the MP2-optimized geometries SCS-MP2 energies were obtained.[29b] Zero-point energies were included in all values. Geometries and vibrations were visualized using Gaussview 4. The syntheses of **1** and allyl azide were performed as described in Appendix. Determination of the reaction kinetics of unsubstituted cyclooctyne (**1**) with benzyl azide was performed according to literature,[11] as described in detail in the Appendix II. Competition experiments of **1**, benzyl azide and allyl azide were performed as described in the Appendix II.

4.3 Results and Discussion

4.3.1. Alkyne-azide cycloadditions

Table 2 depicts the activation energies obtained from calculations with B3LYP, M06-2X, and SCS-MP2 methods for the ten cyclooctynes under investigation. Since all compounds obviously contain strain, triple-ζ [6-311G(d,p)] basis sets were employed for the optimizations, while the single-point energy calculations involved the flexible 6-311+G(2d,2p) basis sets. From experimental studies on reaction kinetics, it is well-known that **3** reacts appreciably faster than **2** and at least an order of magnitude faster than **1** (Table 1). Originally, **1** was published including an alkoxy substituent on the 3-position.[9] The kinetic reaction rate was also published for this compound ($k = 2.4 \times 10^{-3}$ $M^{-1} \cdot s^{-1}$) but considering that the 3-substituent may induce both in the comparison with the calculated activation energy. Therefore, **1** was synthesized (see Appendix II for experimental details). The rate of **1** in the SPAAC reaction with benzyl azide was determined to be $k = 5.8 \times 10^{-3}$ $M^{-1} \cdot s^{-1}$ in CD_3CN/ D_2O (3 : 1).

All currently available kinetic data for the reaction of cyclooctynes **1** - **6** and azides are presented in Table 1, and range over more than two orders of magnitude. The approximate order of experimental reactivity of these compounds in various media is **6** > **5** > **4** ≈ **3** > **2** > **1**. This order was, however, not borne out by B3LYP-based calculations that yielded the relative order of **2** > **1** > **6** > **3** > **5** > **4**. To check whether this discrepancy could be remedied by another DFT functional, thereby keeping the computational advantage of the relatively fast density functional theory, Truhlar's M06-2X functional was employed. However, also the M06-2X functional was unable to reproduce the correct qualitative trend, and yielded a rate order **6** > **5** ≈ **2** > **1** ≈ **3** > **4**.

In contrast, MP2 calculations did follow the order of reactivity (Appendix

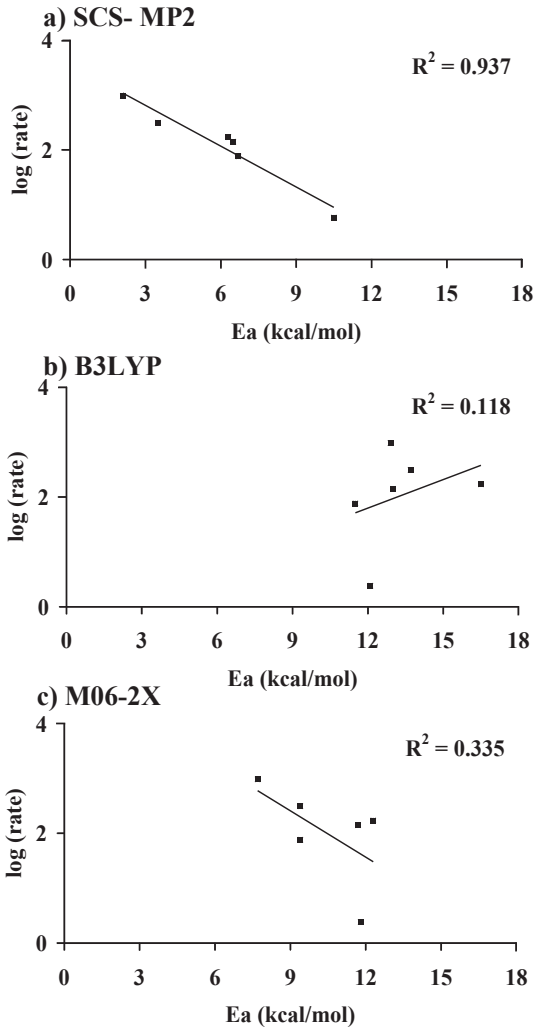

Figure 4. Plot of the logarithm of experimental second-order rate constants (see Table 1 for references) versus calculated activation energies obtained from (a) SCS-MP2/6-311+G(2d,2p)//MP2/6-311G(d,p), (b) B3LYP/6-311+G(2d,2p)//B3LYP/6-311G(d,p), and (c) M06-2X/6-311+G(2d,2p)//M06-2X/6-311G(d,p) calculations.

II Figure S6), but produced incorrect, negative, activation energies. When, however, scaled to SCS-MP2 (Figure 4a), the calculations could properly mimic the complete experimental trend in relative reactivities and also produced realistic activation energies (Table 2). For example, it was clear from these calculations that **6** was the fastest in reacting with azides and **1** the slowest. Application of this method on compounds **7** - **10** confirms the role of ring strain in determining the height of the SPAAC activation energy barrier.

Table 2. Calculated activation energies (kcal·mol-1) in the gas phase and in MeOH (IEFPCM solvent model), of the SPAAC reaction for the studied cyclooctynes with allyl azide (A) or benzyl azide (B) obtained via SCS-MP2, B3LYP, and M06-2X calculations (see text for details).

Compound	SCS-MP2		B3LYP		M06-2X	
	Gas	MeOH	Gas	MeOH	Gas	MeOH
1 + A	10.5	11.3	12.1	13.2	11.8	13.0
1 + B	9.6	10.5	11.9	8.2	11.1	12.7
2 + A[a]	6.7	6.4	11.5	11.6	9.4	9.7
2 + B[a]	6.3	6.0	11.6	11.9	9.6	9.9
3 + A	6.5	7.4	13.0	14.1	11.7	12.9
3 + B	6.2	7.1	ND		ND	
4 + A	6.3	7.7	16.5	17.9	12.3	13.9
4 + B	5.7	7.7	15.0	11.6	11.5	13.4
5 + A	3.5	5.2	13.7	15.4	9.4	11.2
6 + A	2.1	3.5	12.9	14.5	7.7	9.5
7 + A	5.7	6.3	12.0	12.9	10.8	11.6
7 + B	5.4	5.9	12.1	7.9	10.8	11.8
8 + A	8.6	9.5	13.8	15.1	12.6	14.1
9 + A	7.5	8.7	13.3	14.6	12.2	13.8
10 + A	9.6	10.7	15.2	16.5	12.6	14.1

[a] Only 1,4-addition (trans) transition states were calculated. ND = Not Determined.

Increasing the cyclooctyne ring strain in **7** and **8** via inclusion of sp^2-hybridized carbon atoms predicted a significantly increased reactivity towards cycloaddition with azides compared to **1**. Comparison of compound **7** with **4** shows that an increased size of the conjugated system also plays an important role in lowering the activation energy barrier. Both **7** and **4** have a similar ring strain, but **4** has a more extended π-electron system. Next to the ring strain and size of the conjugated system, also conformational stabilities affect the cyclooctyne reactivity. For example, the *trans*-cyclobutyl moiety in **10** restricts the eight-membered ring conformation

to a flattened structure (Figure 3). This impedes the formation of the chair-like conformation that the eight-membered ring in cyclooctynes preferentially adopts in the TS of SPAAC reactions, as is shown for **2**. The analogous *cis*-cyclobutyl-containing **9** adopts a chair conformation and is correspondingly calculated to be more reactive than **10** (see Table 2, and Appendix II Figure S7 for TS geometries).

4.3.2. Transition state activation energies

Figure 4 shows plots of the logarithm of experimental second-order rate constants against the calculated activation energies as obtained by SCS-MP2, B3LYP, and M06-2X calculations. Obviously, the correlations of the experimental rates with B3LYP data (R^2= 0.118) and M06-2X data (R^2 = 0.335) are insufficient to be used in predicting the reaction kinetics of novel cyclooctynes. Given also the significant differences in TS geometries (cf. Figure 6), doubts rise concerning the use of DFT-derived geometries for single-point activation energy determinations. In contrast, when the experimental rate constants were plotted against SCS-MP2 calculated activation energies, using MP2-derived geometries in the gas phase, a clear linear relation with good correlation was found (R^2 = 0.937). The correlation was lower between the SCS-MP2 activation energies in MeOH and the experimental rate constants (Appendix II Figure S8). The used solvent model, however, only provides a rough approximation of the complex interactions between MeOH and molecules in the TS, which probably results in less accurate calculated activation energies.

The correlation between the experimental and computational, gas phase, data might even improve further if the experimental data were determined for one solvent system, which is currently not the case (see Table 1). For example, the experimental data for compounds **3**, **4**, and **5** were reported in protic solvents, which are known to speed up the reaction with respect to acetonitrile.[18] Nevertheless, the found high linear correlation showed that SCS-MP2 data was suitable for use in our evisaged predictive tool. In the remainder of this study we therefore limited ourselves to MP2-optimized geometries and the SCS-MP2 energies thereof. SPAAC rate constants found in the literature have mostly been experimentally determined with benzyl azide as the model compound (Table 1). The number of carbon atoms makes the vibrational frequency calculations on the TS of benzyl azide and a cyclooctyne rather time-consuming to track computationally via Møller-Plesset type calculations. Therefore, we studied the TS properties with allyl azide as well, both theoretically and experimentally. Kinetic data on benzyl

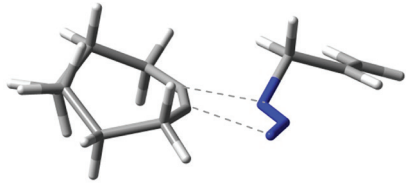

OCT (**1**)	∠ N_3	138.0 º	D N^{term}-C^1	2.10 Å
	∠ C^1-C^2-CH_2	150.0 º	d N^{int}-C^2	2.11 Å
	∠ C^2-C^1-CH_2	153.2 º	d C≡C	1.25 Å

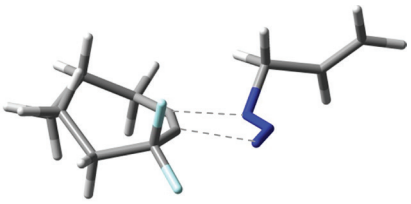

DIFO (**2**)	∠ N_3	137.5 º	d N^{term}-C^1	2.05 Å
	∠ C^1-C^2-CH_2	150.6 º	d N^{int}-C^2	2.07 Å
	∠ C^2-C^1-CF_2	150.0 º	d C≡C	1.26 Å

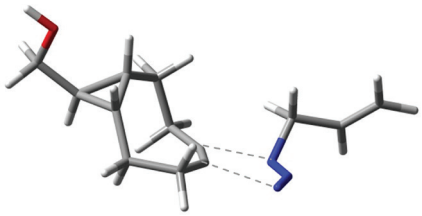

BCN (**3**)	∠ N_3	143.0 º	d N^{term}-C^1	2.19 Å
	∠ C^1-C^2-CH_2	145.8 º	d N^{int}-C^2	2.18 Å
	∠ C^2-C^1-CH_2	145.2 º	d C≡C	1.25 Å

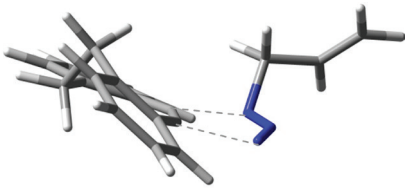

DIBO (**4**)	∠ N_3	136.7 º	d N^{term}-C^1	2.07 Å
	∠ C^1-C^2-C	147.8 º	d N^{int}-C^2	2.04 Å
	∠ C^2-C^1-C	150.0 º	d C≡C	1.27 Å

Figure 5. left) TS geometry of compounds **1** - **4** with allyl azide; right) Structural data that was obtained from MP2/6-311G(d,p) optimization.

azide and allyl azide reactivity with **1** were obtained from second-order rate constant experiments. A five-fold excess of a 1 : 1 mixture of allyl azide and benzyl azide was reacted competitively with compound **1** in CD_3CN/ D_2O (3 : 1), and in a separate experiment with compound **3**. As the product ratios of the allyl and benzyl triazole products were 1 : 1.3 and 1 : 1.4, respectively (see Appendix II), it is clear that the reaction of allyl azide can be compared accurately with that of benzyl azide. This was confirmed computationally: for compounds **1** - **4** the barriers were computed for both allyl azide and benzyl azide, and the difference between allyl azide and benzyl azide was < 0.9 kcal·mol^{-1} for all four cases, with the barrier of benzyl azide consistently lower than that of allyl azide (Table 2). Also, the TS geometries for these two systems are highly similar. For example, in

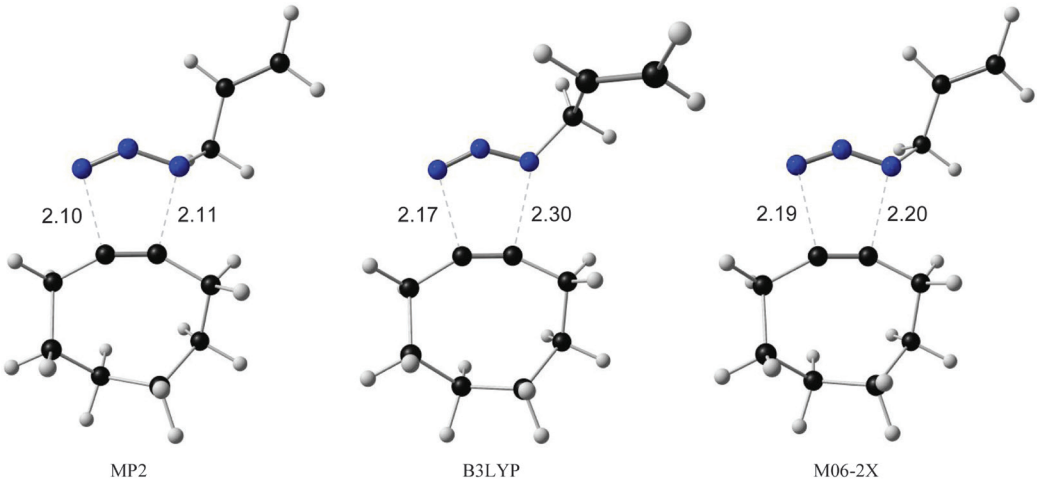

Figure 6. TS conformations of **1** and allyl azide, calculated with MP2, B3LYP, and M06-2X, respectively.

the MP2/6-311G(d,p)-derived TS of **1** with benzyl azide *r*(N^{term}-C) and *r*(N^{int}-C) are 2.100 and 2.099 Å, respectively, while for the allyl azide-derived TS these values are 2.102 and 2.108 Å, respectively (Figure 5). In addition, the imaginary frequencies that track the potential energy curve for approach of the reactants are near- identical: -272.2 and -273.8 cm^{-1}, respectively. Therefore, all TS structures were optimized at the MP2 level of theory for the reaction with allyl azide, while for compounds **1** - **4** these TS structures were also optimized with benzyl azide.

4.3.3. Transition state geometries

To study the correlation of experimental and theoretical data in more detail, an in-depth study was made of the TS geometries. When comparing the geometrical features of the TS as obtained by the various methods, the TSs acquired from MP2 calculations were consistently shown to be significantly 'tighter' than obtained from either B3LYP or M06-2X calculations. As a typical example, Figure 6 shows the relevant bond lengths for the cycloaddition of **1** and allyl azide. With the B3LYP functional, the calculations yielded asymmetric alkyne-azide distances in the order of 2.17 - 2.31 Å. M06-2X calculations showed near-symmetric distances of approximately 2.20 Å, while MP2 calculations showed 'tighter' and also near-identical distances of 2.10 Å. In all three cases, **1** adopted a chair-like conformation.

In Figure 5, the TSs of four cyclooctynes (**1** - **4**) with allyl azide are described

Table 3. Distortion energies per component (cyclooctyne or azide) for the SPAAC reactions of cyclooctynes **1** - **4**, allyl azide (**A**), and benzyl azide (**B**) (in kcal/mol).

Compound	$E_{distortion}$	Compound	$E_{distortion}$
1 (**+ A**)	3.6	**A** (+ **1**)	24.8
1 (**+ B**)	3.7	**B** (+ **1**)	24.4
2 (**+ A**)	1.8	**A** (+ **2**)	24.3
2 (**+ B**)	1.8	**B** (+ **2**)	24.5
3 (**+ A**)	3.0	**A** (+ **3**)	17.9
4 (**+ A**)	5.1	**A** (+ **4**)	26.1
4 (**+ B**)	4.3	**B** (+ **4**)	27.2

as optimized via MP2 calculations. They all exhibit a chair-like conformation in the TS with allyl azide. On a first-level approximation, given the exothermic nature of the reaction, lower activation energies could be expected for an earlier TS conformation, in which the C-N distance is larger. This is indeed the case for the TS of **3** with allyl azide in which the C-N distance is around 2.19 Å, and is more distant in comparison with the 2.10 Å of 1. Also, in the case of allyl azide and **3**, the azide angle is larger, which means that less N-N-N bending is required in order to reach the TS conformation. This latter feature is confirmed by the distortion energy of allyl azide (the energy difference between the azide in the geometry of the optimized reactant and in the geometry it has in the TS), which is 7 kcal/mol lower than that of allyl azide in a TS with **1** (Table 3). However, for the also more rapidly reacting compound **4**, the TS seems to be later than for **1**. For example, the C-N distances are around 2.05 Å, which imply a tighter TS than found for **1**. This corresponds to the larger distortion energy calculated for the allyl azide and benzyl azide components reacting with **4** in comparison to reaction with **1**: 26.1 and 27.2 kcal/mol for **4**, and 24.8 and 24.4 kcal/mol for **1**, respectively. In other words, while both **3** and **4** react appreciably faster than **1**, the TS of **3** is also characterized by a lower distortion energy, while that of **4** is characterized by a higher distortion energy than observed for **1**. A similar discrepancy is observed for compound **2**, which also reacts faster than **1** but has a later TS (Figure 5). In general, plots of the activation energy versus alkyne or azide distortion energies show only a poor correlation for the studied cycloocytnes (see Appendix II Figure S9).

From these observations it can be concluded that the geometries of the TSs and distortion energies of these cyclooctynes cannot be generally correlated

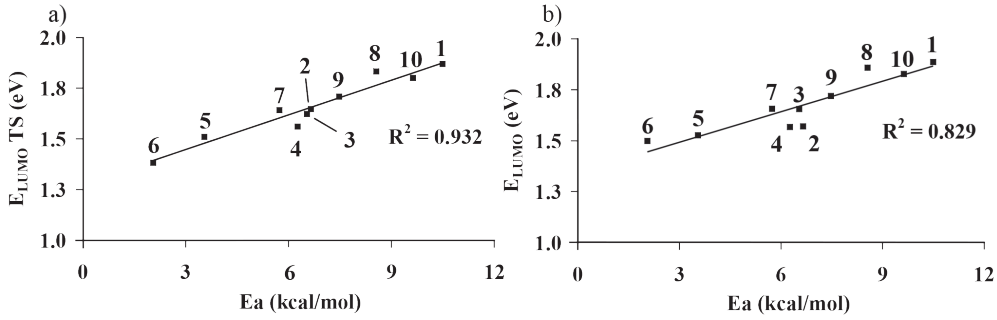

Figure 7. Correlation of the activation energy (Kcal/mol) of the SPAAC transitions states with the LUMO energy (in eV) of the cyclooctynes (**1** - **10**) in the geometry they have (a) in the transition state with allyl azide, or (b) in the geometry they have as a fully optimized reactant.

to activating energies of SPAAC reactions. Also, natural charges on the alkyne carbon atoms and the azide nitrogen atoms could not be related to the reactivity of the cyclooctynes under study.

4.3.4. LUMO energy levels as predictive tools

Besides efforts to correlate activation energies to geometrical features of the TS, interactions between the most-involved molecular orbitals were also studied. This revealed a linear correlation between the activation energy E_a and the LUMO energy of the cycloalkyne as it is distorted in the TS (Figure 7a; R^2 = 0.932), which is quite good given the spread of experimental conditions. A lower LUMO energy of the cyclooctyne (in the MP2-calculated TS geometry; please note: MP2 provides an energy correction on Hartree-Fock level-derived orbitals; as such the LUMO energy is a Hartree-Fock energy) consistently corresponded to a more rapidly

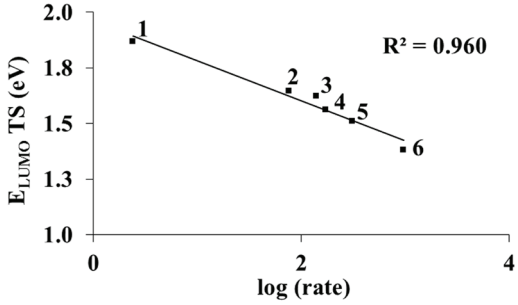

Figure 8. Plot of Logarithm of experimental second-order rate constants for cyclooctynes **1** - **6** versus the calculated MP2 LUMO energies (eV) of their geometry in the SPAAC transition state with allyl azide.

reacting molecule. The HOMO energy of the cyclooctynes could, however, not be related to the activation energy in a good linear fashion (Appendix II Figure S10). These findings confirm that the SPAAC reaction develops predominantly via azide-HOMO and alkyne-LUMO interactions.[12,20,31] However, also the azide-HOMO energies could not be related to the SCS-MP2 activation energy (R^2 = 0.220; Appendix II Figure S11). On the contrary, when cycloocytne LUMO values are correlated to the experimental rate constants, a very good regression is observed: R^2 = 0.960 (Figure 8). This further supports that the reaction is cyclooctyne LUMO-driven and that Hartree-Fock LUMO-values are indeed a good measure for the reactivity of the cycloocytnes in SPAAC reactions with organic azides. Given this success, we wondered whether more simple theoretical tools would be available to rapidly predict the order of reactivity of cyclooctynes in strain-promoted cycloaddition reactions. Therefore, we also plotted the LUMO energy of the MP2-optimized cycloalkyne (i.e. full optimization, without presence of azide) against the calculated activation energies (Figure 7b). This again showed a decent linear correlation (R^2 = 0.829), albeit with obviously more scatter than the linear correlation of the LUMO values that was obtained for the cyclooctynes in the transition state. Even this simplified approach yielded as reactivity order **6** > **5** > **4** ≈ **3** ≈ **2** > **1**, which closely resembles the experimentally observed order **6** > **5** > **4** ≈ **3** > **2** > **1**. Even quicker approaches, involving DFT, were less successful (R^2 = 0.727 and 0.795, for B3LYP and M06-2X, respectively (see Appendix II Figures S12 and S13, respectively). Among the employed methods, only SCS-MP2 is a uniformly robust method that can yield useful SPAAC reactivity predictions. As LUMO energies can be calculated in a straightforward manner in a variety of GUI-assisted molecular simulation programs like Gaussview or ChemBio3D, this may simplify further experimental optimizations of strain-promoted cycloaddition reactions, possibly also with other dipoles like nitrones, nitrile oxides[18] and other alkynes. A step-by-step standard operating procedure for performing these calculations, and thereby giving an indication of the reactivity of novel cyclooctynes in SPAAC reactions, can be found in Appendix II.

4.4 Conclusions

It is possible to predict the relative reactivity of strained alkynes in strain-promoted azide-alkyne cycloaddition (SPAAC) reactions, via the LUMO energy of the alkyne. The LUMO energy in the TS geometry correlates accurately (R^2 = 0.960)

with the experimental rate order for a diverse series of cyclooctynes. Even the alkyne LUMO energy of the relaxed, fully optimized cyclooctyne yields a good indication of relative reactivities. No good correlation between the experimental rates and alkyne distortion energies was observed. By comparing experimental data with theoretically derived activation energies, it was shown that SCS-MP2 yielded accurate data, but that – although popular – the DFT methods B3LYP and M06-2X did not yield theoretical predictions that correlated favorably with experiment. Given the efficiency and accessibility of basic computational chemistry on 21th century personal computers, the calculation of LUMO values of novel cyclooctynes on these machines is a rapid and easily available method to obtain an initial valuable estimate of their reaction kinetics in strain-promoted cycloadditions prior to committing to the development of a synthetic route and actually preparing them.

4.5 References

[1] a) T. K. Tiefenbrunn, P. E. Dawson, *Biopolymers* **2010**, *94*, 95-106; b) B. S. Sumerlin, A. P. Vogt, *Macromolecules* **2010**, *43*, 1-13; c) J. C. Jewett, C. R. Bertozzi, *Chem. Soc. Rev.* **2010**, *39*, 1272-1279; d) M. F. Debets, C. W. J. van der Doelen, F. P. J. T. Rutjes, F. L. van Delft, *ChemBioChem* **2010**, *11*, 1168-1184; e) J. M. Baskin, C. R. Bertozzi, *Aldrichim. Acta* **2010**, *43*, 15-23; f) E. M. Sletten, C. R. Bertozzi, *Angew. Chem., Int. Ed. Engl.* **2009**, *48*, 6974-6998; g) C. R. Becer, R. Hoogenboom, U. S. Schubert, *Angew. Chem., Int. Ed. Engl.* **2009**, *48*, 4900-4908; h) J. A. Prescher, C. R. Bertozzi, *Nature Chem. Biol.* **2005**, *1*, 13-21.

[2] a) R. Huisgen, *Angew. Chem., Int. Ed. Engl.* **1963**, *2*, 565-598; b) C. W. Tornøe, C. Christensen, M. Meldal, *J. Org. Chem.* **2002**, *67*, 3057.

[3] a) V. V. Rostovtsev, L. G. Green, V. V. Fokin, K. B. Sharpless, *Angew. Chem., Int. Ed. Engl.* **2002**, *41*, 2596-2599; b) H. Kolb, C., M. G. Finn, K. B. Sharpless, *Angew. Chem., Int. Ed. Engl.* **2001**, *40*, 2004-2021.

[4] M. E. Letelier, S. Sánchez-Jofré, L. Peredo-Silva, J. Cortés-Troncoso, P. Aracena-Parks, *Chem. -Biol. Interact.* **2010**, *188*, 220-227.

[5] a) S. T. Laughlin, C. R. Bertozzi, *ACS Chem. Biol.* **2009**, *4*, 1068-1072; b) J. M. Baskin, K. W. Dehnert, S. T. Laughlin, S. L. Amacher, C. R. Bertozzi, *Proc. Natl. Acad. Sci. U.S.A.* **2010**, *107*, 10360-10365; c) S. T. Laughlin, J. M. Baskin, S. L. Amacher, C. R. Bertozzi, *Science* **2008**, *320*, 664-667; d) J. M. Baskin, J. A. Prescher, S. T. Laughlin, N. J. Agard, P. V. Chang, I. A. Miller, A. Lo, J. A. Codelli, C. R. Bertozzi, *Proc. Natl. Acad. Sci. U.S.A.* **2007**, *104*, 16793-16797; e) S. T. Laughlin, N. J. Agard, J. M. Baskin, I. S. Carrico, P. V. Chang, A. S. Ganguli, M. J. Hangauer, A. Lo, J. A. Prescher, C. R. Bertozzi, *Method. Enzymol.,* **2006**, 415, 230-250.

[6] A. T. Blomquist, L. H. Liu, *J. Am. Chem. Soc.* **1953**, *75*, 2153-2154.

[7] G. Wittig, A. Krebs, *Chem. Ber.* **1961**, *94*, 3260-3275.

[8] R. B. Turner, A. D. Jarrett, P. Goebel, B. J. Mallon, *J. Am. Chem. Soc.* **1973**, *95*, 790-792.

[9] N. J. Agard, J. A. Prescher, C. R. Bertozzi, *J. Am. Chem. Soc.* **2004**, *126*, 15046-15047.

[10] J. M. Baskin, C. R. Bertozzi, *QSAR & Comb. Sci.* **2007**, *26*, 1211-1219.

[11] J. Dommerholt, S. Schmidt, R. P. Temming, L. J. A. Hendriks, F. P. J. T. Rutjes, J. C. M. van Hest, D. J. Lefeber, P. Friedl, F. L. van Delft, *Angew. Chem., Int. Ed. Engl.* **2010**, *49*, 9422-9425

[12] P. König, J. Zountsas, K. Bleckmann, H. Meier, *Chem. Ber.* **1983**, *116*, 3580-3590.

[13] X. Ning, J. Guo, M. A. Wolfert, G. J. Boons, *Angew. Chem., Int. Ed. Engl.* **2008**, *47*, 2253-2255.

[14] E. M. Sletten, H. Nakamura, J. C. Jewett, R. Bertozzi Carolyn, *J. Am. Chem. Soc.* **2010**, *132*, 11799-11805.
[15] M. F. Debets, S. S. van Berkel, S. Schoffelen, F. P. J. T. Rutjes, J. C. M. van Hest, F. L. van Delft, *Chem. Commun.* **2010**, *46*, 97-99.
[16] A. Kuzmin, A. A. Poloukhtine, M. A. Wolfert, V. V. Popik, *Bioconjugate Chem.* **2010**, *21*, 2076-2085.
[17] J. C. Jewett, E. M. Sletten, C. R. Bertozzi, *J. Am. Chem. Soc.* **2010**, *132*, 3688-3690.
[18] X. Ning, R. P. Temming, J. Dommerholt, J. Guo, D. B. Ania, M. F. Debets, M. A. Wolfert, G. J. Boons, F. L. Van Delft, *Angew. Chem., Int. Ed. Engl.* **2010**, *49*, 3065-3068.
[19] D. H. Ess, G. O. Jones, K. N. Houk, *Org. Lett.* **2008**, *10*, 1633-1636.
[20] F. Schoenebeck, D. H. Ess, G. O. Jones, K. N. Houk, *J. Am. Chem. Soc.* **2009**, *131*, 8121-8133.
[21] R. D. Bach, *J. Am. Chem. Soc.* **2009**, *131*, 5233-5243.
[22] K. Chenoweth, D. Chenoweth, W. A. Goddard, *Org. Biomol. Chem.* **2009**, *7*, 5255-5258.
[23] B. Gold, N. E. Shevchenko, N. Bonus, G. B. Dudley, I. V. Alabugin, *J. Org. Chem.* **2012**, *77*, 75-89.
[24] C. G. Gordon, J. L. Mackey, J. C. Jewett, E. M. Sletten, K. N. Houk, C. R. Bertozzi, *J. Am. Chem. Soc.* **2012**, 134, 9199-9208
[25] a) W. A. van der Linden, N. Li, S. Hoogendoorn, M. Ruben, M. Verdoes, J. Guo, G. J. Boons, G. A. van der Marel, B. I. Florea, H. S. Overkleeft, *Bioorg. Med. Chem.* **2012**, 20, 662-666; b) P. Van Delft, N. J. Meeuwenoord, S. Hoogendoorn, J. Dinkelaar, H. S. Overkleeft, G. A. Van Der Marel, D. V. Filippov, *Org. Lett.* **2010**, *12*, 5486-5489; c) C. S. McKay, J. A. Blake, J. Cheng, D. C. Danielson, J. P. Pezacki, *Chem. Commun.* **2011**, *47*, 10040-10042; d) N. E. Mbua, J. Guo, M. A. Wolfert, R. Steet, G. J. Boons, *ChemBioChem* **2011**, *12*, 1912-1921; e) I. S. Marks, J. S. Kang, B. T. Jones, K. J. Landmark, A. J. Cleland, T. A. Taton, *Bioconjugate Chem.* **2011**, *22*, 1259-1263; f) I. Singh, F. Heaney, *Chem. Commun.* **2011**, *47*, 2706-2708; g) J. C. M. Van Hest, F. L. Van Delft, *ChemBioChem* **2011**, *12*, 1309-1312; h) F. Friscourt, P. A. Ledin, N. E. Mbua, H. R. Flanagan-Steet, M. A. Wolfert, R. Steet, G.-J. Boons, *J. Am. Chem. Soc.* **2012**, *134*, 5381-5389; i) P. van Delft, E. van Schie, N. J. Meeuwenoord, H. S. Overkleeft, G. A. van der Marel, D. V. Filippov, *Synthesis-Stuttgart* **2011**, 2724-2732; j) K. N. Jayaprakash, C. G. Peng, D. Butler, J. P. Varghese, M. A. Maier, K. G. Rajeev, M. Manoharan, *Org. Lett.* **2010**, *12*, 5410-5413; k) K. W. Dehnert, B. J. Beahm, T. T. Huynh, J. M. Baskin, S. T. Laughlin, W. Wang, P. Wu, S. L. Amacher, C. R. Bertozzi, *ACS Chem. Biol.* **2011**, *6*, 548-552; l) N. J. Baumhover, M. E. Martin, S. G. Parameswarappa, K. C. Kloepping, M. S. O'Dorisio, F. C. Pigge, M. K. Schultz, *Bioorg. Med. Chem. Lett.* **2011**, *21*, 5757-5761; m) E. M. Sletten, C. R. Bertozzi, *Acc. Chem. Res.* **2011**, *44*, 666-676; n) M. Shelbourne, X. Chen, T. Brown, A. H. El-Sagheer, *Chem. Commun.* **2011**, *47*, 6257-6259; o) I. Singh, C. Freeman, F. Heaney, *Eur. J. Org. Chem.* **2011**, 6739-6746; p) H. Stoeckmann, A. A. Neves, S. Stairs, H. Ireland-Zecchini, K. M. Brindle, F. J. Leeper, *Chem. Sci.* **2011**, *2*, 932-936; q) V. Bouvet, M. Wuest, F. Wuest, *Org. Biomol. Chem.* **2011**, *9*, 7393-7399; r) A. Bernardin, A. Cazet, L. Guyon, P. Delannoy, F. Vinet, D. Bonnaffé, I. Texier, *Bioconjugate Chem.* **2010**, *21*, 583-588; s) L. A. Canalle, M. Van Der Knaap, M. Overhand, J. C. M. Van Hest, *Macromol. Rapid Commun.* **2011**, *32*, 203-208; t) C. Ornelas, R. Lodescar, A. Durandin, J. W. Canary, R. Pennell, L. F. Liebes, M. Weck, *Chem. Eur. J.* **2011**, *17*, 3619-3629; u) L. A. Canalle, T. Vong, P. H. H. M. Adams, F. L. Van Delft, J. M. H. Raats, R. G. S. Chirivi, J. C. M. Van Hest, *Biomacromolecules* **2011**, *12*, 3692-3697.v) de Almeida, G.; Sletten, E. M.; Nakamura, H.; Palaniappan, K. K.; Bertozzi, C. R. *Angew. Chem. Int. Ed. Engl.* **2012**, *51*, 2443-2447; w) van Geel, R.; Pruijn, G. J. M.; van Delft, F. L.; Boelens, W. C. *Bioconjugate Chem.* **2012**, *23*, 392-398; x) Friscourt, F.; Fahrni, C. J.; Boons, G.-J. *J. Am. Chem. Soc.* **2012**, *134*, 18809-18815; y) Yao, J. Z.; Uttamapinant, C.; Poloukhtine, A.; Baskin, J. M.; Codelli, J. A.; Sletten, E. M.; Bertozzi, C. R.; Popik, V. V.; Ting, A. Y. *J. Am. Chem. Soc.* **2012**, *134*, 3720-3728;
[26] a) R. K. Manova, S. P. Pujari, C. A. G. M. Weijers, H. Zuilhof, T. A. v. Beek, *Langmuir* **2012**, *28*, 8651-8663; b) R. K. Manova, T. A. van Beek, H. Zuilhof, *Angew. Chem., Int. Ed. Engl.* **2011**, *50*, 5428-5430.

[27] C. Lee, W. Yang, R. G. Parr, *Phys. Rev. B* **1988**, *37*, 785.
[28] Y. Zhao, D. G. Truhlar, *Acc. Chem. Res.* **2008**, *41*, 157.
[29] a) C. Møller, M. S. Plesset, *Phys. Rev.* **1934**, *46*, 618; b) S. J. Grimme, *Chem. Phys.* **2003**, *118*, 9095.
[30] M. J. Frisch, *et al.* in *Gaussian Inc.*, Revision A.02 ed., Wallingford Connecticut, **2009,** Gaussian.
[31] I. Fleming, *Molecular Orbitals and Organic Chemical Reactions, Student Edition* John Wiley and Sons Ltd, New York, **2010**.
[32] a) J. J. P. J. Stewart, *Comput. Chem.* **1989**, *10*, 209-220; b) J. J. P. J. Stewart, *Comput. Chem.* **1989**, *10*, 221-264.
[33] J. J. P. J. Stewart, *Mol. Model.* **2007**, *13*, 1173-1213.

4.6 Appendix II

Experimental procedure for the synthesis of **1** and allyl azide. Determination of rate constants of **1** with benzyl azide. Competition experiment procedure of **1** or **3** with benzyl azide and allyl azide. Plots of : E_a (MP2) versus log rate, TS conformation of **9** and **10**, E_a (SCS-MP2) in MeOH versus log rate, E_a (SCS-MP2) versus cyclooctyne distortion energies, E_a (SCS-MP2) versus cyclooctyne E_{HOMO} (MP2), E_a (SCS-MP2) versus allyl azide E_{HOMO} (MP2), E_a (SCS-MP2) versus cyclooctyne E_{LUMO} (B3LYP), and E_{LUMO} (M06-2X), (SCS-MP2) versus $E_{HOMO(azide)}$-$E_{HOMO(cyclooctyne)}$, table with MO energies of allyl azide and benzyl azide in the TS with compounds **1** - **10**, step-by-step guideline for the calculation of cyclooctyne rate values and complete reference 30.

5

The influence of copper on GM1os-based CTB detection assays: CuAAC vs SPAAC

A part of this chapter was subject in a MSc project and documented as *Synthesis of BCN-modified carbohydrates for surface modification via SPAAC reactions*, Geert Noordzij, Wageningen University MSc thesis, **2012**.

Abstract:

In this Chapter, copper-catalyzed azide-alkyne cycloaddition (CuAAC) reactions and strain-promoted azide-alkyne cycloaddtion (SPAAC) reactions are directly compared in biological assays. A GM1 oligosaccharide (GM1os)-bearing compound that presented a hydrophilic spacer and a terminal alkyne was immobilized by CuAAC to microtiter plates. Two novel GM1os compounds were developed to contain cyclooctynes, one attached *via* an aliphatic and lipophilic undecane spacer and the second compound contained both the same aliphatic spacer and an additional hydrophilic hexa-ethyleneoxide (EO_6) spacer. After the ganglioside derivatives were immobilized on microtiter plates by either CuAAC or SPAAC (depending on the nature of the attached alkyne), ELISA experiments were performed on the cholera toxin B-subunit (CTB). It is shown that when copper ions are added to the SPAAC-immobilized carbohydrates their ligand-CTB binding properties increase significantly. The most dramatic effect is shown for the EO_6-containing compound, and therefore employing CuAAC in biological assays in combination with compounds that display such hydrophilic moieties is not recommended. These studies give significant insight on the effects of copper on carbohydrate-CTB avidity.

5.1 Introduction

The pentasaccharide fragment of ganglioside GM1 plays a wide variety of biological roles, some beneficial, some detrimental.[1] In many of these latter cases, GM1 is the targeted entity on cell surfaces. Therefore, it is of general interest to synthesize tailor-made GM1 analogues that can be attached to a platform of interest for detection purposes. The synthesis and biological evaluation of a range of GM1 oligosaccharide (GM1os) fragments are described in Chapter 6. In that study, the synthesized fragments were immobilized on a surface via the copper-catalyzed alkyne-azide cycloaddition (CuAAC) reaction,[2] and assayed for their binding affinity towards a lectin, the cholera toxin B-subunit (CTB),[3] and antibodies (Abs) in the sera from patients with Guillain-Barré syndrome (GBS).[4] In that study and similar previous studies[5] we observed that in some instances the lectins or antibodies showed a significant selective preference for either the wild type GM1, which is the natural antigen for both CTB and many GBS-related Abs, or for the very similar synthetic analogue GM1os. We have previously also observed significant differences in binding affinity of GBS Abs towards a synthetic GM1 analogue that was equipped with either an aliphatic (C_{11}) or an oligo-ethyleneoxide (oligo-EO) aglycone-spacer and immobilized on sepharose beads via the CuAAC reaction (unpublished results). The oligo-EO-linked GM1os showed a marked lower binding affinity.

The question therefore arose if, besides the small structural differences, the use of copper in the CuAAC ligation reaction, and its possible retention after standard washing procedures, might play a role in these observed differences in binding affinity. If indeed so, then changing the ligation reaction and omitting copper might improve the response of the synthetic GM1 derivatives in our ELISA-type experiments. To investigate this, we required a facile ligation reaction that does not involve copper. Therefore, our attention turned to the strain-promoted alkyne-azide cycloaddition (SPAAC) reaction, which can be considered to be the copper-free equivalent of the CuAAC reaction. The SPAAC reaction has in recent years been successfully applied in a still rapidly increasing number of various biological applications.[6]

Since the initial report by Bertozzi and co-workers in 2004,[7] the application of the SPAAC reaction has received a lot of attention.[6] It is especially lauded because it makes the use of toxic copper superfluous. The toxicity of copper is displayed by its ability to take part in oxidative mechanisms that readily

promote the generation of reactive oxygen species (ROS), which are likely to lead to biological damage.[8] An example of a disease that reveals the damage that copper can cause, through the development of ROS, is Wilson's disease, in which a high copper concentration in the patients' blood causes severe damage to liver and brain tissue.[9] Another commonly known property of copper is its ability to be reduced by thiol groups, which are commonly encountered *in vivo* in many proteins in the form of cysteine or methionine residues.[10]

Importantly, it has also been reported that polyethyleneglycol (PEG) moieties coordinate to copper ions (Figure 1).[11] Besides the use of PEG, or oligo-EO moieties as spacers to alter the lipophilicity of organic compounds in biological applications,[12] their other most frequent use is to suppress biofouling, which is an unwanted process initiated by the deposition of biological components on surfaces through aspecific adsorption.[13] Some speculate that copper coordination to the PEG spacer reduces the mobility of the spacer and any attached structures like antigens.[11] When translated to our investigation, this would mean that the antigen, *i.e.* the GM1os that is equipped with an EO spacers and in the presence of Cu ions, may display a lower binding affinity as a result. Because of these drawbacks, it becomes clear why there is a need to replace CuAAC as the tool for bioconjugation.

However, to date, only two studies have been published in which SPAAC was employed in ELISA-type experiments. First, Heemstra and co-workers recently reported an aptamer-based analogue of "sandwich" ELISA experiments, *via* a

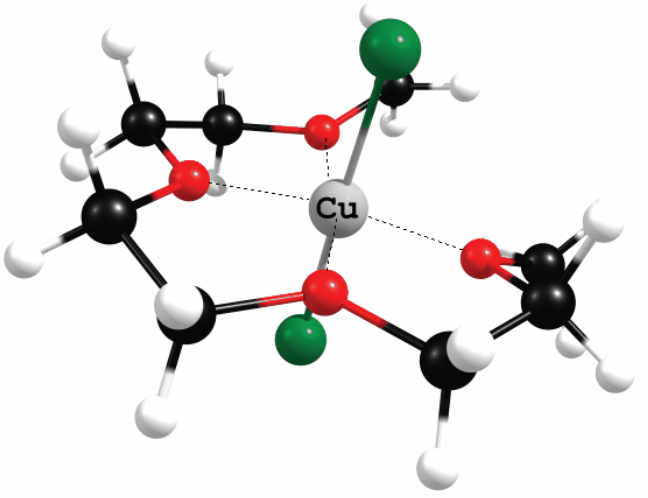

Figure 1. Illustrative example of an octahedral complex formed by coordination of a PEG spacer to copper(II) chloride, proposed by Kaczmarek.[11]

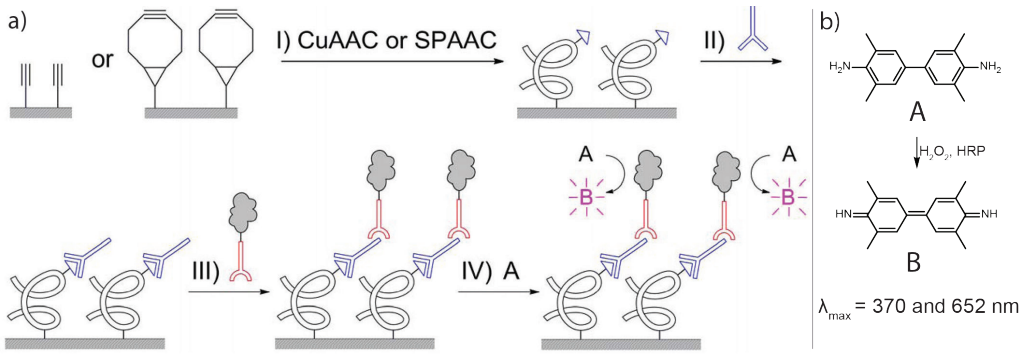

Figure 2. a) Clickable, alkyne or BCN-terminated, microtiter plates to use for ELISA detection of ACA's[16] ; b) HRP-facilitated oxidation of TMB compound **A** to the oxidized TMB product **B**. Figure 2a reproduced from reference.[16]

split aptamer approach that employed the SPAAC reaction, using 2-functionalized cyclooctyne and aza-dibenzocyclooctyne (DIBAC) and, on the opposite terminus, with biotin. The split aptamer approach consists of two DNA strands that only assemble in the presence of a small molecule, in this case cocaine.[14] With this approach they were able to detect µM-level quantities of cocaine in buffer and human blood serum.

More recently, Van Hest and co-workers have reported on an assay in which the cyclooctyne, 9-hydroxymethylbicyclo[6.1.0]nonyne (BCN) (Figure 2),[15] is used to bind an azide-functionalized, citrulline-containing peptide.[16] The employed peptide sequence is recognized, and strongly bound, by anticitrulline antibodies (ACA's) that have found medical application as an early diagnosis for the autoimmune disease rheumatoid arthritis.[17] In an indirect ELISA experiment, the azido-functionalized peptide was immobilized in either terminal alkyne or BCN-functionalized ELISA wells, employing CuAAC or SPAAC, respectively (Figure 2). ACA's were subsequently added to bind to the immobilized peptide after which a secondary antibody, conjugated with horse radish peroxidase (HRP), was added to bind to the (primary) ACA. Finally, oxidation of the HRP-substrate 3,3′,5,5′-Tetramethylbenzidine (TMB, Figure 2b) was measured by OD, which is indicative for peptide-ACA binding efficiency. It was found that the CuAAC strategy showed a high background signal that rendered the test less reliable. This was attributed to coordination of the copper catalyst to nitrogen moieties in the peptide sequence. Instead, the SPAAC strategy proved successful in its application and functioned on a par with a commercially available ELISA test for the ACA antibody.

In the study described in this chapter, we therefore investigate whether using the SPAAC reaction to attach carbohydrates with either oligo-EO spacers or

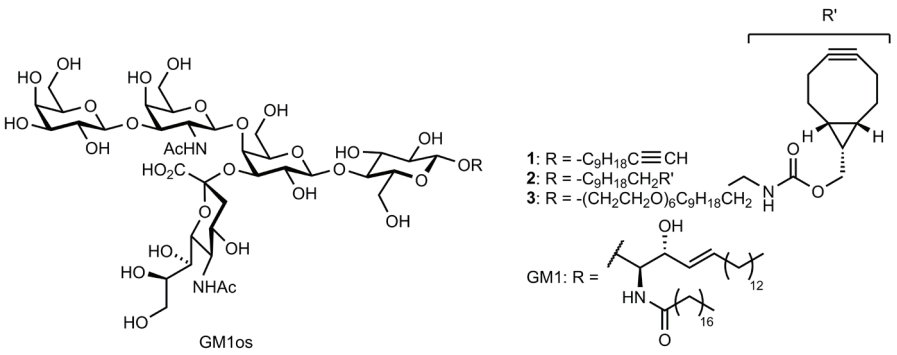

Figure 3: GM1 oligosaccharide-functionalized alkynes **1** - **3** as synthesized and used in ELISA experiments.

aliphatic spacers to our assay surfaces would be beneficial, compared to CuAAC, for the binding ability of these carbohydrates to CTB. We report the application and detailed comparison of SPAAC and CuAAC reactions for the immobilization of ganglioside GM1 epitopes in enzyme-linked lectin assay (ELLA) experiments. For this comparison, we used the well-documented[18] complementary set of the lectin CTB and the ganglioside GM1os (Figure 3). We employed the previously reported GM1os derivative **1**,[5] which contains a lipophilic spacer and a terminal alkyne, and two novel cyclooctyne BCN-containing GM1os derivatives – GM1os derivatives, **2** and **3** – that contained a terminal cyclooctyne and were equipped without and with an oligo-EO spacer, respectively. The terminal alkyne equivalent of compound **3**, displaying also an EO-spacer, was not available at the moment of testing and therefore not included in these experiments. With these target compounds, the effect of adding a hydrophilic EO spacer on the binding to CT could also be directly investigated. Additionally, a direct comparison of CuAAC versus SPAAC is made and insight is obtained on the influence of copper on the compound that contains the hydrophobic EO spacer and its ability to bind CTB.

5.2 Results and discussion

5.2.1 Synthesis

Initially, the approach of choice was to modify the microtiter plate surfaces with alkynes and to use azide-terminated carbohydrates to detect biological agents. This approach was also used for the Guillain-Barré syndrome (GBS)-related experiments

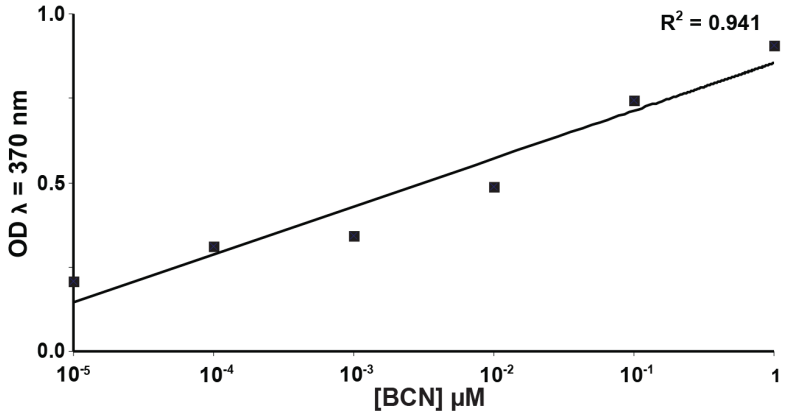

Figure 4: Linear relationship between the concentration of BCN coating applied on ELISA-wells and the deposition of CTB (proportional to the OD) on the surface.

that are described in Chapter 6. In that case, the surfaces were modified by covalently linking propargylamine to commercially available activated ester-terminated microtiter plates. Biological assays have been performed whilst employing SPAAC reactions on BCN-functionalized ELISA plates, *vide supra*.[16] However, there are some notable disadvantages of cyclooctyne-terminated surfaces. One is that cyclooctynes, because of their high intrinsic energy, are prone to oxidation and other unwanted side-reactions. They are therefore not stable for a long period of time and the surfaces need to be used preferably immediately after preparation.[19]

In addition, an unusually high background signal was observed when we tested this BCN-terminated microtiter surface, after ligation with GM1os, for the GM1os-CTB binding affinity in indirect ELLA experiments. This indicated that the toxin interacted with the surface, either chemically or through physisorption. Further investigation indicated that an increasing concentration of BCN on the surface led to a corresponding linear increase in the toxin absorption (Figure 4), even after extensive blocking with bovine serum albumin (BSA) and standard ELISA washing procedures. This contrasts observations by Van Hest and co-workers,[16] who have conducted ELISA experiments with similar cyclooctyne-modified surfaces and do not report having observed this phenomenon. We cannot rule out that the binding to the BCN-functionalized surface by this biological agent is specific, and only the case, for CTB. Anyway, these results discouraged us to further investigate using BCN-terminated surfaces in this manner. When we employed a terminal alkyne coating, and applied CuAAC to immobilize azide-functionalized carbohydrates, a steady and low background signal was measured

independent of the concentration of the surface coating. Hence, rather than applying the alkynes on the surface of the ELISA plates, carbohydrates were synthesized to contain the BCN moiety and commercially available ester-terminated ELISA plates were modified to display azide-functionalized surfaces.

Terminal alkyne-containing **1** (Figure 3) was synthesized as previously reported,[5a] and used without further modifications to immobilize it via the CuAAC reaction on azide-functionalized surfaces. For the synthesis of compounds **2** and **10**, previously reported azido-terminated **4**[5a] and compound **5**[20] were reduced to amines **6** and **7**, respectively. Subsequently, they were attached to cyclooctyne BCN **11**, to afford BCN-functionalized GM1os compounds **2** and **3** (Scheme 1A), respectively. The first step was to investigate the optimal reaction conditions to reduce the azide functionality of the unprotected carbohydrates **4** and **5**. Since the GM1os are precious materials, we aimed for a reduction methodology that is high-yielding, fast, chemoselective, and without byproducts. To prevent unnecessary use of the precious GM1os compounds, reduction experiments were performed on the less complex and easier to synthesize precursor lactoside **8**, which is also discussed in Chapter 6.

First attempts to reduce the azido-lactoside by employing the Staudinger reduction[21] in dioxane, in the presence of PPh_3 were moderately successful due to complexation of the resulting amine to phosphor species in the reaction mixture. After stirring for 4 h in the presence of 0.1 M HCl, more of the desired product was formed. However, the triphenylphosphine oxide (TPPO) byproduct was hard to remove from the mixture by either liquid-liquid extraction or flash chromatography. In order to increase the yield of the reduction and to circumvent the difficult separation from the TPPO byproduct, compound **8** was exposed to polystyrene-bound diphenylphosphine (PS-

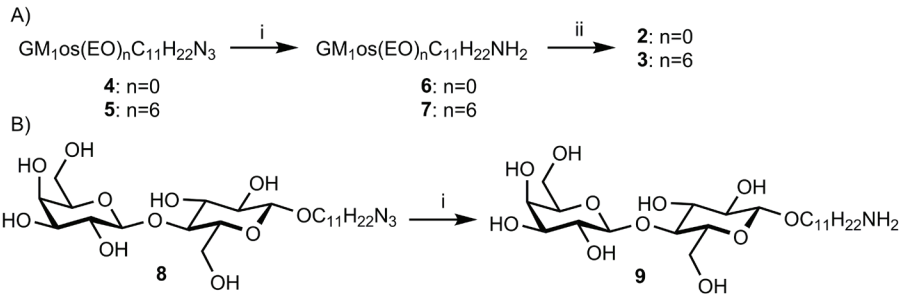

Scheme 1: A) Synthesis of BCN-modified GM1os **2** and **3**; B) Reduction of test compound 1-*O*-(11-azido undecane)-*β*-D-lactoside **8**; i) Pd/C, 4 bar H_2, EtOH, 6 h, 25 °C; ii) **3**, Et_3N, DMF, 2 h, 25 °C; EO = - CH_2CH_2O-.

PPh_2).[22] In this case, as can be expected, TPPO was not observed in the final product after filtration. After overnight stirring of the reaction mixture and additional overnight dissociation of the phosphazene complex in the presence of diluted hydrochloric acid, a still unsatisfactory yield was observed (65%).

At this point, the Staudinger reduction-approach was abandoned, since low yields and the formation of by-products rendered the tests not suitable to be translated to the GM1os. Also, the use of a strong acid is preferably avoided because of the possibility of anomerization[23] and, more importantly, because these complex carbohydrates are prone to acid-mediated hydrolysis of glycoside bonds after prolonged exposure.[24] Reduction in a suspension of Pd/C in water under atmospheric H_2-pressure led to even lower yields (max 20%) than those observed for the experiments with the Staudinger reduction. When this approach was performed in the presence of 0.1 M HCl the desired product was obtained almost quantitatively after overnight reaction. However, again, due to possible acid-induced hydrolysis of the product, the reaction conditions were found to be unsatisfactory for implementation on the valuable GM1 oligosaccharides.

Subsequently, compound **8** was exposed, in two separate experiments, to 4 and 10 bar of H_2 gas for 6 h in the presence of Pd/C in EtOH. This showed that 4 bar was already sufficient for the complete reduction of the azide, as shown by mass spectrometry. A successful reduction could also be easily observed by

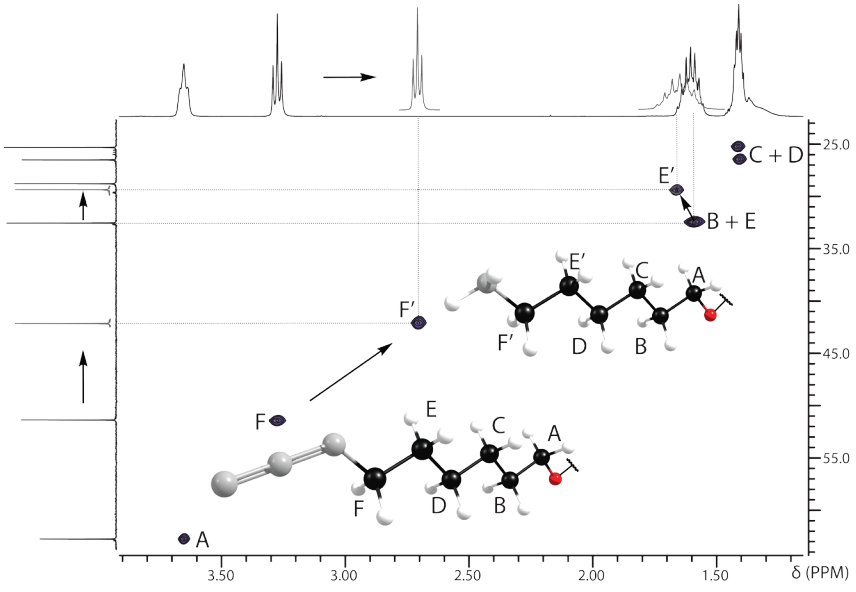

Figure 5: Part of an HSQC spectrum that indicates the typical chemical shift changes seen for azide reductions.

heteronuclear single quantum coherence (HSQC) NMR experiments. Typically, the carbon adjacent to the non-terminal azide nitrogen can be found around δ = 51 ppm (Figure 5, carbon F). After successful reduction, the corresponding carbon adjacent to the amine nitrogen is shifted high field to approximately δ = 42 ppm (Figure 5, carbon F'). After extensive, multistep filtration (see experimental section for details) to remove the Pd/C catalyst, the solvent was removed *in vacuo*. The desired product was obtained in excellent yield (95%). Once this suitable reduction method was found for the azide-terminated lactoside **8** (Scheme 1B), the next step was to reduce the azide-terminated GM1os in a similar fashion (Scheme 1A). High-resolution mass spectrometry analyses confirmed that the desired amine products had formed, and no residual starting materials were observed. Additionally, no degradation products that would imply loss of terminal Gal- and/or Neu5Ac moieties were detected either. Both, products **6** and **7** were obtained in high yield (> 90%) as white solids and were deemed sufficiently pure to be used in subsequent coupling reactions to BCN without further purification.

The synthesis of activated *para*-nitrophenylcarbonate-BCN (*p*NP-BCN) **12** (Scheme 2) proceeded as described in literature.[15] To increase the yield for the first step (from the reported 76%[15] to 87%, namely 40% endo-**11** and 47% exo-**11**), instead of diluting the reactants with DCM, the cyclization was performed in neat cyclooctadiene.[25] For this project, we focussed solely on the slightly more reactive endo-BCN, which was isolated pure from a diastereomeric mixture according to literature.[15] BCN-functionalized GM1 oligosaccharides **2** and **3** were then synthesized by reacting *p*NP-BCN **12** with amines **6** and **7** to obtain compounds GM1BCN **2** and GM1EO$_6$BCN **3**, respectively (Scheme 1). The pure compounds were then obtained as white solids by lyophilisation.

5.2.2 Enzyme-linked lectin assay experiments

Chemical modifications on microtiter plate surfaces are, in general, hard to observe. The effectiveness of such modification is therefore typically indirectly

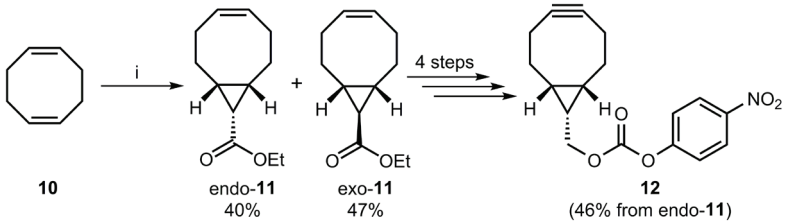

Scheme 2: Synthesis scheme for *p*NP-BCN **12**.[15] i) **10** (neat), Rh(OAc)$_4$, ethyl 2-diazoacetate, 40 h, 0 °C.

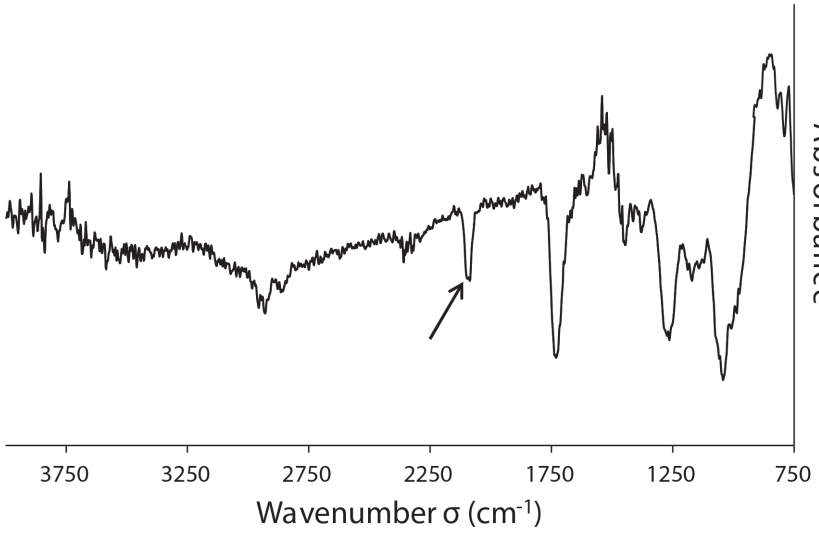

Figure 6. Infrared difference spectrum of terminal azide-functionalized microtiter plate wells. The arrow indicates the N≡N azide stretch signal at σ = 2103 cm^{-1}.

confirmed after the biological assay experiment is completed. For example, if an initial modification was successful, an OD signal is measured through the activity of a secondary enzyme. Direct measurement are, however, of course preferred. To this aim, we performed infrared (IR) absorbance experiments to confirm that the surface of the ELISA plates was indeed azide-functionalized. The bottom part of an unmodified well, as provided by the manufacturer, was used as reference, and a difference spectrum was recorded for the azide-functionalized ELISA surface (Figure 6). A large number of scans (~16,000) was needed to observe a good signal, because ELISA plates absorb a quite significant amount of irradiation in the IR spectrum, but eventually a sharp signal at σ = 2103 cm^{-1} appeared in the typical region of an asymmetric azide N≡N stretch attached to aliphatic spacers.[26]

Subsequently, the synthetic GM1 derivatives were attached via a CuAAC reaction in the case of compound **1**, or a SPAAC reaction in the cases of **2** and **3**. To allow for a fair comparison, the compounds were added in similar quantities to the wells of different rows on the same plate, and all reactions were allowed to run for an equal amount of time, *i.e.* an overnight reaction. It was assumed that an equal amount of each compound was attached to the surfaces of the wells prior to the assays. Subsequently, wells of the microtiter plate were washed (3 ×) with water to remove unattached compounds and unreacted sites were blocked with BSA. The binding experiments were conducted by exposing

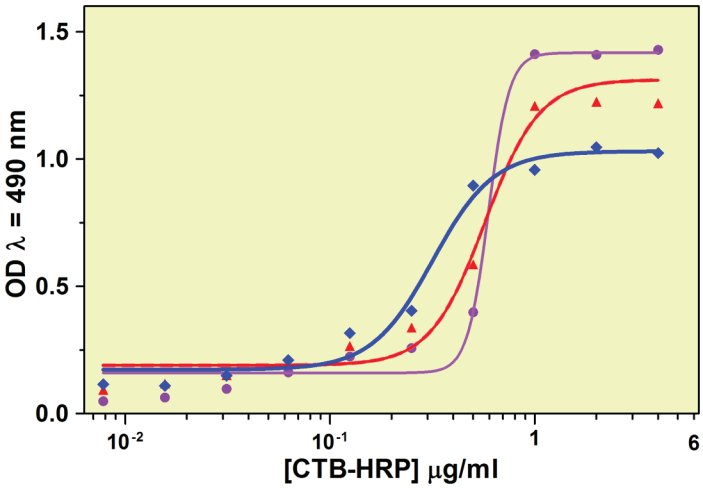

Figure 7. Binding assay on the surface-bound GM1os to a 2-fold dilution series of CTB-HRP. ● **1**, ▲ **2**, ♦ **3**;

the surface-bound carbohydrates to a 2-fold dilution series of CTB-HRP-conjugate. Next, the unbound CTB-HRP was removed by washing and the bound CTB-HRP was exposed to *ortho*-phenylene diamine (OPD). Rather than using TMB – which was also used in the studies that are described in the introduction (Figure 2)[14, 16] and in the previously discussed experiments with BCN-modified surfaces – OPD was used as substrate for HRP, because it showed a higher sensitivity in this system, requiring less GM1os to perform the experiments. After 15 min of exposure to the OPD, the oxidation reaction was quenched by addition of diluted H_2SO_4 and the OD was measured immediately (Figure 7).

Figure 7 shows that CuAAC-attached **1** is slightly more responsive towards CTB than both the BCN-functionalized carbohydrates **2** and **3** that were bound through SPAAC reactions. Clearly, the EO-containing GM1os does not bind as well to the CTB as the GM1os derivatives that do not contain a hydrophilic spacer. The half-maximum binding values for the three compounds in these experiments were determined to be 0.67 μg/ml, 0.59 μg/ml, and 0.35 μg/ml CTB for compounds **1**, **2**, and **3**, respectively. The binding affinities of **1** and **2** show reasonably good similarity. This indicates that the effect of various types of immobilization on a similar compound is negligible. Although compound **1** showed a higher response, it appeared that the oligosaccharide with the EO-spacer **3** has a lower half-maximum binding value. This means that it is “recognized” by the CTB earlier, at lower concentrations, than the two compounds that have non-hydrophilic spacers.

A possible reason for this is that in an aqueous environment, in which these

experiments are performed, the spacer stretches out in the solution whereas the hydrophobic spacer has the tendency to adhere to the hydrophobic bottom of the well. Hence, the chance of a solvated CTB to encounter the pentasaccharide of compound **3,** i.e. the opportunity for the GM1 moiety to present itself in the optimum orientation towards the CTB active site, is greater than for compounds **1** and **2**, which will reside more towards the bottom of the wells with a lower rotational degree of freedom. Nevertheless, the response of the EO-containing compound **3** is significantly lower than those for compounds **1** and **2**. This indicates that – although the CTB "recognizes" the carbohydrate earlier when it stretches out in the solution – the hydrophilic spacer upon binding possibly prevents ideal positioning of the GM1 to the CTB binding pocket and/ or electrostatic interference. The natural inhibitor for CTB, wild-type GM1 (see Chapter 1), contains a hydrophobic ceramide moiety which is more closely related to the hydrophobic spacers that were used for compounds **1** and **2**.

Figure 8 (left) shows again the binding responses of compounds **1** - **3**, but now at three specific CTB concentrations that are around their half-maximum binding values, *i.e.* 0.25, 0.50, and 1.0 µg/ml CTB, respectively. In a subsequent experiment we studied the influence that copper can have on the binding ability of CTB. The three immobilized compounds (including the SPAAC-related compounds) were exposed to 50 µl of a 6 µM $CuSO_4$ solution and 50 µl of a 12 µM sodium ascorbate solution per well for 1 h (Figure 8 right), and washed extensively afterwards. Compound **1** was apparently unaffected by the exposure and showed the same response as in the previous experiment. However, a change was noticed in the copper-exposed SPAAC compounds. Now, both compounds **2** and **3** showed a higher response to the same dose of CTB (at 0.25 and 0.50 µg/ml) than compound **1**. First of all this confirmed that residual copper ions indeed remains on the assay surface even after extensive washing. Furthermore, compound **2** now appeared to have a higher response at the lower CTB concentrations, which would indicate an earlier half-maximum binding. However, the standard error of the mean of the experiments increased significantly after the addition of the copper. The maximum binding is OD ≈ 1.1, which is, within the error, similar to what was observed in the first experiment under standard incubation conditions.

From this, can only be concluded that the binding abilities of both **1** and **2** were, within the error margin, similar to the original experiment in which compound **2** was not exposed to copper, and **1** was. Surprisingly though, EO-containing compound **3** exhibits a higher total response and the ability to bind CTB has

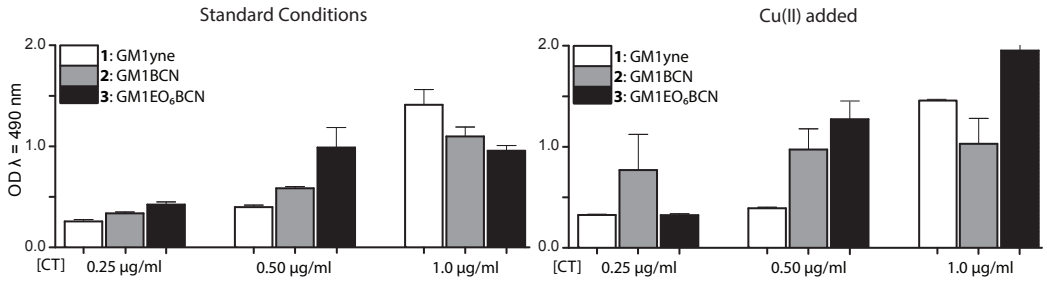

Figure 8. Left) Response of synthetic GM1 derivatives **1** - **3** under standard ELISA conditions. These responses correspond to the curves in Figure 8 between the interval <0.25 - 1.0> µg/ml CTB; Right) Response of synthetic GM1 derivatives after being exposed to small amounts of $CuSO_4$ and ascorbate and subsequently washed prior to the assay; Error bars indicate the standard error of the mean (SEM) of measurements performed in quadruplicate.

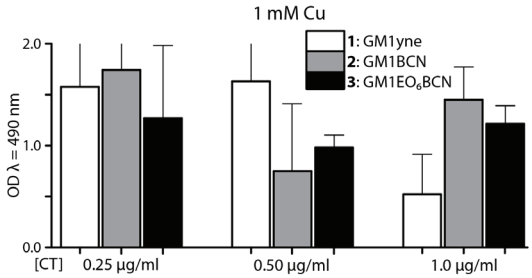

Figure 9. Response of the synthetic GM1 derivatives **1** - **3** that were exposed to 1mM of $CuSO_4$ and ascorbate solution prior to the assay; Error bars indicate the SEM of measurements performed in quadruplicate.

apparently improved due to the influence of copper. The effect that copper has on this compound is possibly too complex to draw conclusions solely based on these experiments. What could be hypothesized from this finding is that the EO-spacer coils around the copper ions and thereby rigidifying the system (see Figure 1) resulting in a loss of entropy. The spacer is thereby "pulled" to the surface and placed in a similar position as the other two compounds that are not equipped with the hydrophilic spacer. Then, when CTB "settles down" on the surface with a lower rotational entropy, as is the natural operating mode of this lectin on cell surfaces, and compound **3** is brought into closer proximity of the binding pockets, CTB is bound more strongly. However, this is a rather meagre explanation on the matter and it requires more research to clarify further.

When the compounds were exposed to an even higher, 1 mM, concentration of copper prior to the biological assays, the responses, even after extensive washing, were prone to high errors and displayed incoherent results that currently are challenging to define (Figure 9). The binding responses are very different from

those of the original experiment and, additionally, the average errors of each of the in quadruplicate measurements were increased significantly, in some cases, even larger than the response. The exaggerated experiment shows to the extreme that exposure to (high quantities of) copper leads to unwanted side-effects and large error in measurements.

5.3 Conclusions

Microtiter plates were successfully functionalized with BCN and used to attach azide-terminated GM1os derivatives. An unprecedented high response of background signal in subsequent biological experiments indicated that the BCN coating itself yields an unwanted binding of CTB. Therefore, BCN-functionalized carbohydrates were synthesized and attached to azide-functionalized ELISA surfaces. CuAAC and SPAAC were employed to attach GM1os derivatives **1** - **3** successfully to the wells and they were subsequently tested on binding affinity towards CTB. Binding affinity experiments showed that there was a slightly better binding for compound **1**, which was attached by CuAAC, but comparable with compound **2**, which was attached to the surface by SPAAC reactions. The EO-spacer-containg compound **3** showed a much lower binding affinity to CTB-HRP. When also compounds **2** and **3** were exposed to $CuSO_4$ before being exposed to CTB, in the subsequent biological assay, especially compound **3** showed a higher binding affinity to CTB than in the case of compound **1**. Even higher, 1 mM Cu^{2+} concentrations explicitly added to both the CuAAC and SPAAC reaction, led to high errors and non-linear results in the subsequent biological binding experiment. This indicated that the biological assays were hampered by the addition of large amounts of copper, and that this copper was insufficiently removed by the standard washing procedure. More importantly, the data from the experiments showed that both CuAAC and SPAAC can be successfully employed to perform binding affinity experiments on the complementary system of GM1os and CTB.

5.4 Experimental Section

5.4.1 Synthesis

General experimental information: Compounds **12** (starting from bicyclic **11**),[15] GM1os-derivatives **1**, **4**, and **5**[5a] were synthesized as described in literature. Spectral data of these compounds were in agreement with literature values. For synthesis and characterization of lactoside **8**, the reader is directed to compound **3** as described in Chapter 6. Reduction reactions were carried out on a Parr multi reactor system. Materials for the ELISA experiments *i.e.* bovine serum albumin (BSA), *ortho*-phenylenediamine (dihydrochloride salt) (OPD), cholera toxin horseradish peroxide (CTB-HRP) conjugate, Tween-20, 30% H_2O_2 solution, sodium citrate, and citric acid were purchased at Sigma Aldrich and used without further modification, phosphate-buffered saline (PBS) 10 × concentrate was diluted ten times with demineralized water prior to use. Nunc immobilizer amino™ 96-well microtiter plates were used as purchased at Thermo Scientific. The microtiter plates were washed using an automated Denville® 2 Microplate Washer. Optical density (OD) was measured between 1.5 and 0.5 units on a Thermo Labsystems Multiskan Spectrum Reader running on Skanit software version 2.4.2. Data analysis and curve fitting of inhibition experiments were performed on Prism Graphpad software version 5.04.

Compound 2: Azido-terminated **4** (10 mg, 7.4 µmol, 1.0 eq) was dissolved in EtOH (10 ml), Pd/C (10% Pd; 10 mol%) was added and the reaction mixture was exposed to 4 bar H_2 gas for the duration of 6 h. After extensive filtration through hyflo, microfiber glass filters, and 0.20 µm syringe filters, the solvent was removed *in vacuo*. The desired product, compound **6**, was obtained in excellent yield as an off-white solid (8.2 mg). **MS** (HR-ESI-): m/z = 1166.5097 [M], calcd. ($C_{48}H_{86}N_3O_{29}$) = 1166.5196; Without further purification, **6** was dissolved in dry DMF (1 ml) and Et_3N (2 µl, 8.6 µmol, 1.2 eq). The reaction mixture was then added dropwise to a solution of *p*NP-BCN **12** (4.1 mg, 13 µmol, 1.9 eq) in dry DMF (0.5 ml) and the solution was stirred for 1 h at room temperature, during which the solution turned yellow, indicating the formation of *p*-nitrophenolate. The desired product was observed by MS (ESI-). However, after observation of the presence of minor peaks of the starting amine in ESI+ mode, additional *p*NP-BCN (20 mg, 62 µmol, 9.0 eq) was added and the reaction was stirred for another hour. Subsequently,

the reaction was quenched by drop-wise addition of 0.1 M formic acid, until full decolouration of the yellow solution was observed. Water was added (1 ml) and the mixture was extracted with toluene (3 × 2 ml) and EtOAc (3 × 2 ml). The volume of the water layer was reduced under high vacuum, and, subsequently, lyophilized to afford compound **2** as a white solid (7.6 mg, 5.7 mmol, 81 % over two steps), remnants of *p*NP-BCN, or derivatives thereof, were not observed by MS (ESI- and ESI+) nor by NMR. **^{1}H-NMR** (MeOD/ D_2O 9 : 1, 400 MHz) δ (ppm) = 4.93 (m, 1H), 4.48 (m, 2H), 4.45 (m, 3H), 4.27 (m, 2H), 4.15 (m, 3H), 4.02 (m, 2H) 3.93-3.81 (m, 7H) 3.78-3.62 (m, 11H) 3.59-3.35 (m, 9H) 3.22 (m, 2H) 2.86 (s, 1H) 2.75 (m, 2H), 2.16 (d, 2H, *J* = 6.8 Hz) 2.00 (m, 6H), 1.66-1.56 (m, 6H), 1.42-1.24 (m, 17H), 1.17 (m, 2H); selected signals **^{13}C-NMR** (MeOD/ D_2O 9 : 1, 100 MHz) δ (ppm) = 105.3, 103.5, 103.0, 102.8, 102.6, 81.6, 80.0, 77.4, 75.0, 74.8, 70.0, 69.0, 68.1, 61.0, 60.1, 48.1, 37.0, 29.0, 25.9, 22.3, 22.1; C_q were not observed; **MS** (HR-ESI-) m/z = 1343.2749 [M], calcd. ($C_{59}H_{97}N_3O_{31}$) = 1343.6106.

Compound 3: Azido-terminated **5** (10 mg, 6.9 µmol, 1.0 eq) was treated in a similar fashion as it is described for compound **4**. The desired intermediate **7** was obtained in excellent yield as an off-white solid (8.9 mg). MS (HR-ESI-) m/z = 1430.6733 [M-H]$^-$, calcd. ($C_{60}H_{110}N_3O_{35}^-$) = 1430.6769; Without further purification, the coupling of **7** to carbonate **12** was performed in a similar fashion as it is described for compound **6**. Compound **3** was obtained as a white solid (7.2 mg, 4.5 µmol, 73% over two steps). MS (HR-ESI-) m/z = 1606.7589 [M-H]$^-$, calcd. ($C_{71}H_{120}N_3O_{37}^-$) = 1606.7601.

5.4.2 Enzyme-linked Lectin Assay

CuAAC Immobilization of compound 1: The following aqueous solutions were added to each well in the following order: 50 µl of a 6 µM $CuSO_4$ solution, 100 µl of a 3 µM solution of compound **1**, 50 µl of a 12 µM sodium ascorbate solution. The plate was incubated overnight at room temperature with gentle agitation. The wells were then washed with water, 3 × 400 µl per well.

SPAAC Immobilization of compounds 2 and 3: Compounds **2**, and **3** were dissolved in 20% DMSO in water and 100 µl of this 3 µM solution was added to each well, followed by 100 µl of demineralized water. The plate was incubated overnight at room temperature with gentle agitation. The wells were then washed with water, 3 × 400 µl per well.

Standard procedure for the binding experiments. Each well of the individual

96-well microtiter plates, Nunc immobilizer Amino, was treated with 200 µl of a 10 mM 1-azido-3-amino-propane solution in 0.1 M Na_2CO_3/ $NaHCO_3$ aqueous buffer (pH 9). The plates were incubated at room temperature for 16 h with gentle agitation. The solution was discarded and the wells were washed with water, 3 × 400 µl per well. The GM1os derivatives (300 pmol/well) were immobilized on the surface of the ELISA plates by either CuAAC (compound **1**) or SPAAC (compounds **2** and **3**) reactions by methods described below. For every compound, two rows on an ELISA plate were reserved, every experiment was performed on two plates. Hence, every data point was obtained in quadruplicate. After GM1os immobilization (*vide infra*), the wells were, blocked with 1% BSA PBS for 30 min at 37 °C. Then, the plate was washed with PBS (3 × 400 µl per well). Binding experiments were performed by addition of a 2-fold dilution series of the CTB-HRP conjugate in 0.1% BSA, 0.05% Tween-20 in PBS, along the columns of an ELISA plate, starting from 5 µg/ml CTB-HRP (100 µl/well). Unattached CTB-HRP was removed by washing with 0.1% BSA, 0.05% Tween-20 in PBS (3 × 400 µl per well). 100 µL of a freshly prepared OPD solution (25 mg OPD·2HCl, 7.5 mL 0.1 M citric acid, 7.5 mL 0.1 M sodium citrate and 6 µL of a 30% H_2O_2 solution, pH was adjusted to 6.0 with NaOH) was added to each well and allowed to react with HRP in the absence of light, at room temperature, for 15 min. The oxidation reaction was quenched by addition of 50 µL 1 M H_2SO_4. Within 5 min, the absorbance was measured at λ = 490 nm.

Binding experiments after additional incubation with copper. These experiments were performed in a similar fashion as described for the standard procedure. However, prior to the exposure of the immobilized carbohydrates to CTB, all wells were incubated with 50 µl of a 6 µM $CuSO_4$ solution and 50 µl of a 12 µM sodium ascorbate solution for 1 h. Subsequently, the plate was washed with water (3 × 400 µl per well) and the assay proceeded as described in the standard procedure. For the third set of experiments, 50 µl of a 1 mM $CuSO_4$ and 50 µl of a 1 mM sodium ascorbate solutions were added to each well and allowed to incubate for 1 h. Subsequently, the plates were washed with water (3 × 400 µl per well) and the assay proceeded as described in the standard procedure.

5.5 References

[1] a) A. Varki, *Glycobiology* **1993**, *3*, 97-130; b) K. Sandhoff, *Proc. Jpn. Acad., Ser. B* **2012**, *4554*, 554-582; c) T. Ariga, *J. Neurosci. Res.* **2014**, *Early view*, DOI: 10.1002/jnr.23411.

[2] a) C. W. Tornøe, C. Christensen, M. Meldal, *J. Org. Chem.* **2002**, *67*, 3057; b) V. V. Rostovtsev, L. G. Green, V. V. Fokin, K. B. Sharpless, *Angew. Chem., Int. Ed. Engl.* **2002**,

41, 2596-2599; c) P. Sengupta, S. Basu, B. P. Chatterjee, *J. Carboh. Chem.* **2000**, *19*, 243-251.
[3] J. Sánchez, J. Holmgren, *Indian J. Med. Res.* **2011**, *133*, 153-163.
[4] G. Guillain, J.-A. Barré, A. Strohl, *Bull. Mem. Soc. Med. Hop. Paris* **1916**, *40*, 1462-1470.
[5] a) A. V. Pukin, C. A. G. M. Weijers, B. van Lagen, R. Wechselberger, B. Sun, M. Gilbert, M.-F. Karwaski, D. E. A. Florack, B. C. Jacobs, A. P. Tio-Gillen, A. van Belkum, H. P. Endtz, G. M. Visser, H. Zuilhof, *Carboh. Res.* **2008**, *343*, 636-650; b) A. V. Pukin, B. C. Jacobs, A. P. Tio-Gillen, M. Gilbert, H. P. Endtz, A. van Belkum, G. M. Visser, H. Zuilhof, *Glycobiol.* **2011**, *21*, 1642-1650; c) K. K. R. Tetala, A. P. Heikema, A. V. Pukin, C. A. G. M. Weijers, A. P. Tio-Gillen, M. Gilbert, H. P. Endtz, A. van Belkum, H. Zuilhof, G. M. Visser, B. C. Jacobs, T. A. van Beek, *J. Med. Chem.* **2011**, *54*, 3500-3505.
[6] a) J. A. Prescher, C. R. Bertozzi, *Nat. Chem. Biol.* **2005**, *1*, 13-21; b) B. S. Sumerlin, A. P. Vogt, *Macromolecules* **2010**, *43*, 1-13; c) J. C. Jewett, C. R. Bertozzi, *Chem. Soc. Rev.* **2010**, *39*, 1272-1279; d) T. K. Tiefenbrunn, P. E. Dawson, *Biopolymers* **2010**, *94*, 95-106; e) E. M. Sletten, C. R. Bertozzi, *Angew. Chem., Int. Ed. Engl.* **2009**, *48*, 6974-6998; f) C. R. Becer, R. Hoogenboom, U. S. Schubert, *Angew. Chem., Int. Ed. Engl.* **2009**, *48*, 4900-4908.
[7] D. Prim, F. Rebeaud, V. Cosandey, R. Marti, P. Passeraub, M. E. Pfeifer, *Molecules* **2013**, *18*, 9833-9849.
[8] S. J. Stohs, D. Bagchi, *Free Radical Biol. Med.* **1995**, *18*, 321-336.
[9] G. J. Brewer, *Chem. Res. Toxicol.* **2010**, *23*, 319-326.
[10] M. E. Letelier, S. Sánchez-Jofré, L. Peredo-Silva, J. Cortés-Troncoso, P. Aracena-Parks, *Chem.-Biol. Interact.* **2010**, *188*, 220–227.
[11] H. Kaczmarek, *J. Photochem. Photobiol. A* **1996**, *95*, 61-65.
[12] F. Lim, X.-H. Yu, S. L. Cooper, *Biomaterials* **1993**, *14*, 537-545.
[13] a) W. Norde, D. Gage, *Langmuir* **2004**, *20*, 4162-4167; b) E. P. K. Currie, W. Norde, M. A. Cohen Stuart, *Adv. Colloid Interface Sci.* **2003**, *100-102*, 205-265.
[14] A. K. Sharma, A. D. Kent, J. M. Heemstra, *Anal. Chem.* **2012**, *84*, 6104-6109.
[15] J. Dommerholt, S. Schmidt, R. P. Temming, L. J. A. Hendriks, P. J. T. Rutjes Floris, C. M. van Hest Jan, D. J. Lefeber, P. Friedl, L. van Delft Floris, *Angew. Chem., Int. Ed. Engl.* **2010**, *49*, 9422-9425.
[16] L. A. Canalle, T. Vong, P. H. H. M. Adams, F. L. Van Delft, J. M. H. Raats, R. G. S. Chirivi, J. C. M. Van Hest, *Biomacromolecules* **2011**, *12*, 3692-3697.
[17] K. Nishimura, D. Sugiyama, Y. Kogata, G. Tsuji, T. Nakazawa, S. Kawano, K. Saigo, A. Morinobu, M. Koshiba, K. M. Kuntz, I. Kamae, S. Kumagai, *Ann. Intern. Med.* **2007**, *146*, 797-808.
[18] a) E. A. Merritt, W. Hol, *Curr. Opin. Struct. Biol.* **1995**, *5*, 165-171; b) E. A. Merritt, S. Sarfaty, T. T. Chang, L. M. Palmer, M. G. Jobling, R. K. Holmes, W. G. J. Hol, *Structure* **1995**, *3*, 561-570; c) E. A. Merritt, S. Sarfaty, F. Vandenakker, C. Lhoir, J. A. Martial, W. G. J. Hol, *Protein Sci.* **1994**, *3*, 166-175.
[19] M. A. Wijdeven, C. Nicosia, A. Borrmann, J. Huskensb, F. L. v. Delft, *R.S.C. Adv.* **2014**, *4*, 10549-10552.
[20] V. D. Matteis, C. A. G. M. Weijers, R. H. v. Doorn, M. Gilbert, B. C. Jacobs, G. M. Visser, H. Zuilhof, unpublished results
[21] a) H. Staudinger, J. Meyer, *Helv. Chim. Acta* **1919**, *2*, 635-646; b) E. Saxon, C. R. Bertozzi, *Science* **2000**, *287*, 2007-2010.
[22] T. Holletz, D. Cech, *Synthesis* **1994**, 789-791.
[23] W. A. Bonner, *J. Am. Chem. Soc.* **1951**, *73*, 2659-2666.
[24] T. E. Timell, *Can. J. Chem.* **1964**, *42*, 1456-1472.
[25] D.-D. Zheng, D.-Y. Fu, Y. Wu, Y.-L. Sun, L.-L. Tan, T. Zhou, S.-Q. Ma, X. Zhab, Y.-W. Yang, *Chem. Commun.* **2014**, *50*, 3201-3203.
[26] C. N. R. Rao, T. S. Chao, C. W. W. Hoffman, *Anal. Chem.* **1957**, *29*, 916-918.

6

Evaluation of synthetic ganglioside-based glycan fragments as epitopes for Guillain-Barré syndrome-associated antibodies

This chapter is *in preparation* for publication.

Abstract:

As part of an ongoing investigation, we aim to improve the understanding at the molecular level of the antibody (Ab)-ganglioside specificity in the pathogenesis of the neuropathological ailment Guillain-Barré syndrome (GBS). Our strategy was to test a small library of ganglioside-based glycans on patient sera. We synthesized eight mono- and disaccharides that display elements from naturally occurring mammalian ganglioside GM1. In addition, these ganglioside fragments were designed to contain chemical handles with which they could be covalently immobilized to microtiter plates. Once immobilized, they were exposed to GBS patient sera that contain anti-ganglioside Abs, and the Ab-carbohydrate binding was evaluated. For most patient sera no significant binding was observed, indicating that their native ganglioside antigen-Ab response could not be recreated by synthetic GM1 fragments or combinations thereof. We did however discover through these assays that some anti-ganglioside Abs bind to compounds displaying the simple monosaccharide galactose and disaccharide lactose epitopes. Especially sera that showed cross-reactivity towards wild type galactocerebroside were shown to bind these two simple saccharides. In addition, applying a relatively short oligo-EO spacer (12 atoms) as a coating on the microtiter plate surfaces had dramatic effects for a select number of GBS patient sera on the Abs-ganglioside fragments binding affinity. This chemical blocking step was applied in addition to the standard blocking step in ELISA with bovine serum albumine. In one case, the Abs-Gal binding response was doubled in relation to when this chemical blocking step was not performed. These results will contribute to the development of future diagnostics, in the form of biosensors, for the rapid detection of certain GBS subtypes.

6.1 Introduction

Our immune system constantly probes our body for the presence of foreign entities. One of many methods it uses for detection is to monitor for non-indigenous glycan structures, and if identified, to initiate an immune response. In rare cases, the antibodies (Abs) that are involved in this immune response are cross-reactive with glycans (carbohydrates) that reside on our own cells, and thereby initiate an autoimmune response. Guillain-Barré syndrome (GBS) is a post-infectious autoimmune disorder that results from such an interaction, in which our own carbohydrates (and as a consequence our cells) are targeted by our immune system. It is a life-threatening disease and patients require immediate hospital treatment. GBS is the leading cause of acute paralysis, and worldwide, 1 - 2 persons per 100.000 are annually affected.[1]

The infection preceding GBS may present itself as an upper respiratory tract infection, gastro-intestinal infection, influenza-like illness or remain subclinical. The main cause of the enteritis that triggers the autoimmune response in GBS is the ingestion of *Campylobacter jejuni* (*C. jejuni*) bacteria. Chickens are considered as the most important source of human infection by *C. jejuni*, which primarily arises from cross-contamination or consumption of not well-baked poultry meats.[2] The bacteria is very common in the guts of chickens and ends up on meat by contamination from accidental fecal spilling during slaughter. [3] Other sources of consumption-based infections are, amongst others, bovine meat, untreated dairy products, contaminated water sources, and pets.[4]

The initial symptoms of the bacterial infection can reach their maximum in about a week after ingestion of the pathogen (Figure 1). The patients usually

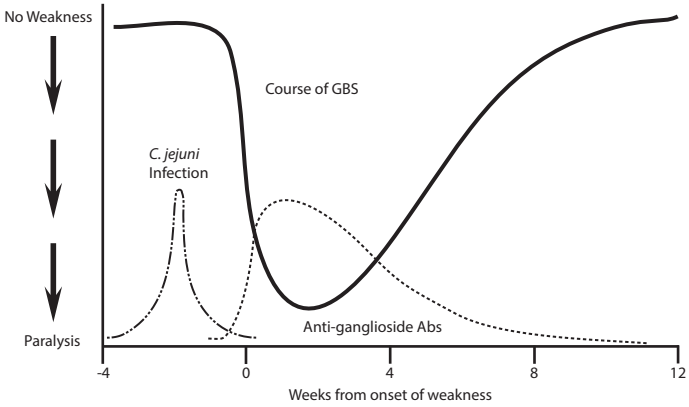

Figure 1. Guillain-Barré syndrome time-scale concerning limb weakness. Figure adapted from reference.[6b]

recover from this by the time the main symptoms of GBS, including motor dysfunction, present themselves. The first signs of GBS are expressed by weakness or numbness, particularly in the limbs. Patients describe tingling sensations, followed by paralysis starting from the base progressing all the way to the top of the body, and extending to the arms. This ascending paralysis increases in intensity and in extreme cases, patients becomes totally paralyzed within 2 days.[5] In at least one-fifth of the patients, the nerves innervating the respiratory muscle become damaged to such extent that respiratory failure may develop and patients need to be ventilated at an intensive care unit. The rapid decline of the patient's health generally reaches its maximum within 4 weeks, but many patients have reached their maximal weakness already within 2 weeks.[6]

The first choice standard treatment for GBS is intravenous immunoglobin (IVIg), and the second choice is plasmapheresis. In IVIg, high doses of immunoglobulins derived from blood from healthy donors are infused. The mechanism of action is unknown but it is believed that IVIg may in part neutralize the harmful Abs or their neurotoxic effects. In plasmapheresis, plasma is extracorporeally separated from the patients' other blood components, leaving the blood cells to be returned to the body while the plasma that contains the malicious Abs is discarded. A major disadvantage of plasmapheresis is that patients with GBS may develop life-threatening autonomic dysfunction. Despite treatment, about 25% of the patients require respiratory assistance; approximately 20% of the patients still experience limb dysfunction after six months. Ultimately, 3 - 10% of the patients die,[7] most commonly of heart failure.[8]

On the molecular level, GBS patients are victimized by pathogens that display carbohydrates that are in part also indigenous of the human body. The terminal parts of the complex bacterial carbohydrates closely resemble glycosphingolipids that are part of the host's peripheral nervous system (PNS) tissue (Figure 2) that are subsequently also attacked by the immune system. Figure 2B shows the lipooligosaccharide (LOS) that resides on the cell wall of *C. jejuni*.[9] The bacterium LOS contains the terminal tetrasaccharide sequence Galβ1-3GalNAcβ1-4(Neu5Acα2-3)Galβ1. The same epitope is displayed on the ganglioside GM1, which resides on PNS nerve cells (Figure 2A). Abs that are formed by the immune system, as a response to the presence of the intruder, cross-react to both types of carbohydrates, and thereby causing the autoimmune response.[10] These phenomena (including other criteria[11]) make GBS a disease that is instigated by molecular mimicry. This mimicry already occurs during

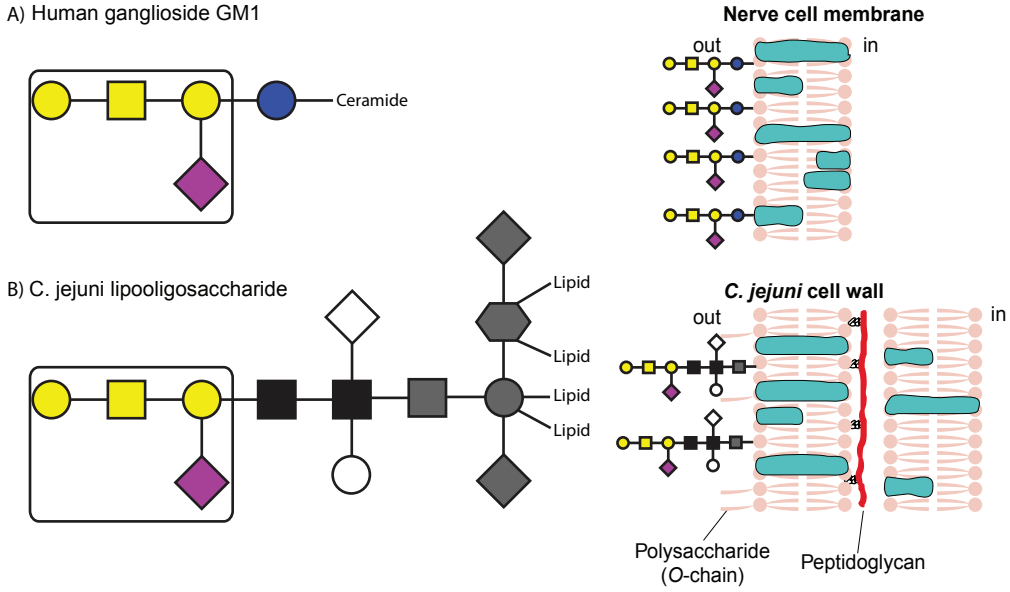

Figure 2. Molecular mimicry of *C. jejuni*. The epitope of the bacterium LOS resembles the terminal tetrasaccharide sequence Galβ1-3GalNAcβ1-4(Neu5Acα2-3)Galβ of ganglioside GM1 (For chemical structure see Figure 4) that resides, amongst others, on PNS nerve cells. Reproduced from reference.[19a]

the infection period, as the host's immune system then forms Abs against the oligosaccharide structures that are displayed on the intruding pathogen.

GBS was first described as a single ailment in 1916 by Guillain, Barré and Strohl.[12] It is nowadays recognized that the range of symptoms observed in GBS patients actually consists of several unique ailments that can be subdivided based on their pathogenesis.[13] Depending on the subtype of GBS, patients develop Abs against varying human gangliosides that each also result in quite different pathogenesis. Patients with acute motor axonal neuropathy (AMAN) predominantly display Abs against GM1, GM1b, GD1a, and GalNAc-GD1a (for structures see Chapter 1). In axonal forms of GBS, the Abs attack appears directed against gangliosides that are displayed on the axon cell membrane and nodes of Ranvier (Figure 3B).[14] In acute inflammatory demyelinating polyneuropathy (AIDP), the myelin sheath and Schwann cells are targeted by the Abs, rather than the axons directly (Figure 3A). Although not always evident, in some cases of AIDP, Abs against GM4, GM3, GM2, GT3, and especially GD3 were encountered.[15] In more recent studies it is, however, debated if gangliosides actually play a role in the pathogenesis of AIDP.[16] It was described that the distinction between the two subtypes AIDP and AMAN is difficult and even unreliable, which resulted in 58%

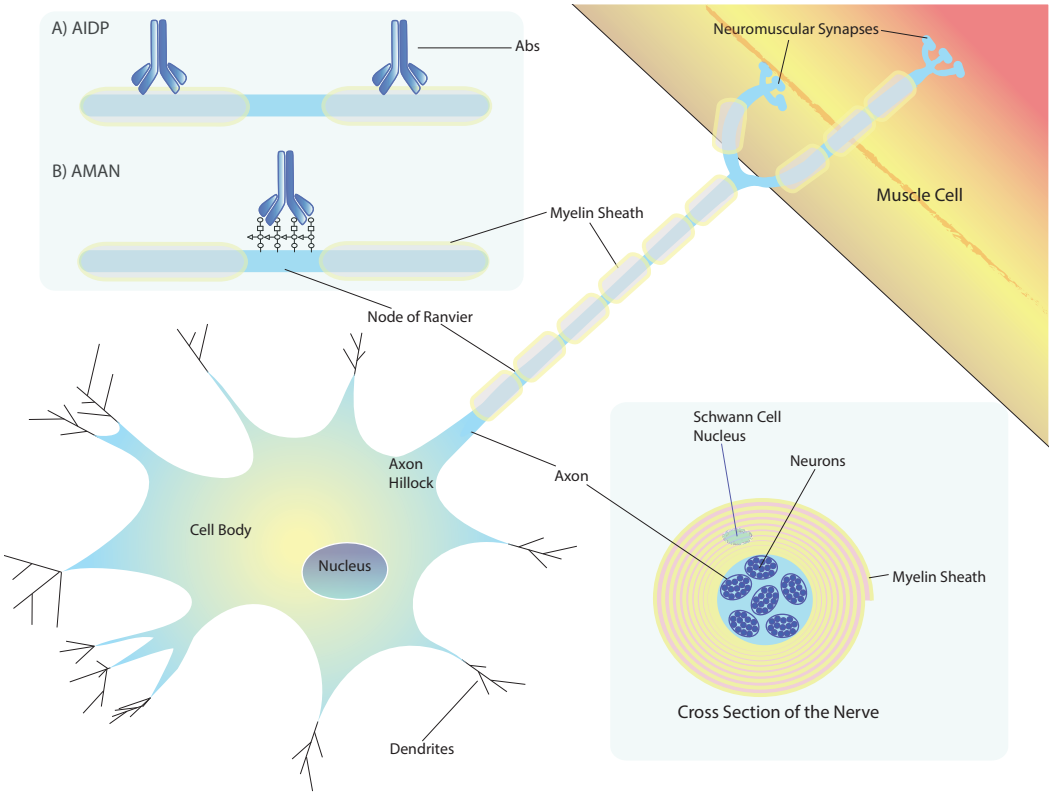

Figure 3. Depiction of an axon, or nerve cell, that sends synapses to the muscle cell to trigger response. A) In AIDP, the myelin sheath is targeted by Abs; B) In AMAN, autoimmune response is caused by Abs that target carbohydrates on the nodes of Ranvier.

of the patients, initially diagnosed with AIDP, to be re-diagnosed with AMAN.[17] The question to what antigens are then the target of auto-immune Abs in AIDP was not answered and therefore remains to be resolved. However, circumstantial evidence for the existence of anti-ganglioside Abs in AIDP is quite strong.[18] Patients with Miller-Fisher syndrome (MFS) that cross-react with *C. jejuni*[19] especially display the presence of Abs against multisialylated gangliosides GQ1b, GD3, and GT1a.

Recent studies indicated that some anti-ganglioside Abs that are able to bind a certain type of ganglioside, say GM1, are also able to bind a mixture of two gangliosides, for example a 1 : 1 combination of GM1 and GD1a. In contrast, other Abs show a positive binding towards the pure ganglioside GM1, but show no signs of binding when combined with GD1a.[20] These results indicate that complexes of gangliosides – complexed through electronic interactions, *e.g.* Van der Waals and H-bonding – are recognized by some Abs

rather than the individual gangliosides. This finding underlines the necessity of applying pure gangliosides in bioassays.[21] Another study[22] involving saturation transfer difference nuclear magnetic resonance (STD-NMR)[23] on two patient sera revealed that, in both cases, the main epitope for the anti-ganglioside Abs were the terminal Gal*β*1-3GalNAc*β* sequence and the Neu5Ac*α*2 moiety. Microarrays that included smaller carbohydrate derivatives, basically ganglioside fragments, have previously been reported in research on the interaction of these ganglioside GM1-related carbohydrates with cholera toxin (for a detailed description of the role of ganglioside in cholera toxin-binding see Chapter 1).[24] To the best of our knowledge, to this date no study has been conducted on synthetic ganglioside fragments to provide more insights on which epitopes are responsible for the recognition by GBS-associated Abs.

In the current study, we aim to improve the understanding of the Abs-ganglioside binding in the pathogenesis of GBS by the design and synthesis of a small library of ganglioside fragments. Previously, synthetic ganglioside analogues were synthesized in our laboratory and used successfully to detect Abs in GBS patient sera.[25] These carbohydrates have the advantage that, since they are synthesized, they are acquired pure. An additional benefit over isolation from natural sources is that the synthesized compounds can be equipped with a handle (*e.g.* an azide) that allows easy bioconjugation or coupling to a surface. In contrast, in current standardized assays native gangliosides are used that are extracted from bovine brain.[26] These are difficult to purify and are therefore potentially contaminated with other glycolipids. Larger bifunctional synthetic ganglioside analogues, presenting two similar epitopes, were also successfully used to detect anti-ganglioside Abs in sera of GBS patients.[25b] The choice for the fragment approach was based on these previous studies and on the additional benefit that fragments are more easily accessible due to shorter synthetic pathways. Patients that have contracted various GBS subtypes express Abs that are able to distinguish between different epitopes, like the multisialylated gangliosides in case of MFS or ganglioside GM1 in AIDP. By deconstruction of such gangliosides – making them less complex, but still providing the epitopes that are essential for binding – we aim to obtain new insights into the binding-mode of these Abs. Any insights gained via such an approach might eventually also lead to a diagnostic test, in the form of a biosensor, that provides rapid and reliable results for GBS subtype typography.

6.2 Results and Discussion

6.2.1 Synthesis of ganglioside fragments

The fragment selection and design was based on the carbohydrate sequence of ganglioside GM1 derivative **1** that contains an undecane-azido spacer (Figure 4). The choice for GM1 was made because it is believed to be the most common target of Abs in GBS patients in the western world.[27] Additionally, it contains almost all epitopes that are also displayed on other gangliosides, except the Neu5Ac*α*2-8Neu5Ac*α*2 disaccharide, which is synthetically challenging to access. However there are sialyltransferases available that are able to form both the *α*2,3- and *α*2,8-glycoside bonds on neuraminic acids.[28] Nevertheless, the optimization and use of these transferases was beyond the scope of this work. Therefore, we focused on a group of mono- and disaccharides that is accessible *via* relatively straightforward synthetic effort. This included the monosaccharides Gal*β*1 **2**, Neu5Ac*α*2 **4**, Neu5Ac*β*2 **7**, GalNAc*β*1 **9**, the non-terminal disaccharide Gal*β*1-4Glc*β*1 (lactoside) **3**, Gal*β*1-3GalNAc*β*1 **5**, which represents the carbohydrates at the terminus of the pentasaccharide ganglioside GM1, Neu5Ac*α*2-3Gal*β*1 **6**, which is ganglioside GM4, and finally GalNAc*β*1-4Gal*β*1 **8** (Figure 4). All fragments contain the anomeric -*O*-$C_{11}H_{22}N_3$ spacer that is also present on the previously synthesized ganglioside GM1 analogue **1**. All compounds have the same stereo- and regiochemistry as the carbohydrates present in the wild type ganglioside. However, since neuraminic acid is possibly the most important epitope in GBS[29] and in fact an essential criterion for a part of a glycosphingolipid to be classified as a ganglioside, we also selected the unnatural *β*-isomer of Neu5Ac (**7**) for this study. This allowed us to assess the effect of a different stereochemistry around the acid moiety.

The synthesis of glycosides **3** and **2** (Figure 4) started with *per*-acetylation of **10** and **11**, respectively, with acetic anhydride in the presence of catalytic iodine[30] (for a detailed insight on the mechanism of this reaction see Chapter 1). After 8 h, the reaction was diluted with DCM, and an equimolar amount of iodine was added to the reaction mixture followed by hexamethyldisilane (HMDS).[31] During this reaction, 2 equivalents of iodotrimethylsilane are generated *in situ*.[32] Substitution of the acetate by an iodine moiety yielded the *α*-iodo-anomer **14** in 74% yield, and in 90% in case of compound **15**, over two steps (Scheme 1). In both cases, only the α-anomers were obtained.

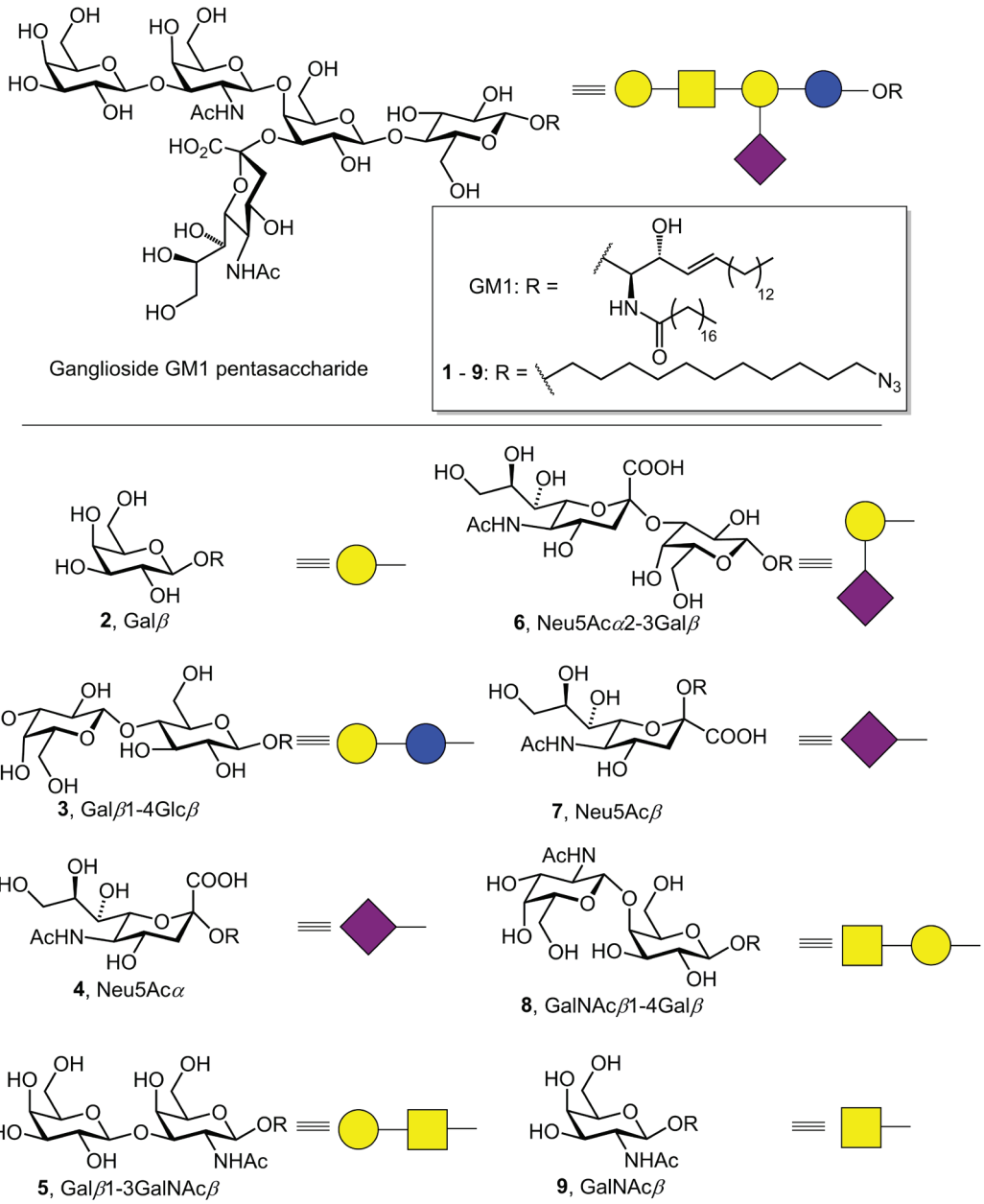

Figure 4. Small library of the synthetic analogue of ganglioside GM1, compound **1**, and ganglioside fragments **2** - **9** that were assayed by exposure to anti-ganglioside Abs in sera from GBS patients.

Activation of donor iodide **15** with iodine, now acting as Lewis acid, and subsequent glycosylation in DCM with acceptor 11-azido undecan-1-ol (**21**)

– which is formed by heating the corresponding 11-bromide analogue **20** with sodium azide in DMF[33] – resulted in a 60% yield of beta galactoside **17** (see Chapter 1 for mechanistic details on this glycosylation step). This reaction yielded both the alpha and the *β* anomer, in a ratio of 1 : 10, based on ^{1}H NMR analysis. The only isolated byproduct was a C-1 hydrolyzed hemiacetal. The glycosylation of the α-iodo lactoside (**14**) yielded 70% of both the *α* and *β* anomers of **16** in a ratio of 15 : 85. Also 2-deprotected lactoside was isolated (20%, *α*/ *β* ratio of 9 : 1) as well as the methyl ester of 11-azido-undecan-1-ol. The reason for the various (by)products being formed during this glycosylation is that various nucleophilic substitution reactions can take place, especially via the mechanism involving neighboring group participation (see Chapter 1 for details).

In an attempt to increase the yield and stereoselectivity of these reactions, the glycosylations were repeated with MeCN as solvent. Now only the β-anomer was obtained in 62% yield in case of the galactoside **17**, and for lactoside **16** in 70% yield. The acetyl-protected 11-azido-undecane glycosides (**16** and **17**) were subsequently deprotected by the standard Zemplén procedure,[34] namely, treatment with NaOMe in MeOH, and subsequent work-up with a H^+-resin resulted in deprotected **2** and **3** in near quantitative amounts. One-step, $SnCl_4$-promoted, glycosylation of *per*-acetyl lactoside **12** or galactoside **13** resulted in mixtures of anomers and disappointing yields: 28% for **18**, and 20% for **19**.

Galactoside **2** was further modified to function as an glycoside acceptor in the glycosylation towards the GalNAc*β*1-4Gal*β*1-*O*-$C_{11}H_{22}N_3$ fragment **8**. Therefore, it first needed to be regiospecifically deprotected at the 4-position (Scheme 2). To accomplish this, a protective group strategy was required that employs a chemoselective deprotection procedure and that keeps the terminal azido moiety intact. In the initial design of the strategy towards disaccharide **8**, galactoside **2** was 4,6-protected with a *p*-methoxybenzyl (PMB) acetal. This route was chosen because PMB acetals, and also the corresponding ethers, can be deprotected under relatively mild conditions. The electron-deficient DDQ facilitates the mild deprotection of PMB ethers[35] by a mechanism of multiple single electron transfers (SET) (see Chapter 1 for mechanistic details on this reaction). Additionally, like benzylidene acetals, the PMB acetals can also be opened regioselectively to form the corresponding 4-*O*- or 6-*O*- ether.[36] Gal*β*1-*O*-$C_{11}H_{22}N_3$ (**2**) was therefore exposed to *p*-anisaldehyde dimethylacetal and *p*-toluenesulphonic acid (PTSA) yielding *p*-methoxybenzylidene acetal **22** (Scheme 2).[35b] When the reaction was performed overnight at 50 °C, a high ratio of *α*-anomer was acquired (*α*/

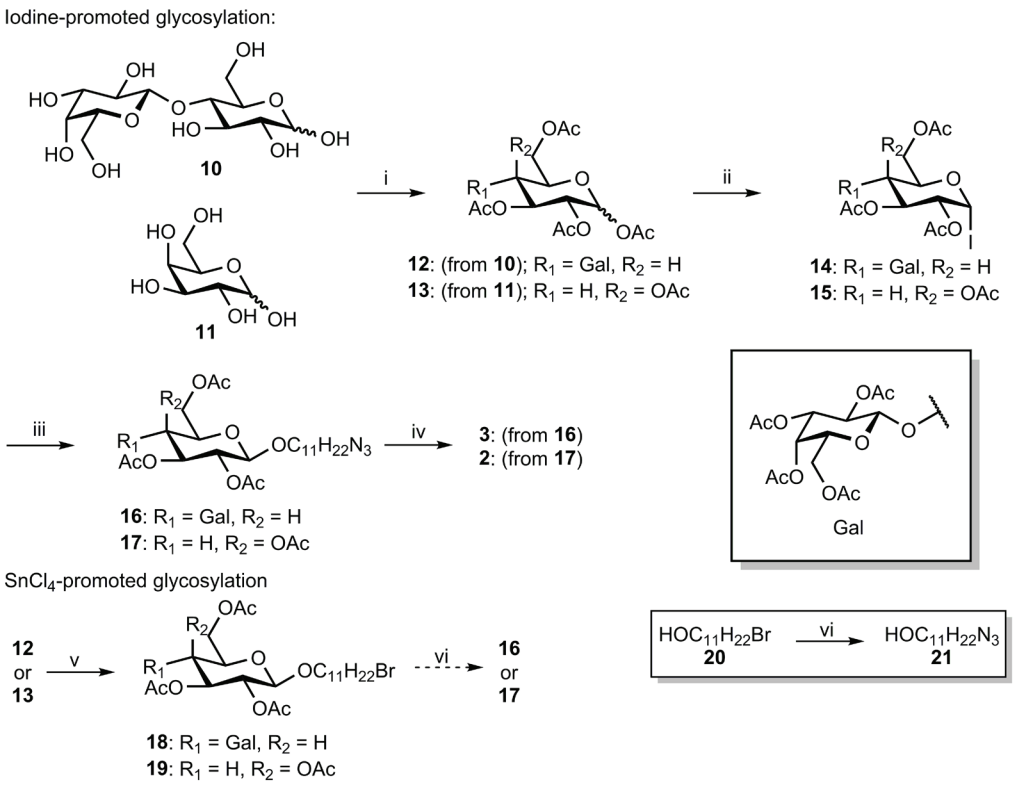

Scheme 1: Iodine-promoted synthesis of fragments **2** and **3**. Reagents and conditions: i) Ac_2O, I_2 (cat.); ii) I_2, HMDS, MeCN, 5 h (**14** 74%, **15** 90% over two steps); iii) **21**, I_2, MeCN, 4 Å MS, (**16** 70%, **17** 62%); iv) NaOMe, MeOH, 10 min. then H^+-resin (**2** 91%, and **3** quant.); v) $SnCl_4$, 4 Å MS, DCM (**18** 28%, **19** 20%); vi) NaN_3, DMF, 100 °C 16 h; **21** 91%; not performed in the direct glycosylation to afford **16** and **17**.

β ratio: 3 : 4, at 72% combined yield). Fortunately, both anomers were easily separated by flash chromatography. When the reaction was repeated at room temperature for 36 h, a significant increase in the desired *β*-anomer, product **22**, was observed (65% *β*) and only trace amounts of the *α*-anomer could be detected.

The remaining hydroxyl-groups at C-2 and C-3 of compound **22** were PMB-protected by reacting them with NaH and PMB-Cl, resulting in 69% yield of compound **23**. The subsequent step was the selective opening of the *para*-methoxybenzylidene and concomitant 4-deprotection of the galactoside to obtain compound **25**. This procedure requires the acetal to be exposed to $NaCNBH_3$ that delivers a nucleophilic hydride.[37] After the ring opening is accomplished, an 1 M HCl solution in ether is added dropwise to protonate the product and to quench the remaining $NaCNBH_3$. In this case, after workup, multiple side products were

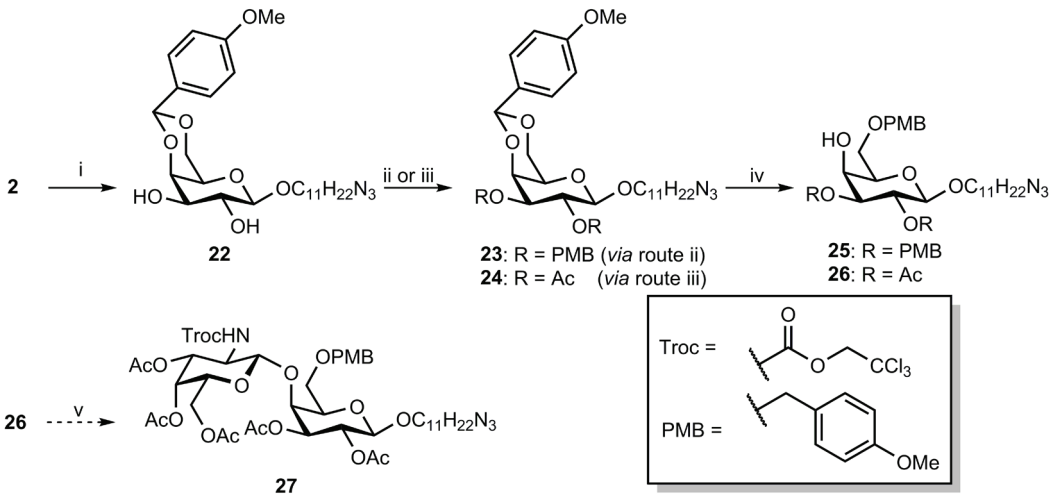

Scheme 2. Protecting group strategies. Reagents and conditions: i) *p*-anisaldehyde dimethyl acetal, PTSA, MeCN, rt, 36 h, 65%; ii) NaH, PMB-Cl, DMF, 18 h, 69%; iii) Ac_2O, pyridine, 18 h, 93%; iv) $NaCNBH_3$, 1 M HCl in Et_2O, THF, 3Å MS, 70% **26**, compound **25** was not isolated; v) **34**, TMSOTf, DCM, 3Å MS -20 °C → 0 °C product not isolated.

detected that indicated that not only the acetal was opened, but that also the 2- and 3-deprotected products had formed. Although it was known that the PMB ether is acid-labile,[38] it was not expected that the deprotection would already be facilitated by addition of minute quantities of acid, and in the presence of a reactive species ($NaCNBH_3$) towards protons. This unfortunate reactivity required an adjustment in the protective group strategy, and it was decided to synthesize the 2,3-di-*O*-acetyl protected compound **26** (Scheme 2) by exposure of **22** to acetic anhydride in pyridine. The resulting diacetyl acetal **24** was then regiospecifically deprotected to obtain 4-*O*-deprotected compound **26** in good yield (70%).

Unfortunately, the subsequent glycosylation with a GalNAc donor did not yield the desired disaccharide **27**. Although, the very similar 2,3-di-*O*-acetyl 6-*O*-benzyl galactoside acceptor has been reported in a successful NIS-promoted glycosylation with a thioglycoside donor.[39] Possibly, the reaction temperature was too high and therefore, some byproducts with displaced PMB protective groups were observed, resulting in a mixture of glycosylation products and (partly) deprotected starting materials that were hard to separate. Since the initial protective group strategy was not successful, we turned to the more commonly used benzyl protective groups as an alternative. Starting from the galactoside **2** (Scheme 3), 4,6-benzylidene protection was applied to provide compound **28**, followed by benzyl-protection of the 2 and 3-positions (**29**). Selective ring

opening of the acetal was achieved, leading to compound **30** in 70% yield.

The galactosamine donor was synthesized, as described in literature[40], by dissolving galactosamine-HCl salt **31** in H_2O and reacting it with trichloroethyloxycarbonyl (Troc) chloride in the presence of base resulting in the Troc carbamate.[41] Subsequent acetylation of the remaining functional sites was performed by addition of pyridine and acetic anhydride, resulting in the Troc carbamate **32**. Specific C-1 deprotection was performed by reaction of **32** with hydrazine acetate to acquire **33** in 85% yield. Subsequent reaction of the resulting hemiacetal with trichloroacetonitrile and DBU resulted in tricholoroacetimidate, or Schmidt imidate,[42] **34** in 75% yield (predominantly α). Alternatively, when $CaCO_3$ was used in this reaction, the product was obtained in 68% (*α*/ *β* ratio: 1 : 2). For

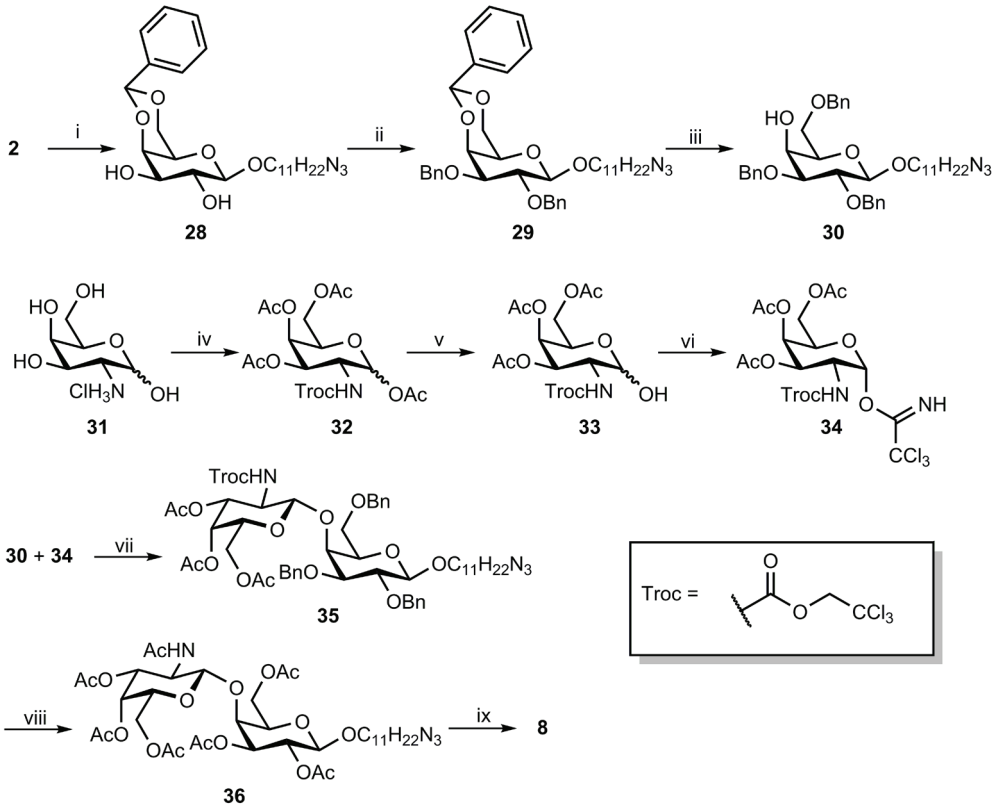

Scheme 3. Synthesis route of disaccharide **8**. Reagents and conditions: i); α,α-dimethoxytoluene, PTSA, MeCN, 6 h, 75%; ii) BnCl, NaH, DMF, 1 h, 86%; iii) $NaCNBH_3$, 1 M HCl in Et_2O, THF, 3Å MS, 70%; iv) K_2CO_3, Troc-Cl, H_2O, 1 h then pyridine/ Ac_2O (1 : 1), 70%; v) hydrazine acetate, DMF, 90 min., 85%; vi) trichloroacetonitrile, DBU, DCM, 20 min., 75%; vii) TMSOTf, DCM, 2 h, -40°C, 53%; viii) a) Activated Zn, Ac_2O, 18 h; b) TMSOTf, Ac_2O; 90 min., 70% over two steps; ix) NaOMe, MeOH 10 min. then H^+-resin, 95%.

this particular compound, a very distinct and characteristic picture arose in the mass spectrum (Figure 5), providing a beautiful example of an isotope pattern of a compound containing six chlorine atoms. In a similar fashion, also the *N*-(4-nitrobenzyl)oxycarbonyl (PNZ) imidate was synthesized as alternative glycosyl donor (see §6.4.3 compound **34b** for more details). Reaction of the galactoside acceptor molecule **30** with the galactosamine imidate **34** in the presence of catalytic amounts of TMSOTf resulted in disaccharide **35** in 53% yield.

The standard benzyl deprotection procedure,[43] which involves Pd/C-catalyzed hydrogenation, is not compatible with the azide functionality that is later required for the immobilization of the carbohydrates in our biological assays. Rather than choosing additional steps – for example, by using an azide transfer reagent after the reduction,[44] which would be able to reestablish the azide functionality from the amine – a method was chosen that exchanges the benzyl protection for acetyl groups after the formation of the disaccharide. Therefore, deprotection of the disaccharide started by interchanging the benzyl groups with acetyl groups via reaction of compound **35** with TMSOTf in acetic anhydride,[45] which was reasonably successful (70% yield). The resulting hexa-acetate **36** was then easily deprotected to form ganglioside GM1 fragment **8** in 95% yield.

Galactoside **2** was also the starting material in the enzymatic synthesis of disaccharide **6** (Scheme 4). This compound contains the disaccharide Neu5Acα2-3Galβ of ganglioside GM4.[46] The commercially available enzyme sialyltransferase II[47] was used to attach its natural substrate, cytidine monophosphate (CMP)-Neu5Ac **37**, to the previously synthesized galactoside **2** to obtain **6** in 77% yield.

Scheme 5 depicts the syntheses of monosaccharide compound **9** and disaccharide **5**. We attempted to synthesize the galactosamine monosaccharide **9** by reacting the previously discussed Schmidt imidate **34** (Scheme 3) with 11-azido-undecan-1-ol (**21**). However, glycosylation attempts with either BF_3OEt_2 or TMSOTf as promoter did not result in the desired compound. Although reactions with galactoside imidate **41** with fairly unreactive alcohols and above-mentioned Lewis acids are described in literature,[48] we did not isolate the desired galactosamine glycoside in acceptable quantities. The iodine-promoted glycosylation, which was described earlier in a successful syntheses of fragments **2** and **3** (Scheme 1), was unsuccessfully employed in an attempt to form an 1-iodo *N*-Troc-protected galactosamine, or its *N*-PNZ protected analogue. Presumably, the α-iodine does not form in these cases due to steric interference of the adjacent bulky carbamate. Ultimately, a microwave-assisted, and H^+-silica-

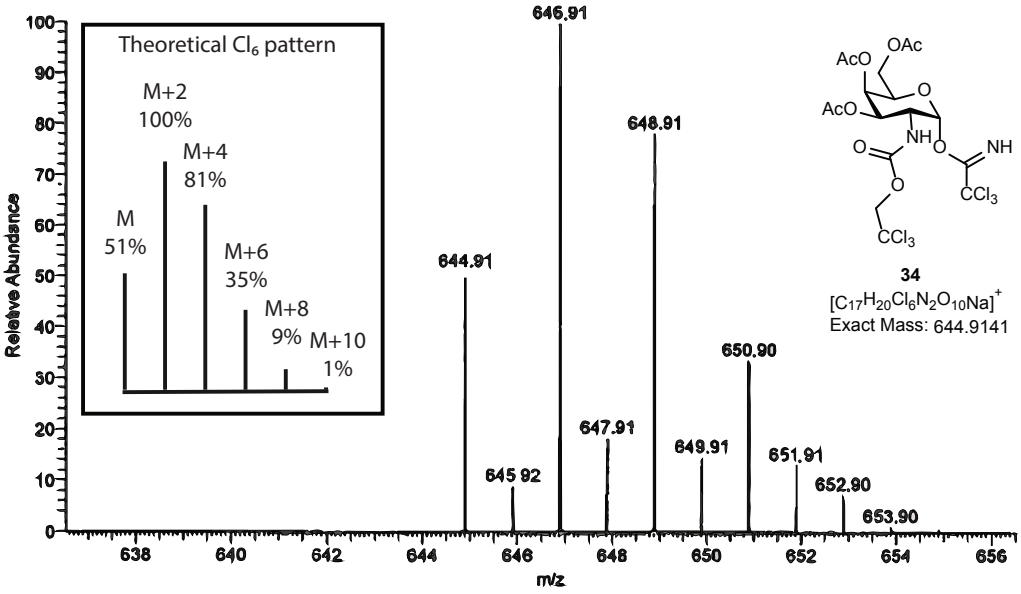

Figure 5. Isotope pattern in a typical ESI+ mass spectrum for 6 Cl-containing compound **34**; $[M+Na]^+$ observed.

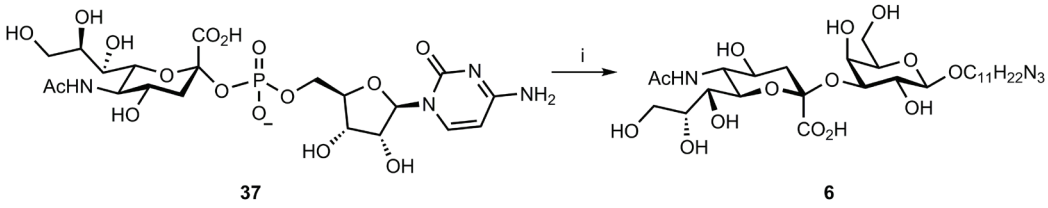

Scheme 4. Enzymatic step in the synthesis of disaccharide **6**. i) **2**, Sialyltransferase II, $MnCl_2$, $MgCl_2$, H_2O, 72 h, 77%.

catalyzed, synthesis was performed,[49] which required the 11-azidoundecan-1-ol (**21**) and the *per-O*-acetylated galactosamine **38** (Scheme 5). Compound **38** was obtained by reacting the galactosamine hydrochloric acid salt **31** with acetic anhydride in pyridine. Generally, a protective group is required on the C-2 position to prevent formation of the stable oxazoline **38b**, in which the acetamide carbonyl-group reacts with the C-1 while approaching from the axial position. In the microwave-assisted reaction, the oxazoline formation is desired since it functions both as a leaving group and prevents approach of a nucleophile, in this case 11-azido-undecan-1-ol **21**, on the α-position, and thereby stimulates *β*-glycosylation. Performing this MW-assisted reaction at 150 °C ensures opening of the oxazoline, reinstating the acetamide on the galactosamine C-2 position and forming solely the desired *β*-product **39** in very good yield (84%). Deprotection by the standard Zemplén procedure ensured formation of galactosamine **9**.

Subsequently, galactosamine fragment **9** was selectively 4,6-protected by a previously described *para*-methoxybenzylacetal (see also Scheme 2), forming acceptor **40** (Scheme 5). Tricholoracetimidate **41** was synthesized in a similar fashion as was described for the GalNAc imidate **34**, by selective C-1 deacetylation of compound **13**, and subsequent reaction with trichloroacetonitrile. Disaccharide Gal*β*1-3GalNAc*β*1 **5** was then synthesized starting by reaction of **40** with galactoside donor **41** to give compound **42**. DDQ-facilitated SET-deprotection of **42** and subsequent Zemplén deacetylation resulted in disaccharide **5**.

The MW-assisted glycosylation that was successfully employed in the synthesis

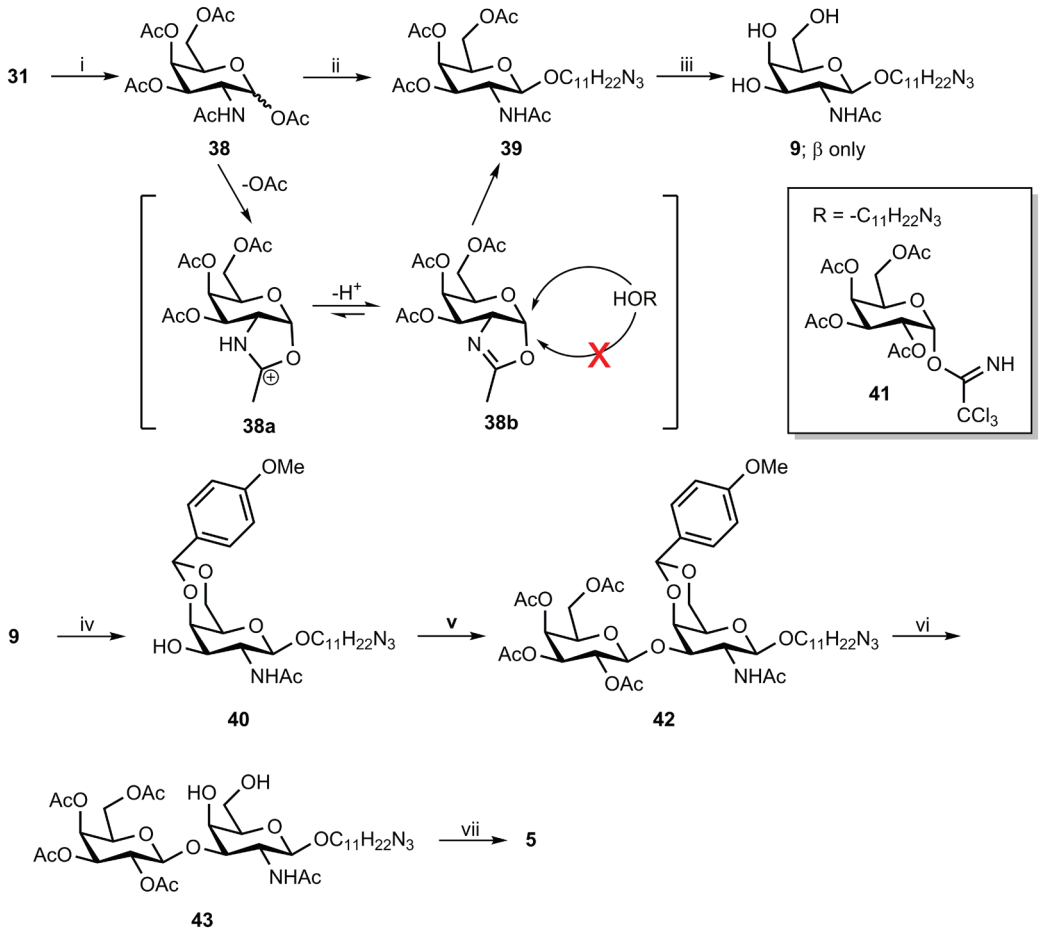

Scheme 5. Synthesis of disaccharide **5**. Reagents and conditions: i) Ac_2O, pyridine, 18 h, 89%; ii) **21**, H^+-silica, DCE, MW, 30 min, 150 °C, 84%; iii) NaOMe, MeOH, 30 min. then H^+-resin, quant.; iv) *p*-anisaldehyde dimethylacetal, PTSA, MeCN, rt, 48 h, 86%; v) **41**, TMSOTf, -30 °C → 0 °C 8 h, 56%; vi) DDQ, MeCN/ H_2O 1 : 4, 2 h, 58%; vii) NaOMe, MeOH, 10 min then H^+-resin, 90%.

of galactosamine **9** was also applied to form *β*-Neu5Ac-derivative, fragment **7**. First, the methyl ester of neuraminic acid **44** was formed by a Fisher esterification, followed by protection of the alcohol groups by reaction with pyridine and acetic anhydride to provide protected **45**.[50] Since the MW-assisted reaction in case of the galactosamine **39** proceeded via neighboring group participation by forming the oxazoline (**38b**), formation of the required product was not expected here, because the neuraminic acid does not have a neighboring group at the C-3 position that can participate. However, mass spectrometry revealed that the target sialoside was present. Additionally, some byproducts had formed that showed intramolecular cyclization, and these resembled structures that were previously described in

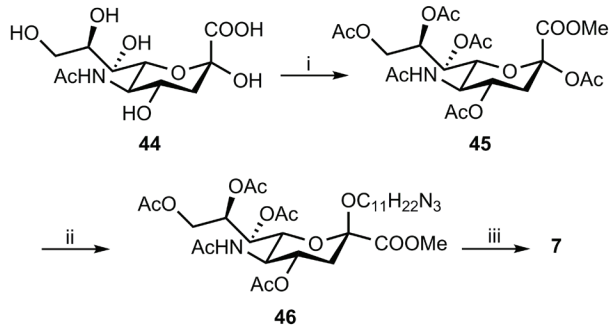

Scheme 6. Reagents and conditions: i) a) H^+-resin, MeOH, 4 days; b) pyridine, Ac_2O, 0 °C → rt, 18 h, 90% over two steps; ii) **21**, H^+-silica, DCE, MW, 20 min, 150 °C, 13%; iii) a) NaOMe, MeOH, 30 min, then H^+-resin; b) KOH, MeOH/ H_2O 1 : 4, 30% over two steps.

literature.[51] Target *β*-compound **46** was obtained in 13% yield after purification. Subsequently, by removing the acetyl protecting groups by the Zemplén procedure and saponification of the methyl-ester with aqueous KOH, compound **7** was obtained in 30% yield (Scheme 6).

In order to synthesize the required natural *α*-anomer **4**, protected Neu5Ac **45** was transformed into 2-Cl-Neu5Ac **47** by applying hydrochloric acid gas through a solution of **45** in acetyl chloride and diethyl ether.[52] Subsequent Koenigs-Knorr glycosylation[53] of chloride **47** with the 11-azidoundecan-1-ol spacer **21** in the presence of silver carbonate[54] yielded the acetyl-protected Neu5Ac*α*2, (**48**) in the modest yield of 47%. After deprotection of the acetyl groups and the methyl ester compound **4** was obtained quantitatively over two steps (Scheme 7).

NMR techniques showed to be of crucial importance for the unambiguous identification of the stereochemistry of the synthesized compounds, which is not a trivial task. For glycosyl pyranosides, assignment of the anomeric configuration

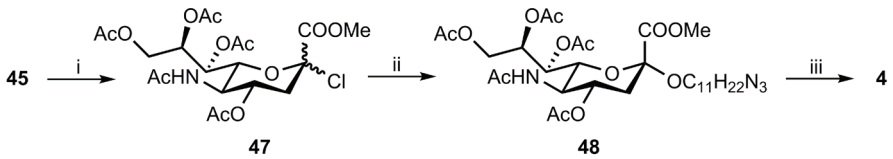

Scheme 7. Synthesis route of Neu5Ac-derivative **4**. Reagents and conditions: i) AcCl, HCl (g), Et_2O, 90%; ii) **21**, $AgCO_3$, DCM, 4 Å MS, rt, 30 min, 47%; iii) a) NaOMe, MeOH, 30 min, then H^+-resin; b) KOH, MeOH/ H_2O (1 : 4), 18 h (71% over 2 steps).

is, partially based on identification of the coupling constant: $^3J_{H\text{-}1,H\text{-}2}$, which hinges on the dihedral angles (φ) between H-1 and H-2 for the two anomers.[55] For carbohydrates with an equatorial C-2 functional group-configuration as in the case of galactose and galactosamine, the α-anomer, φ is close to 60° which corresponds to $J \approx 3.5$ Hz. Whereas for β- anomers, φ is close to 180° yielding $J \approx 8$ Hz. This Karplus relation cannot be used for the structural analysis of neuraminic acid, because of the absence of an anomeric hydrogen (C-2) in that case. Instead, a set of empirical rules has been devised based on chemical shift data and coupling constants of various substituted Neu5Ac derivatives.[56] On unsubstituted neuraminic acid derivatives, the C-3 protons are expected to be found at approximate chemical shifts δ = 1.93 and 2.32 ppm, for H-3ax and H-3eq, respectively.[57] Additionally, the α-substituted neuraminic acid supposedly shows H-3ax, and H-3eq to reside at δ = 1.73, and 2.72 ppm, respectively. The most decisive evidence to determine the anomeric conformation of the neuraminic acid derivative is given through $^3J_{C\text{-}1,H\text{-}3ax}$, which can be measured by the gated-decoupled ^{13}C technique.[57b] The expected value for the hetero-atomic C-1 → H-3a coupling for β-anomers is $^3J_{C\text{-}1,H\text{-}3ax} < 1$ Hz, whereas in the case of an α-anomer $^3J_{C\text{-}1,H\text{-}3ax} = 3 - 6$ Hz. Based on these and other criteria,[56] it could be deduced that Neu5Ac*β*2-*O*-$C_{11}H_{22}N_3$, compound **7**, was formed in the MW-assisted reaction. Following these criteria, we were also able to positively identify the correct stereochemistry of the Neu5Ac*α*2-*O*-$C_{11}H_{22}N_3$ compound **4**.

6.2.2 Enzyme-linked immunosorbent assays (ELISA)

After the successful synthesis of the ganglioside fragments and completion of our library, a set of ELISA experiments was devised to allow for a direct comparison of the synthesized compounds **2** - **9** with the previously synthesized GM1 analogue **1** with regard to their capacity to function as epitopes for GBS-associated Abs. These experiments were also compared to assays on native

gangliosides, which in some cases were performed in parallel. This allowed for a direct comparison between the synthesized compounds that were attached to alkyne-terminated ELISA plates via copper-catalyzed azide-alkyne cycloaddition (CuAAC) reactions, and the naturally occurring gangliosides that were attached to a different type of ELISA plates by hydrophobic interactions.

Prior to exposure of the surface-bound ganglioside GM1 analogue **1** and the GM1 fragments **2** - **9** to the sera of GBS patients, they were tested on human monoclonal IgM Abs SM1 and HA1. Affinity of these Abs towards gangliosides was tested and Figure 6 shows that SM1 preferably binds wild type GM1 and asialo-GM1 (AGM1). Surprisingly, also galactocerebroside (GalC) is recognized by the SM1 Abs. GalC is a glycosphingolipid that contains a D-galactoside bearing a ceramide on its *β*-1 position, and is the major glycolipid in myelin.[58] GalC is also described to play a role in several other neurodegenerative diseases, for example, in Krabbe disease[59] and multiple sclerosis (MS).[60] Additionally, some sera of GBS patients contain cross reacting Abs against ganglioside GM1 and GalC.[61] HA1 specifically binds native multi-sialylated gangliosides in the order: GD3 > GD1b >> GQ1b > GT1a (see §1.2.2 Figure 4 for structures).

Figure 6 (lower left) shows that the monoclonal HA1 Abs does not recognize the synthetic analogue of GM1 **1** nor any of the fragments. The initial hypothesis was that the HA1 might show some preference for disaccharide **6** since it showed especially preference to the wild type gangliosides that contain the terminal Neu5Ac*α*2-3Gal*β* sequence. SM1 showed a comparable response to the chemically immobilized GM1 analogue as to the wild type GM1 (Figure 4, GM1), which is in accordance with previous findings.[62] From the ganglioside fragment library, the Gal*β*1-3GalNAc*β* disaccharide **5** showed a slight response towards SM1 but more importantly, the lactoside **3** (Gal*β*1-4Glc*β*) showed a higher response. Both fragments bear the terminal *β*-galactoside moiety. It is safe to assume that that moiety is one of the major contributors to the binding of SM1 since also the wild type GM1, AGM1, and GalC present this epitope. With this experiment, we confirmed that it is, in fact, possible to detect anti-ganglioside Abs by using synthetic glycan fragments.

Next, we explored the effect of presenting combinations of the synthetic ganglioside fragments to these two Abs. It was hypothesized that the presence of sialic acid moieties in these combinations would increase the response to the antibodies, especially in case of HA1, since this particular Ab shows high preference for multisialylated gangliosides. Therefore, 1 : 1 combinations of *α*-, and *β*-Neu5Ac with other fragments were exposed to the SM1 and HA1 antibodies. However,

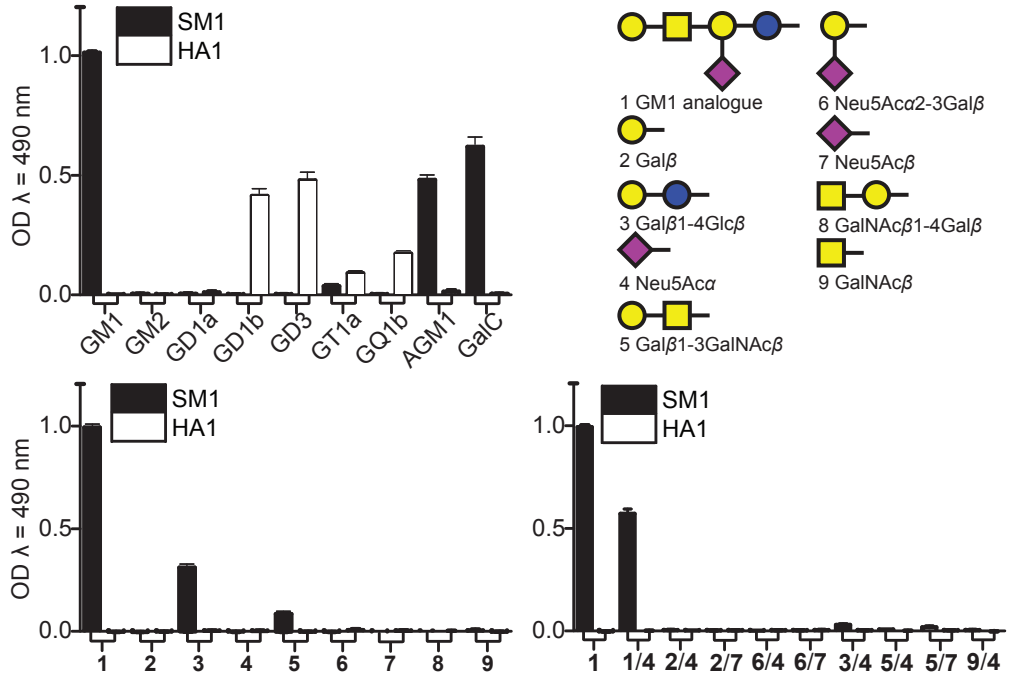

Figure 6. Top Left) Response of human Abs SM1 and HA1 to wild type gangliosides, AGM1 and GalC; Lower Left) Response of SM1 and HA1 Abs to individual the GM1 analogue **1** and fragments **2** - **9**; Lower Right) Response of SM1 and HA1 antibodies to 1 : 1 combinations (compound n/compound m). Error bars indicate the SEM of triplicate measurements.

when 1 : 1 combinations of fragments were exposed to the antibodies (Figure 6 Lower Right), no improvements in binding were observed. This is best indicated by the combination of GM1 analogue **1** and Neu5Ac*α*2, fragment **4**. The response is almost half, in case of the combination of **1** and **4**, with respect to the GM1 analogue **1** when it is not combined. Half the response corresponds to half the concentration of compound **1**. Therefore it is safe to assume that the Neu5Ac*α*2 fragment (**4**) is not recognized by the Abs. It was to be expected that the full complexity of the native ganglioside antigens could not be recreated by combinations of GM1 fragments, even though these combinations do contain the moieties that are presumed to be the Abs epitopes. This mixed fragment-based approach has not been investigated before and therefore this result does contribute to our understanding of the ganglioside-Abs interaction. Taking this result into account, we decided to conduct the subsequent assays, with patient sera, on single fragments or **1**.

In previously reported studies that were based on the synthetic GM1 analogue **1**[25a] it was established that an amount of 100 pmol **1**/well is required to obtain

similar results towards natural Abs as wild type GM1 in standardized ELISA experiments.[26] Based on our preliminary fragment experiments, involving the SM1 and HA1 Abs, we decided that the fragment concentration should be increased 3-fold to match the response of the GM1 analogue. Hence, in the next experiments all fragment amounts are tripled, *i.e.* 300 pmol fragment /well. Also, based on the experiments with SM1 and HA1, several fragments were omitted from further screening to deal economically with the finite Ab sources, *i.e.* GBS patients' sera. Hence, fragment **7**, Neu5Ac*β*, was omitted because the natural α-anomer **4** is more relevant for the subsequent assays. Only a small quantity of compound **6** was acquired *via* chemoenzymatic synthesis and therefore not used in the subsequent reactions unless a high activity towards compound **4** would be registered. Fragment **8** suffered from solubility issues in the immobilization conditions at the indicated concentration, and was therefore omitted as well. Finally, also compound **9** was omitted. Hence, the experiments on GBS patient sera were performed on GM1 analogue **1** and fragments **2** - **5**. The patient sera were coded with either .M or .G, which indicate whether the active components (Abs) belong to either the IgM or IgG immunoglobine class, respectively (Figure 7). Cholera toxin (CT-Bio.SA) was added to these experiments as a standard positive, to give the highest response to ganglioside GM1 analogue **1**.

Figure 7 shows the first set of experiments, together with the blank values. Although the background signals were quite high in some cases, they were deemed acceptable. However, the blank for PC025.M is exceptionally high. High background signals arise from non-specific interaction of serum Abs or other serum components with the surface. Deposition of these components leads to lower signal-to-noise ratios, thereby lowering the sensitivity of the experiments. This issue will be addressed further in §6.2.3. When the blank values are subtracted from the binding responses, the actual response Abs-carbohydrate binding is shown (Figure 8). PC025.M and F263a.G do not give a noticeable response to GM1 mimic **1** nor to any of the fragments, although Abs in both sera do show affinity towards the wild type GM1. This could possibly occur because hydrophobically coated wild type GM1 presumably forms rather disorganized layers and displays random orientation of the glycan part, and may therefore allow orientations that are optimally suited to interact with an antibody.[25b] Instead, the covalently bound ganglioside analogues are coated in a less random and more densely packed order, possibly hampering the availability for Abs interaction. In case of PC025.M, the absence of a positive response can also be caused by the

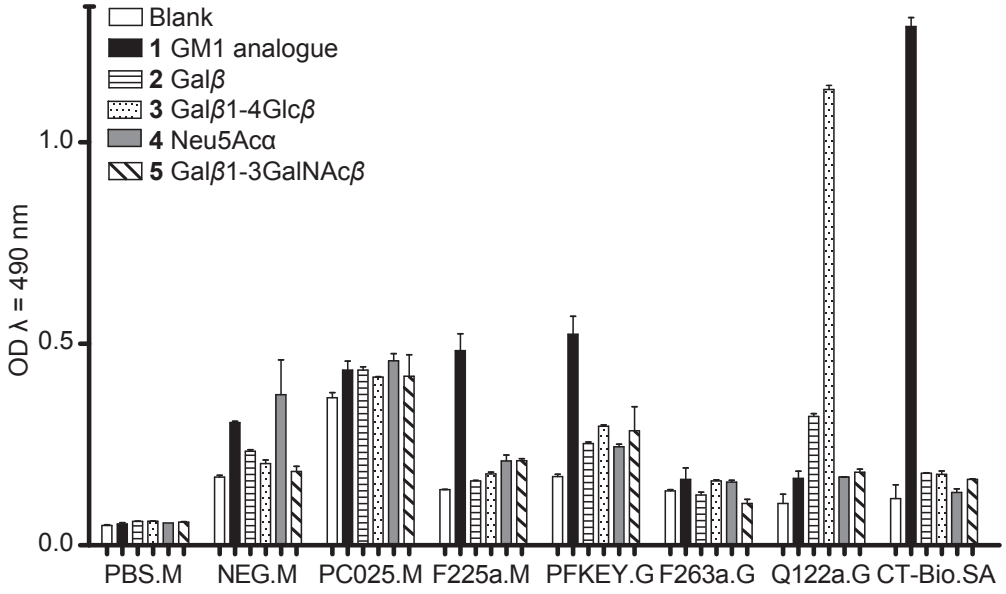

Figure 7. Binding responses of human sera from GBS patients to the synthesized ganglioside GM1 analogue **1** and fragments **2** - **5**. Blank values are not extracted from the OD values in this graph to give an indication of the relatively high background signal. Error bars indicate the mathematical mean of duplicate measurements.

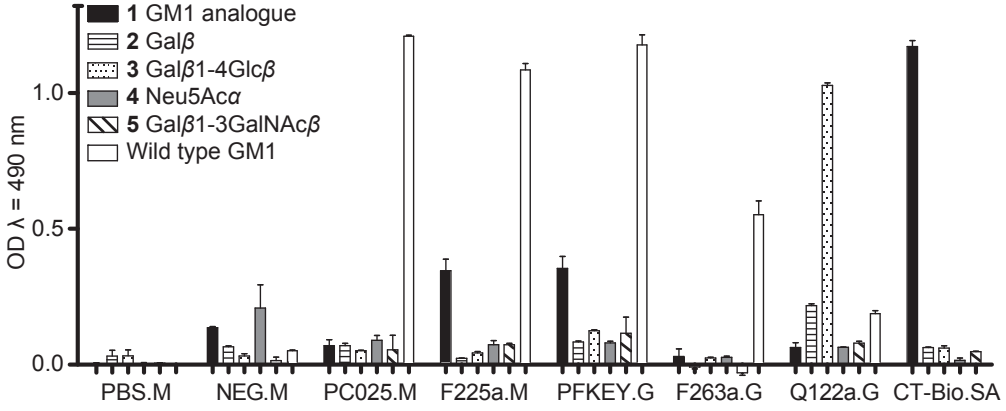

Figure 8. Net response of the reactivity of human sera from GBS patients to the synthesized ganglioside GM1 analogue **1** and fragments **2** - **5** displayed in Figure 7. Error bars indicate the mathematical mean of duplicate measurements.

diminished sensitivity of the test because of the high background signal. Both F225a.M and PFKEY.G show a moderate affinity to the GM1 mimic **1**, although both sera showed to have high titers of antibodies against wild type GM1.

The most remarkable response was given by Q122a.G. Whereas it does not respond well to ganglioside GM1 nor its synthetic analogue **1**, it showed a high

response towards lactoside **3** and also a noticeable response to galactoside **2**. This gave rise to further testing on additional sera that show GalC cross reactivity. This set of sera was tested on **1**, fragments **2** - **3** and, in parallel experiments, also on wild type GalC-coated hydrophobic plates (Figure 9). Q122a.G showed to contain high titers of Abs against GalC. Q122a.G was also used in previous assays and is known as a GBS patients' serum that shows IgG (anti-GalC) cross-reactivity.[61d] This assay also proved that the fragment experiment was reproducible because again both the lactoside and galactoside showed high responses towards Abs in Q122a.G. Also G006.G binds GalC and both the fragments **2** and **3**. Serum Q180.G shows a higher response to **3** than to GalC, and on the contrary, high titers of Abs against GalC are shown in G002.G but not to compound **2** or compound **3**. A conspicuous result in this assay was that neither of these sera showed a high response against **1**, although, many of these sera have previously tested positively against wild type GM1 (not shown). Additionally, F109.G, Q210.G, Q180.G, Q287.G, and Q158.G show to contain titers of Abs that bind **2** and/ or **3** but not GalC. At this stage we considered whether this binding occured due to the presence of other Abs in these sera that are specifically targeting galactoside and lactoside moieties. It is

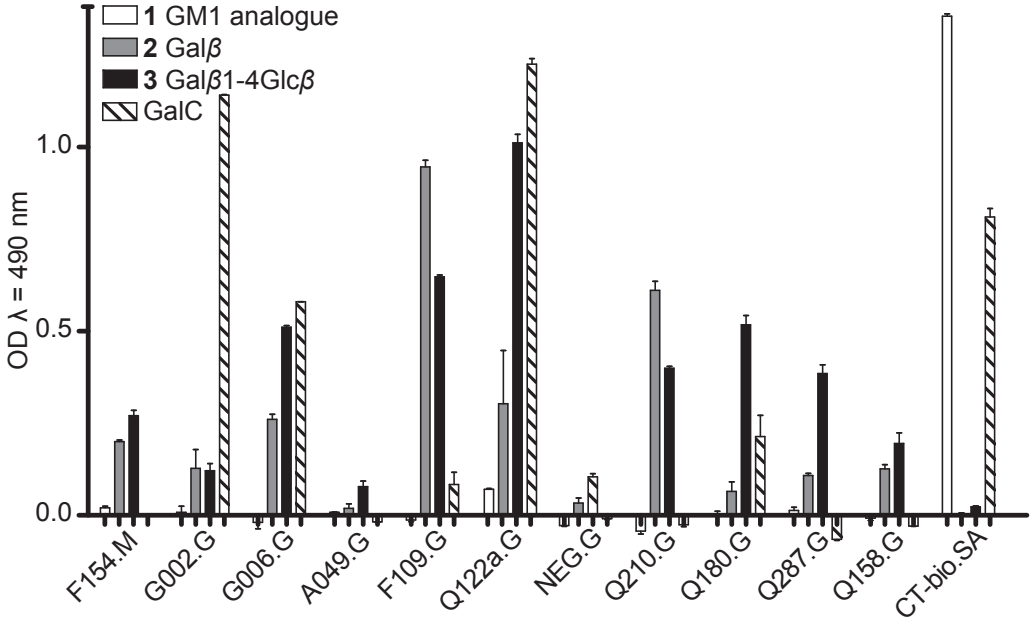

Figure 9. Net response of the reactivity of a second set of human sera from GBS patients, containing also GalC-positive samples G002.G, G006.G, and Q122a.G, to the synthesized ganglioside GM1 analogue **1** and fragments **2** and **3** displayed in Figure 7. Error bars indicate the mathematical mean of duplicate measurements.

known that one of the most abundant Abs (termed anti-Gal) in humans makes up for approx.1% of all Abs and preferably binds a Gal epitope. However, the natural substrate that is targeted by these Abs is the epitope α-Gal, which is present on a complex glycosphingolipid structure that is terminated by the sequence: Gal*α*1-3Gal*β*1-4GlcNAc-R.[63] Also anti-Lac Abs are known that recognize a lactose moiety on the same residue.[64] However, it is debatable whether the effect that is displayed in our assays is caused by anti-Gal Abs, since the epitope, in the case of anti-gal Abs concerns an α-anomer – which is the opposite configuration as that of our fragment **2** –, and because it is attached to a much more complex carbohydrate moiety. Therefore, we can neither exclude nor confirm that the Abs binding responses that we see towards compounds **2** and **3** are the effect of GBS-related Abs that bind these carbohydrates. However, it is likely that the Abs that display anti-GalC cross reactivity also display binding affinity towards the two carbohydrates that display the β-Gal epitope; this is observed in most of our GalC-positive sera.

A further set of sera was tested for their known activity towards native ganglioside GM1 (Figure 10). The results of this assay shows again that the sensitivity of wild type GM1 assays is higher than that for the immobilized synthetic analogues and that these assays cannot always be translated one-to-one. When, for example, F225.M and PC025.M are compared, it shows that the Abs in both sera are able to bind to the natural GM1 but not to the synthetic pentasaccharide (**1**). It must be noted that patient PC025.M was treated for a different autoimmune disease, which is called neuromuscular multifocal motor neuropathy (MMN). Furthermore, most other GM1-positive sera also show a response to **1**. Additionally, F222.G, and F228.M display relatively high responses to **2** and **3**.

6.2.3 Coatings to improve signal-to-noise ratio.

In the experiments that were performed to evaluate Abs-ganglioside binding, we observed in some cases relatively high background signals (Figure 7) for the covalently immobilized fragments. This leads to lower signal-to-noise ratios, thereby lowering the sensitivity of the assays. In an attempt to lower the background due to deposition of the serum components, the exposed alkyne-termini on the ELISA wells that were not used in the immobilization of the synthesized carbohydrates were chemically blocked by reacting them in an additional “click” reaction with either a hydrophilic azido tetra-ethyleneoxide (EO_4N_3) or hydrophobic 11-azidoundecan-1-ol **21** ($HOC_{11}N_3$) (Figure 11).

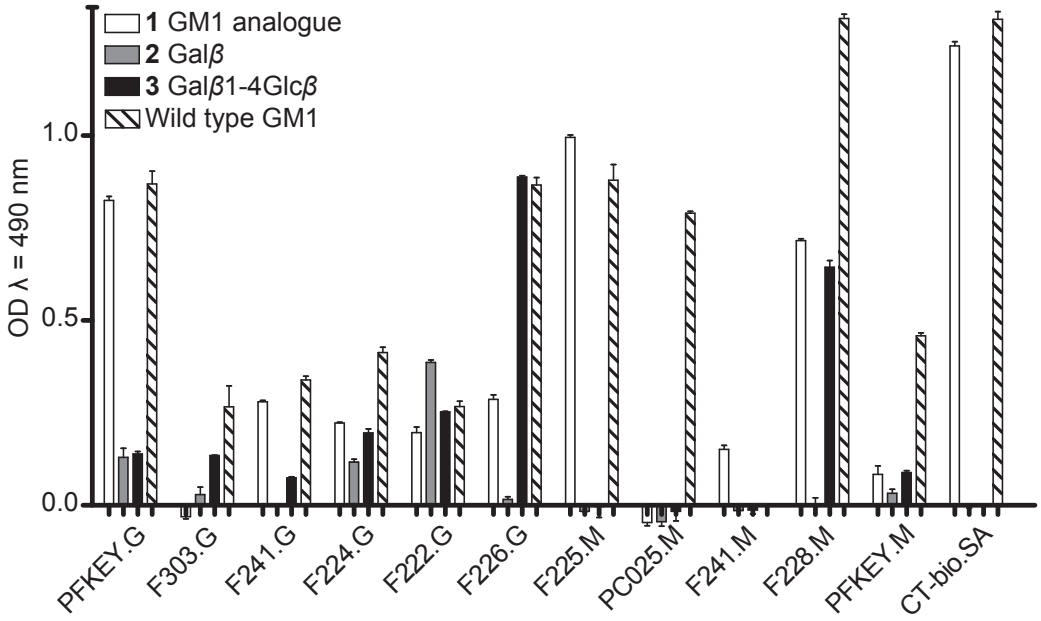

Figure 10. Net response of the reactivity of a third set of patient sera with a selected group of carbohydrates, GM1 mimic **1**, galactoside **2** and lactoside **3**, compared to wild type GM1. Error bars indicate the mathematical mean of duplicate measurements.

In the standard preparation of the microtiter plate surfaces that display alkyne-functionalities, azido-functionalized carbohydrates were covalently immobilized by applying CuAAC reactions. Subsequently, the surfaces were blocked by bovine serum albumin (BSA).[25a] Following this procedure the sites on the ELISA plates that did not react with the azido-terminated carbohydrates, displayed hydrophobic terminal alkyne moieties. In an attempt to reduce the background noise, these "free" alkyne sites were chemically reacted and subsequently blocked by BSA. Surface blocking for sera is preferably done by employing hydrophilic polyethyleneglycol (PEG)[66] rather than by using small chains, but since our antigens are small molecules, the risk existed of being overgrown by the PEG. Hence, as a smaller variant, the tetra-ethyleneoxide was chosen that has the same number of atoms as the linker attached the carbohydrates (*i.e.* 12 atoms, when the anomeric glycoside acetal oxygen is counted as part of the linker). Additionally, the more hydrophobic linker **21** was also applied as surface coating for a comparative study.

Figure 12 shows the blank values that a select group of patient sera displayed when they were deposited on the ELISA wells that were not equipped with any

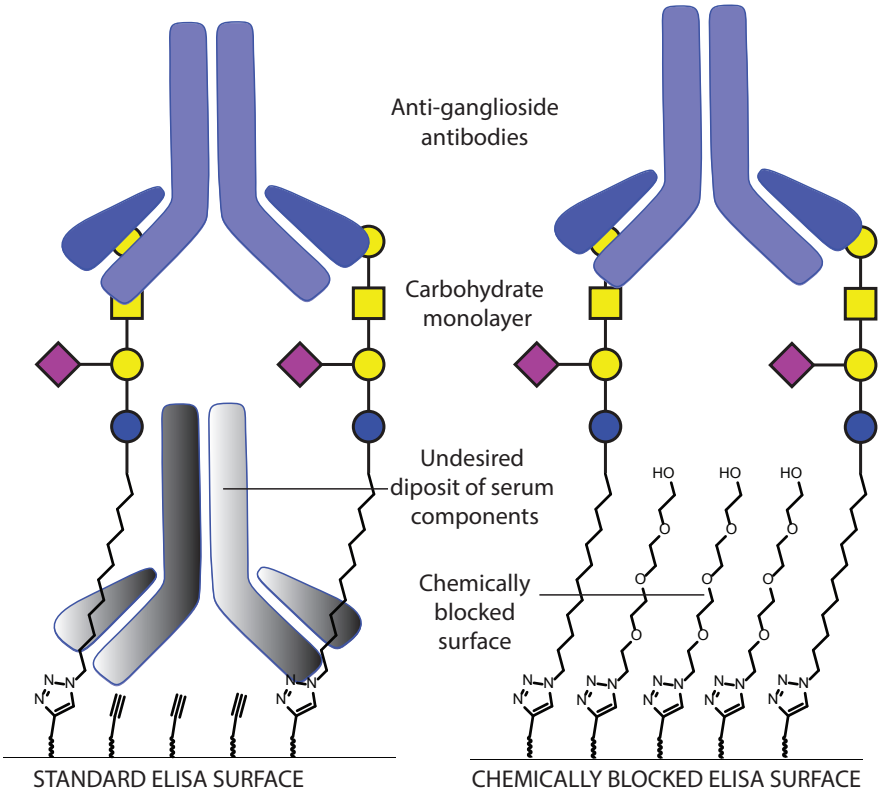

Figure 11. Left) Schematic representation (not on scale) of the standard approach for the ELISA experiments; Right) Chemical blocking of the unreacted free alkyne moieties with hydrophilic oligo-EO spacers. Undecyl spacer **21** was also used as hydrophobic coating (not shown). Standard BSA blocking was applied to all ELISA experiments described in this chapter.

carbohydrates. Comparing the blank values for the various coatings shows that, overall, the changes are not dramatic. In most cases, the chemical blocking shows a slight improvement over the standard procedure without chemical blocking. However, it seems that in the case of serum PC025.M, which was previously already described as suffering from a low signal-to-noise ratio (Figure 7), chemical blocking has a significant advantageous effect for both a hydrophilic or a hydrophobic surface. This is also the case for PFKEY.M, Neg.M, and less prevalent for F292ap.G. In contrast, serum Q122a.G suffers from extensive “sticking” to the hydrophobic undecyl spacer as does F152a.G. From these experiments we could conclude that blocking with hydrophobic spacers does not contribute to a higher signal-to-noise ratio, but applying oligo-EO does

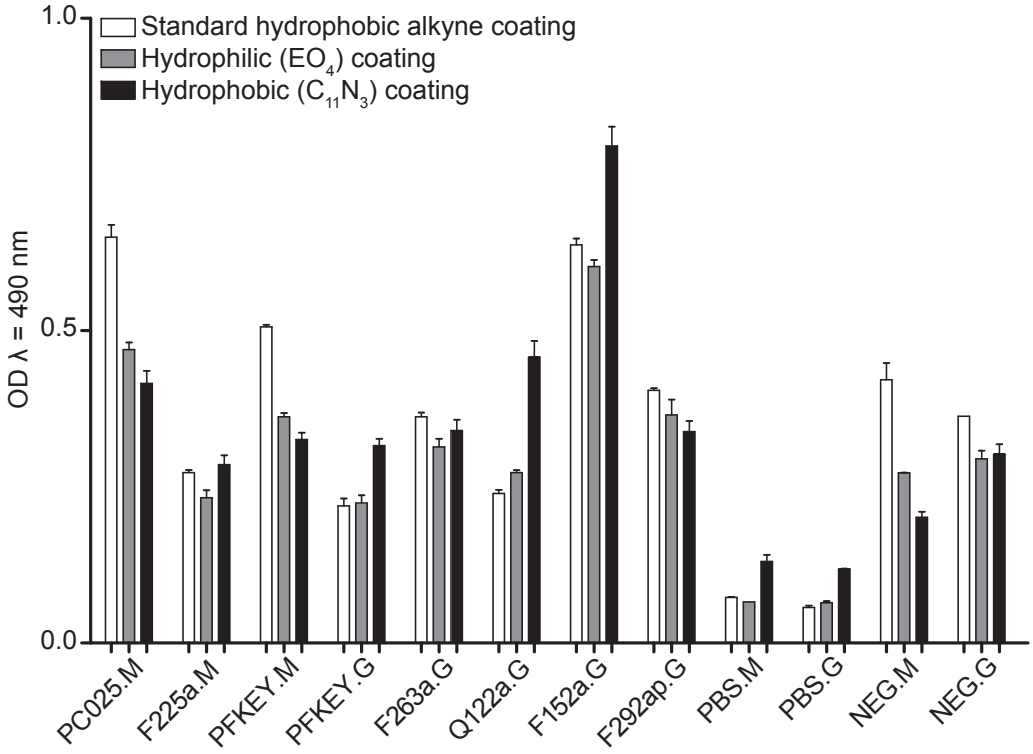

Figure 12. Background measurements: Comparison of patients' sera blanks, deposited on ELISA alkyne-terminated surfaces without or with chemical blocking of the free alkyne sites by reacting them with EO_3N_3 and $HOC_{11}N_3$. Additional, standard, blocking with BSA was performed in all three cases. Error bars indicate the mathematical mean of duplicate measurements.

improve the results in some cases. Therefore, in subsequent experiments, only EO-coating was applied on the free sites on the microtiter plates.

Although the results of the chemically blocked surfaces were not distinctly different from those with the surface that present the free alkyne-terminus, the question was raised what would the influence of the EO-spacer be on the Abs-fragment binding. In Figure 13 the results are shown for the background signals for a select group of sera that were exposed to carbohydrate-functionalized surfaces with only non-covalent blocking (white bars) or both covalent (EO) and non-covalent (BSA) blocking steps (grey bars). In all cases, the response of the background is slightly increased by applying the hydrophilic EO_3 as chemical blocking coating. Additionally, Figure 13 shows also the assay results from the experiments in which compounds **1** - **5** were exposed to the immunoglobins

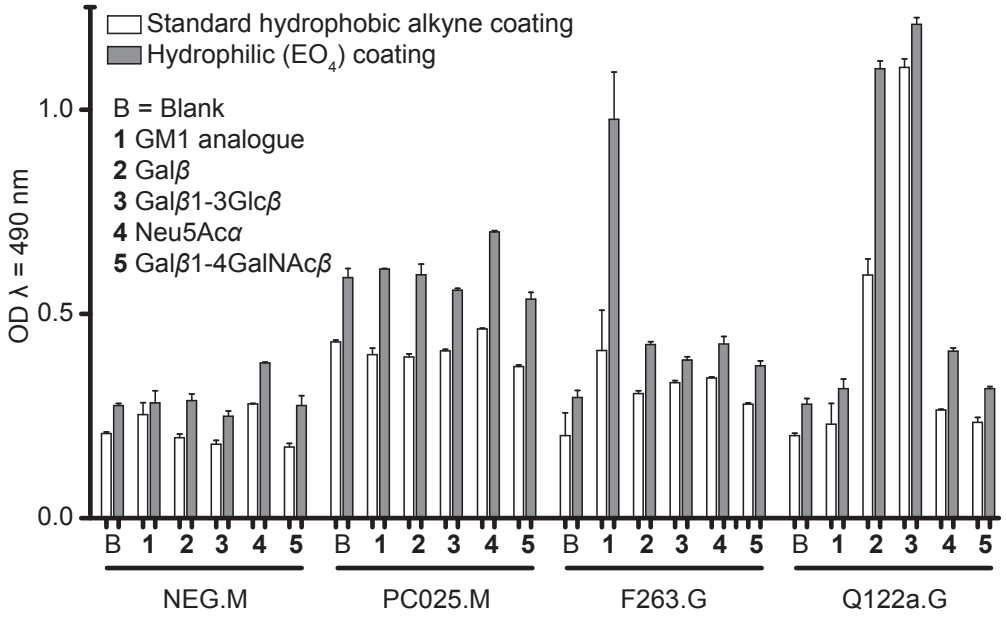

Figure 13. Binding results of the Abs in selected patient sera to compounds **1** - **5** with standard alkyne-terminus or with chemically block EO_4-surface; B = Blank; Error bars indicate the mathematical mean of duplicate measurements.

without and with EO-blocking, white and grey bars, respectively. Again we notice the moderate response to galactoside **2** and the high response to lactoside **3** that is displayed by Q122a.G (see also the discussion belonging to Figure 9) when coated on the alkyne-terminated surface. However, when the free sites were blocked with EO, a much higher response of compound **2** was observed. When the background is subtracted (Figure 14), it can be seen that there is a significant increase and the signal is doubled for the galactoside **2** when the free sites in those corresponding wells were EO_4-blocked rather than alkyne-terminated. This is such a significant difference that it cannot be a result from the slightly higher background signal of the serum when deposited on the EO_4-coated surface. Furthermore, there is also a large increase in activity of the serum F263.G towards GM1 analogue **1** when deposited on the EO_4-blocked wells. In previous experiments, only a minor signal was observed for the synthetic GM1 analogue **1** (Figure 8). When in the presence of the EO_4-coating, F263a.G shows a similar response to the wild-type GM1, and the response is more than three-fold its original. The nature of the higher response, when using chemical EO_4-blocking is not fully understood. Possibly, there is a participating effect of the coating that mimics the complex formation of the gangliosides. On the other

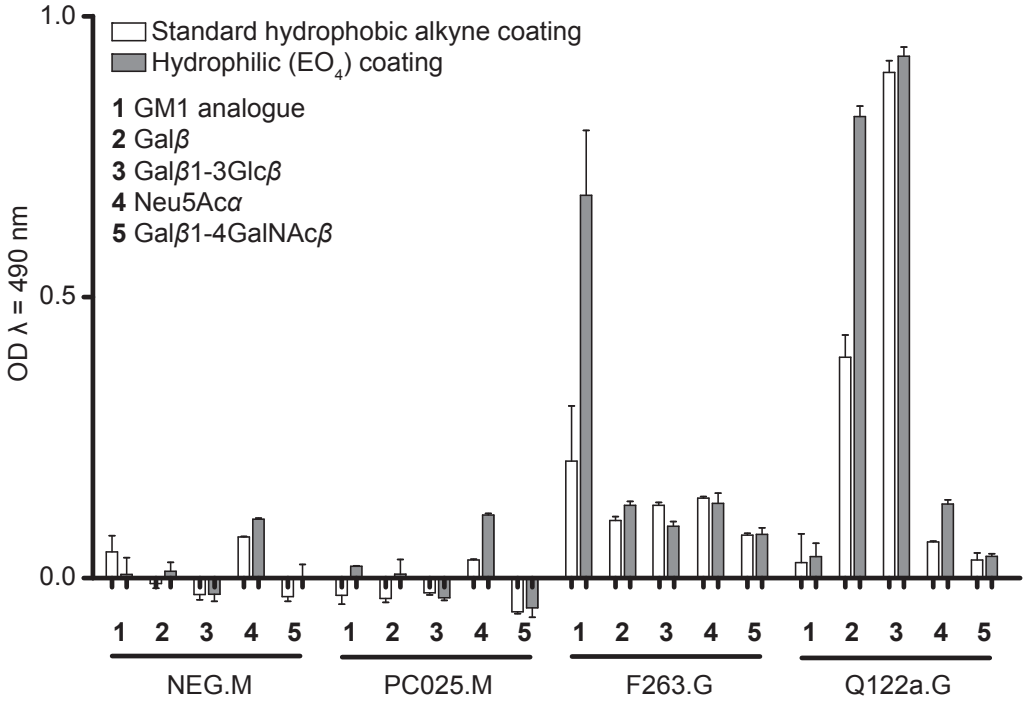

Figure 14. Net binding results of compounds **1** - **5** to immunoglobines with standard alkyne-terminated surface or with chemically blocked EO_4-surface; Error bars indicate the mathematical mean of duplicate measurements.

hand, we have seen in Chapter 5 that the influence of copper on EO-spacers can be quite drastic and sometimes leads to higher response (but also to higher error). In addition, it is not unthinkable that copper also coordinates to the many hydroxyl groups presented on the carbohydrates. This can be either in favour of the binding by filling up essential coordination positions in the Abs binding pockets, but alternatively can also diminish carbohydrate-Abs binding due to unfavourable electronic or steric interactions. Therefore, we cannot exclude that the phenomena described here involve antigen-copper coordination, or that there is a positive interaction of the EO-spacer directly with the Abs. Since the finding with the EO_4-spacers was interesting but not applicable in all cases, the alkyne-terminated microtiter plate surfaces are still preferred for general use. However, these conspicuous findings might be worth to devote follow-up experiments to. For example, changing chain length, chemical appearance (hydrophilicity), as well as the use of other immobilization techniques (*e.g.* SPAAC) may contribute to improved signal-to-noise ratio and analysis of the GBS-related Abs in patient sera.

6.3 Conclusions

As part of an ongoing study to increase the understanding of the pathogenesis of GBS on a molecular level, we focused on the binding mode of GBS-related anti-ganglioside Abs towards synthetic ganglioside-based glycan fragments. Nine compounds were synthesized that are either fragments (**2** - **9**) or a chemical analogue (**1**) of the ganglioside GM1 pentasaccharide, with the aim to form a small library of Abs antigens. All carbohydrates were equipped with an azide handle, with which they could be covalently immobilized onto bio-assay surfaces via CuAAC reactions. These immobilized compounds were then used in ELISA experiments to detect anti-ganglioside Abs in human serum from GBS patients. For most sera no significant binding was observed, indicating that their native ganglioside antigens cannot be recreated by our synthetic GM1 fragments or combinations thereof. We did however discover that some anti-ganglioside Abs bind to compounds displaying the galactoside (**2**) and lactoside (**3**) epitopes. Especially, sera that showed cross-reactivity towards wild type galactocerebroside were shown to bind these two simple saccharides as well. As a confirmation of a previously performed study,[25b] some Abs showed affinity towards the wild type GM1 but not to its chemical analogue **1**. To add to the discussion on this topic, it cannot be ignored that the ceramide hydroxyl and amide functionalities possibly play a role in the assembly, and complex formation, of gangliosides. This specific part of the gangliosides has not been incorporated yet in synthetic ganglioside analogues, and further studies are required to understand its role in anti-ganglioside Abs binding affinity. Finally, in an effort to improve the signal-to-noise ratio, we applied hydrophobic and hydrophilic coatings onto the microtiter (ELISA) surfaces as an additional blocking step. However the effect on the ratio was minimal, applying a relatively short oligo-EO spacer (12 atoms) on the surface had dramatic effect on the binding affinity of some Abs towards the ganglioside fragments. In one case, the Abs-Gal binding response doubled. This surprising result is not fully understood and requires more research. Additional studies on the use of EO spacers in biological assays can be found in Chapter 5.

6.4 Experimental section

6.4.1 General information

All solvents and reagents were obtained commercially and used as received unless stated otherwise. All moisture sensitive reactions were performed under a N_2 or Ar atmosphere. Intermediates that required dry conditions for subsequent reactions were, prior to use, transferred to a dry round-bottom flask, co-evaporated with, EtOAc, Et_2O, and, where possible, the solvent that was used in the subsequent reaction. The concentrated intermediates were then dried for several hours under high vacuum and recovered under Ar atmosphere. Glassware that was used for moisture-sensitive reactions was dried in an oven at 120 °C or heat gun-dried, and, in both cases, charged with reactants under a N_2 or Ar flow prior to use. Dry DCM was acquired by distillation over CaH, THF and Et_2O were distilled over sodium with benzophenone, stored in a Schlenk tube under N_2 or Ar atmosphere over activated 3 Å molecular sieves (MS). Analytical TLC was performed using silica gel plates (Merck 60 F-254 on aluminium) and compounds were visualized, according to the functional groups present on the molecules, with UV light (λ = 254 nm) and/ or stained with Hanessian's Ce/ Mo stain, or 10% sulphuric acid in EtOH, and subsequent charring. Purifications by gravimetric or flash chromatography were performed on Merck silica gel 60 (70 - 230 mesh) using a gradient of the described eluent. The term "purification by automated column chromatography" typically implies purification on a Biotage Isolera One that is running on Spektra software and the 'TLC method'-program, using Biotage SNAP prepacked columns. The applied eluent typically consists of two solvents that are the same as the indicated TLC eluent. Microwave (MW)-assisted reactions were carried out on a CEM Discover labmate 300 W, running on Chemdriver software. MW vials, magnetic stirring bars, and caps were used as provided by the supplier. Standard filtration techniques include: Büchner vacuum filtration, applying Whatman filters; gravity filtration, applying fluted filters; and filtration through hyflo in 3 Å-pore glass filters. NaH was applied as a 60% NaH dispersion in mineral oil and was used as purchased. ^{1}H NMR and ^{13}C NMR spectra were recorded on Bruker Avance III 400 spectrometer, with signal observation around 400 and 100 MHz, respectively. Chemical shifts are reported in parts per million (ppm), calibrated on the residual peak of the solvent, their values are referred to tetramethylsilane (δ_{TMS} = 0.0 ppm), as the internal standard, or the signal of

the deuterated solvent. Where indicated, NMR signal assignments were made using the appropriate 2D NMR experiments. Electrospray ionization (ESI) mass analyses were performed on a Finnigan LXQ, while high resolution ESI mass analyses were recorded on a Thermo Scientific Q Exactive High-Resolution mass spectrometer. Infrared analyses were performed on a Bruker FT-IR spectrometer. Nunc F96 Maxisorp 96-well microtiter plates were used as purchased at Thermo Scientific. Standard Zemplén conditions typically imply the exposure of an acetylated compound – suspended or dissolved in MeOH – to a catalytic amount of an 0.5 M NaOMe in MeOH solution, and subsequent neutralization by Dowex H^+-resin, filtration and concentration by applying reduced pressure.[34]

6.4.2 Enzyme-linked immunosorbent assays

ELISA on wild type gangliosides and serum IgM and IgG anti-ganglioside Abs were performed according to the method previously described[67] and standardized by the INCAT group.[26] Immobilization of ganglioside GM1 analogue **1** and fragments **2** - **9** were immobilized on surfaces according to the procedure involving CuAAC reactions as is described in Chapter 5.

6.4.3 Synthetic procedures

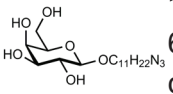

11-Azido-undecyl-β-D-galactopyranoside 2. Tetra-*O*-acetyl **17** 600 mg (1.1 mmol, 1.0 eq) was exposed to standard Zemplén conditions, until TLC indicated that all starting material was consumed. Compound **2** (375 mg, 1.0 mmol, 91%) was obtained as a white solid; **^{1}H NMR** (400 MHz, MeOD): δ = 4.21 (d, 1H, *J* = 7.5 Hz, H-1), 3.90 (m, 1H, -OC***H***$_a$H$_b$-), 3.83 (m, 1H, H-4), 3.74 (m, 2H, H-6a+b), 3.55 - 3.50 (m, 3H, H-2, H-5, -OCH$_a$***H***$_b$-), 3.45 (dd, 1H, *J* = 3.3, 9.7 Hz, H-3), 3.30 (t, 2H, *J* = 6.7 Hz, -C***H***$_2$N$_3$), 1.64 - 1.62 (m, 4H, -C***H***$_2$CH$_2$O-, -C***H***$_2$CH$_2$N$_3$), 1.41 - 1.34 (m, 14H, -C***H***$_2$-spacer); **^{13}C NMR** (100 MHz, MeOD): δ = 105.0 (C-1), 76.6 (C-5), 75.1 (C-3), 72.6 (C-2), 70.8 (-O***C***H$_2$-), 70.4 (C-4), 62.5 (C-6), 51.0 (-***C***H$_2$N$_3$), 30.8 - 27.1 (9 × -CH$_2$-); **MS** (HR-ESI+) m/z = 376.2491 $[M+H]^+$, calcd. ($C_{17}H_{34}N_3O_6^+$) = 376.2442.

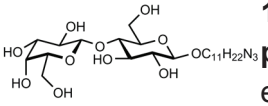

11-azidoundecyl-β-D-galactopyranosyl-(1→4)-β-D-gluco pyranoside 3. Compound **16** (1.0 g, 1.2 mmol, 1.0 eq) was exposed to standard Zemplén conditions, until TLC indicated that all starting material was consumed, affording compound **3** as a white solid

(0.64 g, 1.2 mmol, quant.); **^{1}H NMR** (400 MHz, MeOD): δ = 4.33 (d, 1H, *J* = 7.5, H_{Gal-1}), 4.24 (d, 1H, *J* = 7.8, H_{Glc-1}), 3.91 - 3.85 (m, 2H, $H_{Glc-6a,}$ -C_{Glc-1}OC***H***$_a$$H_b$, 3.83 (dd, 1H, *J* = 4.0, 11.0 Hz, H_{Glc-6b}), 3.79 (m, 1H, H_{Gal-4}), 3.77 (dd, 1H, *J* = 7.3, 11.2 Hz, H_{Gal-6a}), 3.69 (m, 1H, H_{Gal-6b}), 3.60 - 3.48 (m, 4H, H_{Gal-2}, H_{Glc-4}, H_{Gal-5}, -C_{Glc-1}OCH_a***H***$_b$), 3.51 (t, 1H, *J* = 8.9, H_{Glc-3}), 3.47 (dd, 1H, *J* = 3.4, 9.8 Hz, H_{Gal-3}), 3.42 (m, 1H, H_{Glc-5}), 3.26 (t, 2H, *J* = 7.0 Hz, -C***H***$_2$$N_3$), 3.23 (m, 1H, H_{Glc-2}), 1.51 - 1.53 (m, 4H, -C***H***$_2$CH_2O-, -C***H***$_2$C$H_2$$N_3$), 1.42 - 1.28 (m, 14H, -C***H***$_2$-spacer); **^{13}C NMR** (100 MHz, MeOD): δ = 105.7 (C_{Glc-1}), 104.1 (C_{Gal-1}), 81.0 (C_{Glc-4}), 77.6 (C_{Glc-5}), 77.2 (C_{Glc-3}),76.0 (C_{Gal-5}), 75.7 (C_{Glc-2}), 73.7 (C_{Gal-3}), 73.4 (C_{Gal-3}), 71.4 (C_{Gal-2}), 70.6 (-OCH_2-spacer), 69.0 (C_{Gal-4}), 62.5 (C_{Glc-6}), 62.3 (C_{Gal-6}) 52.5 (-C$H_2$$N_3$), 30.5 - 25.0 (9 × -$CH_2$-); **MS** (HR-ESI+) m/z = 536.2921 $[M+H]^+$, calcd. ($C_{23}H_{44}N_3O_{11}^+$) = 536.2970.

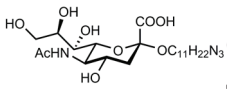

11-azido undecanyl 5-acetamido-3,5-dideoxy-α-D-glycero-D-galacto-2-nonulopyranosonate 4. Deprotection of compound **48** (100 mg, 140 µmol) started by deacetylation by employing the standard Zemplén procedure. After the solvent was removed, the residue was dissolved in 10 ml of a 4 : 1 H_2O/ MeOH mixture that contained 30 mg/ml KOH. The mixture was stirred for 2 days at room temperature after which it was neutralized with Dowex-H^+ resin, filtered, rinsed with 2 ml water, and 2 ml MeOH. By application of a gentle nitrogen flow, MeOH was evaporated from the filtrate and the remaining water was removed by lyophilization overnight. The desired product, compound **4**, was obtained as a white solid (50 mg, 100 µmol, 71%). **^{1}H NMR** (400 MHz, MeOD) δ = 3.86 - 3.81 (m, 2H, H-8, H-9a), 3.77 (m, 1H, -OC*H*a-), 3.73 – 7.69 (m, 2H, H-4, H-5), 3.63 (dd, 1H, *J* = 5.8, 11.5 Hz, H-9b), 3.56 - 3.52 (m, 2H, H-6, H-7), 3.42 (m, 1H, -OC*H*b-), 3.27 (t, 2H, *J* = 6.9 Hz, -C$H_2$$N_3$), 2.77 (dd, 1H, *J* = 3.7, 12.6 Hz, H-3a), 2.01 (s, 3H, -CH_3), 1.68 (m, 1H, H-3b), 1.59 - 1.54 (m, 4H, -OCH_2C***H***$_2$-, N_3OCH_2C***H***$_2$-), 1.40 - 1.30 (9 × -CH_2-); **^{13}C NMR** (100 MHz, $CDCl_3$): δ = 174.0 (-NC(O)-), 73.4 (H-6), 71.5 (H-8), 68.8 (H-7), 67.6 (H-4), 63.8 (-OCH_2-), 63.1 (H-9), 52.6 (H-5), 51.1 (-C$H_2$$N_3$), 40.8 (H-3), 29.4 - 52.7 (9 × -CH_2-), 21.2 (-CH_3); **MS** (ESI-) m/z = 503.2792 $[M-H]^-$, calcd. ($C_{22}H_{39}N_4O_9^-$) = 503.2723.

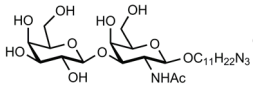

11-azidoundecyl-β-D-galactopyranosyl-(1→4)-β-D-2-acetamido-2-deoxy-galactopyranoside 5. Compound **43** (50 mg, 86 µmol, 1.0 eq) was exposed to standard Zemplén conditions, until TLC indicated that all starting material was consumed, to afford compound **5** (45 mg, 77 µmol, 90%) as a white solid. **^{1}H NMR** (400 MHz, MeOD):

δ = 4.47 (d, 1H, *J* = 8.4 Hz, $H_{GalNAc-1}$), 4.32 (d, 1H, *J* = 7.7 Hz, H_{Gal-1}), 4.10 (m, 1H, $H_{GalNAc-4}$), 3.97 (m, 1H, $H_{GalNAc-2}$), 3.87 (m, 1H, -OC***H***$_a$H$_b$-); 3.82 (m, 1H, $H_{GalNAc-5}$), 3.78 - 3.71 (m, 5H, $H_{GalNAc-3}$, $H_{GalNAc-6,}$ H_{Gal-6}), 3.57 – 3.46 (m, 4H, H_{Gal-2}, H_{Gal-4}, H_{Gal-5}, -OCH$_a$***H***$_b$-), 3.44 (dd, 1H, *J* = 3.1, 9.7 Hz, H_{Gal-3}), 3.27 (t, 2H, *J* = 6.7 Hz, -CH_2N_3), 1.96 (s, 3H, -C(O)CH_3), 1.60 - 1.53 (m, 4H, -C***H***$_2$CH$_2$O-, -C***H***$_2$CH$_2$N$_3$), 1.40 - 1.28 (m, 14H, -C*H*$_2$-spacer); **^{13}C NMR** (100 MHz, MeOD): δ = 174.2 (-NHC(O)-), 106.7 (C_{Gal-1}), 102.7 ($C_{GalNAc-1}$), 81.6 ($C_{GalNAc-3}$), 76.8, 76.3, 74.6, 72.5 (C_{Gal-2}, C_{Gal-3}, C_{Gal-4}, C_{Gal-5},), 70.5 (-OCH_2-spacer), 70.3 ($C_{GalNAc-5}$), 69.6 ($C_{GalNAc-4}$), 62.6, 62.5 ($C_{GalNAc-6}$, C_{Gal-6}), 53.3 ($C_{GalNAc-2}$), 52.5 (-CH_2N_3), 30.8 - 21.1 (-CH_2-spacer), 23.3 (-CH_3); **HRMS** (HR-ESI+) m/z = 579.3333 $[M+H]^+$, calcd. ($C_{25}H_{47}N_4O_{11}^+$) = 579.3236.

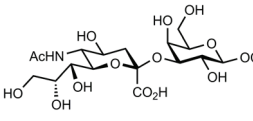

11-azidoundecyl-5-acetamido-3,5-dideoxy-α-D-glycero-D-galacto-2-nonulopyranosonate(2→3)-β-D-galactopyranoside 6. To a solution of 6.7 mM galactoside **2** (5 ml, 34 µmol, 1.0 eq), 10 mM $MgCl_2$, and 10 mM $MnCl_2$ in 50 mM HEPES buffer at pH 7.5, a 9.5 mM solution of donor substrate CMP-Neu5Ac **37** (5 ml, 46 µmol, 1.3 eq) was added. The sialyl transferase II (ST3GalI) (0.5 U) was added to the mixture to start the reaction. The reaction was incubated at 37 °C with gentle agitation for 72 h. After 24 h more 0.2 U of ST3GalI was added, and after 48 h an additional 0.1 U of ST3GalI was added to the reaction mixture. To remove the Mn^{2+}, Mg^{2+} and protein present in the reaction mixture, 1.5 g of Chelex 100 was added to the mixture and the solution was incubated for 15 min at room temperature while shaking. Then, the mixture was centrifuged at 13000 rpm for 10 min. at room temperature and the supernatant was extracted. The Chelex was rinsed and centrifuged two times with 1 ml of MeOH. The combined liquid phases were concentrated under reduced pressure. The disaccharide was charged on a Waters Sep-Pak®Vac C_{18} column and eluted with MeOH. Fractions containing compound **6** were combined and concentrated under reduced pressure. Compound **6** was dissolved in water and lyophilized to result in a white solid with a yield of 77% (16 mg, 25 µmol). **^{1}H NMR** (400 MHz, D_2O) δ = 4.27 (d, 1H, *J* = 8.0 Hz, H_{Gal-1}), 4.20 (m, 1H, H_{Gal-3}), 3.93 (m, 1H, H_{Gal-4}), 3.88 (m, 1H, $H_{Neu5Ac-8}$), 3.84 (m, 1H, $H_{Neu5Ac-9a}$), 3.77 - 3.70 (m, 5H, -OC*H*a-, H_{Gal-6a}, $H_{Neu5Ac-4}$, $H_{Neu5Ac-5}$, H_{Gal-6b}), 3.65 (m ,2H, $H_{Neu5Ac-6}$, $H_{Neu5Ac-9b}$), 3.60 (m, 1H, H_{Gal-5}), 3.58 (m, 1H, H_{Gal-2}), 3.52 (m, 1H, $H_{Neu5Ac-7}$), 3.40 (m, 1H, -OC*H*b-), 2.87 (m, 1H, $H_{Neu5Ac-3eq}$), 2.01 (s, 3H, -CH_3); 1.69 (m, 1H, $H_{Neu5Ac-3ax}$) 1.64 - 1.55 (m, 4H, -OCH$_2$C***H***$_2$-, -OC***H***$_2$CH$_2$N$_3$); 1.42 - 1.32 (m, 4H, -CH_2-spacer); **^{13}C NMR** (100 MHz, D_2O) δ = 175.0, ($C_{Neu5Ac-1}$), 174.0 (-NC(O)-), 105.0 (C_{Gal-1}),

101.1 ($C_{Neu5Ac-2}$), 77.9 (C_{Gal-3}), 76.6 (C_{Gal-5}), 75.1 ($C_{Neu5Ac-6}$), 73.9 ($C_{Neu5Ac-8}$), 72.9 (C_{Gal-2}), 70.6 ($C_{Neu5Ac-7}$), 70.4 (C_{Gal-4}), 70.3 ($C_{Neu5Ac-4}$), 64.4 ($C_{Neu5Ac-9}$), 62.8 (-O*C*H_2-), 62.5 (C_{Gal-6}), 54.1 ($C_{Neu5Ac-5}$), 52.5 (-*C*H_2N_3), 42.4 ($C_{Neu5Ac-3}$), 30.8 - 27.1 (9 × -*C*H_2-spacer), 22.6 (-*C*H_3); **MS** (HR-ESI-) m/z = 665.3345 [M-H]$^-$, calcd. ($C_{28}H_{49}N_4O_{14}^-$) = 665.3251.

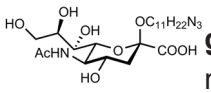

11-azido-undecanyl-5-acetamido-3,5-dideoxy-β-D-glycero-D-galacto-2-nonulopyranosonate 7. Compound **46** (113 mg, 0.2, mmol, 1.0 eq) was suspended in 10 ml MeOH and 100 µl of a 0.5 M NaOMe in MeOH solution was added to the stirred mixture. After 1 h, TLC indicated that the starting material was not completely consumed and an additional 100 µl of the NaOMe solution was added to the mixture. After an additional hour, TLC indicated full conversion to the deprotected material and the mixture was neutralized by addition of Dowex-H^+ resin, filtered and the resin was rinsed with 2 ml of MeOH. The filtrate was concentrated *in vacuo* and redissolved in 10 ml of a 4 : 1 H_2O/ MeOH mixture that contained 30 mg/ml KOH. The mixture stirred for 2 days at room temperature after which it was neutralized with Dowex-H^+ resin, filtered, the resin was rinsed with 2 ml water, and 2 ml MeOH. By application of a gentle nitrogen flow, MeOH was evaporated from the filtrate and the remaining water was removed by lyophilization overnight. Compound **7** was obtained as a white amorphous compound (30 mg, 0.06 mmol, 30%). **^{1}H NMR** (400 MHz, $CDCl_3$): δ = 4.02 (m, 1H, H-4), 3.86 (m, 2H, H-5, H-6), 3.81 - 3.76 (m, 2H, H-9a, H-7 or H-8) 3.68 (m, 2H, H-9b, -OC*H*a-spacer) 3.52 (m, 1H, H-7 or H-8), 3.26 (m, 1H, -OC*H*b-spacer), 3.27 (t, 2H, *J* = 6.8 Hz, -CH_2N_3), 2.37 (dd, 1H, *J* = 4.9, 12.9 Hz, H-3eq), 1.64 - 1.55 (m, 5H, H-3ax, -OCH$_2$CH_2-, -OCH_2CH$_2$N$_3$); 1.38 - 1.31 (m, 14H, -CH$_2$-spacer); **^{13}C NMR** (100 MHz, D_2O) δ = 174.8 (C-1), 173.0 (-NC(O)-), 100.3 (C-2), 72.3 (C-6), 71.4, 70.2, (C-7 and C-8), 67.9 (C-4), 65.2 (C-9), 64.5 (-O*C*H$_2$-spacer), 53.9 (C-5), 52.5 (-*C*H_2N_3), 42.0 (C-3), 30.7 - 27.1 (9 × -*C*H$_2$-spacer), 22.7 (-*C*H_3); **MS** (HR-ESI-) m/z = 503.2721 [M-H]$^-$, calcd. ($C_{22}H_{39}N_4O_9^-$) = 503.2723.

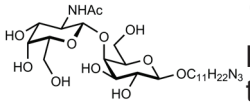

11-azidoundecyl-β-D-2-acetamido-2-deoxy-galacto pyranosyl-(1→4)-β-D-galactopyranoside 8. Hepta-*O*-acetate **36** was exposed to standard Zemplén conditions, until TLC indicated that all starting material was consumed, to afford compound **8** as a white solid (55 mg, 95 µmol, 95%). **^{1}H NMR** (400 MHz, D_2O): δ = 4.50 (d, 1H, *J* = 8.2 Hz, $H_{GalNAc-1}$), 4.21 (d, 1H, *J* = 8.0 Hz, H_{Gal-1}), 4.15 (m, 1H, $H_{GalNAc-3}$), 3.98 (m, 1H), 3.90 (m, 1H, -OC$H_a$$H_b$-), 3.81 (m, 1H, $C_{GalNAc-2}$), 3.81 - 3.51 (m, 9H), 3.39 (m,

1H, H_{Gal-2}), 3.27 (t, 2H, *J* = 6.9 Hz, -C***H***$_2$$N_3$), 2.00 (s, 3H, -C(O)C***H***$_3$), 1.69 - 1.62 (m, 4H, -C***H***$_2$$CH_2O$-, -C***H***$_2$$CH_2N_3$), 1.40 - 1.31 (m, 14H, -C***H***$_2$-spacer); **^{13}C NMR** (100 MHz, D_2O): δ = 169.5 (-N***C***(O)CH_3), 104.0 (C_{Gal-1}), 103.2 ($C_{GalNAc-1}$), 77.0, 75.7, 75.1, 73.2, 70.7 (-O***C***H_2-), 71.9, 71.5, 68.7, 61.0 (C_{Gal-6}), 61.8 ($C_{GalNac-6}$), 52.5 ($C_{GalNAc-2}$), 51.0 (-***C***H_2N_3), 23.2 (-NC(O)***C***H3), 30.5 - 26.8 (9 × -CH_2-spacer); **MS** (HR-ESI+) m/z = 579.3241 $[M+H]^+$, calcd. ($C_{25}H_{47}N_4O_{11}^+$) = 579.3236.

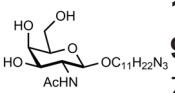

11-Azido-undecyl-2-acetamido-2-deoxy-β-D-galactopyranoside 9. Compound **39** (1.6 g, mmol, 1.0 eq) was exposed to standard Zemplén conditions, until TLC indicated that all starting material was consumed, to afford 1.3 g (3.0 mmol, quant.) **9** as a white solid. **^{1}H-NMR** (400 MHz, MeOD): δ = 4.36 (d, 1H, *J* = 8.4 Hz, H-1), 3.90 (m, 2H, H-2, -OCH_a-spacer), 3.83 (m, 1H, H-4), 3.74 (m, 2H, H-6a+b), 3.59 (dd, 1H, *J* = 3.2, 10.7 Hz, H-3), 3.47 (m, 2H, -OCH_b-spacer, H-5), 3.28 (t, 2H, *J* = 6.8, -C***H***$_2$$N_3$), 1.98 (s, 3H, CH_3), 1.57 (m, 4H), 1.31 (m, 14H); **^{13}C NMR** (100 MHz, MeOD): δ = 174.0 (C=O), 103.1 (C-1), 76.6 (C-5), 73.3 (C-3), 70.6 (-O***C***H_2-spacer), 69.7 (C-4), 62.5 (C-6), 54.4 (C-2), 52.5 (-***C***H_2N_3), 30.8, 30.73, 30.65, 30.5, 30.3, 29.9, 27.8, 27.2, 23.0; **MS** (ESI+) m/z = 439.2580 $[M+Na]^+$, calcd. ($C_{19}H_{36}N_4NaO_6^+$) = 439.2527.

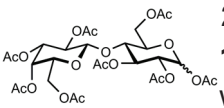

2',3',4',6'-tetra-*O*-acetyl-β-D-galactopyranosyl-(1→4)-1,2,3,6-tetra-*O*-acetyl-β-D-glucopyranoside 12. Dry glassware was charged with lactose (3.4 g, 10 mmol, 1.0 eq) and acetic anhydride (9.4 ml, 10 eq) was added. The suspension was stirred for 5 min. under nitrogen flow and warmed to 35 °C. I_2 (38 mg, 0.15 mmol, 15 mol%) was added and stirring continued for 6 h at 35 °C. Subsequently, the reaction was quenched, while cooling in an ice bath, by slow addition of 1 M $Na_2S_2O_3$. The organic phase was then washed with sat. $NaHCO_3$ (3 × 10 ml), brine (1 × 10 ml), dried over Na_2SO_4, filtered, and concentrated *in vacuo* to afford compound **12** as a white amorphous foam (5.0 g, 7.4 mmol, 74%) and an anomeric mixture of α and β. The mixture was used in subsequent reactions without further purification. **Rf** (chex/EtOAc 1 : 2) = 0.52; **MS** (ESI+) m/z = 679.23 $[M+H]^+$, calcd. ($C_{28}H_{39}O_{19}^+$) = 679.21.

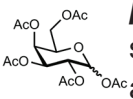

***per-O*-acetyl-D-galactopyranoside 13**. The followed procedure was similar to that of compound **12**, recrystallization from diethyl ether afforded the desired compound as a white solid in 90% yield (19 g, 50 mmol). The resulting mixture of α and β products was used without further

treatment in the next reaction. **Rf** (chex/ EtOAc 2 : 3) = 0.53, (EtOAc/ nhept 1 : 1) = 0.25; **MS** (ESI+) m/z = 391.23 $[M+H]^+$, calcd. ($C_{16}H_{23}O_{11}^+$) = 391.12.

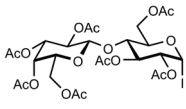

Iodo-2,3,4,6-tetra-*O*-acetyl-β-D-galactopyranosyl-(1→4)-2,3,6-tri-*O*-acetyl-α-D-glucopyranoside 14. A round-bottom flask was charged with lactose (3.4 g, 10 mmol, 1.0 eq), and acetic anhydride (9.4 ml, 10 eq) was added. The suspension was stirred for 5 min under nitrogen flow and warmed to 35 °C. I_2 (38 mg, 0.15 mmol, 15 mol%) was added and stirring continued for 6 h at 35 °C. Subsequently, the reaction mixture was diluted with dry DCM (10 ml) and equimolar I_2 (2.5 g, 10 mmol, 1.0 eq) was added. After allowing the reaction to progress overnight, it was quenched, while cooling in an ice bath, by slow addition of 1 M $Na_2S_2O_3$. The organic phase was then washed with sat. $NaHCO_3$ (3 × 10 ml), brine (1 × 10 ml), dried over Na_2SO_4, filtered, and concentrated *in vacuo* to afford compound **14** as an amorphous white foam (5.0 g, 7.4 mmol, 74%) that was used in subsequent reactions without further purification. **Rf** (nhex/ EtOAc 2 : 3) = 0.49; **^{1}H NMR** (400 MHz, $CDCl_3$): *δ* 6.90 (1H, d, H_{Glc-1}, *J* = 4.36 Hz), 5.45 (1H, t, H_{Glc-3}, *J* = 9.44 Hz), 5.34 (1H, dd, H_{Gal-4}, *J* = 3.38 and 0.88 Hz), 5.11 (1H, dd, H_{Gal-2}, *J* = 10.38 and 7.88 Hz), 4.95 (1H, dd, H_{Gal-3}, *J* = 10.38 and 3.48 Hz), 4.51 (1H, d, H_{Gal-1}, *J* = 7.88 Hz), 4.47 (1H, dd, H_{Glc-6a}, *J* = 12.35 and 1.96 Hz), 4.22-4.05 (4H, m, H_{Glc-2}, H_{Glc-6b}, H_{Gal-6}), 3.98 - 3.92 (1H, m, H_{Glc-5}), 3.90-3.85 (2H, m, H_{Glc-4}, H_{Gal-5}), 2.15 (3H, s, -OC(O)CH_3), 2.11 (3H, s, -OC(O)CH_3), 2.08 (3H, s, -OC(O)CH_3), 2.05 (3H, s, -OC(O)CH_3), 2.04 (6H, s, 2 × -OC(O)CH_3), 1.95 (3H, s, -OC(O)CH_3). **^{13}C NMR** (100 MHz, $CDCl_3$): *δ* 170.3, 170.1, 170.1, 170.0, 169.7, 169.2, 168.9 (7 × C=O), 100.8 (C_{Gal-1}), 75.7 (C_{Glc-5}), 74.7 (C_{Glc-4}), 72.6 (C_{Glc-1}), 71.1 (C_{Glc-3}), 71.0 (C_{Gal-3}), 70.8 (C_{Gal-5}), 70.5 (C_{Glc-2}), 69.1 (C_{Gal-2}), 66.6 (C_{Gal-4}), 61.0 (C_{Glc-6}), 60.9 (C_{Gal-6}), 20.8, 20.8, 20.7, 20.6, 20.6, 20.6, 20.5 (7 × CH_3). **MS** (HR-ESI-) m/z = 745.0832 $[M-H]^-$ calcd. 745.0835 ($C_{26}H_{35}IO_{17}^-$).

Iodo-2,3,4,6-tetra-*O*-acetyl-β-D-galactopyranoside 15. The followed procedure was similar as that for compound **14**. Column chromatography afforded 0.75 g of compound **15** (1.6 mmol, 90%) yellowish solid. **Rf** (hept/ EtOAc 1 : 1) = 0.44; **^{1}H-NMR** (400 MHz, $CDCl_3$): δ = 7.09 (d, 1H, *J* = 4.2, H-1), 5.44 (m, 1H), 5.24 (dd, 1H, *J* = 3.3, 10.5 Hz, H-3), 4.31 (dd, 1H, *J* = 4.2, 10.5 Hz, H-2), 4.24 - 4.13 (m, 2H), 4.10 - 4.02 (m, 1H); **^{13}C NMR** (100 MHz, $CDCl_3$): δ = 170.4, 169.8, 169.5, 169.4, 74.7, 72.9, 71.5, 70.0, 66.7, 60.6, 20.5, 20.4, 20.32, 20.26; **MS** (ESI+) m/z = 347.11 $[M-I+O]^-$, calcd. ($C_{14}H_{19}IO_9$) = 458.00, ($C_{14}H_{19}O_{10}^-$) = 347.10.

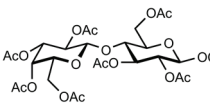

11-Azidoundecyl-2,3,4,6-tetra-*O*-acetyl-β-D-galacto pyranosyl-(1→4)-2,3,6-tri-*O*-acetyl-β-D-glucopyranoside 16. **From** 2,3,4,6-tetra-*O*-acetyl-β-D-galactopyranosyl-(1→4)-1,2,3,6-tetra-*O*-acetyl-β-D-glucopyranoside **12:** Per-*O*-acetate **12** (200 mg, 0.3 mmol, 1.0 eq) and 11-azidoundecan-1-ol compound **21** (800 mg, 0.4 µmol, 1.2 eq) were dissolved in 10 ml dry DCM, 4 Å MS, and 300 µl (0.3 mmol, 1.0 eq) of a 1 M $SnCl_4$ solution in DCM were added to the reaction mixture as subsequently stirred for 16 h at room temperature. The reaction mixture was filtered over hyflo, washed with sat. $NaHCO_3$ (3 × 5 ml), brine (1 × 5 ml), dried over Na_2SO_4, filtered, and concentrated *in vacuo* to afford compound **16** (37 mg, 0.05 mmol, 15 %, anomeric mixture) as a white amorphous foam. **From** Iodo 2,3,4,6-tetra-*O*-acetyl-β-D-galactopyranosyl-(1→4)-2,3,6-tri-*O*-acetyl-α-D-glucopyranoside **14:** Iodide **14** (1.5 g, 2.0 mmol, 1.0 eq) and 11-azido-1-undecanol compound **21** (0.85 g, 4.0 mmol, 2.0 eq) were dissolved in dry MeCN (10 ml). Subsequently, the solution was stirred under dry N_2 for 5 min at 0 °C and I_2 (0.76 g, 3 mmol, 1.5 eq) was added. The reaction was allowed to warm to room temperature while stirring overnight. The reaction was diluted with EtOAc (50 ml), filtered, and the residue rinsed. The filtrate was quenched, while cooling in an ice bath, by slow addition of 1 M $Na_2S_2O_3$ until the dark brown solution maintained a yellow transparent color. The organic phase was washed with sat. NaCl (3 × 50 ml), dried over Na_2SO_4, and concentrated *in vacuo*. The crude was purified by flash chromatography affording compound **16** (1.2 g, 1.4 mmol, 70 %) as a white amorphous foam. **Rf** (EtOAc/ nhept 1 : 2) = 0.50; **^{1}H NMR** (400 MHz, $CDCl_3$): δ = 5.34 (dd, 1H, *J* = 3.3, 0.8 Hz, $H_{Gal\text{-}4}$), 5.18 (t, 1H, *J* = 9.3 Hz, $H_{Glc\text{-}3}$), 5.10 (dd, 1H, *J* = 10.4, 7.9 Hz, $H_{Gal\text{-}2}$), 4.95 (dd, 1H, *J* = 10.4, 3.4 Hz, $H_{Gal\text{-}3}$), 4.87 (dd, 1H, *J* = 9.5, 8.0 Hz, $H_{Glc\text{-}2}$), 4.48 - 4.43 (m, 3H, $H_{Gal\text{-}1}$, $H_{Glc\text{-}6a}$, $H_{Glc\text{-}1}$), 4.15 - 4.05 (m, 3H, $H_{Gal\text{-}6,}$ $H_{Glc\text{-}6b}$), 3.88 - 3.76 (m, 3H, $H_{Gal\text{-}5}$, -OC***H***$_a$H$_b$-spacer, $H_{Glc\text{-}4}$), 3.62 - 3.56 (m, 1H, $H_{Glc\text{-}5}$), 3.47 - 3.41 (m, 1H, -OCH$_a$***H***$_b$-spacer), 3.24 (t, 2H, *J* = 7.0 Hz, -C***H***$_2$N$_3$), 2.14 (s, 3H, -OC(O)C***H***$_3$), 2.11 (s, 3H, -OC(O)C***H***$_3$), 2.05 (s, 3H, -OC(O)C***H***$_3$), 2.03 (s, 6H, 2 × -OC(O)C***H***$_3$), 2.02 (s, 3H, -OC(O)C***H***$_3$), 1.95 (s, 3H, -OC(O)C***H***$_3$), 1.64 - 1.48 (m, 4H, -CH$_2$-spacer), 1.39 - 1.25 (m, 14H, CH$_2$-spacer); **^{13}C NMR** (100 MHz, $CDCl_3$): δ = 170.3, 170.3, 170.1, 170.0, 170.0, 170.0, 169.0 (7 × C=O), 101.0 ($C_{Gal\text{-}1}$), 100.6 ($C_{Glc\text{-}1}$), 76.3 ($C_{Glc\text{-}4}$), 72.8 ($C_{Glc\text{-}3}$), 72.6 ($C_{Glc\text{-}5}$), 71.7 ($C_{Glc\text{-}2}$), 71.0 ($C_{Gal\text{-}5}$), 70.2 (-O***C***H$_2$-spacer), 69.1 ($C_{Gal\text{-}2}$), 66.6 ($C_{Gal\text{-}4}$), 62.1 ($C_{Glc\text{-}6}$), 60.8 ($C_{Gal\text{-}6}$), 51.5 (-***C***H$_2$N$_3$), 29.5, 29.4, 29.4, 29.4, 29.3, 29.1, 28.8, 26.7 25.8 (9 × CH$_2$), 20.8, 20.8, 20.6, 20.6, 20.6, 20.6, 20.5 (7 × CH$_3$). **MS** (HR-ESI-) m/z = 830.3550 [M-H]$^-$, calcd. ($C_{37}H_{57}N_3O_{18}^-$) = 830.3556.

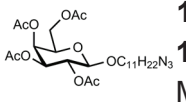

11-Azido-undecyl-2,3,4,6-tetra-*O*-acetyl-D-galactopyranoside 17. To round-bottom flask charged with dry MeCN (20 ml) and 4 Å MS (0.5 g) was added compound **15** (2.0 g, 4.3 mmol, 1.0 eq) and 11-azidoundecan-1-ol **21** (1.8 g, 8.6 mmol, 2.0 eq). The reaction mixture was cooled in an ice bath and small portion of iodine (1.0 g, 3.9 mmol, 1.1 eq) were added and the reaction mixture was allowed to stir for 18 h while gradually warming to room temperature. The reaction was filtered and cooled again in an ice bath. Gradually, a 1M $Na_2S_2O_3$ was added until complete discoloration (turbid brown/ red → clear yellow) of the mixture was observed. The mixture was extracted with EtOAc (3 × 20 ml). The combined organic layers were washed with brine (3 × 30 ml), dried over Na_2SO_4, and concentrated *in vacuo*. Automated column chromatography-purification afforded 1.4 g (2.6 mmol, 62%) of compound **17** as a yellowish syrup. **Rf** (nhex/ EtOAc 1 : 1) = 0.42, **^{1}H-NMR** ($CDCl_3$, 400 MHz): δ (ppm) = 5.38 (m, 1H), 5.21 (m, 1H), 5.01 (dd, 1H, *J* = 3.4, 10.5 Hz), 4.45 (d, 1H, *J* = 8.0, H-1), 4.15 (m, 2H), 3.90 (m, 2H), 3.46 (m, 1H), 3.26 (t, 2H, -CH_2N_3), 2.15 (s, 3H, -C(O)CH_3), 2.05 (s, 3H, -C(O)CH_3), 1.99 (s, 3H, -C(O)CH_3), 1.58 (m, 4H, -C$\boldsymbol{H}_2$CH$_2$O-, -C$\boldsymbol{H}_2$CH$_2$N$_3$), 1.27 (m, 14 H, -CH$_2$-spacer), **^{13}C NMR** (100 MHz, $CDCl_3$): δ = 101.39 (C-1), 71.0, 70.6, 70.3 (-OCH_2-spacer), 69.0, 67.1, 61.3 (C-6), 51.5 (-CH_2N_3), 59.54, 59.47, 59.4, 29.3, 29.1, 28.8, 26.7, 25.8, 20.8, 20.7, 20.6; **MS** (ESI+) m/z = 585.27 $[M+MeCN+H]^+$, calcd. ($C_{27}H_{45}N_4O_{10}^+$) = 585.31.

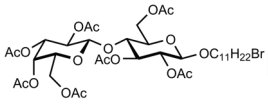

11-Bromo-undecyl-2,3,4,6-tetra-*O*-acetyl-β-D-galacto pyranosyl-(1→4)-2,3,6-tri-*O*-acetyl-β-D-glucopyranoside 18. Per-*O*-acetate **12** (1.0 g, 1.5 mmol, 1.0 eq) and 11-bromoundecan-1-ol (0.4 g, 1.6 mmol, 1.1 eq) were dissolved in 2 ml dry DCM, 4 Å MS, and 0.2 ml (1.6 mmol, 1.1 eq) of a 1M $SnCl_4$ solution in DCM were added to the reaction mixture as subsequently stirred for 16 h at room temperature. The reaction mixture was filtered over hyflo, washed with sat. $NaHCO_3$ (3 × 1 ml), brine (1 × 1 ml), dried over Na_2SO_4, filtered, and concentrated *in vacuo*. Purification on normal-phase silica, eluent: chex/ EtOAc gradient 3 : 2 → 2 : 3, afforded 600 mg (0.4 mmol, 28%) **18** as a white solid as a mixture of anomers (α/ β 1 : 4). **Rf** (chex/ EtOAc 2 : 3) = 0.69, 0.67 (α and β, respectively); **^{1}H NMR** (400 MHz, $CDCl_3$): *δ* 5.30 (1H, d, H_{Gal-4}, *J* = 3.3 Hz), 5.15 (1H, t, *J* = 9.3 Hz, H_{Glc-3}), 5.06 (1H, dd, *J* = 10.4, 7.9 Hz, H_{Gal-2}), 4.92 (1H, dd, *J* = 10.49, 3.48 Hz, H_{Gal-3}), 4.84 (1H, dd, *J* = 9.52, 8.02 Hz, H_{Glc-2}), 4.46 - 4.40 (3H, m, H_{Gal-1}, H_{Glc-6a}, H_{Glc-1}), 4.12 - 4.02 (3H, m, $H_{Gal-6,}$ H_{Glc-6b}), 3.86 - 3.73 (3H, m, H_{Gal-5}, -OC$\boldsymbol{H}_a$H$_b$-spacer, H_{Glc-4}), 3.58 - 3.54 (1H, m, H_{Glc-5}), 3.44 - 3.39

(1H, m, -OCH$_a$***H***$_b$-spacer), 3.36 (2H, t, *J* = 6.8 Hz, -C***H***$_2$Br), 2.11 (3H, s, -OC(O)C***H***$_3$), 2.07 (3H, s, -OC(O)C***H***$_3$), 2.02 (3H, s, -OC(O)C***H***$_3$), 2.00 (6H, s, -OC(O)C***H***$_3$), 1.99 (3H, s, -OC(O)C***H***$_3$), 1.92 (3H, s, -OC(O)C***H***$_3$), 1.84 - 1.77 (2H, m, CH$_2$-spacer), 1.59 - 1.43 (2H, m, CH$_2$-spacer), 1.43-1.32 (2H, m, CH$_2$-spacer), 1.32 - 1.17 (12H, m, CH$_2$-spacer). **^{13}C NMR** (100 MHz, $CDCl_3$): *δ* 170.2, 170.2, 170.0, 169.9, 169.7, 169.4, 168.9 (7 x C=O), 100.9 (C_{Gal-1}), 100.5 (C_{Glc-1}), 76.2 (C_{Glc-4}), 72.8 (C_{Glc-3}), 72.5 (C_{Glc-5}), 71.7 (C_{Glc-2}), 70.9 (C_{Gal-3}), 70.6 (C_{Gal-5}), 70.1 (-O***C***H$_2$-spacer), 69.1 (C_{Gal-2}), 66.6 (C_{Gal-4}), 62.0 (C_{Glc-6}), 60.7 (C_{Gal-6}), 33.9 (-***C***H$_2$Br), 32.7, 29.4, 29.3, 29.3, 29.3, 29.1, 28.6, 28.0, 25.7 (9 x CH$_2$), 20.7, 20.7, 20.6, 20.5, 20.5, 20.5, 20.4 (7 x CH$_3$). **MS** (HR-ESI-) m/z = 867.2660 [M-H]$^-$, calcd. ($C_{37}H_{57}BrO_{18}^-$) = 867.2645.

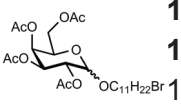

11-Bromo-undecyl-2,3,4,6-tetra-*O*-acetyl-D-galactopyranoside 19. Acetyl-protected galactoside **13** (2.0 g, 5.1 mmol, 1.0 eq) and 1.4 g (5.6 mmol, 1.1 eq) 11-bromo-undecan-1-ol **21** were dissolved in dry DCM (2 ml) and stirred in the presence of 4 Å MS for 30 min. Then, 0.66 ml (5.6 mmol, 1.1 eq) of a 1 M $SnCl_4$ in DCM was added. Stirring continued for 16 h, and then, filtered over hyflo, rinsed with 5 ml DCM, washed with sat. $NaHCO_3$ (3 × 1 ml), and brine (1 × 1 ml), dried over Na_2SO_4, filtered, and concentrated *in vacuo*. Purification on normal-phase silica, eluent: chex/ EtOAc gradient 4 : 1 → 2 : 3, afforded 600 mg (1.0 mmol, 20%, as a mixture of anomers) of **19** as a white solid. **^{1}H-NMR** (β) ($CDCl_3$, 400 MHz): δ (ppm) = 5.39 (m, 1H), 5.20 (m, 1H), 5.02 (m, 1H), 4.45 (d, 1H, *J* = 7.8 Hz, H-1), 4.24 – 4.13 (m, 2H), 3.40 (m, 1H), 3.47 (m, 1H), 3.41 (t, 2H, *J* = 6.7 Hz, -C***H***$_2$Br), 2.15 (s, 3H, -OC(O)C***H***$_3$), 2.05 (s, 6H, 2 × -OC(O)C***H***$_3$), 1.98 (s, 3H, -OC(O)C***H***$_3$), 1.85 (m, 2H), 1.61 (m, 2H), 1.42 (m, 2H), 1.28 (m, 12H); **MS** (ESI+) m/z = 581.20 $[M+H]^+$ (100%), 582.20 (30%), 583.20 (95%), 584.20 (25%), Br-pattern observed, calcd. ($C_{25}H_{42}BrO_{10}^+$) = 581.20 (100.0%), 582.20 (27.0%), 583.20 (97.3%), 584.20 (26.3%), 585.20 (3.4%).

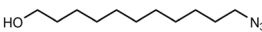

11-Azido-undecan-1-ol 21.[33] To a solution of 11-bromo-undecan-1-ol (10 g, 39 mmol, 1.0 eq) in DMF (50 ml) was added sodium azide (5.2 g 80 mmol, 2.1 eq) and the reaction mixture was heated at 100°C for 16 h. The reaction mixture was diluted with 50 ml of EtOAc, filtered, washed with brine (3 × 50 ml). The organic phase was dried with Na_2SO_4, filtered and dried *in vacuo*. Purification by flash chromatography, eluent: isocratic chex/ EtOAc 1 : 2, afforded the desired compound **21** (7.6 g, 36 mmol, 91%) as a clear and colorless oil. **Rf** (chex/ EtOAc 1

: 2) = 0.60; **^{1}H NMR** ($CDCl_3$, 400 MHz): δ (ppm) = 3.49 (t, 2H, *J* = 6.8 Hz, -CH_2OH), 3.16 (t, 2H, *J* = 7.0 Hz, -CH_2N_3), 2.95 (s, 1H), 1.52-1.44 (m, 4H), 1.20 (m, 14H); **^{13}C NMR** ($CDCl_3$, 100 MHz): 63.1 (-CH_2OH), 51.5 (-CH_2N_3), 32.8, 29.6, 29.5, 29.4, 29.2, 28.9, 26.7, 25.8; **MS** (ESI+) m/z = 214.20 $[M+H]^+$, calcd. ($C_{11}H_{24}N_3O^+$) = 214.19.

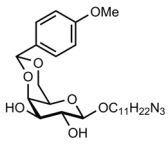

11-Azido-undecyl-4,6-(4-methoxybenzylidene)-β-D-galacto-pyranoside 22. Dry compound **2** (790 mg, 2.1 mmol, 1.0 eq) was suspended in 20 ml MeCN. To the stirred suspension, *p*-anisaldehyde dimethyl acetal (0.72 ml, 4.2 mmol, 2.0 eq) was added, followed by 12 mg (0.06 mmol, 3 mol%) PTSA·H_2O, and stirring continued for 36 h at rt. The resulting clear, red solution was quenched by neutralization with Et_3N, and concentrated *in vacuo*. Purification by automated column chromatography yielded the desired beta product **22** in 670 mg (1.4 mmol, 65%) as a yellowish oil. **β anomer**: **Rf** (EtOAc/ nhept 3 : 1) = 0.18; **^{1}H-NMR** (400 MHz, $CDCl_3$): δ = 7.42 (d, 2H, *J* = 8.6 Hz); 6.88 (d, 2H, *J* = 8.6 Hz); 5.50 (s, 1H); 4.30 (m, 1H); 4.25 (d, 1H, *J* = 7.5 Hz); 4.17 (m, 1H); 4.05 (dd, 1H, *J* = 1.7, 12.5 Hz); 3.95 (m, 1H); 3.79 (s, 3H); 3.72 (m, 1H); 3.67 (m, 1H); 3.50 (m, 1H); 3.43 (m, 1H); 3.24 (t, 2H, *J* = 7.0); 1.68 - 1.56 (m, 4H); 1.39 - 1.27 (m, 16H); **^{13}C NMR** (100 MHz, $CDCl_3$): δ = 127.8; 113.5; 102.8; 101.3; 75.4; 72.8; 72.7; 71.8; 70.0; 69.2; 51.5; 29.5; 29.4; 29.1; 28.8; 26.8; 25.9; **MS** (ESI+) m/z = 494.35 $[M+H]^+$, calcd. ($C_{25}H_{40}N_3O_7^+$) m/z = 494.29. **α anomer**: **Rf** (EtOAc/ nhept 3 : 1) = 0.40; **^{1}H NMR** (400 MHz, $CDCl_3$): δ = 7.39 (d, 2H, *J* = 8.5 Hz); 6.85 (d, 2H, *J* = 8.5 Hz); 5.45 (s, 1H); 4.95 (d, 1H, *J* = 2.6 Hz); 4.17 (m, 1H); 4.00 (d, 1H); 3.85 (m, 2H); 3.76 (s, 3H); 3.68 (m, 1H); 3.62 (m, 1H); 3.46 (m, 1H); 3.23 (t, 2H, *J* = 6.9 Hz); 2.53 (bs, 2H) -OH; 1.56 (m, 4H); 1.26 (m, 14H); **^{13}C NMR** (100 MHz, $CDCl_3$): δ = 127.6; 113.5; 101.3; 99.1; 69.9; 69.7; 69.3; 68.6; 62.9; 68.6; 51.4; 29.6; 29.5; 29.4; 29.3; 29.1; 28.8; 26.7; 26.1; **MS** (ESI+) m/z = 494.28 $[M+H]^+$, calcd. ($C_{25}H_{40}N_3O_7^+$) = 494.28.

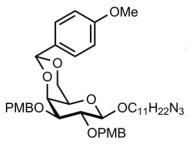

11-Azido-undecyl-4,6-*O*-benzylidene-2,3-di-*O*-(4-methoxyben-zyl)-β-D-galactopyranoside 23. Compound **22** (100 mg, 203 µmol, 1.0 eq) was dissolved in DMF (2 ml) under an applied Ar flow, and treated with NaH (24 mg, 1.0 mmol, 5.0 eq). After 30 min PMB-Cl (0.1 ml, 1.0 mmol, 5.0 eq) was added. The reaction mixture was stirred overnight at rt. TLC analysis indicated that the reaction did not progress any further. Subsequently, it was quenched with NH_4Cl (1 × 10 ml), extracted with EtOAc (3 × 10 ml), the combined organic layers were washed with

brine (1 × 10 ml), dried over Na_2SO_4, filtered, and concentrated *in vacuo* to obtain 258 mg of crude orange oil. Purification by automated column chromatography yielded **23** (102 mg, 140 µmol, 69%) as a white solid. **Rf** (EtOAc/ nhept 3 : 1) = 0.63; **^{1}H NMR** (400 MHz, $CDCl_3$): δ = 7.50 (m, 2H, Ph), 7.31 (m, 4H, Ph), 6.87 (m, 6H, Ph), 5.45 (s, 1H, -C*H* acetal), 4.87 (d, 1H, *J* = 10.5, -(C-2)OC***H***$_a$Ph); 4.70 (m, 3H, -(C-2)OC***H***$_b$Ph, -(C-3)OC***H***$_2$Ph), 4.36 (d, 1H, *J* = 7.5 Hz, H-1), 4.27 (m, 1H, H-6a), 4.06 (m ,1H, H-4), 3.99 (m, 2H, H-6b, -OC*H*$_a$-spacer), 3.81 (m, 11H, H-2, 9 × -C*H*$_3$), 3.50 (m, 2H, H-3, -OC*H*$_b$-spacer), 3.26 (m, 2H, H-5, -C*H*$_2$N$_3$), 1.68 (m, 2H, -C***H***$_2$CH$_2$O-), 1.59 (m, 2H, -C***H***$_2$CH$_2$N$_3$), 1.30 (m, 14H, -C*H*$_2$-spacer); **^{13}C NMR** (100 MHz, $CDCl_3$): δ = 160.0 (C_q Ph) 159.2 (C_q Ph), 159.1 (C_q Ph), 131.2 (C_q Ph), 130.6 (2 × C_q Ph) 129.7 – 127.9 (12 × -*C*H (Ph)) 113.71 (-*C*H$_3$), 113.67 (-*C*H$_3$), 113.4 (-*C*H$_3$), 103.8 (C-1), 101.2 (-CH acetal), 78.9 (C-3), 78.3 (C-2), 74.9 (-(C-2)O***C***H$_2$Ph), 74.1 (C-4), 71.6 (-(C-3)O***C***H$_2$Ph), 70.0 (-O*C*H$_2$-spacer) 69.2 (C-6), 66.4 (C-5), 55.3 (3 × -*C*H$_3$), 51.5 (-*C*H$_2$N$_3$), 29.8 – 26.2 (9 × -*C*H$_2$-spacer); **MS** (ESI+) m/z = 734.38 $[M+H]^+$, calcd. ($C_{41}H_{56}N_3O_9^+$) = 734.40.

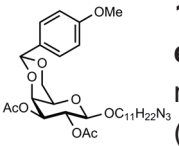

11-Azido-undecyl-2,3-di-*O*-acetyl-4,6-*O*-(4-methoxybenzylidene)-β-D-galactopyranoside 24. Compound **22** (200 mg, 0.4 mmol, 1.0 eq) was dissolved in pyridine and cooled to 0 °C. Ac_2O (0.8 ml, 8.2 mmol, 20 eq) was added drop wise and the reaction mixture was allowed to warm to room temperature and stirred overnight. The reaction mixture was poured into ice cold water and extracted with EtOAc (3 × 5 ml). The combined organic layers were washed with 1 M NH_4Cl (3 × 5 ml), brine (5 ml), dried over Na_2SO_4, filtered, and concentrated, yielding 214 mg (0.4 mmol, 93%) **24** as a colourless oil. The material was used in subsequent reactions without further purification. **^{1}H NMR** (400 MHz, $CDCl_3$): δ = 7.39 (d, 2H, *J* = 8.7 Hz, Ph-*H*a), 6.83 (d, 2H, *J* = 8.7 Hz, Ph-*H*b), 5.40 (s, 1H, -C*H*-Ph), 5.31 (m, 1H), 4.92 (dd, 1H, *J* = 3.6, 10.4 Hz), 4.43 (d, 1H, *J* = 8.0 Hz, H-1), 4.30 (m, 1H), 4.23 (m, 1H), 3.99 (m, 1H), 3.86 (m, 1H), 3.74 (s, 3H, Ph-OC*H*$_3$), 3.43 (m, 2H), 3.20 (t, 2H, *J* = 7.0 Hz, -C*H*$_2$N$_3$), 2.00 (-C(O)CH$_3$), 1.99 (-C(O)CH$_3$), 1.58 - 1.48 (m, 4H,-OCH$_2$C***H***$_2$-, -OC***H***$_2$CH$_2$N$_3$), 1.31 - 1.24 (m, 14H, -CH$_2$-spacer); **MS** (ESI+) m/z = 600.31 $[M+Na]^+$, calcd. ($C_{29}H_{43}N_3NaO_9^+$) = 600.29.

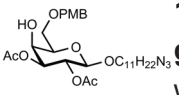

11-Azido-undecyl 2,3-di-*O*-acetyl-6-*O*-(4-methoxybenzyl)-β-D-galactopyranoside 26. Galactoside **24** (1.1 g, 1.9 mmol, 1 eq) was dissolved in THF (20 ml) in the presence of 4 Å MS. After 10

min, $NaCNBH_3$ (1.2 g, 19 mmol, 20 eq) was added and stirring continued for another 10 min, after which, 5 drops of HCl (1 M in Et_2O) were added while gas evacuated. HCl was dropped into the reaction mixture until gas evolution ceased and TLC analysis indicated that all starting material was consumed. The molecular sieves were filtered off and EtOAc (15 ml) was added. The mixture was extracted sat. $NaHCO_3$ (3 × 5 ml) and brine (5 ml), the organic layer was dried over $MgSO_4$, filtered and concentrated *in vacuo*. Purification by automated column chromatography yielded compound **26** in 70% yield (0.8 g, 1.3 mmol) as a colorless oil; **Rf** (EtOAc/ toluene 1 : 2) = 0.67; **^{1}H NMR** (400 MHz, $CDCl_3$): δ = 7.22 (d, 2H, *J* = 8.6 Hz); 6.84 (d, 2H, *J* = 8.6 Hz); 5.23 (dd, 1H, *J* = 8.0, 10.3 Hz); 4.89 (dd, 1H, *J* = 10.3, 3.3 Hz); 4.48 (m, 2H); 4.40 (d, 1H, *J* = 8.0 Hz); 4.09 (m, 1H); 3.85 (m, 1H); 3.77 (s, 3H); 3.70 - 3.62 (m, 3H); 3.45 (m, 1H); 3.22 (t, 2H, *J* = 7.0 Hz); 2.88 (bs, 1H) -OH; 2.05 (s, 3H); 2.01 (s, 3H); 1.60 - 1.49 (m, 4H); 1.36 - 1.22 (m, 14H) **^{13}C NMR** (100 MHz, $CDCl_3$): δ = 170.2; 169.4; 159.3; 129.4; 101.3, 73.5; 73.3; 73.2; 69.7; 69.5; 68.8; 67.9; 55.2; 51.4; 29.5; 29.4; 29.3; 29.1; 28.8; 26.7; 25.8; 20.8; 20.7; **MS** (ESI+) m/z = 602.43 $[M+Na]^+$, 1180.96 $[2M+Na]^+$, calcd. ($C_{29}H_{45}N_3NaO_9^+$) = 602.30, ($C_{58}H_{90}N_6NaO_{18}^+$) = 1181.62.

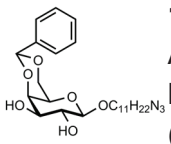

11-Azido undecyl 4,6-*O*-benzylidene-β-D-galactopyranoside 28. A suspension of β-D-galactopyranoside **2** (1.8 g, 3.4 mmol, 1.0 eq) benzaldehyde dimethylacetal (1.0 g, 6.7 mmol, 2.0 eq), and 40 mg (0.17 mmol, 5 mol%) camphor-10-sulphonic acid were added and the reaction mixture was refluxed for 3 h. Automated column chromatography yielded the β-product **28** in 460 mg (1.0 mmol, 30%) as a white solid. The α-anomer was obtained in 26% yield (400 mg, 0.86 mmol) as an off-white solid; **β anomer**: **Rf** (nhex/ EtOAc 1 : 1) = 0.28; **^{1}H NMR** (400 MHz, $CDCl_3$): δ = 7.50 (m, 2H, Ph-*H*), 7.36 (m, 3H, Ph-*H*), 5.56 (-C*H*-Ph), 4.30 (m, 1H, H-6a), 4.28 (d, 1H, *J* = 7.4 Hz, H-1), 4.21 (m, 1H), 4.10 (m, 1H, H-6b), 3.95 (m, 1H, -OC*H*a-spacer), 3.79 - 3.65 (m, 2H), 3.51 (m, 1H, -OC*H*b-spacer), 3.48 (m, 1H), 3.25 (t, 2H, *J* = 7.0 Hz, -CH_2N_3), 1.65 - 1.59 (m, 4H, -OCH$_2$C$\boldsymbol{H}_2$-, -OC$\boldsymbol{H}_2$CH$_2$N$_3$), 1.36 - 1.30 (m, 14H, -CH$_2$-spacer); **^{13}C NMR** (100 MHz, $CDCl_3$): δ = 137.5 (Cq), 129.2, 218.2 (2 ×), 126.4 (2 ×) (5 × Ph), 102.3 (C-1), 101.5 (-*C*H-Ph), 75.4, 72.8, 72.0, 70.1 (-OCH$_2$-spacer), 69.2 (C-6), 66.8, 51.5 (-*C*H$_2$N$_3$), 29.6 - 26.0 (9 × -*C*H$_2$-spacer); **MS** (HR-ESI+) m/z = 464.27 $[M+H]^+$, calcd. ($C_{24}H_{38}N_3O_6^+$) = 464.28; **α anomer**: **Rf** (nhex/ EtOAc 1: 1) = 0.28; **^{1}H NMR** (400 MHz, $CDCl_3$): δ = 7.50 (m, 2H, Ph-*H*), 7.37 (m, 3H, Ph-*H*), 5.57 (s, 1H, -*C*H-Ph), 5.04 (d, 1H, *J* = 2.8 Hz, H-1), 4.30 (m, 2H), 4.16

- 4.06 (m, 2H), 3.90 (m, 2H), 3.78 - 3.70 (m, 2H), 2.37 (t, 2H, *J* = 7.0 Hz, -C*H*$_2$N$_3$), 2.35 (bs, 1H, -OH), 2.00 (bs, 1H, -OH), 1.67 - 1.57 (m, 4H, -OCH$_2$C***H***$_2$-, -OC***H***$_2$CH$_2$N$_3$), 1.40 - 1.28 (m, 14H, -CH$_2$-spacer); **^{13}C NMR** (100 MHz, CDCl$_3$): δ = 137.6 (Cq), 129.2, 128.3 (2 ×), 126.3 (2 ×) (5 × Ph), 101.3 (-*C*H-Ph), 99.1 (C-1), 76.0, 70.2, 69.9, 69.4, 68.7, 62.9, 51.5 (-*C*H$_2$N$_3$), 29.5 - 26.2 (9 × -*C*H$_2$-spacer).

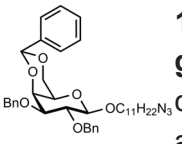

11-Azido undecyl 2,3-di-*O*-benzyl-4,6-*O*-benzylidene-β-D-galactopyranoside 29. To a stirred and cooled (0 °C) solution of compound **28** (280 mg, 0.6 mmol, 1.0 eq) in DMF (10 ml) was added 70 mg NaH (1.8 mmol, 3.0 eq). After 1 h, 0.2 ml (1.8 mmol, 3.0 eq) BnCl was added drop wise to the solution and stirring continued for an additional hour. The reaction was quenched by addition of 10 ml 1 M NH_4Cl and extracted with EtOAc (3 × 5 ml). The combined organic layers were washed with brine (1 × 10 ml), dried over Na_2SO_4, filtered, and concentrated *in vacuo*. Automated column chromatography yielded 336 mg (0.52 mmol, 86%) of compound **29** as a white solid. **Rf** (EtOAc/ nhex 2 : 3) = 0.41; **^{1}H NMR** (400 MHz, CDCl$_3$): δ = 7.58 (m, 2H, Ph-H), 7.42 - 7.28 (m, 13H, Ph-H), 5.52 (s, 1H, -C*H*-acetal), 4.97 (d, 1H, *J* = 10.9 Hz, -C*H*a-Ph), 4.82 - 4.75 (m, 3H, -C*H*b-Ph, -CH$_2$-Ph), 4.40 (d, 1H, *J* = 7.8 Hz, H-1), 4.31 (d, 1H, *J* = 1.4, 12.3, H-6a), 4.13 (m, 1H, H-4), 4.04 - 4.00 (m, 2H, H-6b, -OC*H*a-spacer), 3.86 (m, 1H, H-3), 3.58 (dd, 1H, *J* = 3.7, 9.7 Hz, H-2), 3.52 (m, 1H, -OC*H*b-spacer), 3.31 (m, 1H, H-5), 3.26 (t, 2H, *J* = 7.0 Hz, -C*H*$_2$N$_3$), 1.72 - 1.57 (m, 4H, -OCH$_2$C***H***$_2$-, -OC***H***$_2$CH$_2$N$_3$), 1.44 - 1.29 (m, 14H, -CH$_2$-spacer); **^{13}C NMR** (100 MHz, CDCl$_3$): δ = 139.1, 138.6, 138.1 (3 × Cq Ph), 129.0 - 126.6 (15 × Ph), 103.8 (C-1), 101.39 (-*C*H-Ph), 79.4 (C-2), 78.6 (C-3), 75.3 (-*C*H$_2$Ph), 74.1 (C-4), 72.1 (-*C*H$_2$Ph), 70.0 (-O*C*H$_2$-spacer), 69.4 (C-6), 66.5 (C-5), 51.6 (-*C*H$_2$N$_3$), 29.8 - 26.3 (9 × -*C*H$_2$-spacer); **MS** (HR-ESI+) m/z = 644.36 [M+H]$^+$, calcd. ($C_{38}H_{50}N_3O_6^+$) = 644.37.

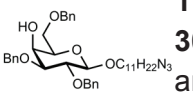

11-Azido-undecyl 2,3,6-tetra-*O*-benzyl-β-D-galactopyranoside 30. Acetal **29** 1.4 g (2.1 mmol, 1.0 eq) was dissolved in dry THF and stirred under Ar in the presence of 3 Å MS for 1 h. $NaCNBH_3$ (1.3 g, 21 mmol, 10 eq) was added to the solution and stirred for an additional 10 min. A 1 M HCl solution in Et_2O was added drop wise until evolution of gas ceased and TLC indicated that all starting material was consumed. The molecular sieves were filtered off and EtOAc (15 ml) was added. The mixture was extracted sat. $NaHCO_3$ (3 × 5 ml) and brine (5 ml), the organic layer was dried over $MgSO_4$, filtered and concentrated *in vacuo*. Purification by automated column

chromatography yielded compound **29** in 70% yield (1.0 g, 1.5 mmol) as a yellowish oil; **Rf** (toluene/ EtOAc 7 : 1) = 0.38; **^{1}H NMR** (400 MHz, $CDCl_3$): δ = 7.27 - 7.13 (m, 15H, 15 × Bn-H), 4.82 (d, 1H, *J* = 11.1 Hz, -C-2C***H***$_a$Ph), 4.62 (d, 1H, *J* = 11.1 Hz, -(C-2)OC***H***$_b$Ph), 4.58 (s, 2H, -(C-3)OC***H***$_3$Ph), 4.46 (s, 2H, -(C-6) OC***H***$_3$Ph), 4.24 (d, 1H, *J* = 7.8 Hz), 3.88 - 3.82 (m, 2H, H-4 -OC*H*$_a$-spacer), 3.68 (dd, 1H, *J* = 5.9, 10.0 Hz, H-6a), 3.61 (dd, 1H, *J* = 6.0, 10.0 Hz, H-6b), 3.55 (m, 1H, H-2), 3.45 - 3.35 (m, 3H, -OC*H*$_a$-spacer, H-3, H-5), 3.09 (t, 2H, *J* = 7.0 Hz, -C*H*$_2$N$_3$), 2.53 (s, 1H, -OH), 1.53 (m, 2H, -C***H***$_2$CH$_2$O-), 1.45 (m, 2H, -C***H***$_2$CH$_2$N$_3$), 1.16 (m, 14H, -C*H*$_2$-spacer); **^{13}C NMR** (100 MHz, $CDCl_3$): δ = 138.8 (C_q Bn), 138.2 (C_q Bn), 138.1 (C_q Bn), 128.5 - 127.6 (15 × Bn), 103.8 (C-1), 80.7 (C-3), 79.1 (C-2), 75.2 (-(C-2)O***C***H$_2$Ph), 73.7 (-(C-6)O***C***H$_2$Ph), 73.3 (C-5), 72.4 (-(C-3) O***C***H$_2$Ph), 70.0 (-O*C*H$_2$-spacer), 69.4 (C-6), 67.0 (C-4), 51.5 (-*C*H$_2$N$_3$), 29.8 -26.2 (9 × -*C*H$_2$-spacer). **MS** (ESI+) m/z = 668.58 $[M+Na]^+$, 1313.11 $[2M+Na]^+$, calcd. ($C_{38}H_{51}N_3NaO_6^+$) = 668.37, ($C_{76}H_{102}N_6NaO_{12}^+$) = 1313.74.

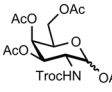

2,3,4,6-Tetra-*O*-acetyl-2-deoxy-2-*N*-(2,2,2-trichloroethyloxycarbonyl amino)-α/β-D-galactopyranoside 32. A solution of galactosamine hydrochloride **31** (2.0 g, 9.3 mmol, 1.0 eq) and 1.9 g (23 mmol, 2.5 eq) of K_2CO_3 in H_2O (30 mL) was cooled to at 0 °C. After 10 min, 1.7 mL TrocCl (2.6 g, 12 mmol, 1.3 eq) was added dropwise. The mixture was allowed to stir for 10 h while gradually warming to room temperature. The resulting suspension was cooled to 0 °C, and filtered. The residue was rinsed with cold Et_2O, and dried *in vacuo*. The residue was then stirred overnight in 50 mL of a mixture of pyridine/ Ac_2O (1 : 1). The reaction mixture was poured into cold water (200 mL), and extracted, while still cold, with EtOAc (3 × 50 mL). The combined organic extracts were washed with H_2O (3 × 50 mL), 1 M HCl (50 mL), and saturated aqueous $NaHCO_3$ (50 mL), dried over Na_2SO_4, and concentrated *in vacuo* to afford 3.4 g (6.5 mmol, 70%) **32** (mixture of anomers) as a colorless solid. The mixture was used in subsequent reactions without further purification. **MS** (ESI+) m/z = 522.67 $[M+H]^+$ (100%), 524.67 (95%), 526.67 (30%), Cl_3-pattern observed, calcd. ($C_{17}H_{23}Cl_3NO_{11}^+$) m/z = 522.03 (100.0%), 524.03 (95.9%), 526.03 (30.6%).

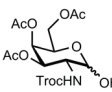

3,4,6-Tri-*O*-acetyl-2-deoxy-2-*N*-(2,2,2-trichloroethyloxycarbonyl amino)-α/β-D-galactopyranoside 33. Compound **32** (2.3 g, 4.5 mmol, 1.0 eq) was dissolved in 100 ml DMF and exposed to 0.5 g (5.9 mmol, 1.3 eq) hydrazine acetate and stirred at room temperature for 1 h. TLC indicated that the starting material was still present so additional 0.6 eq hydrazine acetate

were added to the solution and stirring continued for 30 min at room temperature. Upon completion, the reaction mixture was diluted with 100 ml EtOAc and washed with brine (2 × 200 ml), demi water (2 × 200 ml), dried over Na_2SO_4, filtered, and concentrated *in vacuo*. Automated column chromatography-purification afforded 1.3 g (2.7 mmol, 85%) of compound **33** in a mixture of both anomers as a white solid. **Rf** (nhex/ EtOAc 1 : 2) = 0.55 (both anomers); **MS** (ESI+) m/z = 480.07 $[M+H]^+$ (100%), 481.07 (15%), 482.08 (95%), 483.07 (15%), 484.06 (30%), 485.08 (5%), 486.07 (3%), Cl_3 isotope pattern observed, calcd. [$C_{15}H_{21}Cl_3NO_{10}^+$] = 480.02 (100.0%), 481.03 (16.2%), 482.02 (95.9%), 483.02 (15.6%), 484.02 (30.6%), 485.02 (5.0%), 486.01 (3.3%). Spectral data in agreement with literature values.[40]

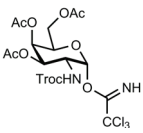

3,4,6-Tri-*O*-acetyl-2-deoxy-2-(2,2,2-trichloroethoxycarbonyl amino)-α-D-galactopyranosyl trichloroacetimidate 34.[40, 68] A solution of hemi-acetal **33** (0.9 g, 1.9 mmol, 1.0 eq), trichloroacetonitrile (2.9 g, 19 mmol, 10 eq), and DBU (75 mg, 0.5 mmol, 0.3 eq) in 10 ml DCM was stirred at room temperature for 20 minutes and subsequently concentrated *in vacuo*. The residual orange/brown oil was purified by column chromatography, eluent: gradient nhex/EtOAc 10 : 1 → 1 : 2, affording 510 mg (0.9 mmol, 75%) **34** as yellowish oil. **Rf** (nhex/ EtOAc 1 : 2) = 0.33; **^{1}H NMR** (400 MHz, $CDCl_3$): δ = 8.78 (s, 1H, -N*H*CCl_3), 6.45 (d, 1H, *J* = 3.4 Hz, H-1); 5.50 (m, 1H, H-4); 5.30 (m, 1H, H-3); 4.74 (d, 1H, *J* = 7.5 Hz, -C*H*$_a$$CCl_3$), 4.68 (d, 1H, *J* = 7.5, -C*H*$_b$$CCl_3$); 4.50 (m, 1H, H-2); 4.35 (m, 1H, H-5); 4.15 (m, 1H, H-6a), 4.08 (m, 1H, H-6b), 2.17 (s, 3H -C(O)C*H*$_3$), 2.01 (s, 6H 2 × -C(O)C*H*$_3$); **^{13}C NMR** (100 MHz, $CDCl_3$): δ = 170.7 (C-3O***C***(O)), 170.2 (C-6O***C***(O)), 170.0 (C-4O***C***(O)), 160.4 (*C*=NH), 154.3 (-NH*C*(O)O-); 95.2 (-*C*Cl_3), 95.2 (C-1), 90.7 (NH*C*Cl_3), 74.6 (-***C***H$_2$$CCl_3$); 69.1 (C-5); 67.9 (C-3); 66.8 (C-4); 49.5 (C-2); 20.6 (3 × -C(O)***C***H$_3$); **MS** (ESI+) m/z = 644.91 $[M+Na]^+$ (51%), 645.92 (10), 646.91 (100%), 647.91 (20%), 648.91 (81%), 649.91 650.90 (35%), (15%), 651.91 (5%), 652.90 (8%), Cl_6 isotope pattern observed., calcd. ($C_{17}H_{20}Cl_6N_2O_{10}Na^+$) m/z = 644.91 (52.1%), 645.92 (9.6%), 646.91 (100.0%), 647.91 (18.4%), 648.91 (79.9%), 649.91 (14.7%), 650.91 (34.1%), 651.91 (6.3%), 652.90 (8.2%), 653.91 (1.5%), 654.90 (1.0%).

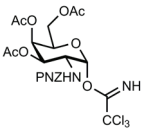

3,4,6-Tri-O-acetyl-2-deoxy-2-*N*-(4-nitrobenzyloxycarbonyl-amino)-α-D-galactopyranosyl trichloroacetimidate 34b.[40, 68] A solution of **33** (1.0 g, 2.0 mmol, 1.0 eq), trichloroacetonitrile (2 ml, 20 mmol, 10 eq), and DBU (75 µl, 0.3 mmol, 0.25 eq) in 10 ml DCM was

stirred at 0 °C until TLC analysis indicated that all starting material **33** had reacted (approx. 1 h). Then, the reaction mixture was concentrated *in vacuo* to afford compound **34b** as a white solid in 60% yield (0.5 g, 1.2 mmol). **^{1}H-NMR** (400 MHz, $CDCl_3$): δ = 8.75 (s, 1H, -N*H*CCl_3), 8.23 (d, 2H, *J* = 7.5 Hz, Ph-*H*a), 7.51 (d, 2H, *J* = 7.5 Hz, Ph-*H*b), 6.44 (d, 1H, 3.8 Hz, H-1), 5.55 (m, 1H, H-4), 5.29 (dd, 1H, *J* = 3.1, 11.4 Hz) H-3, 5.20 (s, 2H, -C*H*$_2$Ph), 4.98 (d, 1H, *J* = 9.8 Hz, -N*H*PNZ); 4.50 (m, 1H, H-2), 4.37 (m, 1H, H-5), 4.23 (m, 2H, H-6a+b), 2.03 (s, 6H, 2 × -OC(O)C*H*$_3$), 2.01 (s, 3H, -OC(O)C*H*$_3$); **^{13}C NMR** (100 MHz, $CDCl_3$): δ = 170.72, 170.68, 169.5, 155.5, 152.6, 144.8, 125.1, 121.9, 95.4 (C-1), 69.1 (C-5), 68.1 (C-3), 66.6 (C-4), 65.5 (*C*H_2Ph), 61.1 (C-6), 49.4 (C-2), 20.7, 20.6, 20.5.

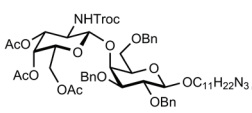

3,4,6-Tri-*O*-acetyl-2-deoxy-2-*N*-(2,2,2-trichloroethyl oxycarbonyl amino)-β-D-galactopyranosyl-(1→4)-2,3,6-tri-*O*-benzyl-β-D-galactopyranoside 35. GalNAc donor **34** (438 mg, 0.70 mmol, 1.5 eq) and Gal acceptor **30** (300 mg, 0.46 mmol, 1.0 eq) were dissolved in DCM (1 ml) in the presence of 3 Å MS and cooled to -40 °C. Subsequently, TMSOTf (4.1 µl, 24 µmol, 5 mol%) was added to initiate the glycosylation and the mixture was allowed to stir at a constant temperature (-40 °C) for 2 h. The reaction mixture was allowed to warm to room temperature in 1 h and quenched with three drops of Et_3N. The reaction mixture was filtered, rinsed with DCM (2 ml), and the filtrate concentrated *in vacuo*. Purification by automated column chromatography afforded disaccharide **35** as a white solid (245 mg, 0.24 mmol, 53%). **Rf** (EtOAc/ nhept 1 : 2) = 0.18, **^{1}H NMR** (400 MHz, $CDCl_3$) δ = 7.38 - 7.27 (m, 15H, Ph-*H*), 5.26 (m, 1H, -N*H*-), 4.93 (m, 2H), 4.75 - 4.52 (m, 7H), 4.36 (m, 1H), 4.34 (d, 1H, *J* = 8.0 Hz, $H_{Gal\text{-}1}$), 4.11 - 3.89 (m, 5H), 3.81 - 3.45 (m, 7H), 3.24 (t, 2H, *J* = 7.0 Hz, -C*H*$_2$$N_3$), 2.13 (s, 3H, -C(O)C*H*$_3$), 1.99 (s, 3H, -C(O)C*H*$_3$), 1.93 (s, 3H, -C(O)C*H*$_3$), 1.67 - 1.54 (m, 4H, -C***H***$_2$$N_3$, -$OC_2$HC***H***$_2$-), 1.38 - 1.26 (m, 14H, -C*H*$_2$-spacer); **^{13}C NMR** (100 MHz, $CDCl_3$): δ = 170.3, 170.2, 170.1 (3 × -***C***(O)CH_3); 154.3 (-N*C*(O)O-), 138.2 (2 × Cq Ph), 137.3 (Cq Ph), 129.0 - 127.6 (15 × Ph), 103.7 ($C_{Gal\text{-}1}$), 102.0 ($C_{GalNAc\text{-}1}$), 95.8 (-CCl_3), 81.7, 80.0, 75.7, 75.5, 74.6, 74.3, 73.6, 73.1, 71.9, 70.9, 70.1, 69.1, 66.6, 61.1, 52.7, 51.5 (-*C*$H_2$$N_3$), 29.5 - 26.7 (9 × -*C*$H_2$-spacer), 26.2, 20.64, 20.61, 20.55 (3 × -OC(O)***C***H_3, -NC(O)***C***H_3) **MS** (ESI+) m/z = 1107.39 (100%), 1109.39 (95%), 1111.38 (30%), 1113.38 (5%) $[M+H]^+$ Cl_3 pattern observed, calcd. ($C_{53}H_{70}Cl_3N_4O_{15}^+$) = 1107.39 (100.0%), 1109.39 (95.9%), 1111.38 (30.6%), 1113.38 (3.3%).

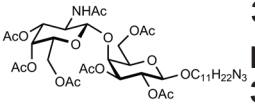

3,4,6-Tri-*O*-acetyl-2-deoxy-2-*N*-acetamido-β-D-galacto pyranosyl-(1→4)-2,3,6-tri-*O*-acetyl-β-D-galactopyranoside 36. **Zn dust activation**: To 3 g (46 mmol) powdered Zn was added 3 M HCl (30 ml) and stirred for 2 h (gas evolution was no longer observed). Subsequently, the suspension was filtered, rinsed with EtOH (20 ml), Et_2O (20 ml) and concentrated *in vacuo*. **Deprotection**: To a solution of disaccharide **35** (120 mg, 0.11 mmol, 1.0 eq) in Ac_2O, was added the previously activated powdered Zn (200 mg, 3.2 mmol, 30 eq). The suspension was stirred overnight at room temperature. The reaction mixture was then diluted with toluene (2 ml), filtered, the residue was rinsed with toluene (2 ml), EtOAc (2 ml), and then concentrated *in vacuo*. **Rf** (EtOAc/ nhept 3 : 1) = 0.31. A solution of the crude material (200 mg) in Ac_2O (2 ml) was cooled to -35 °C. A solution of TMSOTf (365 µl, 2.0 mmol) in Ac_2O (1 ml) was added drop wise. The resulting reaction mixture was stirred overnight at -35 °C. Subsequently, the reaction was warmed to 0 °C and quenched by the addition of sat. $NaHCO_3$. The mixture was extracted with EtOAc (3 × 2 ml), the combined organic layers where washed with sat NaCl (3 × 2 ml), dried over Na_2SO_4, filtered, and concentrated *in vacuo*. Purification by automated column chromatography yielded compound **36** as a white solid in 70% yield (64 mg, 80 µmol) over two steps; **^{1}H NMR** (400 MHz, $CDCl_3$): δ = 5.93 (m, 1H), 5.73 (d, 1H, *J* = 8.0 Hz, -N*H*-), 5.35 (m, 1H), 5.32 (m, 1H), 5.12 (d, *J* = 8.5 Hz, $H_{GalNAc-1}$), 5.00 (dd, 1H, *J* = 3.0, 10.5 Hz), 4.60 (d, 1H, *J* = 8.0 Hz, H_{Gal-1}), 4.25 (m, 2H), 4.17 (m, 1H), 4.05 (m, 2H), 3.92 (m, 1H), 3.73 (m, 2H), 3.34 (m, 2H), 3.26 (t, 2H, *J* = 6.9 Hz, -C$H_2$$N_3$), 2.30 - 2.00 (7 × -C(O)CH_2), 1.62 - 1.55 (m, 4H, -OCH_2C$\boldsymbol{H}_2$-, -OC$\boldsymbol{H}_2$$CH_2N_3$), 1.34 - 1.26 (m, 14H, -CH_2-spacer); **^{13}C NMR** (100 MHz, $CDCl_3$): δ = 170.7, 170.54, 170.49, 170.0, 169.9, 169.5, 169.1, (7 × -***C***(O)CH_3), 100.5 (C_{Gal-1}), 99.0 ($C_{GalNAc-1}$), 73.0, 72.5, 70.5, 70.3, 68.7, 68.2, 67.1, 61.1, 63.2, 53.5, 51.5 (-***C***H_2N_3), 29.5 - 25.8 (9 × -CH_2-spacer), 25.5, 23.6, 23.5 (2 ×), 21.0, 20.63, 20.59 (7 × -C(O)***C***H_2); **MS** (ESI+) m/z = 853.35 $[M+Na]^+$, calcd. ($C_{37}H_{58}N_4NaO_{17}^+$) = 853.37.

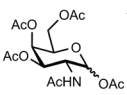

Acetyl 2-acetamido-2-deoxy-3,4,6-tri-acetyl-D-galactopyranoside 38.[69] To a cooled suspension (0 °C) of 1.0 g (4.6 mmol, 1.0 eq) HCl-salt **31** in 9.3 ml (115 mmol, 25 eq) pyridine, 13 ml (138 mmol, 30 eq) acetic anhydride was added drop wise in 15 min, stirring continued for an additional 48 h, while warming to room temperature. The reaction mixture was precipitated in 75 mL cold water (no ice), filtered with a Büchner setup, and the residue was rinsed with cold water, and lyophilized, affording 1.6 g (4.1 mmol, 89%) of compound

38 as a white solid. The product was sufficiently pure to be used in subsequent reactions; **MS** (ESI+) m/z = 390.20 $[M+H]^+$, calcd. ($C_{16}H_{24}NO_{10}^+$) = 390.14.

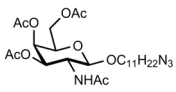

11-Azido-undecyl 2-acetamido-2-deoxy-3,4,6-tri-*O*-acetyl-β-D-galactopyranoside 39.[49] A mixture of 0.50 g (1.3 mmol, 1.0 eq) acetylated **38**, 0.33 g (1.5 mmol, 1.2 eq) 11-azido undecan-1-ol **21**, and 10 mg H_2SO_4-silica in 3 ml DCE were exposed to MW irradiation (150 W) for 30 min at 110 °C. The white suspension turned into a clear brown solution during the reaction. The reaction mixture was filtered through hyflo, and concentrated *in vacuo*. Purification by column chromatography, eluent: hept/ EtOAc 4 : 1, afforded 0.60 g (1.1 mmol, 84%) **39** as yellowish oil. **Rf** (hept/ EtOAc 4 : 1) = 0.35; **^{1}H NMR** (400 MHz, $CDCl_3$): δ = 6.43 (d, 1H, *J* = 8.8, -NH), 5.21 (m, 1H, H-4), 5.15 (m, 1H, H-3), 4.56 (d, 1H, *J* = 8.4 Hz, H-1), 4.00 (m, 2H, H-6a+b), 3.82 (m, 2H, H-2, H-5), 3.71 (m, 1H, -OCH_a-spacer), 3.34 (m, 1H, -OCH_b-spacer), 3.11 (t, 2H, *J* = 7.0 Hz, -CH_2N_3), 2.00 (s, 3H, -C(O)CH_3) 1.90 (s, 3H, -C(O)CH_3), 1.84 (s, 3H, -C(O)CH_3), 1.80 (s, 3H, -NHC(O)C$\boldsymbol{H}_3$), 1.43 (m, 4H, -C$\boldsymbol{H}_2$CH$_2$N$_3$, -C$\boldsymbol{H}_2$CH$_2$O-), 1.13 (m, 14H, -CH$_2$-spacer); **^{13}C NMR** (100 MHz, $CDCl_3$): δ = 170.2 (C=O), 170.1 (C=O), 170.0 (2 × C=O), 100.7 (C-1), 70.1 (C-5), 69.8 (C-3), 69.5 (-OCH_2-spacer), 61.3 (C-6), 51.0 (-CH_2N_3), 50.9 (C-2), 29.2, 29.1, 29.0, 28.7, 28.4, 26.3, 25.5, 22.9 (-NHC(O)$\boldsymbol{C}$H$_3$) 20.3 (3 × -C(O)$\boldsymbol{C}$H$_3$); **MS** (ESI+) m/z = 543.30 $[M+H]^+$, calcd. ($C_{25}H_{43}N_4O_9^+$) = 543.30.

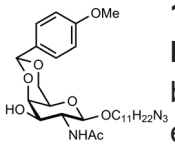

11-Azido undecyl 2-acetamido-2-deoxy-4,6-*O*-(4-methoxy benzylidene)-β-D-galactopyranoside 40. Compound **9** was dried by co-evaporation with EtOAc, Et_2O, MeCN and subsequently exposed to high vacuum overnight. PTSA·H_2O (6 mg, 30 µmol) was dissolved in 10 ml dry MeCN under Ar and stirred for 1 h in the presence of 3Å MS. Dried **9** (0.90 g, 2.2 mmol, 1.0 eq) was dissolved in 20 ml dry MeCN, while under Ar, *p*-anisaldehyde dimethyl acetal (0.78 g, 4.3 mmol, 2.0 eq) was added and the mixture was warmed to 50 °C. To the warmed solution, 2 ml of the freshly prepared PTSA-solution was added drop wise and stirring continued for 4 h at 50 °C and 48 h at room temperature. The resulting pink suspension was filtered on a Büchner setup and the residue was rinsed with additional MeCN, affording the desired compound **40** as a white solid (0.84 g). Purification by column chromatography of the filtrate resulted in additional yield (0.16 g). Combined yield: 1.0 g (1.9 mmol, 86%) **40** as a white solid. **Rf** (toluene/acetone 1:4) = 0.47; **^{1}H NMR** (400 MHz, $CDCl_3$): δ = 7.44 (d, 2H, *J* = 8.7, Ph-H$_a$), 6.88 (d, 2H, *J* = 8.7, Ph-H$_b$), 5.61 (m, 1H,

-N*H*-), 5.53 (s, 1H, acetal-H), 4.69 (d, 1H, *J* = 8.3, H-1), 4.32 (m, 1H), 4.19 (m, 1H), 4.09 (m, 2H), 3.93 (m, 1H), 3.81 (s, 3H, -OMe), 3.70 (m, 1H, H-2), 3.49 (m, 2H), 3.25 (t, 2H, *J* = 6.9, -C*H*$_2$N$_3$), 2.03 (s, 3H, -C(O)C*H*$_3$), 1.58 (m, 4H, -OCH$_2$C***H***$_2$-, -C***H***$_2$CH$_2$N$_3$), 1.28 (m, 14H, -CH$_2$-spacer); **^{13}C NMR** (100 MHz, $CDCl_3$): δ = 171.7 (C_q Ph), 160.2 (C_q Ph), 127.8 (Ph-H_a), 113.5 (Ph-H_b), 101.3 (acetal-H), 100.0 (C-1), 75.1, 70.7, 69.3, 69.1, 66.8, 55.7 (C-2), 55.3 (-O*C*H$_3$), 51.5 (-*C*H$_2$N$_3$), 29.5 - 23.7 (spacer); **MS** (ESI+) m/z = 535.33 $[M+H]^+$, calcd. ($C_{27}H_{43}N_4O_7^+$) = 535.31.

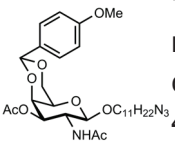

11-Azido undecyl 2-acetamido-2-deoxy-3-*O*-acetyl-4,6-*O*-(4-methoxybenzylidene)-β-D-galactopyranoside 40b (used as test compound for subsequent DDQ-mediated selective 4,6-deprotection). Monohydroxy **40** (164 mg, 0.3 mmol, 1.0 eq) was dissolved in pyridine (620 µl, 7.7 mmol, 25 eq) and cooled to 0 °C. After 10 min, 820 ml (9.2 mmol, 30 eq) Ac_2O was added drop wise and stirring continued at 0 °C for 16 h. The reaction mixture was poured in 10 ml ice cold water (no ice) and the resulting precipitate was recovered by filtration and dried overnight *in vacuo*, resulting in 61 mg (0.1 mmol, 35%) of **40b** as a white solid. The yield was increased by extracting the water layer with EtOAc (3 × 5 ml), the combined organic layers were concentrated *in vacuo* to obtain an additional 50 mg (0.08 mmol, 29%) off-white solid, 64% combined yield. **Rf** (toluene/ acetone 2:1) = 0.38; **^{1}H NMR** (400 MHz, $CDCl_3$): δ = 7.43 (m, 2H, Ph-H_a), 6.88 (m, 2H, Ph-H_b), 5.48 (s, 1H, acetal-H), 5.43 (m, 1H, -N*H*-), 4.92 (d, 1H, *J* = 8.3 Hz, H-1), 4.36 (m, 1H), 4.33 (m, 1H), 4.03 (m, 1H), 3.91 (m, 2H), 3.81 (s, 3H, -OMe), 3.50 (m, 2H), 3.26 (t, 2H, *J* = 7.0 Hz, -C*H*$_2$N$_3$), 2.08 (s, 3H, -C(O)C*H*$_3$), 1.95 (s, 3H, -C(O)C*H*$_3$), 1.59 (m, 4H, -OCH$_2$C***H***$_2$-, -C***H***$_2$CH$_2$N$_3$) 1.23 (m, 14H, -CH$_2$-spacer); **MS** (ESI+) m/z = 599.30 $[M+Na]^+$, calcd. ($C_{29}H_{44}N_4NaO_8^+$) m/z = 599.31.

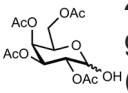

2,3,4,6-Tetra-*O*-acetyl-D-galactopyranoside 41a. Per-*O*-acetate **13** (1.8 g, 4.5 mmol, 1.0 eq) was dissolved in 100 ml DMF and exposed to 0.5 g (5.9 mmol, 1.3 eq) hydrazine acetate and stirred at rt until TLC indicated that the starting material had reacted (~ 1 h). Upon completion, the reaction mixture was diluted with 100 ml EtOAc and washed with brine (2 × 200 ml), demi water (2 × 200 ml), dried over Na_2SO_4, filtered, and concentrated *in vacuo*. Purification by automated column chromatography afforded an anomeric mixture of compound **41a** in 75% (1.2 g, 3.4 mmol) yield as a colorless oil. **Rf** (EtOAc/ nhept 2 : 1) = 0.39; **MS** (ESI+) m/z = 349.11 $[M+H]^+$, calcd. ($C_{14}H_{21}O_{10}^+$) = 349.11.

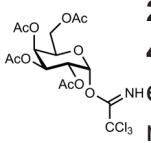

2,3,4,6-Tetra-*O*-acetyl-α-D-galactopyranosyl-trichloroacetimidate 41. Hemi-acetal **41a** (300 mg, 0.9 mmol, 1.0 eq) in 10 ml DCM was exposed to trichloroacetonitrile (0.7 g, 4.5 mmol, 5 eq), and $CaCO_3$ (27 mg, 0.3 mmol, 0.3 eq), stirred at room temperature for 20 min, and subsequently concentrated *in vacuo*. The residual orange/brown oil was purified by column chromatography, eluent: gradient hept/ EtOAc 10 : 1 → 1 : 2, afforded **41**(*α*) 91 mg (0.2 mmol, 22%) and the *β*-imidate in 175 mg (0.4 mmol, 43%). Alternatively, when the reaction was performed with DBU, rather than $CaCO_3$, predominantly the *α*-imidate, compound **41**, was formed and isolated in 57% yield as a white solid. **Rf** (hept/ EtOAc 1 : 2) = 0.76, 0.68 (α and β, respectively); **α anomer**: **^{1}H NMR** (400 MHz, $CDCl_3$): δ = 8.66 (s, 1H, =N*H*), 6.59 (d, 1H, *J* = 3.5 Hz, H-1), 5.56 (dd, 1H, *J* = 1.1, 3.2 Hz, H-4), 5.36 (dd, 1H, *J* = 3.1, 10.8 Hz, H-3), 5.30 (dd, 1H, *J* = 3.5, 10.8, H-2), 4.37 (m, 1H, H-5), 4.12 - 4.00 (m, 2H, H-6a+b), 2.10 (s, 3H, -C(O)CH_3), 1.97 (s, 3H, -C(O)CH_3), 1.96 (s, 3H, -C(O)CH_3), 1.95 (s, 3H, -C(O)CH_3); **^{13}C NMR** (100 MHz, $CDCl_3$): δ = 170.3 (-*C*=O), 170.09 (-*C*=O), 170.07 (-*C*=O), 169.67 (-*C*=O), 160.9 (-*C*=N*H*), 93.5 (C-1), 90.8 (-CCl_3), 69.0 (C-5), 67.5 (C-4), 67.3 (C-3), 66.9 (C-2), 61.2 (C-6), 20.7 (-CH_3), 20.6 (2 × -CH_3), 20.5 (-CH_3); **β anomer**: **^{1}H NMR** δ = 8.71 (s, 1H, =N*H*), 5.82 (d, 1H, *J* = 8.2 Hz, H-1), 5.49 (m, 1H, H-2), 5.46 (m, 1H, H-4), 5.11 (dd, 1H, *J* = 3.6, 10.4 H-3), 4.18 (m, 1H, H-6), 4.11 (m, 1H H-5), 2.18 (s, 3H, -C(O)CH_3), 2.05 (s, 3H, -C(O)CH_3), 2.03 (s, 3H, -C(O)CH_3), 2.01 (s, 3H, -C(O)CH_3); **^{13}C NMR** (100 MHz, $CDCl_3$): δ = 170.3 (-*C*=O), 170.2 (-*C*=O), 170.0 (-*C*=O), 169.1 (-*C*=O), 161.0 (-*C*=N*H*), 96.0 (C-1), 90.3 (-CCl_3), 71.7 (C-5), 70.7 (C-3), 67.7 (C-2), 66.7 (C-4), 60.9 (C-6), 20.7 (4 × -CH_3) **MS** (ESI+) m/z = 514.01 $[M+Na]^+$(100.0%), 515.00 (15%), 516.00 (95%), 517.01 (15%), 518.00 (30%), 519.00 (5%), Cl_3-pattern observed, calcd. ($C_{16}H_{20}Cl_3NNaO_{10}^+$) = 514.00 (100.0%), 515.00 (17.3%), 516.00 (95.9%), 517.00 (16.6%), 517.99 (30.6%), 519.00 (5.3%); (HR-ESI+) m/z = 331.0265 Corresponds to C-2 → C-1 acetal, calcd. ($C_{14}H_{19}O_9^+$) = 331.1024.

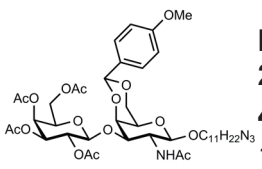

11-Azido undecyl 2,3,4,6-tetra-*O*-acetyl-β-D-galacto pyranosyl-(1→3)-4,6-(4-methoxybenzylidene) 2-acetamido-2-deoxy-β-D-galactopyranoside 42. Galactosamine acceptor **40** (515 mg, 1.0 mmol, 1.0 eq), galactose donor **41** (617 mg, 1.3 mmol, 1.3 eq), and activated 3 Å MS were dried under vacuum for 4 h, then recovered under Ar atmosphere. Dry DCM (10 ml) was added to the dried compounds and the reaction mixture was cooled to -30 °C.

After 10 min stirring, 13 µl (0.07 mmol, 7 mol%) TMSOTf was added and stirring continued for 2 h at -30 °C. TLC indicated only slow conversion, additional drop of TMSOTf was added and stirring continued for 16 h while warming up to 0 °C and subsequently for 3 h at room temperature. The reaction mixture was quenched by addition of a drop of Et_3N and concentrated *in vacuo*. Purification by automated column chromatography (toluene/ acetone), resulted in compound **42** as a white sold in 56% yield (465 mg, 0.6 mmol). **Rf** (acetone/ toluene 1 : 1) = 0.60; **^{1}H NMR** (400 MHz, $CDCl_3$): δ = 7.46 (d, 2H, *J* = 8.7 Hz, (Ph-*H*a), 6.88 (d, 2H, *J* = 8.7 Hz, (Ph-*H*b), 5.69 (d, 1H, *J* = 5.7 Hz, -NH-), 5.51 (s, 1H, acetal-*H*), 5.36 (m, 1H), 5.22 (m, 2H), 5.13 (d, 1H, *J* = 8.0 Hz, $H_{GalNAc-1}$), 4.99 (dd, *J* = 3.4, 10.3 Hz) 4.80 (d, 1H, *J* = 7.9 Hz, H_{Gal-1}), 4.73 (dd, *J* = 3.30, 11.1 Hz, $H_{GalNAc-2}$), 4.31 – 4.26 (m, 2H), 4.14 (m, 2H), 4.03 (m, 1H), 3.89 (m, 2H), 3.81 (s, 3H, -OMe), 3.45 (m, 2H, $H_{GalNAc-4}$, $H_{GalNAc-2}$), 3.25 (t, 2H, *J* = 7.0 Hz, -CH_2N_3), 2.14 (s, 3H, -C(O)CH_3), 2.04 (s, 6H, -C(O)CH_3), 1.97 (s, 6H, -C(O)CH_3), 1.58 (m, 4H, -OCH_2C***H***$_2$-, -C***H***$_2$CH_2N_3), 1.27 (m, 14H, -CH_2-spacer); **MS** (ESI+) m/z = 866.01 $[M+H]^+$, calcd. ($C_{41}H_{61}N_4O_{16}^+$) = 865.95.

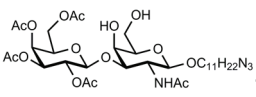

11-azidoundecyl-2,3,4,6-tetra-*O*-acetyl-β-D-galactopyranosyl-(1→3)-β-D-2-acetamido-2-deoxy-galactopyranoside 43. The following procedure was carried out in the dark. The selective 4,6-deprotection of compound **42** (200 mg, 0.23 mmol, 1.0 eq) was performed in MeCN (10 ml) by stirring the starting material at room temperature in the presence of DDQ (105 mg, 0.46 mmol, 2.0 eq). After 30 min., H_2O (1 ml) was added and the reaction mixture was allowed to stir for an additional 90 min., after which, TLC analysis indicated that the reaction was complete. The reaction mixture was quenched by addition of sat. $NaHCO_3$ (10 ml), the organic phase was washed with sat. NaCl (3 × 10 ml), dried over Na_2SO_4, filtered, and concentrated *in vacuo*. Purification by automated column chromatography afforded 100 mg (0.13 mmol, 58%) compound **43** as a white solid. **Rf** (toluene/ acetone 1 : 1) = 0.30; **^{1}H NMR** (400 MHz, $CDCl_3$): δ = 5.82 (bs, -N*H*-), 5.39 (m, 1H, H_{Gal-4}), 5.20 (dd, 1H, *J* = 7.9, 10.3 Hz, H_{Gal-2}), 5.02 (dd, 1H, *J* = 3.4, 10.4 Hz, H_{Gal-3}), 4.97 (d, 1H, *J* = 8.3 Hz, $H_{GalNAc-1}$), 4.65 (d, 1H, *J* = 8.0, H_{Gal-1}), 4.60 (m, 1H, $H_{GalNAc-3}$), 4.13 - 4.08 (m, 3H, $H_{GalNAc-4}$, $H_{GalNAc-6}$), 3.96 (m, 2H, $H_{GalNAc-5}$, H_{Gal-6a}), 3.86 (m, 2H, -OC*H*a-spacer, H_{Gal-6b}), 3.63 (m, 1H, H_{Gal-5}), 3.48 (m, 1H, -OC*H*b-spacer), 3.34 (m, 1H, $H_{GalNAc-2}$), 3.26 (t, *J* = 7.0 Hz, -CH_2N_3), 2.17, 2.07 (2 ×), 1.99, 1.98 (5 × -C(O)CH_3), 1.64 - 1.54 (m, 4H, -C***H***$_2N_3$, -OC_2HC***H***$_2$-), 1.39 - 1.28 (m, 14H, -CH_2-spacer); **^{13}C NMR** (100 MHz, $CDCl_3$): δ = 170.8, 170.5, 170.0,

169.9, 169.5 (5 × -***C***(O)CH_3), 100.3 (C_{Gal-1}), 98.5 ($C_{GalNAc-1}$), 78.5 ($C_{GalNAc-3}$), 73.4 (C_{Gal-5}), 71.1 ($C_{GalNAc-5}$), 70.6 (C_{Gal-3}), 69.9 (C_{Gal-5}), 68.8 (-O***C***H_2-spacer), 68.4 ($C_{GalNAc-4}$), 66.9 (C_{Gal-4}), 62.6 (C_{Gal-6}), 61.6 ($C_{GalNAc-6}$), 54.5 ($C_{GalNAc-2}$), 51.5 (-***C***H_2N_3) 29.5 - 28.8 (9 × -***C***H_2-spacer), 25.9, 20.8, 20.59, 20.57, 20.49 (4 × -OC(O)***C***H_3, -NC(O)***C***H_3); **MS** (ESI+) m/z = 769.36 $[M+Na]^+$, calcd. ($C_{33}H_{54}N_4NaO_{15}^+$) = 769.35.

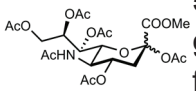

5-acetamido-2,4,7,8,9-penta-*O*-acetyl-3,5-didexoy-D-glycero-D-galacto-2-nonulopyranosonate 45. Compound **45** was synthesized from *N*-acetyl neuraminic acid **44** according to literature procedures.[52] Compound **45** was obtained as a mixture of anomers as an off-white solid in 90% yield over two steps. Spectral data was in agreement with literature values.[52b, 56, 70]

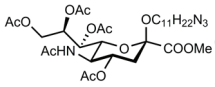

11-Azido undecyl-5-acetamido-4,7,8,9-tetra-O-acetyl-3,5-didexoy-β-D-glycero-D-galacto-2-nonulopyranosonate 46. Similar procedure as described for compound **39**. The resulting brownish oil was purified by automated column chromatography, eluent: gradient hept/ EtOAc, to afford 113 mg (0.2 mmol, 13%) **46** as a white solid. **Rf** (EtOAc/ nhept 4 : 1) = 0.18; **^{1}H NMR** (400 MHz, $CDCl_3$): δ = 5.73 (dd, 1H, *J* = 2.2, 3.3 Hz, H-7), 5.32 (d, 1H, *J* = 10.2 Hz, -NH-), 5.24 (m, 1H, H-4), 5.17 (m, 1H, H-8), 4.77 (dd, 1H, *J* = 2.3, 12.4 Hz, H-9a), 4.09 (m, 2H, H-5, H-9b, 3.90 (dd, 1H, *J* = 2.2, 10.5 Hz, H-6), 3.77 (s, 3H, -C(O)OC***H***$_3$), 3.43 (m, 1H, -OC***H***a-spacer), 3.29 (m, 1H, -OC***H***b-spacer), 3.23 (t, 2H, *J* = 6.8 Hz, -CH_2N_3), 2.43 (dd, 1H, *J* = 4.9, 12.9 Hz, H-3eq), 2.12, 2.04, 2.00, 1.99, (4 × -OC(O)C***H***$_3$), 1.85 (m, 4H, -NC(O)C***H***$_3$, H-3ax), 1.61 - 1.52 (m, 4H, -OCH$_2$C***H***$_2$-, -OC***H***$_2$CH$_2$N$_3$); 1.32 - 1.36 (m, 14H, -CH_2-spacer); **^{13}C NMR** (100 MHz, $CDCl_3$): δ = 171.0, 170.6, 170.4, 170.2, 170.1, (5 × -O***C***(O)CH_3, -N***C***(O)CH_3), 167.6 (-***C***(O)OCH_3), 98.5 (C-2), 72.1 (C-8), 71.7 (C-6), 69.0 (C-4), 68.5 (C-7), 64.2 , 62.4 (C-9), 52.5 (-C(O)O***C***H_3), 51.4 (-***C***H_2N_3), 49.4 (C-5), 37.4 (C-3), 29.6 - 26.0 (9 × -***C***H_2-spacer), 23.1 (-NC(O)***C***H_3), 21.0 - 20.7 (4 × -OC(O)***C***H_3); **MS** (ESI+) m/z = 687.36 $[M+H]^+$, calcd. ($C_{31}H_{51}N_4O_{13}^+$) m/z = 687.34.

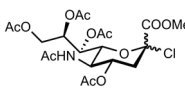

Chloro 5-acetamido-4,7,8,9-tetra-O-acetyl-3,5-dideoxy-D-glycero -D-galacto-2-nonulopyranosonate 47. Compound **47** was synthesized from **45** according to literature procedures.[52] Compound **47** was obtained as a mixture of anomers in 90% yield as an off-white solid. Spectral data was in agreement with literature values.[52b, 56, 70]

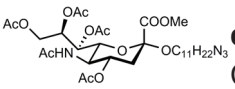

11-Azido undecyl-5-acetamido-4,7,8,9-tetra-O-acetyl-3,5-di dexoy-α-D-glycero-D-galacto-2-nonulopyranosonate 48. Chlorine compound **47** (470 mg, 0.9 mmol, 1.0 eq) and 11-azido-undecan-1-ol **21** (508 mg, 1.8 mmol, 2.0 eq) were dissolved in 5 ml dry DCM and stirred for 30 min. with 4Å MS. $AgCO_3$ (589 mg, 2.8 mmol, 3.0 eq) was added and stirring continued overnight in a closed vessel, deprived from light. The reaction mixture was filtered through hyflo, rinsed with DCM and concentrated *in vacuo*. The crude yellow oil was purified by automated column chromatography, eluent EtOAc/ nhept 10 : 1, to afford 290 mg **48** as a white solid (0.42 mmol, 47%. **Rf** (EtOAc/ nhept 10 : 1) = 0.21; **^{1}H NMR** (400 MHz, $CDCl_3$): δ = 5.78 (d, 1H, *J* = 9.4 Hz, -N*H*-), 5.28 (m, 1H, H-8), 5.25 (dd, 1H, *J* = 1.7, 7.8 Hz), 4.74 (m, 1H, H-4), 4.25 (dd, 1H, *J* = 2.4, 12.4 Hz, H-9a), 4.01 (m, 3H, H-5, H-6, H-9b), 3.69 (s, 3H, -C(O)OCH_3), 3.65 (m, 1H, -OC*H*a-spacer), 3.16 (t, 3H, *J* = 7.0 Hz, -CH_2N_3), 3.12 (m, 1H, -OC*H*b-spacer), 2.49 (dd, 1H, *J* = 4.6, 12.8 Hz, H-3eq), 2.05, 2.04, 1.94, 1.93 (4 × -OC(O)CH_3), 1.78 (m, 4H, -NC(O)CH_3, H-3ax), 1.50 (m, 2H, -C$\boldsymbol{H}_2N_3$), 1.43 (m, 2H, -$OC_2HC\boldsymbol{H}_2$-), 1.26 - 1.19 (m, 14H, -CH_2-spacer); **^{13}C NMR** (100 MHz, $CDCl_3$): δ = 170.8, 170.5, 170.2, 170.03, 169.98, (4 × -O***C***(O)CH_3, -N***C***(O)CH_3), 168.5 (-***C***(O)OCH_3), 98.7 (C-2), 72.5 (C-6), 69.3 (C-4), 69.1 (C-8), 67.4 (C-7), 64.9 (-*C*H_2O-spacer), 62.3 (C-9), 52.4 (-C(O)O***C***H_3), 51.3 (-CH_2N_3), 49.1 (C-5), 38.0 (C-3), 29.4 - 25.7 (9 × -*C*H_2-spacer), 23.0, 21.0, 20.7 (2×), 20.6 (4 × -OC(O)***C***H_3, -NC(O)***C***H_3); **MS** (HR-ESI+) m/z = 709.3198 $[M+Na]^+$, calcd. ($C_{31}H_{50}N_4NaO_{13}^+$) = 709.3267.

6.5 References

[1] World Health Organization (WHO), *Weekly epidemiological record* **2008**, *83*, 37-44.
[2] Y. Hu, J. Huang, X.-a. Jiao, *J. Microbiol. Biotech.* **2014**, *24*, 217-224.
[3] A.-K. Llarena, K. Sivonen, M.-L. Hänninen, *Lett. Appl. Microbiol.* **2013**, *58*, 408-413.
[4] k. T. Young, L. M. Davis, V. J. DiRita, *Nat. Rev. Microbiol.* **2007**, *5*, 665-679.
[5] J. B. Winer, R. A. C. Hughes, C. Osmond, *J. Neurol. Neurosurg. Psychiatry* **1988**, *51*, 605-612.
[6] a) A. K. Asbury, D. R. Cornblath, *Ann. Neurol.* **1990**, *27(Suppl.)*, S21-24. b) P. A. van Doorn, *Presse Med.* **2013**, *42*, e193-201.
[7] B. van den Berg, C. Bunschoten, A. van Doorn Pieter, C. Jacobs Bart, *Neurology* **2013**, *80*, 1650-1654.
[8] L. Ruts, P. A. van Doorn, R. Lombardi, E. D. Haasdijk, P. Penza, J. H. M. Tulen, R. J. Hempel, A. H. van den Meiracker, G. Lauria, *Pain* **2012**, *153*, 399-409.
[9] R. W. Ledeen, R. K. Yu, *Methods Enzymol.* **1982**, *83*, 139-191.
[10] R. K. Yu, S. Usuki, T. Ariga, *Infect. Immun.* **2006**, *74*, 6517-6527.
[11] A. C. Horsfall, *Mol. Biol. Rep.* **1992**, *16*, 139-147.
[12] G. Guillain, J.-A. Barré, A. Strohl, *Bull. Mem. Soc. Med. Hop. Paris* **1916**, *40*, 1462-1470.
[13] A. F. Hahn, *Lancet* **1998**, *352*, 635-641.
[14] T. W. Ho, H. J. Willison, I. Nachamkin, C. Y. Li, J. Veitch, H. Ung, G. R. Wang, R. C. Liu, D. R. Cornblath, A. K. Asbury, J. W. Griffin, G. M. McKhann, *Ann. Neurol.* **1999**, *45*, 168-173.
[15] S. Usuki, J. Sanchez, T. Ariga, I. Utsunomiya, K. Taguchi, M. H. Rivner, R. K. Yu, *J. Neurol. Sci.* **2005**, *232*, 37-44.
[16] a) Y. Sekiguchi, A. Uncini, N. Yuki, S. Misawa, F. Notturno, S. Nasu, K. Kanai, Y.-i. Noto, Y. Fujimaki, K. Shibuya, S. Ohmori, Y. Sato, S. Kuwabara, *J. Neurol. Neurosurg. Psychiatry* **2012**, *83*, 23-28; b) N. Yuki, H.-P. Hartung, *N. Engl. J. Med.* **2012**, *366*, 2294-2304.
[17] A. Uncini, C. Manzoli, F. Notturno, M. Capasso, *J. Neurol. Neurosurg. Psychiatry* **2010**, *81*, 1157-1163.
[18] S. Rinaldi, K. M. Brennan, G. Kalna, C. Walgaard, P. van Doorn, B. C. Jacobs, R. K. Yu, J.-E. Mansson, C. S. Goodyear, H. J. Willison, *PLoS One* **2013**, *8*, e82337/82331-e82337/82313, 82313 pp.
[19] a) C. W. Ang, B. C. Jacobs, J. D. Laman, *Trends Immunol.* **2004**, *25*, 61-66; b) H. J. Willison, *Nat. Clin. Pract. Neuro.* **2005**, *1*, 2-3; c) H. J. Willison, *J. Peripher. Nerv. Syst.* **2005**, *10*, 94-112; d) A. van Doorn Pieter, L. Ruts, C. Jacobs Bart, *Lancet Neurol.* **2008**, *7*, 939-950.
[20] F. Galban-Horcajo, K. Halstead Susan, R. McGonigal, J. Willison Hugh, *Curr. Opin. Chem. Biol.* **2014**, *18*, 78-86.
[21] K.-i. Kaida, D. Morita, M. Kanzaki, K. Kamakura, K. Motoyoshi, M. Hirakawa, S. Kusunoki, *Ann.Neurol.* **2004**, *56*, 567-571.
[22] R. S. Houliston, B. C. Jacobs, A. P. Tio-Gillen, J. J. Verschuuren, N. H. Khieu, M. Gilbert, H. C. Jarrell, *Biochemistry* **2009**, *48*, 220-222.
[23] M. Mayer, B. Meyer, *J. Am. Chem. Soc.* **2001**, *123* 6108–6117.
[24] a) C. S. Kim, J. H. Seo, H. J. Cha, *Anal. Chem.* **2012**, *84*, 6884-6890; b) E. Arigi, O. Blixt, K. Buschard, H. Clausen, S. B. Levery, *Glycoconjugate J.* **2012**, *29*, 1-12.
[25] a) A. V. Pukin, C. A. G. M. Weijers, B. van Lagen, R. Wechselberger, B. Sun, M. Gilbert, M.-F. Karwaski, D. E. A. Florack, B. C. Jacobs, A. P. Tio-Gillen, A. van Belkum, H. P. Endtz, G. M. Visser, H. Zuilhof, *Carboh. Res.* **2008**, *343*, 636-650; b) A. V. Pukin, B. C. Jacobs, A. P. Tio-Gillen, M. Gilbert, H. P. Endtz, A. van Belkum, G. M. Visser, H. Zuilhof, *Glycobiology* **2011**, *21*, 1642-1650; c) K. K. R. Tetala, A. P. Heikema, A. V. Pukin, C. A. G. M. Weijers, A. P. Tio-Gillen, M. Gilbert, H. P. Endtz, A. van Belkum, H. Zuilhof, G. M. Visser, B. C. Jacobs, T. A. van Beek, *J. Med. Chem.* **2011**, *54*, 3500-3505.
[26] a) H. J. Willison, J. Veitch, A. V. Swan, N. Baumann, G. Comi, N. A. Gregson, I. Illa, J. Zielasek, R. A. Hughes, *Eur. J. Neurol.* **1999**, *6*, 71-77; b) M. L. Kuijf, P. A. Van Doorn, A. P. Tio-Gillen, K. Geleijns, C. W. Ang, H. Hooijkaas, W. C. J. Hop, B. C. Jacobs, *J. Neurol.*

Sci. **2005**, *239*, 37-44.
[27] R. A. C. Hughes, R. D. Hadden, N. A. Gregson, K. J. Smith, *J. Neuroimmunol.* **1999**, *100*, 74-97.
[28] a) W. Wakarchuk, M. Gilbert, patent, (National Research Council of Canada, Can.). Application: WO, **2007**, p. 70pp; b) L. M. Willis, M. Gilbert, M.-F. Karwaski, M.-C. Blanchard, W. W. Wakarchuk, *Glycobiology* **2008**, *18*, 177-186.
[29] B. C. Jacobs, M. P. Hazenberg, P. A. v. Doorn, H. P. Endtz, F. G. v. d. Meché, *J. Infect. Dis.* **1997**, *175*, 729-733.
[30] K. P. R. Kartha, R. A. Field, *Tetrahedron* **1997**, *53*, 11753-11766.
[31] J. Gervay, T. N. Nguyen, M. J. Hadd, *Carbohydr. Res.* **1997**, *300*, 119-125.
[32] a) G. A. Olah, S. C. Narang, B. G. B. Gupta, R. Malhotra, *Angew. Chem. Int. Ed.* **1979**, *18*, 612-614; b) G. A. Olah, S. C. Narang, *Tetrahedron* **1982**, *38*, 2225-2277.
[33] S. M. Andersen, C.-C. Ling, P. Zhang, K. Townson, H. J. Willison, D. R. Bundle, *Org. Biomol. Chem.* **2004**, *2*, 1199-1212.
[34] G. Zemplén, E. Pascu, *Ber. Dtsch. Chem. Ges.* **1929**, *62*, 1613.
[35] a) Y. Oikawa, T. Yoshioka, O. Yonemitsu, *Tetrahedron Lett.* **1982**, *23*, 889-892; b) Z. Zhang, G. Magnusson, *J. Org. Chem.* **1996**, *61*, 2394-2400.
[36] a) R. Johansson, B. Samuelsson, *J. Chem. Soc. Perk. Trans. 1* **1984**, 2371-2374; b) J. M. Hernández-Torres, J. Achkar, A. Wei, *J. Org. Chem.* **2004**, *69*, 7206-7211.
[37] a) P. J. Garegg, H. Hultberg, *Carboh. Res.* **1981**, *93*, C10-C11; b) P. J. Garegg, H. Hultberg, S. Wallin, *Carboh. Res.* **1982**, *108*, 97-101.
[38] a) L. Yan, D. Kahne, *Synlett* **1995**, 523; b) D. J. Jenkins, A. M. Riley, B. V. L. Potter, *J. Org. Chem.* **1996**, *61*, 7719-7726.
[39] R. Autar, R. M. J. Liskamp, R. J. Pieters, *Carbohydr. Res.* **2005**, *340* 2436–2442.
[40] W. Dullenkopf, J. C. Castro-Palomino, L. Manzoni, R. R. Schmidt, *Carboh. Res.* **1996**, *296*, 135-147.
[41] a) S. Kusumoto, H. Yoshimura, M. Imoto, T. Shimamoto, T. Shiba, *Tetrahedron Lett.* **1985**, *26*, 909-912; b) P. Boullanger, M. Jouineau, B. Bouammali, D. Lafont, G. Descotes, *Carboh. Res.* **1990**, *202*, 151-164; c) U. Ellervik, G. Magnusson, *Carboh. Res.* **1996**, *280*, 251-260.
[42] G. Grundler, R. R. Schmidt, *Carbohydr. Res.* **1985**, *135*, 203-218.
[43] a) W. H. Hartung, C. Simonoff, *Org. React.* **1953**, *7*, 263–326; b) C. H. Heathcock, R. Ratcliffe, *J. Am Chem. Soc.* **1971**, *93*, 1746–1757.
[44] a) E. D. Goddard-Borger, R. V. Stick, *Org. Lett.* **2007**, *9*, 3797-3800; b) K. Weidner, A. Giroult, P. Panchaud, P. Renaud, *J. Am. Chem. Soc.* **2010**, *132*, 17511-17515; c) R. Lartia, P. Murat, P. Dumy, E. Defrancq, *Org. Lett.* **2011**, *13*, 5672-5675.
[45] a) P. Angibeaud, J.-P. utille, *Synthesis* **1991**, *9*, 737-738; b) J. Alzeer, A. Vasella, *Helv. Chim. Acta* **1995**, *78*, 177-193.
[46] S. Uemura, S. Go, F. Shishido, J.-i. Inokuchi, *Glycoconj. J.* **2014**, *31*, 101-108.
[47] C. A. G. M. Weijers, M. C. R. Franssen, G. M. Visser, *Biotech. Adv.* **2008**, *26*, 436-456.
[48] a) T. Ren, D. Liu, *Tetrahedron Lett.* **1999**, *40*, 7621-7625; b) H. Cheng, X. Cao, M. Xian, L. Fang, T. B. Cai, J. J. Ji, J. B. Tunac, D. Sun, P. G. Wang, *J. Med. Chem.* **2005**, *48*, 645-652; c) G. Stübs, B. Rupp, R. R. Schumann, N. W. J. Schröder, J. Rademann, *Chem. Eur. J.* **2010**.
[49] S. Mandal, N. Sharma, B. Mukhopadhyay, *Synlett* **2009**, 3111-3114.
[50] R. Kuhn, P. Lutz, D. L. MacDonald, *Chem. Ber.* **1966**, 611-617.
[51] P. Allevi, P. Rota, R. Scaringi, R. Colombo, M. Anastasia, *J. Org. Chem.* **2010**, *75*, 5542-5548.
[52] a) P. Meindl, H. Tuppy, *Monatsh. Chem.* **1965**, *96*, 802-815; b) M. N. Sharma, R. Eby, *Carbohydr. Res.* **1984**, *127*, 201-210.
[53] W. Koenigs, E. Knorr, *Ber. Dtsch. Chem. Ges.* **1901**, *34*, 957–981.
[54] R. Sardzık, R. Sharma, S. Kaloo, J. Voglmeir, P. R. Crocker, S. L. Flitsch, *Chem. Commun.* **2011**, *47*, 5425-5427.
[55] M. Karpluss, *J. Am. Chem. Soc.* **1963**, *85*, 2870–2871.

[56] G.-J. Boons, A. V. Demchenko, *Chem. Rev.* **2000**, *100*, 4539-4566.
[57] a) J. Haverkamp, H. v. Halbeek, L. Dorland, F. G. Vliegenthart, R. Pfeil, R. Schauer, *Eur. J. Biochem.* **1982**, *122*, 305-311; b) H. Hori, T. Nakajima, Y. Nishida, H. Ohrui, H. Meguro, *Tetrahedron Lett.* **1988**, *29*, 6317-6320; c) S. Prytulla, J. Lauterwein, M. Klessinger, J. Thiem, *Carboh. Res.* **1990**, *215*, 345-349; d) T. Klepach, W. Zhang, I. Carmichael, A. S. Serianni, *J. Org. Chem.* **2008**, *73*, 4376–4387.
[58] a) R. Mirsky, K. R. Jessen, *Ann. N. Y. Acad. Sci.* **1986**, *486*, 132-146; b) K. R. Jessen, R. Mirsky, *NATO ASI Ser., Series H: Cell Biology* **1987**, *2*, 699-707.
[59] G. M. Pastores, *Int. J. Pept. Res. Ther.* **2009**, *47*, S75-S81.
[60] a) N. Kasai, A. R. Pachner, R. K. Yu, *J. Neurol. Sci.* **1986**, *75*, 33-42; b) T. Ichioka, K. Uobe, M. Stoskopf, Y. Kishimoto, G. Tennekoon, W. W. Tourtellotte, *Neurochem. Res.* **1988**, *13*, 203-207.
[61] a) Q. Hao, T. Saida, S. Kuroki, M. Nishimura, M. Nukina, H. Obayashi, K. Saida, *J. Neuroimmunol.* **1998**, *81*, 116-126; b) J. Kasuya, T. Miyazono, S. Takenaga, K. Arimura, M. Osame, S. Kusunoki, *Clin. Neurol.* **1999**, *39*, 538-541; c) S. Kusunoki, M. Shiina, I. Kanazawa, *Neurology* **2001**, *57*, 736-738; d) C. W. Ang, A. P. Tio-Gillen, J. Groen, P. Herbrink, B. C. Jacobs, R. Van Koningsveld, A. D. M. E. Osterhaus, F. G. A. Van der Meche, P. A. van Doorn, *J. Neuroimmunol.* **2002**, *130*, 179-183; e) M. Samukawa, Y. Hamada, M. Kuwahara, K. Takada, Y. Mitsui, M. Hirano, M. Sonoo, S. Kusunoki, *J. Neurol. Sci.* **2014**, *337*, 55-60.
[62] A. V. Pukin, C. A. G. M. Weijers, B. v. Lagen, R. Wechselberger, B. Sun, M. Gilbert, M.-F. Karwaski, D. E. A. Florack, B. C. Jacobs, A. P. Tio-Gillen, A. v. Belkum, H. P. Endtz, G. M. Visser, H. Zuilhof, *Carboh. Res.* **2008**, *343*, 636-650.
[63] U. Galili, *Immunol. Today* **1993**, *14*, 480-482.
[64] J. H. Pazur, K. L. Dreher, L. S. Forsberg, *J. Bio. Chem.* **1978**, *253*, 1832-1837.
[65] P. H. H. Lopez, G. Zhang, M. A. Bianchet, R. L. Schnaar, K. A. Sheikh, *Brain : J. Neurol.* **2008**, *131*, 1926-1937.
[66] a) D. Leckband, S. Sheth, A. Halperin, *J. Biomater. Sci., Polym. Ed.* **1999**, *10*, 1125; b) W. Norde, D. Gage, *Langmuir* **2004**, *20*, 4162-4167.
[67] B. C. Jacobs, P. A. van Doorn, P. I. M. Schmitz, A. P. Tio Gillen, P. Herbrink, L. H. Visser, H. Hooijkaas, F. G. A. van der Meche, *Ann. Neurol.* **1996**, *40*, 181-187.
[68] a) R. Batchelor, P. T. Northcote, J. E. Harvey, *J. Chem. Educ.* **2008**, *85*, 689-691; b) H. Paulsen, B. Helpap, *Carbohydr. Res.* **1991**, *216*, 289-313; c) X. Qian, O. Hindsgaul, *Chem. Commun.* **1997**, 1059-1060.
[69] Toray Industries, patent*, Vol. EP1787661 A1*, **2007**.
[70] N. E. Byramova, A. B. Tuzikov, N. V. Bovin, *Carboh. Res.* **1992**, *237*, 161-175.

7

General discussion

7.1 Introduction

In the studies presented in the preceding chapters we used functional glycomics in an effort to increase the understanding on biological processes at the molecular level. All these studies revolve around the idea to covalently attach functionalized synthetic oligosaccharide ligands onto platforms for the detection of cholera and Guilliain-Barré syndrome (GBS). Obtaining such a sensor was the overarching goal of the Unihealth research program,[1] of which these studies were a part.

We designed and synthesized relatively small molecules that are similar in appearance to natural carbohydrates that occur in the human macromolecular glycocalyx, which is on the surface of almost every cell. We applied them on multivalent scaffolds that showed very good ligand-protein binding affinities and attached them to surfaces *via* copper-catalyzed azide-alkyne cycloaddition (CuAAC) reactions or strain-promoted azide-alkyne cycloaddition (SPAAC)-type ligations. A specific computational tool was developed so that novel cyclooctynes can be valued for their reactivity with azides in SPAAC reactions before their actual time-consuming synthesis. Additionally, very interesting results were obtained when synthetic ganglioside GM1 oligosaccharide (GM1os) fragments were applied on surfaces and used for the detection of GBS-related anti-ganglioside antibodies (Abs). In the research presented in this thesis it is clear how the combination of several disciplins is fundamental to reach fixed goals. Computational chemistry, organic synthesis and biological assays were applied in synergy to increase the knowledge of the biological processes involved in the diseases cholera and Guillain-Barré syndrome. The sections below, provide a general discussion and future prospects for each research chapter. These studies show that the past and future of science are only separated by the infinitesimally thin present time in which the research is performed.

7.2 Chapters 2 and 3: 'Getting one-on-one with cholera: Picomolar inhibition of cholera toxin by a pentavalent ganglioside GM1os-calix[5]arene' and 'Nanomolar cholera toxin inhibitors based on symmetrical pentavalent ganglioside GM1os-*sym*-corannulenes'

Multivalency is the key factor in the studies presented in these two chapters. A single protein-carbohydrate interaction, albeit with high specificity, usually shows

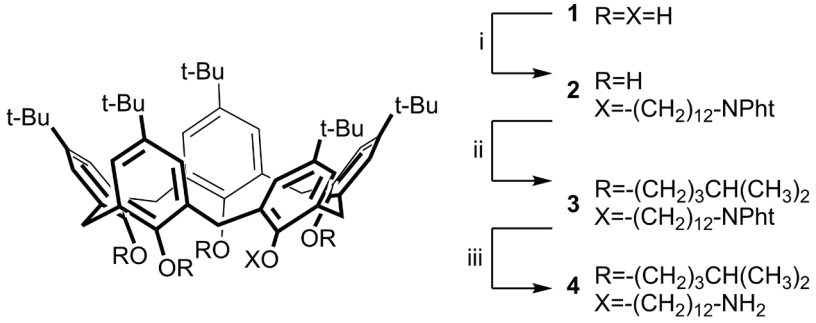

Figure 1. A spacer can be attached to the lower rim of a calixarene and equipped with a suitable reactive handle to enable covalent immobilization onto surfaces. Reagents and conditions: i) PhtN-$(CH_2)_{12}$Br, $KHCO_3$/ CH_3CN; ii) $CH_3CH(CH_2)_3Br$, K_2CO_3/ CH_3CN; iii) H_2NNH_2/ EtOH. Figure reproduced from reference.[4]

weak binding affinities with dissociation constants in the micromolar or millimolar range. Enhancement of the protein-ligand binding affinity can be achieved by presenting multiple ligands on a multivalent scaffold so that the glycoside cluster effect is mimicked to some extend. It has been shown on several occasions that compounds bearing multiple copies of the GM1os provide an effective strategy for inhibiting the pentameric receptor of the cholera toxin B-subunit (CTB).[2] In Chapters 2 and 3, we presented the first examples of pentameric GM1os CTB inhibitors. Binding experiments of three corannulene-based compounds presenting the GM1os – that was attached to the platforms *via* spacers with three different lengths – with CTB showed that the corannulene compound with the "mid-sized" hexa-ethyleneoxide (EO_6) spacer was able to inhibit CTB the strongest with IC_{50} = 5 nM. The calix[5]arene scaffold that was synthesized to also present five GM1os ligands showed an even better inhibitory potency of IC_{50} = 450 pM, amounting to a hundred thousand fold increase in relative inhibitory potency with respect to the monovalent control compound. We showed here again that exposing a multivalent receptor to a multivalent ligand has a positive synergetic effect on the receptor-ligand binding and leads to interactions that are thermodynamically and kinetically more favorable than if monovalent ligands would be used.[3]

Our multivalent ligands could be used as diagnostic tools for pathogen detection. It would be interesting to functionalize surfaces to present multivalent platforms rather than individual molecules so that the structural complexity of the glycocalyx on cell surfaces[5] is mimicked. Besides, when multivalent ligands are presented, instead of the monovalent counterparts, the overall concentration can be reduced to maintain the same binding affinities. This

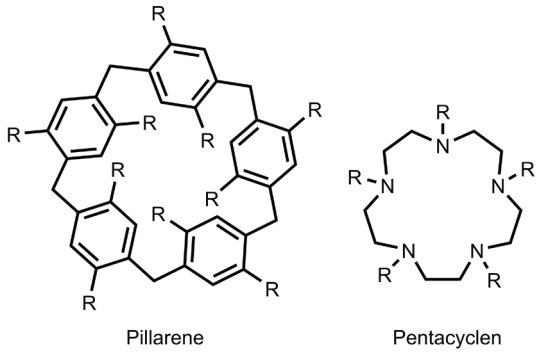

Figure 2. Pillarenes and pentacyclens are suitable alternatives as carbohydrate-modified pentavalent scaffolds, or even decavalent scaffolds in case of the pillarenes; R = suitable spacer and GM1os (or fragments).

is advantageous because high overall concentration can lead to overcrowded surfaces on which epitope-movability might be restricted or the epitopes might be unavailable for a protein binding pocket due to steric reasons.[6]

To meet the requirements of being attached to a surface, our current scaffolds need to be modified. Whereas, for the corannulene derivatives, this is not really an option, due to the lack of reactive functionalities in these compounds, for calix[5] arenes monofunctionalization on the lower rim can be performed so that they can be immobilized on a surface. Figure 1 depicts an example of a possible approach to obtain such a calix[5]arene.[4] In that case, they could function as detectors in for example a biosensor or also to remove cholera toxin from solutions *via* a dialysis approach.[7]

Spacer length and morphology remain important issues to be further investigated.[8] We showed in Chapter 2 that optimizing spacer length is important for the binding affinity. In the case of our corannulenes, tuning the spacer length led to a factor 100 better binding. Crystallography studies by Hol and coworkers[9] on the binding site of CT (bound to ganglioside GM1) revealed that the ceramide functionalities clearly do not participate in the protein-carbohydrate binding interaction on the cell surface (although it plays a significant role in the follow-up steps in the pathogenesis of cholera[10]). So further investigation on the ceramide functionalities in order to increase the binding affinity to CTB is not relevant for our purpose. However, the ceramide structures are suspected to contribute to ganlgioside clustering that is important for the recognition by some anti-ganglioside Abs in GBS (this aspect is discussed in §7.5).

An avenue that *is* worth investigating to reach even more potent CTB inhibitors is to use alternative pentameric platforms such as pentacyclen structures

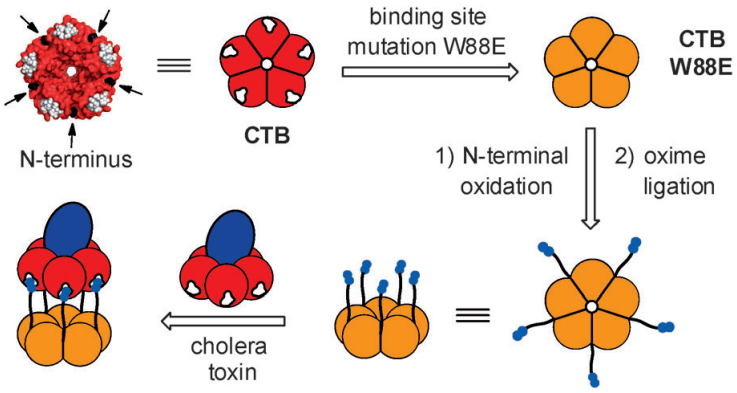

Figure 3. A protein-based pentavalent inhibitor of CTB. Figure reproduced from reference.[14]

(1,4,7,10,13-pentaazacyclopentadecane) (Figure 2).[11] Fan and coworkers synthesized a series of pentavalent CTB inhibitors in which a pentacyclen core was conjugated to five linkers, each one ending with a galactose unit.[12] Although a single monomeric galactose unit presents a rather low CTB affinity, thanks to multivalency the pentavalent galactose compound revealed a CTB-binding that was in the same order of magnitude as the inhibition potency of monovalent GM1. It showed a 260-fold higher potency compared to the monomeric galactose-derivative. However, pentacyclens suffer from the same deficiency as the corannulene scaffold *i.e.* a lack of a sixth site to modify for surface immobilization. This is imperative for our goal to develop a suitable biosensor, although it could be useful for therapeutic purposes since this relatively small scaffold is likely to be good water soluble when attached to multiple copies of the GM1os.

In addition, pillarenes are also worth investigating.[13] Since pillarenes do not have chemically distinguishable sides/ sites as equivalents of the calixarene upper and lower rims, they can only be functionalized in a decavalent fashion (or a mixture of asymmetric compounds). This means that, when equipped with the appropriate spacers, they are potentially able to inhibit two toxin proteins simultaneously.

After focusing on purely synthetic small molecule scaffolds, our attention recently also turned to multimeric proteins as scaffolds to appropriately display the ganglioside GM1 pentasaccharide.[14] We reasoned that the ideal pentavalent protein scaffold to bear GM1os would be CTB itself and therefore we explored a strategy to achieve this. Tryptophan (Trp) residues in the binding pockets of CTB were replaced by glutamic acid (Glu) residues by site-directed mutagenesis. This rendered the protein incapable of binding ganglioside GM1.

This site-specific mutant of CTB was subsequently equipped with suitable GM1 analogues at the *N*-termini (Figure 3). The site-specific modification of a protein scaffold, that perfectly matches the target toxin in both size and valency provided a convenient route to an effective multivalent inhibitor. This synthetic pentavalent neoglycoprotein displayed an IC_{50} of 104 pM for CTB,[14] which makes it the most potent pentavalent inhibitor for CTB reported thus far.

7.3 Chapter 4: Electronic effects versus distortion energies during strain-promoted alkyne-azide cycloadditions: A theoretical tool to predict reaction kinetics

Strain-promoted azide-alkyne cycloaddition (SPAAC) reactions are increasingly used as the preferred ligation method in biological assays. The high intrinsic energy of cyclooctynes and their high reactivity towards azides caught the attention of scientists from many disciplines. Therefore, novel cyclooctynes are developed on a regular basis. The design of new cyclooctynes might be aimed at improving specific characteristics like water solubility that is achieved chemically by incorporation of hydrophilic moieties. However, other properties that are of interest are less easily predicted like the reactivity of the cyclooctyne towards azides. A theoretical exploration of the reactivity of several cyclooctynes towards allyl azide and benzyl azide led to the development of a new predictive tool. We have used the designed method – that involves MP2-derived LUMO values as a measure for the reactivity of cyclooctynes with azides in the SPAAC reaction – to calculate the reactivity of several novel cyclooctynes and related structures that have not yet been synthesized. This study confirmed that inducing electron deficiency indeed improves the reactivity of the cyclooctynes. Therefore, it is definitely worthwhile exploring the design of cyclooctynes, or related strained compounds, that carry positive charges within their ring structure. We are currently focusing in this direction in the ongoing work on these compounds.

7.4 Chapter 5: The influence of copper on GM1os-based CTB detection assays: CuAAC vs SPAAC

In Chapters 2 and 3 we went “one-on-one” with cholera by strong inhibition of CTB with multivalent corannulene and calix[5]arene compounds. These compounds were synthesized in a convergent manner by employing the CuAAC reaction to

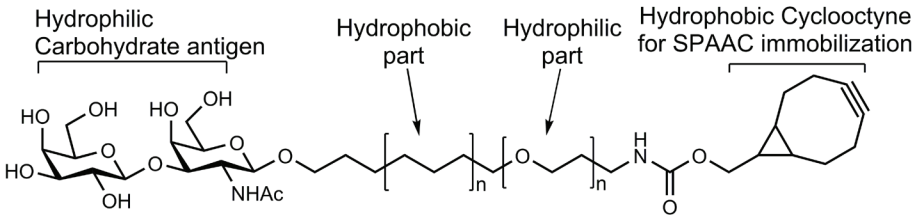

Figure 4. Amphipathic carbohydrate as a potential antigen that does not require metals to be immobilized on a surface.

attach five copies of the GM1os to the pentameric scaffolds. In Chapter 4, the nature of the high reactivity of cyclooctynes with azides in SPAAC reactions was investigated on a quantum mechanical level. In Chapter 5 we then combined knowledge gained from the three preceding chapters by directly comparing CuAAC and SPAAC in biological assays, while employing again the natural complementary system of CTB and the ganglioside GM1os. Three GM1os-bearing compounds were immobilized on azide-terminated microtiter plates *via* either CuAAC or SPAAC conditions depending on the nature of the attached alkyne moieties (either terminal alkyne or cyclooctyne). From these experiments we learned that the influence of residual copper on binding assays may be significantly greater than initially expected. Therefore, it can be concluded that ligation techniques that do not require metals are preferred to immobilize antigens on a surface. However, the solubility of compounds that bear relatively large lipophilic cyclooctynes is expected to be limited in the assay conditions. Therefore, hydrophilic spacers need to be added. On the other hand, we also saw that the addition of a hydrophilic spacer results in lower protein-carbohydrate binding. Perhaps this is because of disadvantageous interactions between the hydrophilic spacer and the CTB. Wild type gangliosides display a lipophilic aglycon part (ceramide) rather than a polar one. This then leads to a specific synthetic proposal: rather than attaching the EO directly to the carbohydrate, it should first be attached to an lipophilic part that in turn is then attached to an EO spacer suitably functionalized for surface attachment (Figure 4) much like the design of our calix[5]arene and corannulene compounds. In this way, an amphipathic antigen is created that has increased solubility in assay conditions and is therefore better presented in the aqueous environment and is expected to be recognized better by the target proteins.

7.5 Chapter 6: Evaluation of synthetic ganglioside-based glycan fragments as epitopes for Guillain-Barré syndrome-associated antibodies

As part of an ongoing investigation, we aimed to improve the understanding at a molecular level of the Abs-ganglioside specificity in Guillain-Barré syndrome (GBS). A small library of nine compounds was assembled that included fragments of the ganglioside GM1 pentasaccharide or a chemical analogue of it, the GM1os. All carbohydrates were equipped with an azide-functionality, with which they were covalently immobilized on bioassay surfaces via CuAAC reactions. Previous studies by our laboratory[6] showed that improvements for GBS-related Abs detection need to be directed to variation of the spacers (length and polarity) and to the density of GM1 molecules on the surface. A GM1 surface coverage that is too low leads to insufficient gangliosides to bind the Abs strongly, a density that is too high on the other hand impairs Abs-carbohydrate interactions because of steric reasons. Based on our current study, described in Chapter 6, it cannot be ignored that also the ceramide hydroxyl and amide functionalities possibly play a role in the assembly, and complex formation, of gangliosides. This specific part of the gangliosides has not yet been incorporated in synthetic ganglioside analogues and further studies are required to understand its role in ganglioside-Ab binding affinities.

It is also required to determined if residual copper on microtiter plates is of influence on the Ab binding response towards our synthetic carbohydrates. In line with the proposition of Chapter 5 (concerning Figure 4), the influence of copper on Ab-fragment interactions can be studied by using carbohydrates that are equipped with cyclooctynes. After being immobilized by SPAAC ligations on microtiter plates, these compounds can then be compared in an ELISA study with carbohydrate analogues that require to be immobilized *via* the CuAAC reaction.

It is clear from our research that reducing complexity of the gangliosides has only limited success for the detection of GBS-related anti-ganglioside Abs. Saturation transfer difference NMR (STD-NMR)[15] studies by Houliston *et al*. indicated that the major contributors to the GM1-Abs binding are the terminal Gal*β*1-3GalNAc*β* and Neu5Ac*α*2 epitopes.[16] This, as a stand-alone study, would suggest that presenting either of these epitopes would enable significant binding to the Abs. However, it is also obvious from our study that the complexity of the Ab-ganglioside binding interaction cannot always be mimicked in a one-to-one fashion by presenting these separate glycan fragments to the Abs. GBS-

related Abs, in contrast to CTB, have less specifically defined binding sites. Their recognition sites are more complex and some Abs are known to recognize ganglioside complexes of different ganglioside composition rather than separate unique compounds.[17] Thus, mimicking the ganglioside complexes by presenting the carbohydrate epitopes on multivalent platforms might drastically increase the Ab-carbohydrate binding. In that case, also mixtures of epitopes (such as the Gal*β*1-3GalNAc*β* epitope depicted in Figure 4 in combination with a similar Neu5Ac*α*2-bearing compound) could be attached to these platforms. This would reintroduce some of the complexity of the gangliosides but would still maintain the relative ease of synthesizing ganglioside fragments. In line with the future prospects of Chapters 2 and 3, also such novel compounds will be fit to be used for protein-detection with next generation biosensors, like the Unihealth sensor. They eventually should lead to the development of new biosensors that will be faster, cheaper and more accurate alternatives for the current detection methods.

An additional, potential therapeutic, application of our finding is that patients that test positive to our galactose and/ or lactose fragments could be treated with the unmodified galactose or lactose by IV administration. In this approach, the carbohydrates might be able to inhibit the malicious Abs and prevent them to target cells. Since these carbohydrates are part of our natural diet, unwanted effects are expected to be limited.

7.6 References

[1] http://www.unihealth.info/index.php?id=94

[2] For references and more information on this topic see Chapter 1.

[3] A. Mulder, J. Huskens, D. N. Reinhoudt, *Org. Biomol. Chem.* **2004**, *2*, 3409-3424.

[4] S. Pappalardo, V. Villari, S. Slovak, Y. Cohen, G. Gattuso, A. Notti, A. Pappalardo, I. Pisagatti, M. R. Parisi, *Chem. Eur. J.* **2007**, *13*, 8164-8173.

[5] R. L. Schnaar, R. Gerardy-Schahn, H. Hildebrandt, *Physiol. Rev.* **2014**, *94*, 461–518.

[6] A. V. Pukin, B. C. Jacobs, A. P. Tio-Gillen, M. Gilbert, H. P. Endtz, A. van Belkum, G. M. Visser, H. Zuilhof, *Glycobiology* **2011**, *21*, 1642-1650.

[7] K. K. R. Tetala, A. P. Heikema, A. V. Pukin, C. A. G. M. Weijers, A. P. Tio-Gillen, M. Gilbert, H. P. Endtz, A. van Belkum, H. Zuilhof, G. M. Visser, B. C. Jacobs, T. A. van Beek, *J. Med. Chem.* **2011**, *54*, 3500-3505.

[8] F. Sansone, A. Casnati, *Chem. Soc. Rev.* **2013**.

[9] E. A. Merritt, S. Sarfaty, F. Vandenakker, C. Lhoir, J. A. Martial, W. G. J. Hol, *Protein Sci.* **1994**, *3*, 166-175.

[10] a) D. E. Saslowsky, Y. M. Te Welscher, D. J. F. Chinnapen, J. S. Wagner, J. Wan, E. Kern, W. I. Lencer, *J. Biol. Chem.* **2013**, *288*, 25804-25809; b) M. Panasiewicz, H. Domek, G. Hoser, M. Kawalec, T. Pacuszka, *Biochemistry* **2003**, *42*, 6608-6619.

[11] a) E. Fan, Z. Zhang, W. E. Minke, Z. Hou, C. L. M. J. Verlinde, W. G. J. Hol, *J. Am. Chem. Soc.* **2000**, *122*, 2663-2664; b) E. A. Merritt, Z. Zhang, J. C. Pickens, M. Ahn, W. G. J. Hol, E. Fan, *J. Am. Chem. Soc.* **2002**, *124*, 8818.

[12] Z. S. Zhang, E. A. Merritt, M. Ahn, C. Roach, Z. Hou, C. Verlinde, W. G. J. Hol, E. Fan, *J. Am. Chem. Soc.* **2002**, *124*, 12991-12998.
[13] D.-D. Zheng, D.-Y. Fu, Y. Wu, Y.-L. Sun, L.-L. Tan, T. Zhou, S.-Q. Ma, X. Zhab, Y.-W. Yang, *Chem. Commun.* **2014**, *50*, 3201-3203.
[14] T. R. Branson, T. E. McAllister, J. Garcia-Hartjes, M. A. Fascione, J. F. Ross, S. L. Warriner, T. Wennekes, H. Zuilhof, W. B. Turnbull, *Angew. Chem. Int. Ed.* **2014**, *in press*, DOI: 10.1002/anie.201404397.
[15] M. Mayer, B. Meyer, *J. Am. Chem. Soc.* **2001**, *123* 6108–6117.
[16] R. S. Houliston, B. C. Jacobs, A. P. Tio-Gillen, J. J. Verschuuren, N. H. Khieu, M. Gilbert, H. C. Jarrell, *Biochemistry* **2009**, *48*, 220-222.
[17] F. Galban-Horcajo, S. K. Halstead, R. McGonigal, H. J. Willison, *Cur. Opin. Chem. Biol.* **2014**, *18*, 78-86.

8

Summary & Samenvatting

8.1 SUMMARY

In the studies presented in this dissertation we used functional glycomics in an effort to increase the understanding of several biological processes on a molecular level. The main goal was to use this knowledge to aid in the development of the Unihealth biosensor.[1] These studies focused on the design and synthesis of oligosaccharide-based antigens with good binding properties for the cholera toxin B-subunit (CTB) and Guillain-Barré syndrome (GBS)-related antibodies (Abs). In addition, and equally important, we studied the optimal means to attach these antigens onto a sensor surface. To achieve these goals it was essential to combine a broad spectrum of disciplines *e.g.* theoretical predictions, biological assays, and organic synthesis.

In **Chapters 2 and 3**, we presented the first examples of pentameric GM1 oligosaccharide (GM1os)-displaying CTB inhibitors that are based on two distinct pentameric scaffolds. In the pathogenesis of the disease cholera, CTB is used for recognition and binding to cell surfaces that display the complex glycan ganglioside GM1. It has been shown on several occasions that compounds bearing multiple copies of that ligand provide an effective strategy for inhibiting these pentameric receptors.[2] However, none of these previously reported compounds simultaneously displayed five GM1 pentasaccharides that would match the toxin's valency.

In **Chapter 2**, we presented how the pentameric GM1-bearing corannulene scaffolds were synthesized to display the GM1os *via* spacers of three different sizes *i.e.* three, six, or nine ethyleneglycol moieties. Besides resulting in a good nanomolar

Figure 1. A) bowl-like Corannulene scaffold; B) Flexible calix[5]arene scaffold.

inhibitor of CTB, importantly, it also proved that size *does* matter, because not the compound with the longest spacer, but rather, the intermediate length showed to have the best nanomolar inhibitory potency of the three corannulene derivatives.

The studies presented in **Chapter 3** showed that also the shape of the platform is of importance. A pentameric compound was designed to display five ganglioside GM1 oligosaccharides on a calix[5]arene platform. Whereas the corannulene shows bowl-like characteristics (Figure 1), with the carbohydrate-bearing spacers directed outwards, the calix[5]arene, which is functionalized at the lower rim with methoxy groups, presents conformational mobility that allow the five pentasaccharides to point also in the same direction adapting itself to the CT structure. The GM1os calix[5]arene showed a higher inhibitory potency than any of the corannulenes did with an IC_{50} of 450 pM, this amounted to a hundred thousand-fold increase in inhibitory potency with respect to the monovalent control compound. When the five terminal galactose moieties from the GM1os were omitted to display five GM2 oligosaccharides, the inhibitory potency dropped significantly and a much higher half maximal inhibition concentration was measured (IC_{50} = 9 μM).

Strain-promoted azide-alkyne cycloaddition (SPAAC, Figure 2) reactions are increasingly used as the preferred ligation method in bioorthogonal reactions and biological assays.[3] As this becomes more important, novel cyclooctynes are developed on a regular basis. Synthesis of new cyclooctynes might be aimed at improving specific characteristics like water solubility, which is achieved chemically by incorporation of hydrophilic moieties. However, other properties that are of interest are less easily predicted like the reactivity of the cyclooctyne towards azides. **Chapter 4** describes a theoretical exploration of cyclooctyne reactivity towards allyl azide and benzyl azide that was performed with three types of computational methods (B3LYP[4], M06-2X[5] and SCS-MP2[6]). While the DFT-type

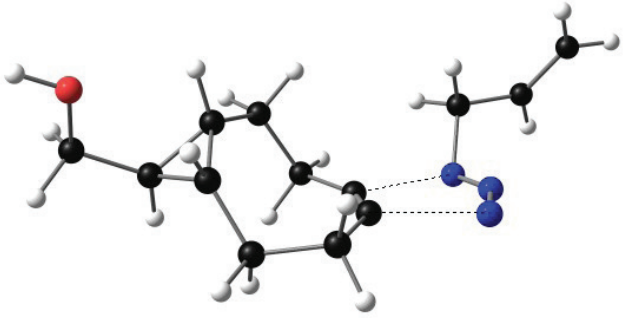

Figure 2. LUMO-driven SPAAC reaction of 9-hydroxymethylbicyclo[6.1.0]non-4-yne (BCN) with allyl azide.

calculations, B3LYP and M06-2X, did not provide good correlations between an extensive set of experimentally observed reaction rates and calculated parameters, SCS-MP2 calculations yielded clear, synthetically useful predictions. This allowed the discovery of a clear correlation of MP2-derived LUMO energies of the alkynes in the geometry they have in the transition state (TS, Figure 2) with the empirical reaction rate. In contrast to what has been claimed in literature,[7] no correlation between the experimental rates and alkyne distortion energies was established. Furthermore, we used these results to develop a tool that can aid synthetic chemists to determine SPAAC reaction kinetics of novel cyclooctynes prior to the actual synthesis. As a somewhat less accurate but much simpler predictive tool, the LUMO energy level of the fully MP2-optimized cyclooctyne reactant can also be used instead of the TS LUMO energy. When cyclooctyne TS LUMO values were correlated to the experimental rate constants, a good linear regression of $R^2 = 0.960$ was observed. Our study further supports the idea that the reaction is cyclooctyne LUMO-driven and that Hartree-Fock LUMO values are indeed a good measure for the reactivity of the cyclooctynes with organic azides in SPAAC reactions.

The SPAAC reaction is a potentially good replacement for the copper azide-alkyne cycloaddition (CuAAC)[3, 8] reaction in biological assays. One reason for that is that copper is suspected to have a negative influence on ligand-protein binding measurements. Experiments were devised to investigate the influence of copper on such measurements. Therefore in **Chapter 5**, we combined elements from the three previous chapters by directly comparing CuAAC reactions and SPAAC reactions in biological assays. A GM1os-bearing compound that presented a terminal alkyne[9] was immobilized by CuAAC to microtiter plates. Two novel GM1os-bearing compounds were developed to contain cyclooctynes, one was attached to an aliphatic and lipophilic undecane spacer and the second compound contained both the same aliphatic spacer and an additional hydrophilic spacer.

The initial assays were performed on the compounds after they had been immobilized on azide-terminated microtiter plates via either CuAAC or SPAAC conditions depending on the nature of the alkyne. The GM1os-bearing compounds were then exposed to CTB in indirect ELISA experiments. Both compounds without the EO-spacer were found to be recognized by the CTB protein in an approximate equal binding affinity, independent of the used immobilization technique. On the other hand, the compound that contained the EO-spacer showed significant lower binding affinity towards CTB. In a second set of experiments, the compounds were attached to the surface and then exposed to the CuAAC catalyst *i.e.* a

$CuSO_4$ solution was added to all microtiter wells, including the ones that contained the SPAAC-ligated carbohydrates. This was followed by an extensive washing procedure in an attempt to remove the residual copper. Within the margin of error, the compound that was connected to the surface *via* CuAAC and the SPAAC-ligated compound that both contain only the hydrophilic spacer again showed similar binding responses, although some changes were noted. On the other hand, for the EO-containing compound unprecedented high binding affinities were observed. This is undoubtedly a result from coordination of the residual copper to the EO spacer as was described previously by Kaczmarek *et al*.[10]

Interestingly, the observed binding affinities are thus influenced by copper and, specifically in the case of the EO-containing BCN compound, the presence of copper boosts the ligand-protein interaction, at least in the case of CTB. The exact nature of this phenomenon and its physical manifestation, for example if the copper also enters the CTB binding pocket, is unclear at the moment. This raises the question whether copper coordination also occurs to the carbohydrate epitope. In **Chapter 6** we observed that some GBS-related Abs recognize wild type ganglioside GM1, but not the very similar synthetic analogue that is attached to a microtiter surface via CuAAC (or *vice versa*). It cannot be excluded that the copper is of negative influence here and prevents the epitope from reaching the Ab binding pocket, or that the carbohydrate conformation is altered, or its movement is restricted in such a way that the Abs do not recognize it anymore.

Further in Chapter 6, an evaluation is presented of synthetic ganglioside-based glycan fragments that were used as epitopes for the detection of GBS-associated Abs. GBS is an autoimmune disorder that results from molecular mimicry by complex glycans that are present on the bacterium *Campylobacter jejuni*.[11] Parts of ganglioside epitopes that reside on our cell surfaces can also be found in the glycans on the pathogen, and in case of an GBS-related autoimmune response the carbohydrate moieties that reside on the surface of the bacteria are targeted by anti-ganglioside Abs. These Abs in turn also target the structurally similar gangliosides that reside on human nerve cells.[11] As part of an ongoing investigation, we aimed to improve the understanding at a molecular level of the antibody-ganglioside specificity of GBS. A small library of nine compounds was assembled that include fragments of the ganglioside GM1 pentasaccharide or a synthetic analogue of it, the GM1os. All carbohydrates were equipped with a chemical handle *i.e.* azide-functionality, with which they could be covalently immobilized on bio-assay surfaces via CuAAC reactions.

Saturation transfer difference NMR (STD-NMR)[12] studies by Houliston *et al.* indicated that the major contributors to the GM1-Abs binding are the terminal Gal*β*1-3GalNAc*β* and Neu5Ac*α*2 epitopes,[13] which would suggest that either of these ganglioside fragments would by themselves also bind the Abs significantly. It became obvious from our study that the complexity of the Abs-ganglioside binding cannot always be mimicked in a one-to-one fashion by presenting these epitopes as smaller synthetic fragments to the Abs. Surprisingly, we discovered that some anti-ganglioside Abs bind to compounds displaying the simple monosaccharide galactose and disaccharide lactose. Especially sera that show cross-reactivity towards wild type galactocerebroside were shown to bind these two simple saccharides, which opens up a new line of future investigations.

Applying a relatively short oligo-EO spacer (12 atoms) on the microtiter plate surfaces as chemical blocking agent – next to the immobilized GM1os fragments – had a dramatic effect in a select number of GBS patient sera on the binding affinity of Abs towards the ganglioside fragments. In one case, the Abs-Gal binding response was even doubled in relation to when no chemical blocking step was performed. This indicates a positive effect of the increased surface polarity towards the Abs-fragment binding affinity. When there is no EO coating the carbohydrate epitope will be pulled close to the surface because of the hydrophobic nature of the undecane spacer. The EO coating can function as a supporting construction for the epitope that allows the epitope to rise further from the surface to increase the presentation of the epitope in the solution. This then contributes to an increase of the epitope's degrees of freedom, which also has a positive effect on Ab-ligand recognition. On the other hand, we have learned from the studies described in Chapter 5 that compounds bearing an EO spacer suffer from coordination by residual copper from CuAAC chemistry. This could mean that the EO-coated surface contained a higher concentration of residual copper than in the cases where no chemical blocking step was performed. This higher concentration of residual copper then possibly influences the Abs-carbohydrate recognition, and in this case also boosts the binding response.

The studies presented in this dissertation show that small tailor-made synthetic carbohydrate moieties have the potential to be used in detection methods for specific Abs. However, tuning is required to adjust their design to the binding pocket characteristics of the proteins. This involves changing (the polarity of) the spacers, adjusting the epitope, and creating suitable functionalized surfaces to perform inhibitory experiments. Also applying suitable coatings on the surface,

in the form of chemical blocking steps, may aid the ligand-protein binding. In additon, it is clear from these studies that copper influences measurements in biological assays, sometimes beneficial and sometimes detrimental. But the main issue remains that it *does* influence the system. Therefore, to avoid this, it can be concluded that ligation techniques that do not require metals are preferred. Finally, exploiting multivalent structures achieves binding affinities that are multiple orders of magnitude higher than employing monovalent equivalents.

It is clear that there are many tuneable parameters in functional glycomics, and optimizing them is one of the challenges for every glycoscientist. These studies show the power of custom design and synthesis of tailor-made glycan derivatives to support functional glycomics in order to gain knowledge on natural mechanisms. Based on the knowledge gained from these studies we formed a precedent to create novel pentavalent CTB inhibitors as medicinal drugs, dialysis methods, and biosensors that contain GM1-derived carbohydrates for pathogen and antibody detection.

8.2 Samenvatting

Voor de studies die in dit proefschrift worden besproken is *functional glycomics* gebruikt om meer kennis te ontwikkelen over diverse biologische processen op moleculair niveau. Het hoofddoel was om deze kennis toe te passen op sensoren en daarbij bij te dragen aan de ontwikkeling van de Unihealth biosensor.[1] Deze studies draaiden voornamelijk om het ontwerp en de synthese van antigenen, gemaakt van oligosachariden, die goede bindingseigenschappen vertonen met de cholera toxine B-eenheid (CTB) en de antilichamen (Abs) die gerelateerd zijn aan de neuropathologische aandoening Guillain-Barré syndrome (GBS). Als toevoeging daarop zijn de optimale condities bestudeerd om deze antigenen op sensoroppervlakten te immobiliseren. Om deze doelen te behalen was het essentieel om een groot scala aan disciplines te combineren waaronder: theoretische chemie, biologische experimenten (bioassays) en organische synthese.

In **Hoofdstukken 2 en 3** zijn de eerste voorbeelden beschreven van pentamere GM1 oligosacharide-bevattende CTB inhibitoren die gebaseerd zijn op twee typische, pentamere platformen. In de pathogenese van de ziekte cholera wordt CTB gebruikt voor celherkenning en celbinding. Deze cellen worden herkend door de aanwezigheid van een specifiek ligand, de complexe glycan koolhydraat ganglioside GM1. Er zijn diverse voorbeelden van synthetische materialen die

deze ligand in veelvoud bevatten.[2] Deze studies hebben uitgewezen dat het gebruik van multivalente materialen een effectieve strategie behelst voor de inhibitie van de pentamere receptor CTB en soortgelijke ziektemakers.[2] Echter heeft geen van deze synthetische materialen de fysieke eigenschap dat ze vijf GM1 pentasacchariden vertonen, overeenkomstig met de valentie van het toxine. In **Hoofdstuk 2** wordt de synthese beschreven van het pentamere GM1 oligosaccharide-bevattende corannuleen platform. De oligosacchariden werden gekoppeld aan het corannuleen platform met ethyleenoxides (EO) van drie verschillende lengten, drie, zes of negen EO-eenheden lang. Naast dat ze goede, nanomolaire, bindingsaffiniteit vertoonden als inhibitoren van CTB, bewijzen deze structuren ook dat de lengte er *toch* toe doet. Het is namelijk zo dat niet het materiaal met de langste “armen” maar het molecuul met de intermediaire lengte de beste inhibitiepotentie vertoonde. Uit de studie die in **Hoofdstuk 3** wordt gepresenteerd kon worden geconcludeerd dat ook de vorm van het platform belangrijk is voor de bindingsaffiniteit met CTB. Een calix[5] areen platform werd voorzien van vijf ganglioside GM1 oligosacharide. Waar de corannuleen een komachtige vorm heeft, is dit platform meer bekervormig (Figuur 1). Hierdoor zijn bij laatstgenoemde de koolhydraten meer gericht in één richting daar komt ook bij dat de onderste rand van de calix[5]areen is voorzien van methoxidegroepen waardoor conformationele mobiliteit van het molecuul behouden blijft. De GM1os-calix[5]areen vertoonde een betere inhibitiepotentie bij de biologische testen met CTB dan de corannulenen. Met een IC_{50} van 450 pM werd een honderdduizend maal betere inhibitiepotentie vastgesteld ten opzicht van het monovalente controlemateriaal. Wanneer het calix[5]areen-platform werd voorzien van GM2 oligosacharide (waarbij de galactose-eenheid van de GM1os-terminus is weggelaten) liet de inhibitiepotentie een significant verschil zien en verslechterde de half maximale inhibitieconcentratie drastisch naar IC_{50} = 9 μM.

Strain-promoted azide-alkyne cycloaddition (SPAAC) reacties worden met enige voorkeur in toenemende mate gebruikt als ligatiereactie in biologische experimenten. Omdat dit soort reacties met deze toepassingen steeds belangrijker worden, worden er steeds weer nieuwe cyclooctynen ontwikkeld. Synthese van de nieuwe structuren kan gericht zijn op het verbeteren van specifieke karaktereigenschappen van bestaande moleculen zoals het verbeteren van wateroplosbaarheid dat kan worden bewerkstelligd door het toevoegen van hydrofiele eenheden aan het molecuul. Echter is het gebleken dat andere intrinsieke eigenschappen van deze moleculen zich lastig laten voorspellen en

zijn niet zo eenvoudig te bepalen, zoals de mate van reactiviteit van cyclooctynen met azides. **Hoofdstuk 4** beschrijft een theoretische verkenning van de reactiviteit van cyclooctynen met allyl- en benzylazide in SPAAC reacties. Dit werd berekend met drie verschillende typen theoretische methoden (B3LYP[4], M06-2X[5] en SCS-MP2[6]). Terwijl de methoden van het DFT-type, B3LYP en M06-2X, geen goede correlatie lieten zien voor een uitgebreide set van experimenteel bepaalde reactiekinetiek met berekende parameters, gaven SCS-MP2-berkeningen daarentegen een heldere voorspelling. Hieruit kwam een goede correlatie voort met op MP2-gebasseerde LUMO energieën van de cyclooctynen – in de geometrie die de alkynen hebben in de overgangstoestand (TS, Figuur 2) – en hun empirische reactiekinetiek. In tegenstelling tot wat in de literatuur[7] wordt beweerd hebben we geen relatie kunnen ontdekken tussen empirische data en energieën die het alkyn nodig heeft om te vervormen (*distortion energy*) om de overgangstoestand te bereieken. Verder zijn deze resultaten gebruikt om een methode te ontwikkelen waarmee het mogelijk is om de reactiekinetiek van een cyclooctyn in een SPAAC-reactie te bepalen alvorens het stofje daadwerkelijk is gesynthetiseerd. Voor een iets mindere accurate maar veel simpelere voorspellingsmethode kunnen ook LUMO-energieën gebruikt worden van het reactant waarvan de geometrie volledig is geoptimaliseerd met de MP2 methode (in plaats van de geometrie van de TS). Als de cyclooctyn TS LUMO-waarden gecorreleerd worden met de experimentele reactieconstanten, wordt een goede lineaire regressie weergegeven van $R^2 = 0.960$. Tevens onderstreept deze studie de theorie dat de SPAAC reacties gedreven worden door LUMO-energieën en dat Hartree-Fock LUMO-waarden inderdaad een goede maat zijn voor de reactiviteit van cyclooctynen met organische azides in SPAAC reacties.

De SPAAC reactie is in potentie een goede vervanger voor de copper azide-alkyne cyclooaddtion (CuAAC)[3,8] reactie in biologische testen. Een van de redenen is dat koper in potentie een negatieve invloed heeft op metingen die betrekking hebben op ligand-proteïne interacties. We hebben experimenten bedacht waarbij de invloed van koper op deze bindingen kon worden onderzocht. In **Hoofdstuk 5** combineren we daarom elementen die voorkomen in de voorgaande drie hoofdstukken door een directe vergelijking te trekken tussen CuAAC- en SPAAC-reacties in bindingsexperimenten. Reeds gesynthetiseerd GM1os materiaal[9] dat was voorzien van een alkynterminus werd geïmmobiliseerd op een microtiterplaat. Twee nieuwe materialen, die eveneens het GM1os bevatten, zijn zo gemodificeerd dat ze cyclooctynen bevatten. Één

daarvan met een verbindingsstuk tussen het koolhydraat en het cyclooctyn dat bestond uit een alifatisch, lipofiel undecaangedeelte en een tweede met hetzelfde verbindingsstuk en een additioneel hydrofiel EO-verbindingsstuk.

De eerste set van biologische experimenten werd verricht nadat de materialen waren geïmmobiliseerd op microtiterplaten d.m.v. CuAAC of SPAAC, afhankelijk van het alkyntype. Beide materialen zonder het EO-verbindingsstuk werden door de CTB proteïne in min of meer gelijke mate “herkend”, dus er is in dit geval een zekere mate van onafhankelijk van de gebruikte immobilisatietechniek vastgesteld. In tegenstelling daartoe werd voor de EO-bevattende stof een significant lagere bindingsaffiniteit vastgesteld t.o.v. CTB. Een tweede set experimenten werd verricht onder soortgelijke condities, echter werd er in deze set aan *alle* materialen koperkatalysator toegevoegd na de immobilisatiestap (in dezelfde kwantiteit als voor de standaard CuAAC-reactie), dus ook aan de cyclooctyne-bevattende materialen. Dit werd gevolgd door een uitgebreide wasprocedure in een poging om alle residuele koperdeeltjes te verwijderen. Binnen de foutenmarge lieten de beide materialen zonder het EO-verbindingsstuk wederom een soortgelijke bindingsaffiniteit zien, echter was het verschil dit maal wel aanzienlijk groter dan voor de eerste set. Voor het EO-bevattende materiaal werden buitensporig hogere waarden waargenomen dan voorheen. Het is onbetwistbaar dat dit het resultaat is van coördinatie van residueel koper met het EO-verbindingsstuk zoals eerder is beschreven in de literatuur door Kaczmarek *et al.*[10]

Interessant genoeg zijn de bindingsaffiniteiten dus beïnvloedbaar door de aanwezigheid van (kleine hoeveelheden) koper. Specifiek in het geval van het materiaal met het EO-verbindingsstuk, werkt het koper synergetisch op de ligand-proteïne-interactie. De exacte reden van dit fenomeen is onduidelijk. Het is bijvoorbeeld onduidelijk of de koper ook het bindingsdomein van CTB binnendringt en of de koper ook coördineert aan het koolhydraatgedeelte en daardoor de interactie van het koolhydraat met de proteïne beïnvloed. In de studie die is beschreven in **Hoofdstuk 6** is waargenomen dat sommige Abs, die zijn gerelateerd aan GBS, natuurlijke ganglioside GM1 herkennen maar niet het synthetische, structureel vrijwel identieke materiaal dat d.m.v. CuAAC reacties geïmmobiliseerd werd op microtiterplaten. Het kan niet worden uitgesloten dat koper een negatief effect heeft op deze experimenten en het de koolhydraten bemoeilijkt de bindingsdomeinen van de Abs te bereiken of dat de koolhydraatconformatie dusdanig wordt veranderd dat de Abs de koolhydraten niet meer herkennen. Verder wordt in Hoofdstuk 6 een evaluatie gepresenteerd van synthetische, op ganglioside-gebaseerde glycanfragmenten die

gebruikt zijn als liganden voor de detectie van Abs die geassocieerd worden met GBS. GBS is een auto-immuunziekte die het resultaat is van moleculaire nabootsing (*molecular mimicry*) van glycans die voorkomen op de celwand van o.a. de bacterie *Campylobacter jejuni*.[11] Gedeelten van structuren van gangliosiden die in het menselijke stelsel voorkomen op celwanden kunnen ook teruggevonden worden in deze glycans op de bacterie. In het geval van een auto-immuun respons (in GBS), worden er Abs gemaakt die deze glycans kunnen herkennen en de bacteriën markeren om te worden vernietigd. Echter worden in het menselijk zenuwstelsel hierdoor ook gezonde cellen gevlagd die soortgelijke glycanstructuren bevatten en eveneens vernietigd.[11] Als onderdeel van een doorlopend onderzoek naar deze ziekte pogen wij een beter begrip te vormen van de Abs-ganglioside specificiteit op het moleculaire niveau. Een kleine bibliotheek met negen verbindingen werd samengesteld en bevatte fragmenten van het ganglioside GM1 pentasacharide en een synthetische analoog daarvan. Alle koolhydraten werden voorzien van een chemisch handvat d.w.z. een azide-functionaliteit waarmee ze covalent geïmmobiliseerd konden worden op microtiterplaten d.m.v. CuAAC reacties.

Studies die waren gebasseerd op saturation transfer difference NMR (STD-NMR)[12] door Houliston *et al*.[13] gaven de indicatie dat de termini Gal*β*1-3GalNAc*β* en Neu5Ac*α*2 de koolhydraatstructuren zijn die het meest bijdragen aan de GM1-Abs-binding. Dit wekt de suggestie dat deze koolhydraten afzonderlijk van elkaar een significante bijdrage kunnen leveren aan de GM1-Abs-binding. Het werd echter al snel duidelijk in onze experimenten dat dit niet het geval is en dat de complexiteit van de bindingen niet altijd één-op-één kan worden nagebootst door (kleinere) synthetische fragmenten. Een verassende ontdekking was wel dat sommige anti-ganlgioside Abs zich binden aan de simpele galactoside monosacharide en lactoside disacharide. Dit zijn in het bijzonder de Abs die voorkomen in patientensera die tevens kruisreactiviteit vertonen met natuurlijke galactocerebroside. Deze ontdekking heeft een nieuwe richting voor toekomstige onderzoeken geopend.

Het toepassen van relatief korte oligo-EO-materialen, van 12 atomen lang, op een microtiterplaat – om te voorkomen dat serumcomponenten ongewild adheren aan het oppervlakte – had een dramatisch effect op een select groepje GBS patiëntensera op de Abs-ligand-binding. In een enkel geval verdubbelde de bindingsrespons t.o.v. experimenten waarin deze vorm van chemisch blokken niet werd toegepast. Dit duidde op een positief effect van de verhoogde polariteit van het oppervlakte. Bij afwezigheid van de hydrofiele EO-modificatie bevindt het ligand zich wellicht dichter op het oppervlakte. Door het hydrofobische karakter

van het undecaan verbindingsstuk adheert het aan het eveneens hydrofobe oppervlakte. In het geval van de hydrofiele oppervlakte, kan het EO fungeren als een ondersteunende structuur die het mogelijk maakt voor het koolhydraat om zich verder in de oplossing van de biologische experimenten te bevinden. Dit draagt bij aan een toename van de vrijheidsgraden van het ligand en levert daarmee een positieve bijdrage aan de Abs-ligand-interactie. Het is uit de studie die is beschreven in Hoofdstuk 5 echter ook duidelijk geworden dat EO-materialen participeren aan kopercoördinatie en dat dit van invloed kan zijn op de uitkomst van een biologisch experiment. Het kan daarom zijn dat de residuele koper in het geval van een EO-oppervlakte in het experiment hoger is dan wanneer een hydrofoob oppervlakte wordt gebruikt. De hogere bindingsuitkomst zou dus het resultaat kunnen zijn van een hogere concentratie koperionen in het systeem.

De studies die in dit proefschrift zijn beschreven bewijzen dat kleine, op-maat-gemaakte synthetische moleculen de potentie hebben om gebruikt te worden als onderdeel van detectiemethoden voor specifieke Abs en toxines. Het blijft echter nodig om het ontwerp aan te passen en zo te modeleren naar de karakteristieke bindingseigenschappen van de te detecteren proteïnes. Dit houdt in dat de (polariteit van de) verbindingsmoleculen en de koolhydraatsamenstelling aangepast moeten worden en tevens geschikte, correct gefunctionaliseerde oppervlakten ter beschikking moeten zijn voor de inhibitie-experimenten. Het is ook duidelijk geworden dat het gebruik van koper van invloed is op de uitkomst van de experimenten, soms komt het ten goede aan de binding, soms niet. De meest belangrijke conclusie is dat koper het systeem beïnvloed en dat daarom beter naar alternatieven gezocht kan worden waarbij het gebruik van metalen overbodig is. Tot slot is in dit proefschrift ook multivalentie geëxploiteerd in materialen die vijf maal het GM1 ligand vertonen. Deze pentavalente structuren vertoonden een bindingaffiniteit die meerdere orden van grootte beter is dan wanneer de monovalente equivalenten werden toegepast in proteïne-ligand bindingstudies.

Het is duidelijk dat er veel aanpasbare parameters zijn in *functional glycomics* en dat het optimaliseren daarvan één van de uitdagingen is voor iedere glycochemicus. Deze studies laten zien wat de kracht is van handmatig ontwerp en synthese van glycanderivaten om de *functional glycomics* te gebruiken om een beter begrip te creëren van biologische mechanismen. De kennis opgedaan in deze studies scheppen precedent om nieuwe pentavalente CTB inhibitoren te creëren voor medicinaal gebruik, dialysemethoden of het gebruik in nieuwe biosensoren die synthetische GM1 derivaten bevatten voor pathogeen- en antilichaamdetectie.

8.3 References

[1] http://www.unihealth.info/index.php?id=94

[2] For references and more information on this topic see Chapter 1.

[3] a) J. A. Prescher, C. R. Bertozzi, *Nature Chem. Biol.* **2005**, *1*, 13-21; b) E. M. Sletten, C. R. Bertozzi, *Angew. Chem., Int. Ed. Engl.* **2009**, *48*, 6974-6998; c) C. R. Becer, R. Hoogenboom, U. S. Schubert, *Angew. Chem., Int. Ed. Engl.* **2009**, *48*, 4900-4908; d) J. C. Jewett, C. R. Bertozzi, *Chem. Soc. Rev.* **2010**, *39*, 1272-1279; e) T. K. Tiefenbrunn, P. E. Dawson, *Biopolymers* **2010**, *94*, 95-106; f) B. S. Sumerlin, A. P. Vogt, *Macromolecules* **2010**, *43*, 1-13; g) M. F. Debets, C. W. J. van der Doelen, F. P. J. T. Rutjes, F. L. van Delft, *Chembiochem* **2010**, *11*, 1168-1184; h) J. M. Baskin, C. R. Bertozzi, *Aldrichimica Acta* **2010**, *43*, 15-23.

[4] C. Lee, W. Yang, R. G. Parr, *Phys. Rev. B* **1988**, *37*, 785.

[5] Y. Zhao, D. G. Truhlar, *Accounts Chem. Res.* **2008**, *41*, 157.

[6] a) C. Møller, M. S. Plesset, *Phys. Rev.* **1934**, *46*, 618; b) S. J. Grimme, *Chem. Phys.* **2003**, *118*, 9095.

[7] D. H. Ess, G. O. Jones, K. N. Houk, *Org. Lett.* **2008**, *10*, 1633-1636.

[8] a) R. Huisgen, *Angew. Chem., Int. Ed. Engl.* **1963**, *2*, 565-598; b) C. W. Tornøe, C. Christensen, M. Meldal, *Journal of Organic Chemistry* **2002**, *67*, 3057; c) V. V. Rostovtsev, L. G. Green, V. V. Fokin, K. B. Sharpless, *Angew. Chem., Int. Ed. Engl.* **2002**, *41*, 2596-2599; d) H. Kolb, C., M. G. Finn, K. B. Sharpless, *Angew. Chem., Int. Ed. Engl.* **2001**, *40*, 2004-2021.

[9] A. V. Pukin, C. A. G. M. Weijers, B. v. Lagen, R. Wechselberger, B. Sun, M. Gilbert, M.-F. Karwaski, D. E. A. Florack, B. C. Jacobs, A. P. Tio-Gillen, A. v. Belkum, H. P. Endtz, G.M. Visser, H. Zuilhof, *Carboh. Res.* **2008**, *343*, 636-650.

[10] H. Kaczmarek, *J. Photochem. Photobiol. A* **1996**, *95*, 61-65.

[11] C. W. Ang, B. C. Jacobs, J. D. Laman, *Trends in Immunol.* **2004**, *25*, 61-66.

[12] M. Mayer, B. Meyer, *J. Am. Chem. Soc.* **2001**, *123* 6108–6117.

[13] R. S. Houliston, B. C. Jacobs, A. P. Tio-Gillen, J. J. Verschuuren, N. H. Khieu, M. Gilbert, H. C. Jarrell, *Biochemistry* **2009**, *48*, 220-222.

I

Appendix I

Chapter 2: Nanomolar cholera toxin inhibitors based on symmetrical pentavalent ganglioside GM1os-*sym*-corannulenes

This Chapter is published as supporting information to:

M. Mattarella,‡ J. Garcia-Hartjes,‡ T. Wennekes, H. Zuilhof, J. S. Siegel, *Org. Biomol. Chem.* **2013**, *11*, 4333-4339, DOI: 10.1039/c3ob40438b

‡Both authors contributed equally to this work.

I.1 General notes

Microwave reactions were carried out in a dedicated CEM Discovery microwave oven. The microwave power was limited by temperature control once the desired temperature was reached. All reagents and solvents were reagent grade and were used without further purification unless otherwise specified. Flash chromatographic purification was performed using silica gel Merck 60 (particle size 0.040 - 0.063 mm); the eluting solvent for each purification was determined by thin layer chromatography (TLC). Size exclusion chromatographic purifications were performed using Sephadex® G-15 and Sephadex® G-25. Analytical thin-layer chromatography was performed using Merck TLC silica gel 60 F254. Solvents for chromatography were technical grade and freshly distilled before use. ^{1}H NMR spectra were recorded on a Bruker AV2-500 (500 MHz) or Bruker AV2-600 (600 MHz) spectrometers. Solvent for NMR spectroscopy were purchased from ARMAR chemicals, degassed with nitrogen and dried over molecular sieves. Chemical shifts are reported in parts per million (ppm) relative to the solvent residual peak: $CDCl_3$ = 7.26 ppm, MeOD = 3.31 ppm, D_2O = 4.79 ppm. Multiplicities are given as: s (singlet), br (broad), d (doublet), t (triplet), q (quadruplet), m (multiplet). ^{1}H-decoupled ^{13}C NMR spectra were obtained on Bruker AV2-500 (125 MHz) or Bruker AV2-600 (150 MHz) spectrometer. ^{13}C NMR chemical shifts are reported relative to the solvent residual peak: $CDCl_3$ = 77.2 ppm, d^4-MeOD = 49.00 ppm. HR-ESI-MS: Finnigan Mat 900 MS. Materials for the ELLA experiments *i.e.* bovine serum albumin (BSA), bovine brain GM1, *ortho*-phenylenediamine (dihydrochloride salt) (OPD), cholera toxin horse-radisch peroxide (CTB-HRP) conjugate, Tween-20, 30% H_2O_2 solution, sodium citrate, and citric acid were purchased at Sigma Aldrich and used without further modification, phosphate-buffered saline (PBS) 10x concentrate was diluted ten times with demi water prior to use. Nunc F96 Maxisorp™ 96-wells microtiter plates were used as purchased at thermo scientific. The microtiter plates were washed using an automated Denville® 2 Microplate Washer. Optical density (OD) was measured between 1.5 and 0.5 units on a Thermo Labsystems Multiskan Spectrum Reader running on Skanit software version 2.4.2. Compounds **s1**, **s2**, and **s3** were synthesized according to literature.[S1]

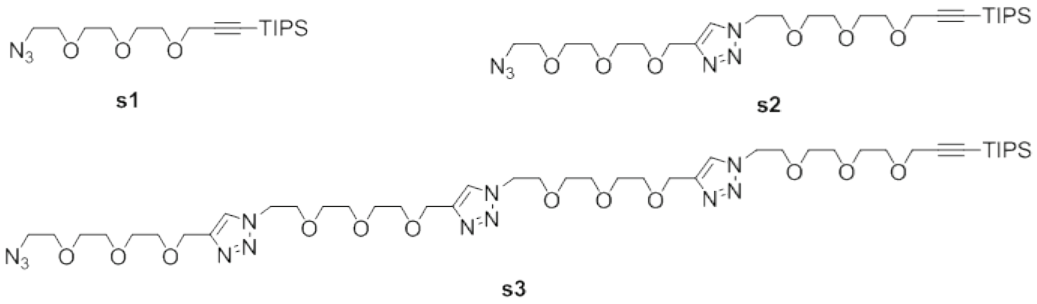

Figure S1. Compounds **s1**, **s2**, and **s3** were prepared according to literature procedure.

I.2 Synthetic details

Compound 5. A mixture of **3** (15 mg, 29 µmol), **s1** (67 mg, 0.18 mmol) and copper nanoparticles (12 mg, 0.19 mmol) in DMF (1.5 mL) was loaded in a microwave vessel was heated at 60 °C in a microwave reactor for 2 h. The mixture was filtrated over Celite® and the solvent evaporated. The crude was purified by column chromatography on silica gel (DCM/ MeOH 95 : 5) to yield a reddish oil (58 mg, 83%); **^{1}H NMR** (500 MHz, $CDCl_3$): δ = 7.64 (s, 5H), 7.52 (s, 5H), 4.49 (t, 10H, *J* = 5.5 Hz), 4.18 (s, 10H), 3.82 (t, 10H, *J* = 5.5 Hz), 3.66 - 3.45 (m, 50H), 3.26 (t, 10H, *J* =8.0 Hz), 1.02 (s, 105H); **^{13}C NMR** (125 MHz, $CDCl_3$): δ = 147.1, 140.4, 134.9, 129.7, 123.0, 122.4, 103.2, 87.7, 70.5, 70.5, 70.4, 69.7, 68.7, 59.2, 50.2, 33.4, 28.5, 18.6, 11.2; **MS** (HR-ESI+) m/z = 1201.2173 $[M+2Na]^{2+}$, calcd. ($C_{130}H_{205}N_{15}Na_2O_{15}Si_5^{2+}$) = 1201.2185.

Compound 6. A mixture of **3** (9.4 mg, 18 µmol), **s2** (83 mg, 0.14 mmol) and copper nanoparticles (12 mg, 0.18 mmol) in DMF (1.0 mL) was loaded in a microwave vessel and was heated at 80 °C in a microwave reactor for 2 h. The reaction mixture was filtrated over Celite® and the solvent evaporated. The crude mixture was purified by column chromatography on silica gel (from DCM/ MeOH 94 : 6 to DCM/ MeOH 9 : 1) to yield a reddish oil (49 mg, 79%); **^{1}H NMR** (500 MHz, $CDCl_3$): δ = 7.69 (s, 5H), 7.64 (s, 5H), 7.53 (s, 5H), 4.62 (s, 10H), 4.48 (q, 20 H, *J* = 5.5 Hz), 4.21 (s, 10H), 3.82 (t, 20H, *J* = 5.0 Hz), 3.69 - 3.47 (m, 90H), 3.26 (t, 10H, *J*=8.0 Hz), 1.04 (s, 105H); **^{13}C NMR** (125 MHz, $CDCl_3$): δ = 147.1, 144.8, 140.4, 134.9, 129.7, 123.9, 123.1, 122.5, 103.2, 87.8, 70.6, 70.54 70.51, 70.47, 69.7, 69.6, 69.5, 68.7, 64.6, 59.3, 50.3, 50.3, 33.4, 28.5, 18.7, 11.2. **MS** (HR-ESI+) m/z = 1163.6590 $[M+3Na]^{3+}$, calcd. ($C_{175}H_{280}N_{30}Na_3O_{30}Si_5^{3+}$) = 1163.6609.

Compound 7. A mixture of **3** (20 mg, 38 µmol), **s3** (296 mg, 0.29 mmol) and copper nanoparticles (23.0 mg, 0.36 mmol) in DMF (2.0 mL) was loaded in a microwave vessel and was heated at 80 °C in a microwave reactor for 2 h. The reaction mixture was filtrated over Celite® and the solvent evaporated. The crude mixture was purified by column chromatography on silica gel (DCM:MeOH 9:1) to yield a reddish oil (147 mg, 70%); **^{1}H NMR** (500 MHz, $CDCl_3$): δ = 7.66 - 7.62 (m, 15H), 7.56 (s, 5H), 7.47 (s, 5H), 4.56 - 4.52 (m, 30H), 4.43 - 4.38 (m, 40H), 4.11 (s, 10H), 3.77 - 3.73 (m, 40H), 3.61 - 3.41 (m, 165H), 3.17 (bs, 10H), 0.96 (s, 105H). **^{13}C NMR** (125 MHz, $CDCl_3$): δ = 146.8, 144.5, 140.2, 134.6, 129.5, 123.7, 122.8, 122.2, 103.0, 87.5, 70.4, 70.34, 70.29, 70.2, 69.4, 69.3, 69.3, 68.5, 64.4, 64.4, 58.9, 50.07, 50.02, 50.00, 49.96, 49.9, 33.1, 28.2, 18.4, 10.9. MS (HR-ESI+) m/z = 794.3097 $[M+7H]^{7+}$, calcd. ($C_{265}H_{437}N_{60}O_{60}Si_5^{7+}$) = 794.3114.

Compound 8. A solution of TBAF in THF (1 M, 0.77 mL, 0.77 mmol) was added to a solution of **5** (55 mg, 23 µmol) in THF (0.33 mL) and the reaction mixture was stirred at rt for 2 h. The solution was then diluted with a saturated aqueous solution of NH_4Cl and extracted with ethyl acetate. The combined organic phases were dried over Na_2SO_4 and evaporated to yield the crude product. The crude was then heated at 75 °C under high vacuum for 18 h. The product was then purified by column chromatography on silica gel (DCM/ MeOH 95 : 5) to yield a reddish oil (15 mg, 40%); **^{1}H NMR** (500 MHz, $CDCl_3$): δ = 7.64 (s, 5H), 7.53 (s, 5H), 4.50 (t, 10H, *J* = 5.0 Hz), 4.13 (d, 10H, *J* = 2.0Hz), 3.82 (t, 10H, *J* = 5.0 Hz), 3.62 - 3.50 (m, 50H), 3.26 (t, 10H, *J* = 8.0 Hz), 2.40 (t, 5H, *J* = 2.0 Hz); **^{13}C NMR** (125 MHz, $CDCl_3$): δ = 147.1, 140.5, 134.9, 129.8, 123.1, 122.5, 79.7, 74.8, 70.6, 70.4, 69.7, 69.1, 58.5, 50.3, 33.4, 28.5. **MS** (HR-ESI) m/z = 526.2709 $[M+2H]^{2+}$, calcd. ($C_{85}H_{108}N_{15}O_{15}^{2+}$) 526.2711.

Compound 9. A solution of TBAF in THF (1 M, 1.0 mL, 1.0 mmol) was added to a solution of **6** (103 mg, 30 µmol) in THF (1.0 mL) and the reaction mixture was stirred at rt for 2 h. The solution was then diluted with a saturated aqueous solution of NH_4Cl and extracted with ethyl acetate. The collected organic phases were dried over Na_2SO_4 and evaporated to yield the crude product. The crude was then heated at 75 °C under high vacuum for 18 h. The product was then purified by column chromatography on silica gel (DCM/ MeOH 9 : 1) to yield a reddish oil (24 mg, 30%); **^{1}H NMR** (500 MHz, $CDCl_3$): δ = 7.70 (s, 5H), 7.64 (s, 5H), 7.53 (s, 5H), 4.62 (s, 10H), 4.50 - 4.46 (m, 20 H), 4.16 (d, 10H, *J* = 2.5 Hz), 3.82 (t, 20H, *J* = 5.0 Hz), 3.64 - 3.51 (m, 90H), 3.23 (t, 10H, *J* = 8.0 Hz), 2.44 (d, 5H, *J* = 2.5 Hz). **^{13}C-NMR** (125 MHz, $CDCl_3$): δ = 147.1, 144.8, 140.5, 134.9, 129.8, 124.0, 123.1,

122.5, 79.7, 74.9, 70.6, 70.6, 70.5, 69.7, 69.5, 69.1, 64.7, 58.5, 50.3, 50.2, 33.4, 28.5; **MS** (HR-ESI+) m/z = 529.2767 $[M+5H]^{5+}$, calcd. ($C_{130}H_{185}N_{30}O_{30}^{5+}$) 529.2769.

Compound 10. A solution of TBAF in THF (1M, 0.9 mL, 0.9 mmol) was added to a solution of **6** (143 mg, 25.7 µmol) in THF (1.0 mL) and the reaction mixture was stirred at rt for 2 h. The solution was then diluted with a saturated aqueous solution of NH_4Cl and extracted with ethyl acetate. The collected organic phases were dried over Na_2SO_4 and evaporated to yield the crude product. The crude was then heated at 75 °C under high vacuum for 18 h. The product was then purified by column chromatography on silica gel (DCM/ MeOH 9 : 1) to yield a reddish oil (81 mg, 66%); **^{1}H NMR** (500 MHz, $CDCl_3$): δ = 7.69 - 7.65 (m, 15H), 7.60 (s, 5H), 7.50 (s, 5H), 4.60 - 4.56 (m, 30H), 4.48 - 4.41 (m, 40H), 4.13 (d, 10H, *J* = 2.0 Hz), 3.81 - 3.80 (m, 40H), 3.62 - 3.52 (m, 165H), 3.18 (t br, 10H, *J* = 7.5 Hz), 2.41 (s, 5H); **^{13}C NMR** (125 MHz, $CDCl_3$): δ = 146.9, 144.7, 140.3, 134.8, 129.7, 123.8, 123.8, 122.9, 122.3, 79.6, 74.7, 70.47, 70.46, 70.44, 70.42, 70.35, 69.6, 69.41, 69.39, 69.0, 64.5, 58.4, 50.17, 50.16, 50.12, 50.07, 33.2, 28.4; **MS** (HR-ESI+) m/z = 1216.1057 $[M+4Na]^{4+}$, calcd. ($C_{220}H_{330}N_{60}Na_4O_{60}^{4+}$) 1216.1052.

Compound 13. A mixture of 2,3,4,6-tetra-*O*-acetyl-*α*-D-galactopyranosyl bromide (**11**, 1.6 g, 4.0 mmol), 2[-2-(2-{2-[2-(2-hydroxyethoxy)-ethoxy]-ethoxy}-ethoxy)-ethoxy]- ethyl azide (**12**, 1.7 g, 5.6 mmol) and molecular sieves in dry dichloromethane (35 mL) was stirred at rt for 50 min; $HgBr_2$ (1.43 g, 4.0 mmol) was added to the reaction and the mixture was stirred at r. t. for 3 days. The mixture was then filtrated and the solid washed with dichloromethane, methanol and THF. The filtrate was concentrated *in vacuo*. The product was purified by column chromatography on silica gel eluted with AcOEt/ Hexane 1 : 1. The solvent was evaporated to yield a yellow syrup (1.4 g, 55%). ^{1}H-NMR (500 MHz, $CDCl_3$): δ = 5.36 (d, 1H, *J* = 3.0 Hz), 5.17 (dd, 1H, *J* = 8.0, 10.0 Hz), 5.00 (dd, 1H, *J* = 3.5, 10.5 Hz), 4.55 (d, 1H 3.5), 4.16 - 4.10 (m, 2H), 3.97 - 3.89 (m, 2H) 3.76 - 3.62 (m, 23H), 3.39 (t, 2H, *J* = 5.0 Hz), 2.12 (s, 3H), 2.07 (s, 3H), 2.05 (s, 3H), 1.99 (s, 3H); **^{13}C NMR** (135 MHz, $CDCl_3$): δ = 170.6, 170.4, 170.3, 101.7, 71.1, 70.9, 70.8, 70.6, 70.5, 70.1, 69.3, 69.1, 67.3, 61.5, 50.9, 21.0, 20.9, 20.9, 20.8; **MS** (HR-ESI+) m/z = 660.2580 $[M+Na]^+$, calcd. ($C_{26}H_{43}N_3NaO_{15}^+$) = 660.2586.

Compound 14. A solution of sodium methoxide (3.0 g in 10 mL of methanol) was added to a solution of **13** (1.3 g, 2.1 mmol) in methanol (10 mL.) until pH 12 was reached. The reaction mixture was stirred at r. t. for 2 days. Dowex 50

was added to the reaction until pH 6 was reached; the mixture was then filtrated and the solvent evaporated. The crude was purified by chromatography (DCM/ MeOH 85 : 15). The product is a yellow syrup (560 mg, 58%), **^{1}H NMR** (500 MHz, D_2O): δ = 4.44 (d, 1H, *J* = 8.0 Hz), 4.12 - 4.08 (m, 1H), 3.94 (d, 1H, *J* = 3.5), 3.88 - 3.66 (m, 25H), 3.58 - 3.52 (m, 3H); **^{13}C NMR** (125 MHz, MeOD): δ = 104.3, 76.4, 74.1, 72.1, 71.0, 70.91, 70.87, 70.8, 70.5, 69.9, 69.7, 62.1, 51.4; **MS** (HR-ESI+) m/z = 492.2159 $[M+Na]^+$, calcd. ($C_{18}H_{35}N_3NaO_{11}^+$) = 492.2164.

Compound 15. A mixture of **3** (11 mg, 21.5 µmol), **14** (89 mg, 0.19 mmol) and copper nanoparticles (12 mg, 0.19 mmol) in DMF (1.0 mL) was loaded in a microwave vessel was heated at 80 °C in a microwave reactor for 2 h. The mixture was filtrated over Celite® and the solvent evaporated. The crude was purified by size exclusion chromatography (Sephadex® G-25, water) to yield a reddish solid (147 mg, 47%); **^{1}H NMR** (600 MHz, MeOD): δ = 7.83 (s, 5H), 7.71 (s, 5H), 4.54 (t br, 10H, *J* = 5.0 Hz), 4.26 (d, 5H, *J* = 5.0 Hz), 3.99 - 3.85 (m, 5H), 3.82 - 3.70 (m, 20H), 3.68 - 3.59 (m, 30H), 3.53 - 3.29 (m, 125H); **^{13}C NMR** (150 MHz, MeOD): δ = 148.1, 141.7, 135.8, 130.9, 124.7, 124.4, 104.9, 76.7, 74.9, 72.5, 71.4, 71.31, 71.27, 71.25, 71.24, 71.22, 70.4, 70.3, 69.5, 62.5, 51.3, 34.1, 29.1; **MS** (HR-ESI+) m/z = 737.0824 $[M+4Na]^{4+}$; calcd. ($C_{130}H_{205}N_{14}Na_4O_{55}^{4+}$) = 737.0819.

Compound 16. A mixture of **8** (4.5 mg, 2.9 µmol), **14** (11.3 mg, 24.1 µmol) and copper nanoparticles (1.5 mg, 24 µmol) in DMF (300 µL) was loaded in a microwave vessel and was heated at 80 °C in a microwave reactor for 2 h. The mixture was filtrated over Celite® and the solid was washed with water. The crude was lyophilized and purified by size exclusion chromatography (Sephadex® G-25, water) to yield a reddish solid (5.0 mg, 44%); **^{1}H NMR** (500 MHz, D_2O/ MeOD): δ = 7.81 (s, 5H), 7.57 (s, 5H), 7.52 (s, 5H), 4.41 - 397 (m, 40H), 3.85 (m, 5H), 3.71 - 2.99 (m, 220H); **^{13}C NMR** (125 MHz, D_2O/ MeOD): δ = 144.8, 141.3, 137.4, 126.1, 124.8, 124.4, 103.8, 76.1, 73.7, 71.7, 70.7, 70.5, 70.34, 70.26, 70.22, 70.18, 69.8, 69.7, 69.6, 69.5, 66.9, 64.0, 61.9, 50.9, 50.8; **MS** (HR-ESI+) m/z = 807.3734 $[M+5Na]^{5+}$; calcd. ($C_{175}H_{280}N_{30}Na_5O_{70}$) = 807.3747.

Compound 17. A mixture of **9** (8.5 mg, 3.2 µmol), **14** (11 mg, 24 µmol) and copper nanoparticles (1.5 mg, 24 µmol) in DMF (300 µL) was loaded in a microwave vessel was heated at 80 °C in a microwave reactor for 2 h. The mixture was filtrated over Celite® and the solid was washed with water. The crude was lyophilized and purified by size exclusion chromatography (Sephadex® G-25,

water) to yield a reddish solid (9 mg, 57%); **^{1}H NMR** (500 MHz, D_2O/ MeOD): δ = 8.01 (s, 5H), 7.88 (s, 5H), 7.68 (s, 5H), 7.60 (s, 5H), 4.58 - 4.39 (m, 50H), 4.08 - 4.06 (m, 5H), 3.98 - 3.12 (m, 255H); **^{13}C NMR** (125 MHz, D_2O/ MeOD): δ = 147.9, 144.8, 141.3, 134.8, 130.4, 126.3, 126.1, 124.8 124.2, 103.9, 76.1, 73.7, 71.7, 70.7, 70.6, 70.5, 70.42, 70.41, 70.35, 70.3, 70.2, 69.9, 69.8, 69.73, 69.65, 69.6, 69.5, 64.0, 61.9, 50.9, 50.8, 49.5, 34.0, 28.1; **MS** (HR-ESI+) m/z = 854.2378 $[M+6Na]^{6+}$, calcd. ($C_{220}H_{355}N_{45}Na_6O_{85}^{6+}$) = 854.2366.

Compound 18. A mixture of **10** (16 mg, 3.4 µmol), **14** (14 mg, 29 µmol) and copper nanoparticles (1.8 mg, 28 µmol) in DMF (300 µL) was loaded in a microwave vessel was heated at 80 °C in a microwave reactor for 2 h. The mixture was filtrated over Celite® and the solid was washed with water. The crude was lyophilized and purified by size exclusion chromatography (Sephadex® G-25, water) to yield a reddish solid (10 mg, 43%); **^{1}H NMR** (500 MHz, D_2O/ MeOD): δ = 8.07 (d, 5H, *J* = 5.0 Hz), 8.02 (d, 5H, *J* = 5.0 Hz), 7.98 (d, 5H, *J* = 5.0 Hz), 7.90 (d, 5H, *J*=5.0 Hz), 7.89 (d, 5H, *J* = 5.0 Hz), 7.63 (s, 5H), 4.69 - 4.39 (m, 90H), 4.08 (m, 5H), 3.96 - 3.16 (m, 345H); **^{13}C NMR** (125 MHz, D_2O/ MeOD): δ = 147.9, 145.0, 141.4, 134.8, 130.3, 126.2, 126.1, 126.0, 125.9, 124.6, 124.1, 103.8, 99.5, 76.0, 73.7, 71.7, 70.61, 70.58, 70.5, 70.4, 70.3, 70.3, 70.2, 69.9, 69.59, 69.57, 69.55, 69.5, 64.0, 61.9, 50.89, 50.87, 50.8, 50.7, 32.9, 28.1; **MS** (HR-ESI) m/z = 912.8149 $[M+8Na]^{8+}$, calcd. ($C_{310}H_{505}N_{75}Na_8O_{115}^{8+}$) = 912.8139.

Compound 20. A mixture of **8** (0.8 mg, 0.5 µmol), **19** (5.5 mg, 4.6 µmol) and copper nanoparticles (0.3 mg, 5.2 µmol) in water (150 µL) was loaded in a microwave vessel was heated at 80 °C in a microwave reactor for 2 h. The mixture was filtrated over Celite® and the solid was washed with water. The crude was lyophilized and purified by size exclusion chromatography (Sephadex® G-15, water) to yield a colorless solid (1.8 mg, 45%). ^{1}H-NMR (500 MHz, D_2O/ MeOD): δ = 7.86 - 7.70 (m, 15H), 4.55 (t, 25H, *J* = 10.0 Hz), 3.81 (d, 10H, *J* = 10.0 Hz), 3.76 (t, 5H, *J* = 5.0 Hz), 3.85 - 3.79 (m, 15H), 3.75 - 3.59 (m, 40H), 3.58 - 3.52 (m, 20H), 3.47 - 3.41 (m, 20H), 3.64 - 3.33 (m, 25H), 2.69 (d, 5H, *J* = 10.0 Hz), 1.98 (d, 15H, *J* = 15.0 Hz), 1.93 - 1.84 (m, 5H), 1.55 - 1.54 (m br, 5H), 1.47 - 1.37 (m br, 10H), 1.26 - 1.12 (m br, 20H), 1.07 - 0.83 (m br, 30H); **^{13}C NMR** insufficient material was acquired to record an ^{13}C NMR spectrum; **MS** (HR-ESI) m/z =1507.8678 $[M-5H]^{5-}$, calcd. ($C_{325}H_{515}N_{40}O_{160}^{5-}$) = 1507.6684.

Compound 21. A mixture of **9** (2.9 mg, 1.1 µmol), **19** (11 mg, 9.3 µmol) and copper

nanoparticles (0.8 mg, 12 µmol) in water (300 µL) was loaded in a microwave vessel was heated at 80 °C in a microwave reactor for 2 h. The mixture was filtrated over Celite® and the solid was washed with water. The crude was lyophilized and purified by size exclusion chromatography (Sephadex® G-25, water) to yield a colorless solid (4.8 mg, 51%); **^{1}H NMR** (500 MHz, D_2O/ MeOD): δ = 7.96 - 7.75 (m, 20H), 4.57 - 4.54 (m, 70H), 4.18 - 4.05 (m, 45H), 3.94 - 3.34 (m, 286H), 2.70 (d, 5H, *J* = 10.0 Hz), 2.06 (d, 35H, *J* = 15.0 Hz), 1.98 - 1.94 (t, 5H, *J*=10.0 Hz), 1.62 - 1.45 (m br, 25H), 1.28 - 1.25 (m br, 20H), 1.11 - 0.90 (m br, 75H); **^{13}C NMR** (125 MHz, D_2O/ MeOD): δ = 176.0, 175.1, 105.7, 103.6, 103.5, 103.2, 102.7, 75.8, 75.3, 73.5, 71.7, 70.7, 70.64, 70.62, 70.52, 70.50, 70.48, 70.47, 70.45, 69.59, 69.57, 61.9, 52.6, 52.1, 51.13, 51.11, 29.7, 26.6, 26.2, 23.6, 23.0; **MS** (HR-ESI-) m/z = 1721.1778 $[M-5H]^{5-}$, calcd. ($C_{370}H_{590}N_{55}O_{175}^{5-}$) = 1720.7797.

Compound 22. A mixture of **10** (4.8 mg, 1.0 µmol), **19** (8.4 mg, 7.0 µmol) and copper nanoparticles (0.5 mg, 8.0 µmol) in water (300 µL) was loaded in a microwave vessel was heated at 80 °C in a microwave reactor for 2 h. The mixture was filtrated over Celite® and the solid was washed with water. The crude was lyophilized and purified by size exclusion chromatography (Sephadex® G-25, water) to yield a colorless solid (6.2 mg, 58%); ^{1}H-NMR (500 MHz, D_2O/ MeOD): δ = 7.91 - 7.67 (m, 25H), 4.47 - 4.35 (m br, 75H), 4,07 (m 20H), 3.98 (t, 10H, *J* = 5.0 Hz), 3.88 - 3.15 (m, 280H), 2.60 (d, 5H, *J* = 10.0 Hz), 1.95 (d, 25H, *J* = 15.0 Hz), 1.85 (s, 40H), 1.55 (s br, 10H), 1.40 (s br, 10H), 1.07 - 0.91 (m br, 60H); **^{13}C NMR** (125 MHz, D_2O/ MeOD): δ = 176.0, 175.6, 175.1, 171.9, 144.9, 126.28, 126.25, 126.20, 126.17, 126.06, 126.05, 125.5, 105.7, 103.6, 103.5, 103.1, 102.7, 81.4, 79.7, 78.2, 75.8, 75.7, 75.5, 75.3, 75.04, 75.03, 74.07, 74.06, 73.77, 73.76, 73.7, 73.51, 73.47, 73.2, 71.7, 71.4, 71.0, 70.64, 70.62, 70.59, 70.49, 70.45, 69.91, 69.87, 69.7, 69.6, 69.0, 68.9, 64.09, 64.06, 63.8, 62.1, 61.9, 61.5, 52.6, 52.1, 51.1, 50.9, 50.8, 37.9, 30.4, 30.34, 30.33, 30.31, 30.0, 29.89, 29.86, 29.80, 29.79, 29.74, 29.72, 29.70, 29.68, 29.64, 29.62, 29.2, 26.60, 26.58, 26.18, 26.16, 24.2, 23.6, 23.0; **MS** (HR-ESI-) m/z = 2147.2039 $[M-5H]^{5-}$, calcd. ($C_{460}H_{740}N_{85}O_{205}^{5-}$) 2147.0024.

I.3 ELLA experiments

Each well of a 96-well microtiter plate was coated with a 100 µL native GM1 solution (1.3 µM in ethanol) after which the solvent was evaporated. Unattached GM1 was removed by washing with PBS (3 × 450 µL), the remaining free binding sites were blocked by incubation with 100 µL of a 1% (w/v) BSA solution in PBS for 30 min at 37 °C. Subsequently, the wells were washed with PBS (3 × 450 µL). In separate vials, a logarithmic serial dilution, starting from 2.0 mM, of 150 µL saccharide-corannulenes in 0.1% BSA, 0.05% Tween-20 in PBS, mixed with 150 µL of a 50 ng/mL CTB-HRP solution in the same buffer were incubated. This gave an initial inhibitor concentration of 1.0 mM. In the case of potent inhibitors, based on the logarithmic experiments, a more accurate, serial dilution of a factor two was performed around the expected IC_{50} values. The inhibitor-toxin mixtures were incubated at room temperature for 2 h and then transferred to the coated wells. After 30 min of incubation at room temperature, unbound CTB-HRP-corannulene complexes were removed from the wells by washing with 0.1% BSA, 0.05% Tween-20 in PBS (3 x 500 µL). 100 µL of a freshly prepared OPD solution (25 mg OPD·2HCl, 7.5 mL 0.1 M citric acid, 7.5 mL 0.1 M sodium citrate and 6 µL of a 30% H_2O_2 solution, pH was adjusted to 6.0 with NaOH) was added to each well and allowed to react with HRP in absence of light, at room temperature, for 15 min. The oxidation reaction was quenched by addition of 50 µL 1M H_2SO_4. Within 5 min, the adsorbance was measured at 490 nm.

I.4 ^{1}H-NMR, UV-vis and Emission Spectroscopy Investigation on the Aggregation of s4

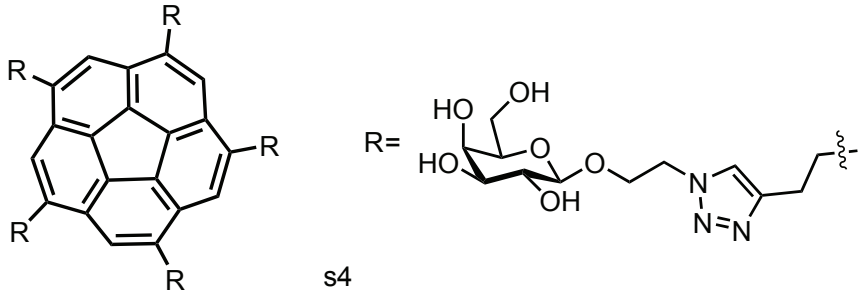

s4

Figure S2. C_5-symmetric galactose conjugated corannulene prepared according to literature procedure.[S2]

The thermodynamic behavior of the aggregation process of compound **S4** was studied by measuring the ^{1}H-NMR chemical shift of the five homotopic hydrogen atoms on the corannulene ring at different concentrations and temperatures (Figure S3).

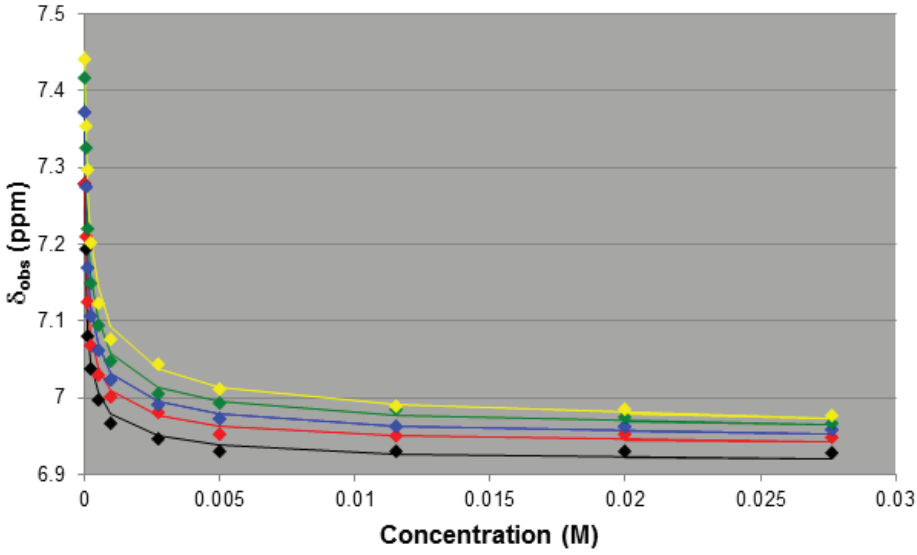

Figure S3. δ_{obs} vs. concentration of **s4**; experimental data and fitting curves at 300 K (black), 310 K(red), 320 K (blue), 330 K (green) and 340 K (yellow).

NMR samples were prepared over a range of concentrations and measured at different temperatures after 15 minutes equilibration. The association constants K_a (Table s1) were calculated based on an equal *K* model described by Martin[S3] (eq. s1), where δ_{obs} is the observed chemical shift, δ_{mon} is the chemical shift of monomer, K_a is the association constant, *c* is the molar concentration of the sample, and Δ is the difference in chemical shift between monomer and dimer. The chemical shifts *vs* concentration data were analyzed by nonlinear least-squared fitting using Prism 6.0 (GraphPad).

$$\delta_{obs} = \delta_{mon} - \Delta\left\{1 + \left[1 - \sqrt{(4K_a c + 1)}\right] / 2K_a c\right\} \quad \text{eq. S1}$$

Table S1. Association constant of **s4** in water at different temperatures.

T (K)	K_a (x10^5)
300	2 ± 1
310	0.5 ± 0.2
320	0.6 ± 0.2
330	0.3 ± 0.1
340	0.14 ± 0.03

The aggregation number *N, i.e.* the number of monomers included in the aggregate, was determined by eq. 2, where δ_{obs} is the observed chemical shift, δ_{mon} is the chemical shift of monomer, K_a is the association constant, *c* is the molar concentration of the sample and N is the aggregation number.

$$\ln\left[c\left(\delta_{mon}-\delta_{obs}\right)\right]=N\ln\left[c\left(\delta_{obs}-\delta_{agg}\right)\right]+\ln K_a+\ln N-\left(N-1\right)\ln\left(\delta_{mon}-\delta_{agg}\right) \quad \text{eq. S2}$$

The aggregation number was estimated to 2 assuming that compound **s4** is in equilibrium between the monomer and the aggregate. [S4] The thermodynamic parameters ΔH (-13 ± 1 kcal mol^{-1}) and ΔS (-18 ± 4 cal mol^{-1}) for the dimerization process were determined based on the van't Hoff plots revealing that the driving force for the aggregation of compound **s4** in solution is not the increasing of the entropy of the system, like for the most amphiphilic molecules, but the exothermicity of the process. UV-vis absorption spectra were recorder for a 10^{-4} M solution of compound **s4** at different temperature after 15 minutes equilibration (Figure s4). Emission spectra of solutions of compound **s4** at different concentration were measured at room temperature after excitation at 300 nm (Figure s5). The hypsochromic shift in the absorption spectra, upon increasing of the temperature, and the quenching of the fluorescence due to the increasing of the concentration of compound **s4** suggest the formation of H-dimers in solution.[S5]

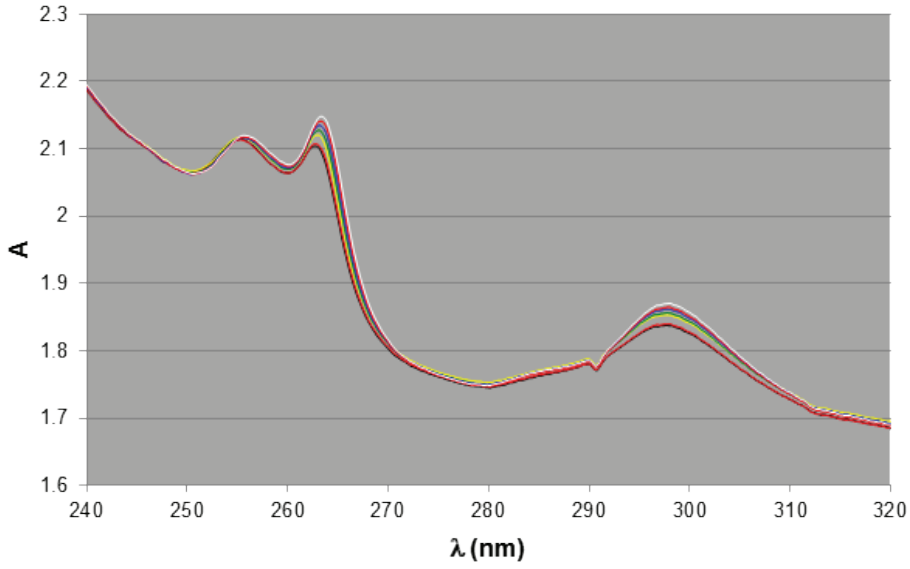

Figure S4. UV-vis spectra of a 10^{-4} M solution of compound **s4** at 280 K (black), 285 K (red), 290 K (yellow), 295 K (green), 305 K (blue), 315 K (violet), 325 K (white).

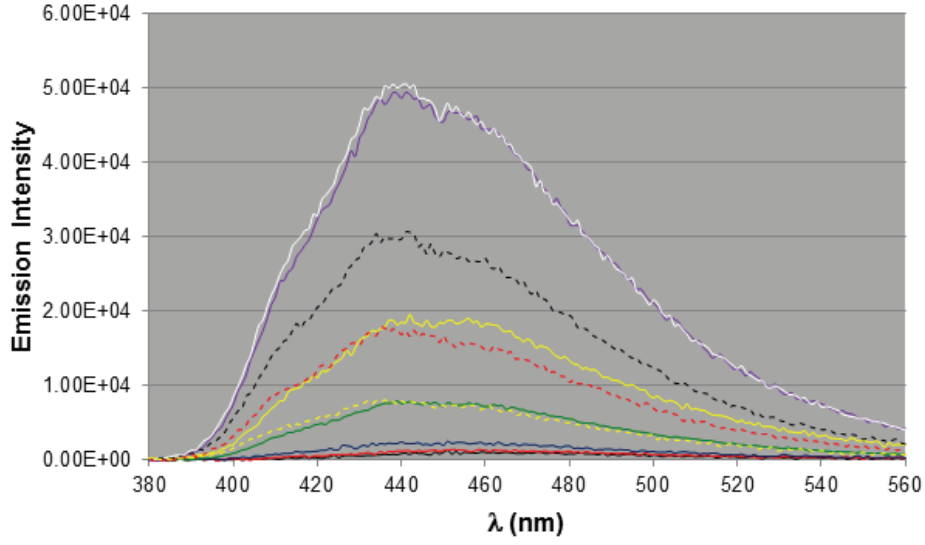

Figure S5. Emission spectra of compound **S4** at different concentrations: 2.63 $x10^{-3}$ M (black, solid line), 1.31 $x10^{-3}$ M (red, solid line), 6.57 $x10^{-4}$ M (blue, solid line), 2.42 $x10^{-4}$ M (green, solid line), 2.31 $x10^{-4}$ M (yellow, solid line), 1.64 $x10^{-4}$ M (violet, solid line), 8.22 $x10^{-5}$ M (white, solid line), 4.11 $x10^{-5}$ (black, dashed line), 2.05 $x10^{-5}$ (red, dashed line) and 1.03 $x10^{-5}$ M (yellow, dashed line).

I.5 References

S1. S. Binauld, C. J. Hawker, E. Fleury, E. Drockenmuller, *Angew. Chem. Int. Ed.,* 2009, **48**, 6654.
S2. M. Mattarella, J. S. Siegel, *Org. Biomol. Chem.* 2012, **10**, 5799.
S3. R. B. Martin, *Chem. Rev.* 1996, **96**, 3043.
S4. a) P. Taboada, D. Attwood, J. M. Ruso, M. Garcia, F. Sarmiento, V. Mosquera, *Langmuir* 2000, **10**, 3175. b) H. Sun, K. Ye, C. Wang, H. Qi, F. Li, T. Wang, *J. Phys. Chem. A* 2006, **110**, 10750.
S5. a) M. Wang, G. L. Silva, B. A. Armitage, *J. Am. Chem. Soc.* 2000, **122**, 9977. b) H. Yao, K. Domoto, T. Isohashi, K. Kimura, *Langmuir* 2005, **21**, 1067.

Appendix II

Chapter 4: Electronic Effects versus Distortion Energies During Strain-Promoted Alkyne-Azide Cycloadditions:

A Theoretical Tool to Predict Reaction Kinetics

This Chapter is published as supporting information to:

J. Garcia-Hartjes, J. Dommerholt, T. Wennekes, F. L. Van Delft, H. Zuilhof, *Eur. J. Org. Chem.* **2013**, 3712-3720. DOI: 10.1002/ejoc.201201627

II.1 General Methods

Reagents. Unless otherwise stated, reactions were carried out in a small glass tube at room temperature, no special conditions/atmosphere were needed. Chemicals were purchased from Sigma-Aldrich and used without further purification. Solvents CH_2Cl_2, acetonitrile, THF, Et_2O and toluene were obtained dry from a MBRAUN SPS-800 solvent purification system. Analytical thin layer chromatography (TLC) was performed on silica gel-coated plates (Merck 60 F254) with the indicated solvent mixture; visualization was done using ultraviolet (UV) irradiation (λ = 260 nm) and/or staining with $KMnO_4$.

Analytical Methods. New compounds were characterized by ^1H NMR and ^{13}C NMR (where applicable), IR spectroscopy and HRMS. ^1H NMR spectra were recorded on a Varian Inova 400 (400 MHz), ^{13}C NMR spectra were recorded on a Bruker DMX300 (75 MHz) spectrometer. Infrared spectra were recorded on an ATI Mattson Genesis Series FTIR spectrometer. High resolution mass analyses were performed using Electrospray Ionization on a JEOL AccuTOF. All ^1H NMR spectra are reported in parts per million (ppm) downfield of TMS and were measured relative to the signals for $CHCl_3$ (7.27 ppm). All ^{13}C NMR spectra were reported in ppm relative to residual $CHCl_3$ (77.2 ppm) and were obtained with ^1H decoupling. The pure compounds are estimated to be > 95% pure as determined by ^1H NMR.

II.2 Synthesis

Synthesis of allyl azide. To a solution of NaN_3 (11 g, 173 mmol) in DMSO (150 ml) was added dropwise allyl bromide (7.5 ml, 87 mmol). After stirring for 16 h at room temperature the mixture was poured in an ice/water mixture (150 ml). The layers were separated; allyl azide was washed with water (2 × 10 mL), and dried (Na_2SO_4).*

* There are some dangers that are associated with low molecular weight azides, as well with the synthesis of some organic azides. These include explosion hazard. This is particularly true in instances where elevated temperatures are required for azide formation.

Synthesis of cyclooctyne. To a solution of cyclooctene (33 ml, 0.25 mol) in CH_2Cl_2 (100 ml) was added dropwise at −40 °C a solution of Br_2 (13 mL, 0.25 mol) in CH_2Cl_2 (12 ml) until the yellow color persisted. The reaction mixture was quenched with a 10% $Na_2S_2O_3$ solution (50 ml), and

extracted with CH_2Cl_2 (2 × 100 ml). The organic layer was dried (Na_2SO_4) and concentrated *in vacuo* to afford *trans*-1,2-dibromocyclooctane (66 g, 97%).

Without further purification the dibromide (66 g, 244 mmol) was dissolved in THF (100 ml). A solution of KO*t*Bu (41 g, 370 mmol) in THF (40 mL) was added dropwise at 0 °C. The reaction mixture was quenched with a saturated NH_4Cl solution (100 ml), the THF was evaporated and the remaining water layer was extracted with CH_2Cl_2 (2 × 100 ml). The organic layer was dried (Na_2SO_4) and concentrated *in vacuo*. The residue was purified by distillation (bp: 73 - 80 °C/ 10 mbar) yielding 1-bromocyclooctene (37 g, 80%) as a colorless liquid.

To a solution of *i*Pr_2NH (11.5 mL, 81 mmol) in THF (30 ml) was added dropwise at −25 °C *n*-BuLi (51 ml, 81 mmol, 1.6 M in hexane). 1-Bromocyclooctene (15 g, 81 mmol) was added at once to this solution. The temperature of the reaction mixture was allowed to rise gradually over a period of 45 min to 15 °C and was kept at this level for another 90 min. The mixture was then quenched with a 3 M HCl-solution (30 ml) and extracted with pentane (5 × 20 ml). The combined extracts were washed with water (3 × 20 ml) to remove the THF, dried (Na_2SO_4) and concentrated *in vacuo* carefully. The residue was purified by distillation (bp: 55 - 63 °C/ 30 mbar) giving cyclooctyne (4.8 g, 54%) as a clear liquid.

II.3 Determination of rate constants of cyclooctyne with benzyl azide

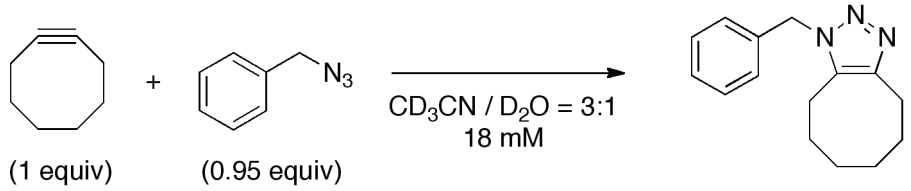

Scheme S1. ^{1}H NMR rate constant determination with benzyl azide.

^{1}H NMR monitoring of cycloaddition of OCT with BnN_3 was performed by rapid mixing (t = 0) of stock solutions of **A** and **B** (0.3 mL each) in an NMR tube and immediate insertion into a 400 MHz NMR spectrometer. NMR spectra were measured at preset intervals. The experiment was performed in duplo. Stock solution A: **1** was dissolved in a mixture of CD_3CN and D_2O (ratio 3 : 1, 10 ml) to give a 36 mM solution. Stock solution B: Benzyl azide was dissolved in a mixture of CD_3CN and D_2O (ratio 3 : 1, 10 mL) to give a 54 mM solution.

Kinetics of the reaction of **1** with benzyl azide was determined by measuring the decrease of the integral of the signal caused by benzyl azide methylene protons, with the integral of the CD_3CN solvent-peak as internal standard. Due to the fact that cycloaddition had already proceeded significantly by the time of the first measurement, a starting value for the integral of benzyl azide methylene signals was estimated based on the average of the summation of signals of benzyl azide and triazole product.

From the conversion plots thus obtained, the second order rate plots were calculated according to equation:

$$kt = \frac{1}{[B]_0 - [A]_0} \times \ln \frac{[A]_0([B]_0 - [P])}{([A]_0 - [P])[B]_0} \quad \text{eq. s1}$$

with k = 2nd order rate constant ($M^{-1} \cdot s^{-1}$), t = reaction time (s), $[A]_0$ = the initial concentration of substrate A (mmol/ml), $[B]_0$ = the initial concentration of substrate B (mmol/ml) and $[P]$ = the concentration of product (mmol/ml). Calculated rate constants were averaged, giving a k = 0.0058 $M^{-1}s^{-1}$ for cycloaddition of benzyl azide and **1**.

Exp.	Based on disappearance of BnN_3	Based on formation of triazole
I	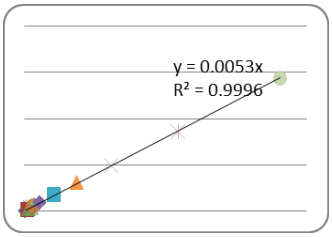	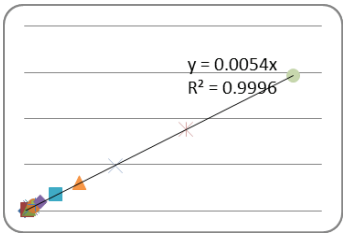
II	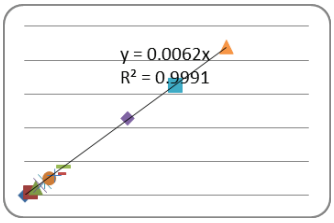	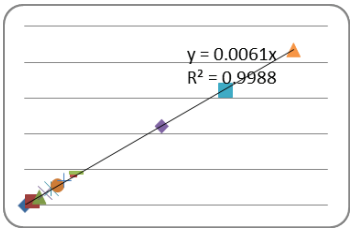

Figure S1. Rate plots used for the determination of rate constants of cyclooctyne with benzyl azide.

II.4 Competition experiments of 1 and 3 with benzyl azide and allyl azide

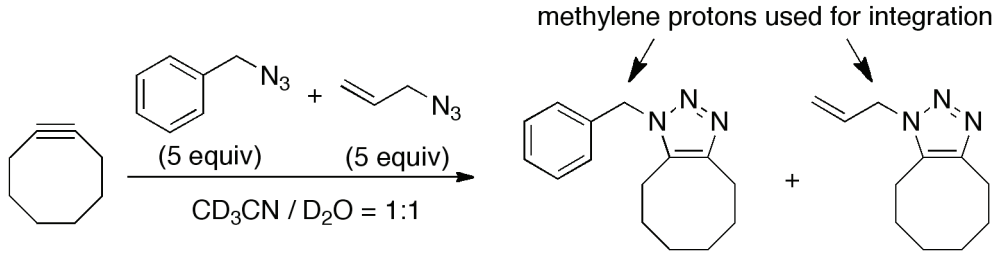

Scheme S2. Competition experiments of OCT with benzyl azide and allyl azide.

Cyclooctyne (OCT, compound **1**): Allyl azide (23 µL, 0.25 mmol, 5.0 equiv.) and benzyl azide (33 µL, 0.25 mmol, 5.0 equiv.) were dissolved in CD_3CN/ D_2O (1 : 1, 10 ml). The 1 : 1 ratio of allyl azide and benzyl azide was corroborated by ^1H NMR, before addition of cyclooctyne (6.2 µL, 0.05 mmol, 1.0 equiv.). The mixture was stirred at room temperature for 16 h, then solvents and excess allyl azide and benzyl azide were removed in vacuo. The residue was redissolved in $CDCl_3$ and ^1H NMR analysis was used to determine the ratio of allyl- and benzyltriazole adduct.

Bicyclononyne (BCN, compound **3**): Allyl azide (23 µL, 0.25 mmol, 5.0 equiv.) and benzyl azide (33 µL, 0.25 mmol, 5.0 equiv.) were dissolved in CD_3CN/ D_2O (1 : 1, 10 ml). The 1:1 ratio between allyl azide and benzyl azide was corroborated by ^1H NMR, before addition of *endo*-BCN (7.5 mg, 50 µmol, 1 equiv.). The mixture was stirred at room temperature for 16 h, then solvents and excess allyl azide and benzyl azide were removed *in vacuo*. The residue was redissolved in $CDCl_3$ and ^1H NMR analysis was used to determine the ratio of allyl- and benzyltriazole adduct.

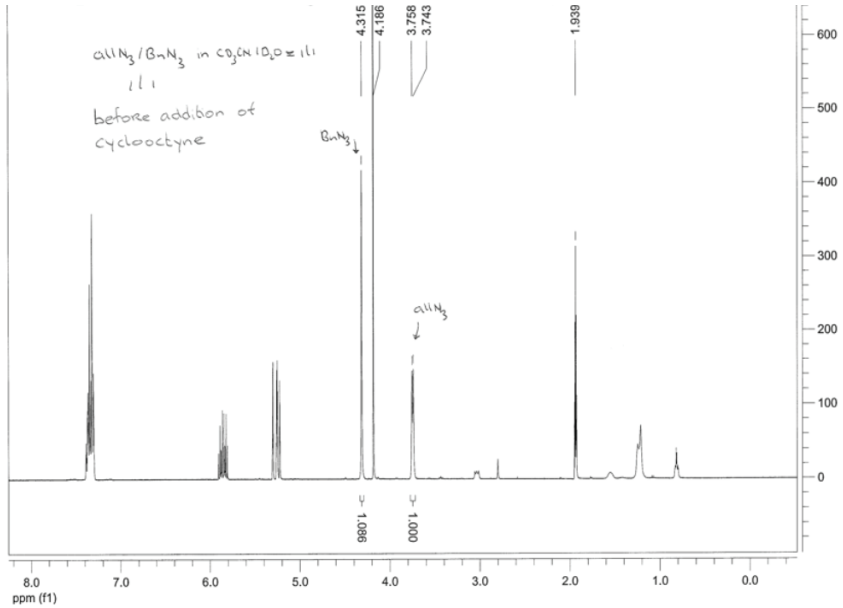

Figure S2. ^{1}H NMR spectrum of BnN_3 and $allylN_3$ in CD_3CN/D_2O before addition of **1**.

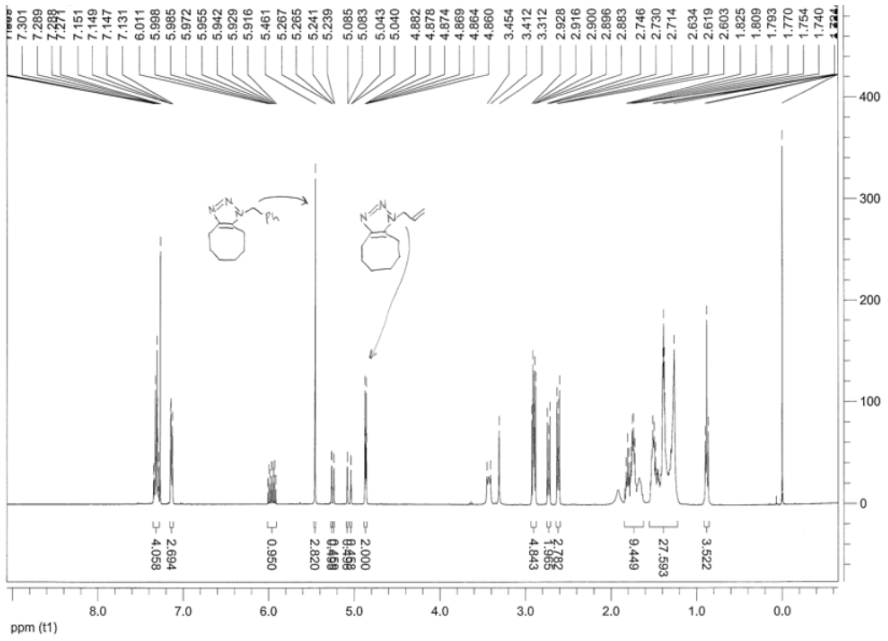

Figure S3. ^{1}H NMR spectrum of mixture of triazole products from OCT in $CDCl_3$.

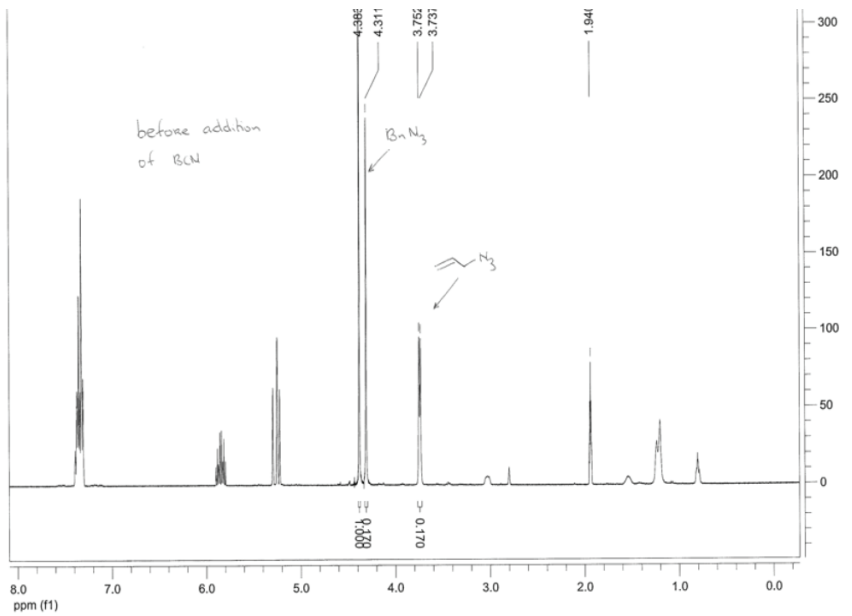

Figure S4. ^{1}H NMR spectrum of BnN_3 and $allylN_3$ in CD_3CN/D_2O before addition of compound **3**.

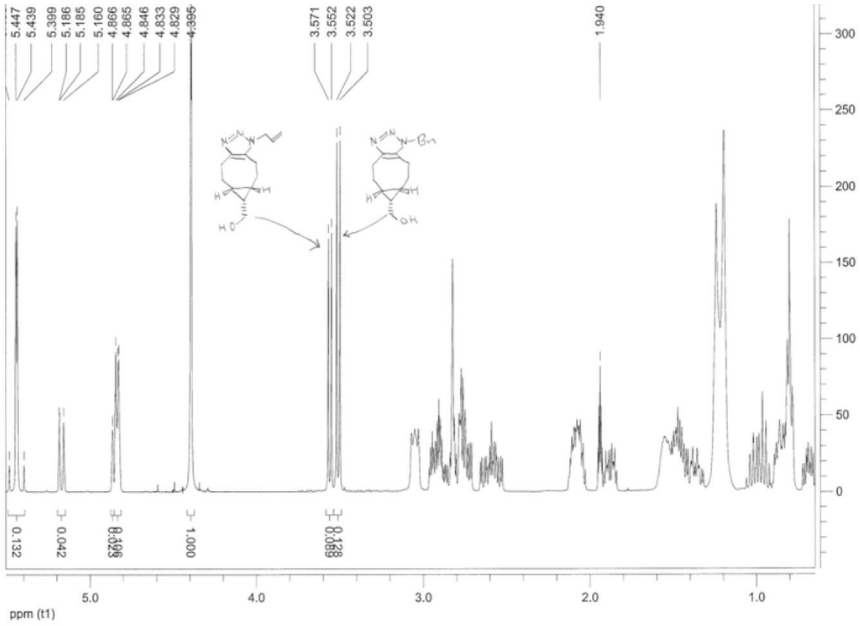

Figure S5. ^{1}H NMR spectrum of mixture of triazole products from BCN in $CDCl_3$.

II.5 Activation energies vs. calculable parameters

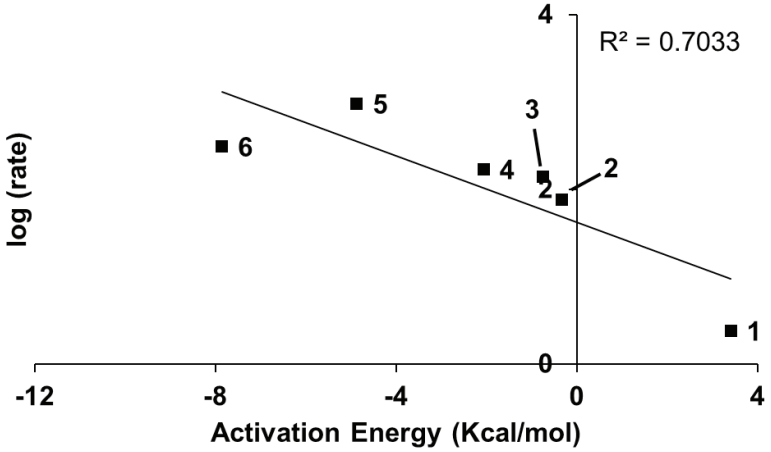

Figure S6. MP2 activation energy (kcal/mol) of the TS in the gas phase of cyclooctynes **1** - **6** with allyl azide versus the logarithm of the experimental rate.

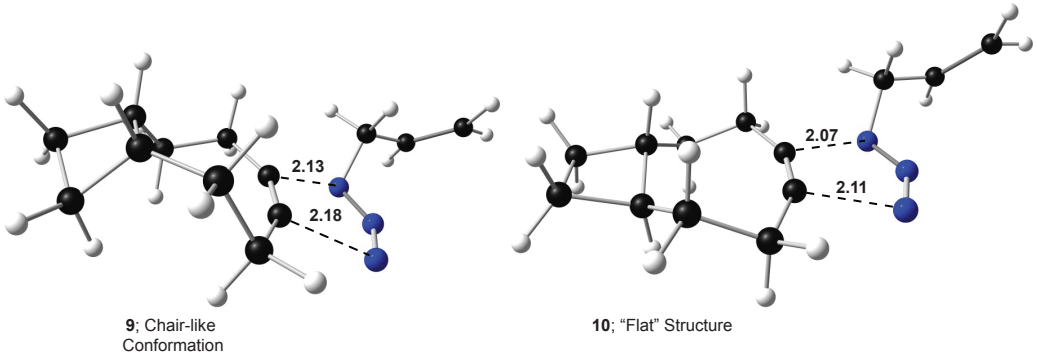

9; Chair-like Conformation

10; "Flat" Structure

Figure S7. Transition state conformations of (left) *cis*-cyclobutyl-substituted cyclooctyne, compound **9** and (right) *trans*-cyclobutyl-substituted compound **10** with allyl azide.

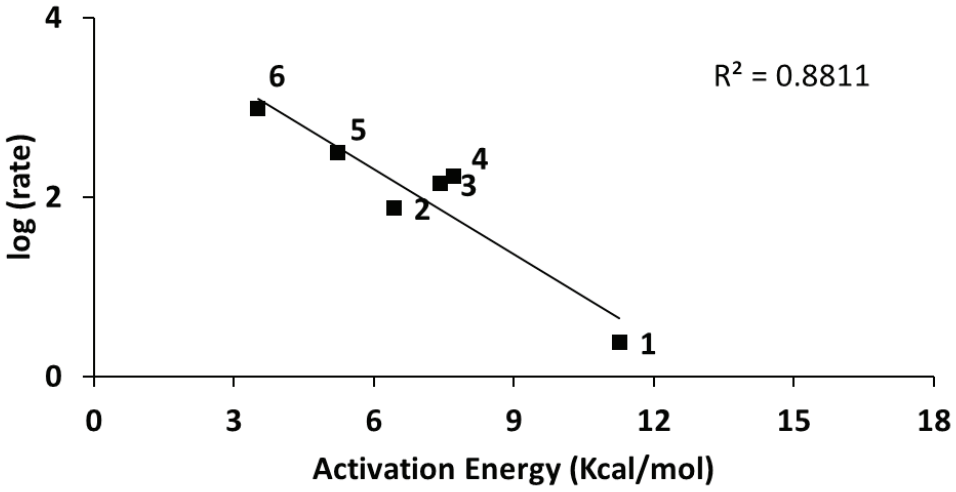

Figure S8. SCS-MP2 activation energy (kcal/mol) of the TS in MeOH of cyccloctynes **1** - **6** with allylazide versus the logarithm of the experimental rate.

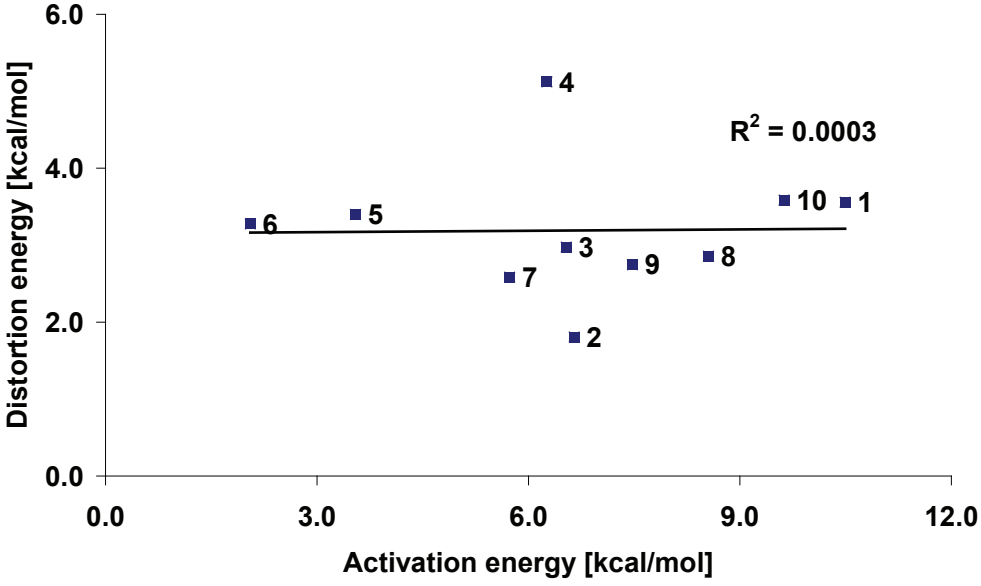

Figure S9. SCS-MP2 activation energies (kcal/mol) versus SCS-MP2 cyclooctyne distortion energies (kcal/mol).

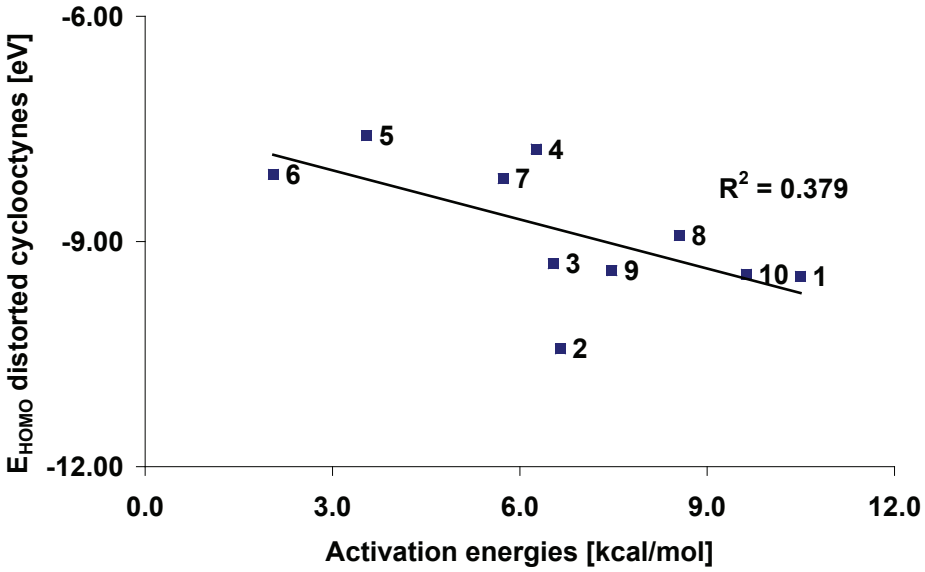

Figure S10. SCS-MP2 activation energies (kcal/mol) versus HOMO energy (eV) values of the distorted cyclooctynes **1** – **10** acquired from MP2 calculations.

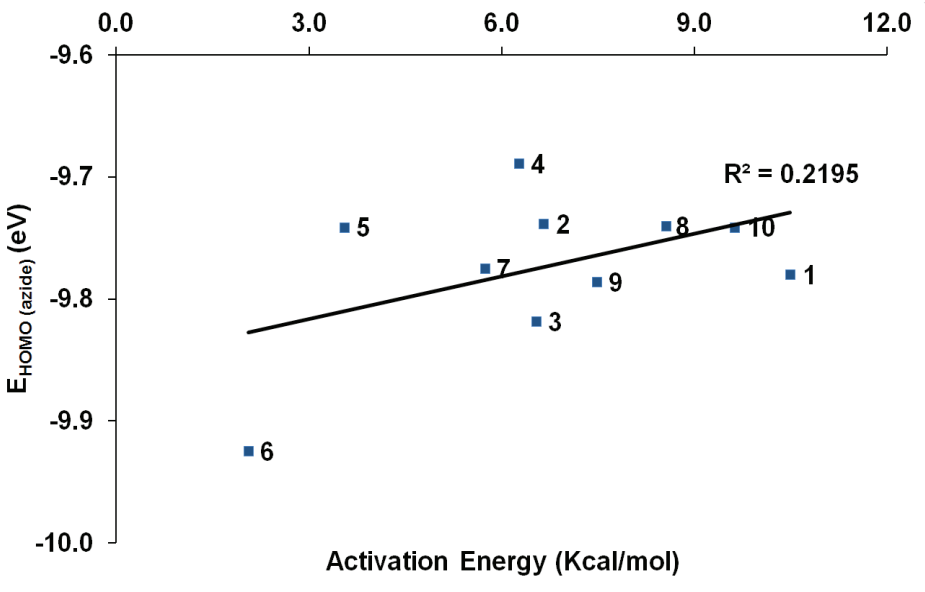

Figure S11. SCS-MP2 activation energy (kcal/mol) versus HOMO energy (eV) values of allyl azide acquired from MP2 calculations.

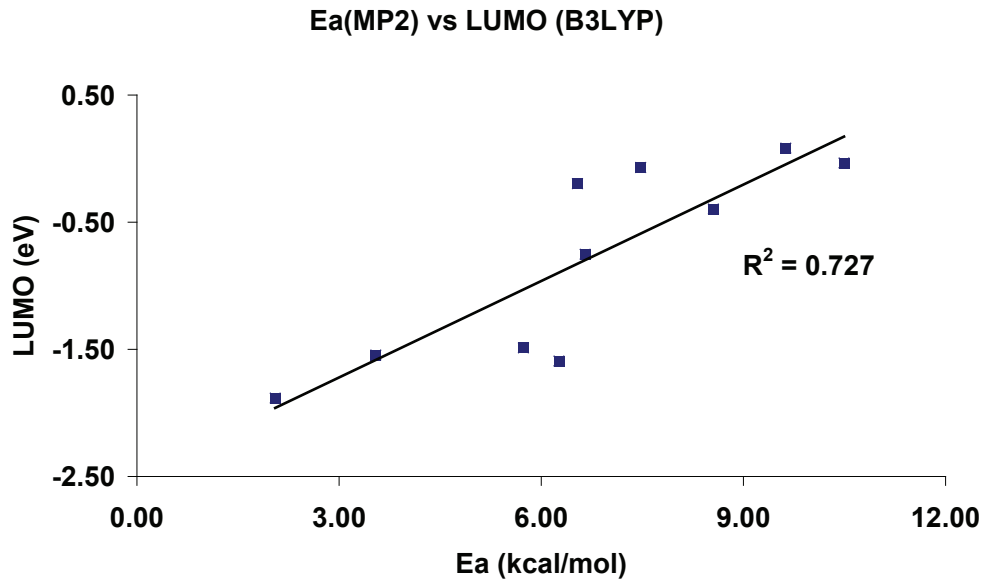

Figure S12. SCS-MP2 activation energy (kcal/mol) versus LUMO energies (eV) acquired from B3LYP calculations.

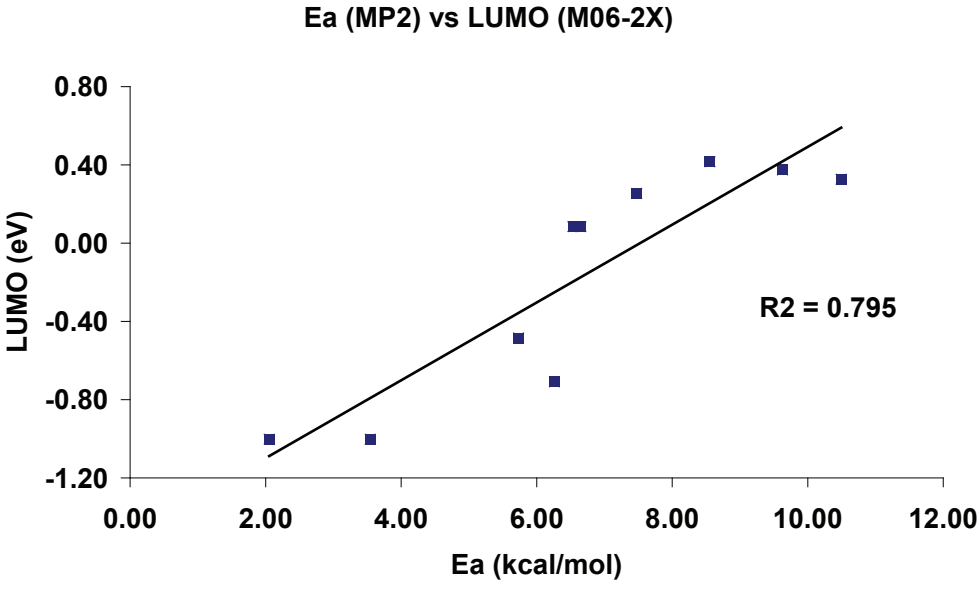

Figure S13. MP2 activation energies (kcal/mol) versus LUMO energies (eV) acquired from M06-2X calculations.

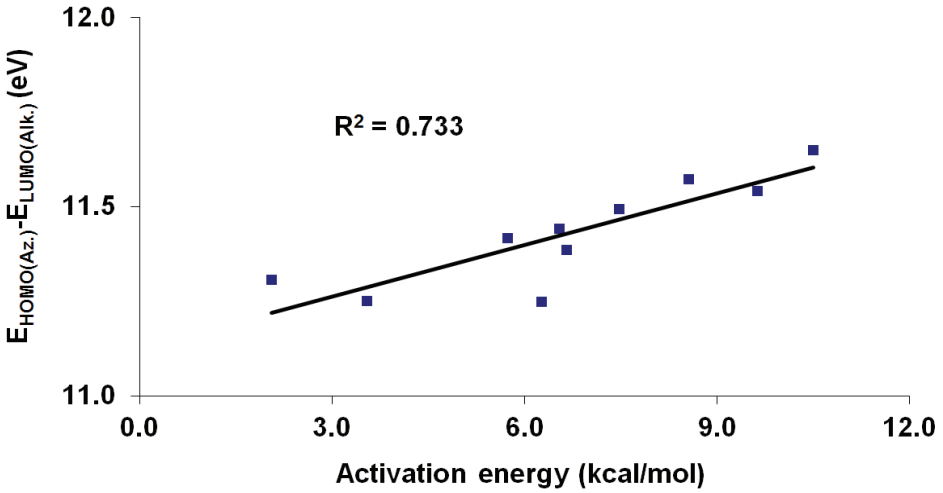

Figure S14. SCS-MP2 activation energy (kcal/mol) versus $E_{HOMO(azide)}$- $E_{LUMO(alkyne)}$ (eV).**Table S1.** SCS-MP2 MO energies of allyl azide (**A**) and benzyl azide (**B**) in the TS (with compounds **1** - **10**).

Table S1. SCS-MP2 MO energies of allyl azide (**A**) and benzyl azide (**B**) in the TS (with compounds **1** - **10**).

Azide (cyclooctyne)	HOMO-1 (eV)	HOMO (eV)	LUMO (eV)	LUMO+1 (eV)
A (+1)	-10.40	-9.78	1.03	1.85
B (+1)	-9.34	-9.01	1.05	1.64
A (+2)	-10.55	-9.74	1.04	1.86
B (+2)	-9.35	-9.02	1.05	1.64
A (+3)	-10.57	-9.82	1.35	1.87
B (+3)	-9.36	-9.06	1.36	1.64
A (+4)	-10.53	-9.69	0.97	1.86
B (+4)	-9.26	-8.99	0.92	1.68
A (+5)	-10.55	-9.74	1.14	1.86
A (+6)	-10.29	-9.92	1.06	1.88
A (+7)	-10.56	-9.78	1.21	1.87
B (+7)	-9.35	-9.04	1.22	1.64
A (+8)	-10.54	-9.74	1.00	1.86
A (+9)	-10.56	-9.79	1.24	1.87
A (+10)	-10.55	-9.74	1.14	1.86

Table S2. Calculated LUMO energies for the investigated cyclooctynes (in the state as fully optimized reagents) and corresponding activation energies for the SPAAC reaction with allyl amine.

Compound #	Abbreviation	LUMO (kcal/mol)	Ea (kcal/mol)
1	OCT	43.5	10.49
2	DIFO	36.2	6.65
3	BCN	38.2	6.54
4	DIBO	36.1	6.26
5	DIBAC	35.2	3.55
6	BARAC	34.6	2.05
7	diene	38.2	5.73
8	5,6-ene	42.9	8.56
9	*trans* c-butyl	42.1	9.63
10	*cis* c-butyl	39.6	7.47

II.6 Complete Reference 30

Frisch, M. J.; Trucks, G. W.; Schlegel, H. B.; G. E. Scuseria; Robb, M. A.; Cheeseman, J. R.; Scalmani, G.; Barone, V.; B. Mennucci; Petersson, G. A.; Nakatsuji, H.; Caricato, M.; Li, X.; Hratchian, H. P.; Izmaylov, A. F.; Bloino, J.; Zheng, G.; Sonnenberg, J. L.; Hada, M.; Ehara, M.; Toyota, K.; Fukuda, R.; Hasegawa, J.; Ishida, M.; Nakajima, T.; Honda, Y.; Kitao, O.; Nakai, H.; Vreven, T.; J. A. Montgomery, J.; Peralta, J. E.; Ogliaro, F.; Bearpark, M.; Heyd, J. J.; Brothers, E.; Kudin, K. N.; Staroverov, V. N.; Kobayashi, R.; Normand, J.; Raghavachari, K.; Rendell, A.; Burant, J. C.; Iyengar, S. S.; Tomasi, J.; Cossi, M.; Rega, N.; Millam, J. M.; Klene, M.; Knox, J. E.; Cross, J. B.; Bakken, V.; Adamo, C.; Jaramillo, J.; Gomperts, R.; Stratmann, R. E.; Yazyev, O.; Austin, A. J.; Cammi, R.; Pomelli, C.; Ochterski, J. W.; Martin, R. L.; Morokuma, K.; Zakrzewski, V. G.; Voth, G. A.; Salvador, P.; Dannenberg, J. J.; Dapprich, S.; Daniels, A. D.; Farkas, O.; Foresman, J. B.; Ortiz, J. V.; Cioslowski, J.; Fox, D. J. In *Gaussian Inc.*; Revision A.02 ed. Wallingford Connecticut, 2009, Gaussian.

II.7 Step-by-step manual for minimum energy-calculations on MP2 level of theory

1. Start by drawing the envisaged cycloalkyne in ChemDraw and copy (Figure S15).
2. Paste in ChemBio3D.
3. Select “Calculations → GAMESS Interface → Minimize Energy/Geometry” (Figure S16).
4. Enter the parameters for the MP2 calculations and press “Run” (Figure S17).

a. Job type:	Minimize (Energy/Geometry)
b. Method:	MP2
c. Basis Set:	6-311G
d. Wave function:	R-closed shell
e. Polarization:	2d,2p
f. Diffuse:	s
g. Exponent:	POPN311
h. Opt. Algorithm:	QA
i. Move Which:	All Atoms
j. Coord. System:	Cartesian
k. Spin Multiplicity:	1
l. Net Charge:	0 (Use Formal Charge)

5. The output file will appear in the “GAMESS Interface” folder, which for windows OS is in the “my documents” folder by default.
6. Open the output file “name.out” in a text editor.
7. Search for “Alpha occ. Eigenvalues”, the highest value is the HF LUMO value in Hartree.
8. Multiply this value with 627.51, the product is the energy of this orbital in kcal/mol.
9. Repeat this procedure for cyclooctyne. [By making one’s own reference to cyclooctyne, other, slightly smaller basis sets, can also be used.]
10. Compare the obtained energy difference of the cycloalkyne of interest to cyclooctyne with that calculated for compounds in Table S2.

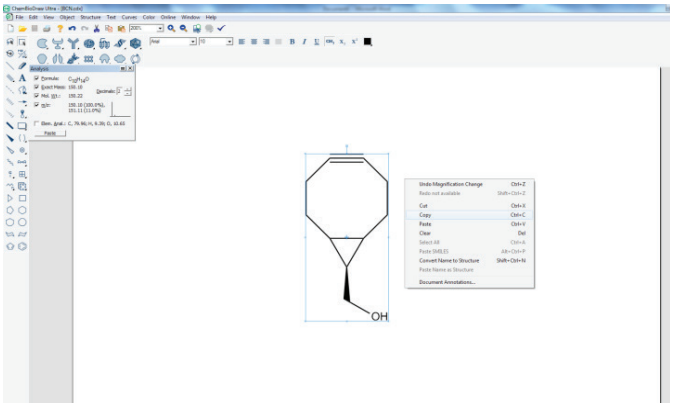

Figure S15: Draw the cyclooctyne in ChemDraw.

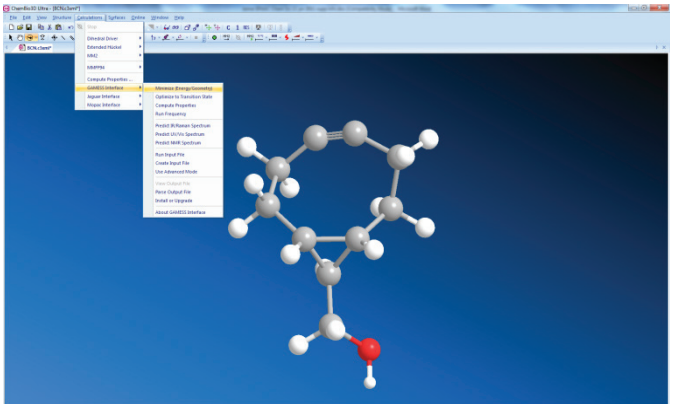

Figure S16. Select the GAMESS “Minimize (Energy/Geometry)” option.

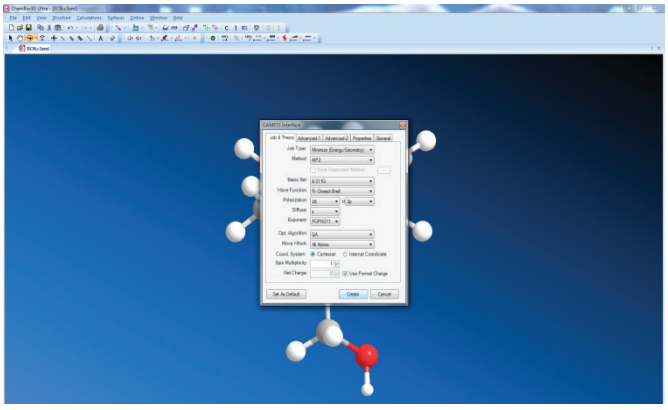

Figure S17. Enter the parameters.

Dankwoord

Om maar even met een cliché te beginnen: een proefschrift schrijf je niet alleen. Hier wil ik dan ook van de gelegenheid gebruik maken om een aantal mensen te bedanken die op de één of andere manier bijgedragen hebben aan het ontstaan van dit proefschrift en aan mijn persoonlijke ontwikkeling gedurende mijn promotie.

Als traditie begin ik natuurlijk met mijn promotoren, Professor Han Zuilhof, promotor van dit proefschrift en ook tijdelijk mijn dagelijkse begeleider: Van een promovendus wordt er verwacht dat hij/zij tijdens het promotietraject een persoonlijke ontwikkeling ondergaat tot zelfstandig professioneel wetenschapper. Ik heb mijn promotie echter ervaren als een uitdaging die zich ver buiten het wetenschappelijke uitstrekte, ik heb in de afgelopen paar jaar dan ook veel van je geleerd. Daar naast hebben we op wetenschappelijk vlak ook leuke resultaten gehaald en wil ik in het bijzonder mijn waardering uiten voor de nauwe samenwerking t.b.v. de SPAAC-studie. Ik wil je bedanken voor de mogelijkheid die je me hebt geboden om bij ORC te promoveren.
dr. Tom Wennekes, Tom, co-promotor van dit proefschrift, als vierde dagelijkse begeleider heb je nog zeker je stempel op het project weten te drukken. Jouw kennis van chemie, in het bijzonder de suikerchemie, was precies wat dit project nog nodig had. Ik loof je voor je geduld en de enorme toewijding waarmee je mij het laatste anderhalve jaar en voornamelijk met de laatste loodjes hebt geholpen. Jij bezit tevens de capaciteit om leven in de (ORC)brouwerij te brengen, bedankt voor de gezellige momenten die hiervan het gevolg waren!
dr. Carel Weijers, Carel, na Richard en Han heb jij de supervisie van mijn projecten op je genomen, helaas hebben we niet de kans gekregen deze samen af te maken. Je achtergrond in de biotechnologie hebben mij een hele andere kant van de wetenschap laten zien en ik heb hierdoor veel van je kunnen leren. Ik bedank je voor de prettige samenwerking in het bijzonder voor de hoofdstukken 3 en 6 en het werk dat je hierin hebt gestoken.
dr. Richard Jagt, Richard, ongeveer zes maanden nadat ik aan dit traject ben begonnen heb je de vakgroep verlaten. Voor je rol als mijn eerste begeleider/ co-promoter wil ik je toch zeer bedanken voor de ondersteuning die je me hebt gegeven bij het opstarten van het project en voor het mij wegwijs maken binnen de universiteit.

Professor Hans Tramper, uw ervaring, wijsheid en geduld hebben mij enorm geholpen bij het zoeken naar oplossingen voor complexe situaties.

dr. Aart van Amerongen en dr. Truus Posthuma-Trumpie, ik heb aan jullie veel kennis te danken met betrekking tot het plannen, opzetten en uitvoeren van ELISA experimenten. Bedankt voor de prettige discussies en de samenwerking. In het bijzonder wil ik Truus bedanken omdat je mij wegwijs gemaakt hebt in het lab bij FBR, mij de details voor het vakkundig uitvoeren van biologische experimenten hebt bijgebracht en je met een kritische blik naar de experimenten van hoofdstukken 2 en 3 hebt gekeken.
Anne Tio-Gillen, dr. Astrid Heikema, dr. Bart Jacobs: Ik had graag wat meer met jullie samengewerkt. Ik heb jullie namelijk leren kennen als zeer prettige persoonlijkheden en heb het Guillain-Barré-project, dat is beschreven in Hoofdstuk 6, als enorm interessant ervaren. In het bijzonder wil ik Anne bedanken voor het uitvoeren van de sera-experimenten die zijn beschreven in Hoofdstuk 6 maar voornamelijk voor de professionele maar zeer aangename manier waarop je me wegwijs hebt gemaakt met de gestandaardiseerde methoden van het uitvoeren van ELISA experimenten.
Prof. Jay Siegel and Dr Martin Mattarella, thank you both for the collaboration. Together with your expertise of your corannulenes we achieved nice scientific results that led to the publication described in Chapter 2. Especially, Martin, thanks for the pleasant cooperation and leasure time after work.
Prof. Alessandro Casnati and Dr Francesco Sansone, thank you for sharing your (expertise on) calixarenes to achieve the nice scientific results that led to the publication described in Chapter 3 and allowing me to work in your department on these compounds.
dr. Floris van Delft en Jan Dommerholt, bedankt voor de prettige samenwerking t.b.v. de SPAAC-studie, die is beschreven in Hoofdstuk 4.
To all the Unihealth project partners I would like to extend many thanks for the inspiring discussions and collaboration that kept us moving forward in this interesting project.
dr. Teris van Beek, Teris, bedankt voor je gezelschap tijdens de ritjes naar Duisburg, Nijmegen en Rotterdam, je advies en ondersteuning in het Unihealth project.
Of course thanks to all my many colleagues at ORC: Frank, Barend, Elbert, Elly, Aleida, Anita, Cees, Maurice, Michel, Ton, Jos, Ronald, Marcel, Maarten, Erik,

Anne-Marie, Remco, Ai (especially for the xá xíu (I hope now that I didn't write anything offensive! ☺)), Jacob, Tu Ha, Jurjen, Alexandre, Kim, Aliaksei, Loes, Luc, Bart, Willem, Nagesh, Wouter, Tin, Mabel, Florine, Steven, Anke, Sidhu, Radostina, Umesh, Saurabh, Satesh, Yao, Aline, Wilco, Sweccha, Rickdeb, Christie, Sjoerd, Esther for the great time that we have shared at ORC.
Een speciaal bedankje voor de oud-studenten Marjon en Baris, ik wens jullie veel succes met het vervolg van jullie carrières, Ana for your small contribution to Chapter 5 en Geert, jouw capita selecta en MSc-project onder mijn begeleiding hebben mede geleid tot de wetenschappelijke studie die is beschreven in hoofdstuk 5. Ik wil je bedanken voor de samenwerking en het mooie werk dat je hebt afgeleverd, daar kun je trots op zijn. Ik wens je veel succes met je eigen promotieonderzoek.
Sourav, for you an honorable mention. I laud your ability to regulate and manage, and I especially enjoyed our many discussions, like the one in the train from Newcastle to Edinburgh. Hopefully there are many such to come, I wish you all the best in Ireland, and keep in touch.
Ik wil ook graag "the usual suspects" bedanken voor jullie rol als kartrekkers als het gaat om het organiseren van de sociale activiteiten binnen de vakgroep. Bas, Tjerk en Jorin bedankt voor de gezellige avonden die jullie hebben georganiseerd. Tevens bedankt voor het kritisch lezen van (delen van) mijn manuscript en ik ben ervan overtuigd dat we elkaar nog regelmatig zullen treffen bij de "Vlaam" of het Ernemse equivalent.

Dan zijn mijn paranimfen aan de beurt:

Nishant, van studiegenoot bij de VU en UVA tot collega bij een stagebedrijf, van labmaat tot goede vriend. Onze wegen hebben elkaar onbewust al meerdere malen gekruist tijdens onze relatief korte chemiecarrières. Het is pas sinds het laatste anderhalf jaar dat je bij de WUR werkte dat we elkaar echt goed hebben leren kennen. Bedankt voor je kameraadschap en natuurlijk ook voor de technische ondersteuning in het project dat is beschreven in Hoofdstuk 6, voor het kritisch lezen van mijn teksten en het helpen organiseren van mijn verdediging.

Bas, jij bent zowaar de enige die tweemaal genoemd wordt in dit dankwoord. Jij verdient dan ook wel wat extra lof. Je staat altijd klaar voor anderen en schuwt het niet om de leiding te nemen in zaken die anderen niet aandurven. Daarbij ben ik je

zeer verdienstelijk voor de enorme hulp die je me hebt geboden bij het organiseren van mijn verdediging.

Natuurlijk wil ik mijn vrienden bedanken, jullie allemaal bedankt voor jullie vriendschap en het nodige vertier!
Natuurlijk Roy, “Professor G”, bedanken voor de gezellige avondjes, ik ben er van overtuigd dat er nog veel zullen volgen.
Schoutûh, my brother-from-another-mother, er kunnen veel dingen in mijn leven veranderen maar één ding is zeker, jij bent er bij. Melanie en Hein (pokpoook), jullie legendarische kaartavonden staan altijd garant voor hilarische momenten. Mijn “Nijmeegse vrienden” Sjakie, Marleen, Linda, Dennis, Hanneke, Al, Sanne en Hans, inmiddels woont het gros van jullie er al niet meer (dé gros nog wel) maar we zullen altijd verbonden blijven door deze stad. Jullie wil ik bedanken voor de vele fijne avondjes/weekendjes en steun van de afgelopen jaren. Dewi, jij hebt een speciaal plekje hier, mijn woorden zijn hier ontoereikend maar jouw affectie, kracht en doorzettingsvermogen hebben door de jaren heen bijgedragen aan het vormen van de persoon die ik nu ben. Bedankt voor alles!

Tamara, René, Noor en Milou, mijn familie… Bedankt dat jullie er altijd voor me zijn wanneer het nodig is en het vormen van een stabiel en levendig thuisfront.

Ora, una persona che è molto speciale per me. Silvia, non so dove devo iniziare. Grazie per la colloborazione. Mi hai aiutato anche molto con la mia tesi, ma più importante: grazie che sei con me, per tutte le emozioni che mi fai sentire e per tutte le cose belle che sempre facciamo insieme. Anche la tua famiglia voglio ringraziare: Rita, Massimo e Francesca grazie per sempre. Mi fate sentire come se fossi a casa mia. Vi prometto che imparerò meglio e presto la lingua ;)

Tot slot mijn ouders, pa en ma, toen ik op mijn 17e stopte met VWO vonden jullie dat jammer omdat ik *“dokter” zou kunnen worden*. Nu gaat het uiteindelijk dan toch gebeuren, zij het dat dit wellicht niet de “doctor” is waar jullie toentertijd op doelden. Ik wil jullie bedanken voor alle onvoorwaardelijke steun die jullie mij altijd weer bieden en het creëren van een liefdevolle thuishaven. Daarom is dit proefschrift opgedragen aan jullie.

Jaime

Overview of training activities

Discipline specific activities

Courses
Advanced Organic Chemistry I, Wageningen (2009-2010)
Advanced Organic Chemistry II, Wageningen (2010-2012)
VLAG Summer Course Glycoscience 11th ed., Wageningen (2010)
COST Trainingschool Supramolecular Chemistry in Water, Riccione (2012)

Meetings
NWO Annual Conference, Lunteren (2009-2013)
KNCV eendaagse sectiebijeenkomst, Wageningen (2012)
KNCV Wageningen Symposium on Organic Chemistry, Wageningen (2010)
KNCV Wageningen Symposium on Organic Chemistry, Wageningen (2012)

General courses

PhD-week, Baarlo (2010)
Information literacy and endnote, Wageningen (2010)
Advanced course guide to scientific artwork, Wageningen (2013)
Adobe Indesign, Wageningen (2013)

Optionals

Preparation PhD research proposal, Wageningen (2010)
Group meetings, laboratory of organic chemistry, Wageningen (2009-2014)
Colloquia, laboratory of organic chemistry, Wageningen (2009-2014)
PhD-trip, UK (2011)
Organization PhD-trip, UK (2011)
PhD representative “group of change”, Wageningen (2011-2013)

The research presented in this dissertation was financed by the INTERREG IV A Germany-Netherlands programme through the EU funding from the European Regional Development Fund (ERDF), the Ministry for Economic Affairs, Energy, Building, Housing and Transport of the State of North-Rhine Westphalia, the Dutch Ministry of Economic Affairs, and the Province of Gelderland; it is accompanied by the program management Euregio Rhein-Waal.

Design and Layout: Jaime Garcia Hartjes*
Printed by: Editoo B.V., Arnhem

*Cover CT image: 1XTC.pdb
*Cover Ab image: 1IGT.pdb